

# VU Research Portal

## Imaging neurodegeneration across the Alzheimer's disease continuum

Pelkmans, Wiesje

2022

### **document version**

Publisher's PDF, also known as Version of record

[Link to publication in VU Research Portal](#)

### **citation for published version (APA)**

Pelkmans, W. (2022). *Imaging neurodegeneration across the Alzheimer's disease continuum: The contribution of biomarkers to understanding clinical progression*. Optima.

### **General rights**

Copyright and moral rights for the publications made accessible in the public portal are retained by the authors and/or other copyright owners and it is a condition of accessing publications that users recognise and abide by the legal requirements associated with these rights.

- Users may download and print one copy of any publication from the public portal for the purpose of private study or research.
- You may not further distribute the material or use it for any profit-making activity or commercial gain
- You may freely distribute the URL identifying the publication in the public portal ?

### **Take down policy**

If you believe that this document breaches copyright please contact us providing details, and we will remove access to the work immediately and investigate your claim.

### **E-mail address:**

[vuresearchportal.ub@vu.nl](mailto:vuresearchportal.ub@vu.nl)



**IMAGING NEURODEGENERATION**  
**ACROSS THE ALZHEIMER'S DISEASE CONTINUUM**

*The contribution of biomarkers to understanding clinical progression*

Wiesje Pelkmans

## Colofon

The studies described in this thesis were carried out at the Alzheimer Center Amsterdam, Neurology, Vrije Universiteit Amsterdam, Amsterdam UMC location VUmc, the Netherlands. The Alzheimer Center Amsterdam is part of the Neurodegeneration research program of Amsterdam Neuroscience. Chapter 4 of this thesis described research that was carried out at the Clinical Memory Research Unit of Lund University, Sweden, and was funded by a research fellowship grant from Alzheimer Nederland (WE.15-2019-14). Printing costs of this thesis were sponsored by Alzheimer Nederland, Danone Nutricia Research, and Vrije Universiteit Amsterdam.

Wiesje Pelkmans ISBN: 978-94-6361-733-8

Printing: Optima

Layout and cover design: Wiesje Pelkmans

Copyright 2022 © Wiesje Pelkmans

All rights reserved. No parts of this thesis may be reproduced, stored in a retrieval system or transmitted in any form or by any means without permission of the author.



VRIJE UNIVERSITEIT

**IMAGING NEURODEGENERATION  
ACROSS THE ALZHEIMER'S DISEASE CONTINUUM**

The contribution of biomarkers to understanding clinical progression

ACADEMISCH PROEFSCHRIFT

ter verkrijging van de graad Doctor of Philosophy aan  
de Vrije Universiteit Amsterdam,  
op gezag van de rector magnificus  
prof.dr. J.J.G. Geurts,  
in het openbaar te verdedigen  
ten overstaan van de promotiecommissie  
van de Faculteit der Geneeskunde  
op maandag 3 oktober 2022 om 13.45 uur  
in een bijeenkomst van de universiteit,  
De Boelelaan 1105

door

Wiesje Pelkmans

geboren te Tilburg

promotoren:            prof.dr. W.M. van der Flier  
                              prof.dr. F. Barkhof

copromotor:            dr. B.M. Tijms

promotiecommissie:    prof.dr. L. Reneman  
                              prof.dr. W.J. Niessen  
                              prof.dr. L. van der Weerd  
                              dr. J. Pereira  
                              dr. S.A.M. Sikkes  
                              dr. J.D. Gispert

## Table of contents

<b>Chapter 1.</b>	General introduction	7
<b>Chapter 2</b>	Amyloid- $\beta$ , cortical thickness, and subsequent cognitive decline in cognitively normal oldest-old.	23
<b>Chapter 3</b>	Association of CSF, blood and imaging markers of neurodegeneration with clinical progression in people with subjective cognitive decline.	67
<b>Chapter 4</b>	Tau-related grey matter network breakdown across the Alzheimer's disease continuum.	105
<b>Chapter 5</b>	Grey matter T1-w/T2-w ratios are higher in Alzheimer's disease	145
<b>Chapter 6</b>	Grey matter network markers identify individuals with prodromal Alzheimer's disease who will show rapid clinical decline	199
<b>Chapter 7</b>	Summary and general discussion	233
<b>Appendix</b>	Nederlandse samenvatting (Dutch summary) List of publications List of author affiliations List of PhD theses Alzheimer Center Amsterdam Portfolio Acknowledgements About the author	255





# CHAPTER 1

## **General introduction**



## GENERAL INTRODUCTION

### **The Alzheimer's disease continuum**

Alzheimer's disease (AD) is a progressive neurodegenerative disorder and the most common cause of dementia. Traditionally, an AD diagnosis has been based on the patient's clinical presentation, namely a progressive impairment of multiple cognitive domains that interferes with daily life activities (McKhann et al. 1984). A definitive biological diagnosis of AD could only be established by autopsy. Post-mortem studies, however, revealed that about one-third of clinical AD dementia cases did not exhibit the neuropathological changes associated with AD (Nelson et al. 2012; Elobeid et al. 2016).

Over the past two decades, the development of biomarkers that can detect AD pathology in living individuals has transformed the field of AD research. The key pathological features of AD, namely amyloid- $\beta$  (A $\beta$ ) plaques and tau neurofibrillary tangles, can be measured *in vivo* using positron emission tomography (PET), as well as in the cerebrospinal fluid (CSF), and accurate blood-based assays are on the horizon (Hansson 2021). Furthermore, structural magnetic resonance imaging (MRI) can provide estimates of regional neurodegeneration and patterns of brain atrophy. Consequently, it has become apparent that AD pathology begins to accumulate approximately 20 years prior to the onset of symptoms of dementia.

The amyloid cascade hypothesis proposes that aggregation of A $\beta$  plays an initiating role in the onset of the disease by initiating a cascade of events leading to synaptic dysfunction, the formation of neurofibrillary tangles, inflammation, neuronal loss, cognitive dysfunction, and dementia (Jack et al. 2013; Selkoe and Hardy 2016; Busche and Hyman 2020). As a

result, AD has been conceptualized as a biological construct along a continuum of preclinical, prodromal and dementia stages rather than a clinical symptomology. Therefore, AD can now be defined by markers indicating the underlying pathology, regardless of the clinical presentation. These insights have led to the publication of the 'ATN' research framework that binarizes three classes of AD biomarkers (i.e. A = Amyloid, T = hyperphosphorylated Tau, N = Neurodegeneration). A+T+ pathology can be used to define AD, while N biomarkers are not specific to AD but can be used for disease severity staging (Jack et al. 2018).

### **Imaging correlates of neurodegeneration**

Synaptic loss and neuronal cell death are characteristic neurodegenerative features of AD that are closely related to cognitive decline. The grey matter of the brain is made up of neuronal cells and their connections, and loss of grey matter can be detected *in vivo* using structural MRI. Several biomarkers for grey matter integrity have been associated with cognitive impairments and can be used to accurately predict future deterioration in early disease stages (Dickerson and Wolk 2012; Tondelli et al. 2012; Mormino et al. 2014; Pettigrew et al. 2016; ten Kate et al. 2017; Bilgel et al. 2018). However, to date the mechanism of cognitive decline in AD cannot fully be explained by grey matter integrity. In addition, it remains unclear how neurodegeneration is associated with AD pathology across different disease stages.

In this thesis we investigated the structural brain changes of four neurodegeneration measures that occur during the progression of Alzheimer's disease: hippocampal volume, cortical thickness, grey matter networks, and cortical myelin. Furthermore, we studied their relationship with AD pathology markers and clinical progression.

*Hippocampal volume and cortical thickness*

Neuronal loss in predominantly medial temporal regions, including the hippocampus, entorhinal cortex and surrounding parahippocampal cortex, is a consistent finding in AD patients and a predictor of decline in memory functioning (den Heijer et al. 2010; Verfaillie et al. 2016). As a result, macrostructural brain changes of atrophy and cortical thinning can typically be observed on MRI, which are widely used as diagnostic indicators of AD (Frisoni et al. 2010; McKhann et al. 2011). Aside from visual assessment, automated quantitative software can be used to calculate structural changes in the brain indicative of neuronal loss and/or a decrease in neuronal complexity (Bobinski et al. 1999).

Even though hippocampal volume loss and regional cortical thinning are typical in individuals with A $\beta$  aggregation, it is not specific to AD since there are multiple other pathologies that can cause hippocampal atrophy and cognitive impairments, including TDP-43, hippocampal sclerosis, and vascular damage (Wirth et al. 2013; Josephs et al. 2017; Flores et al. 2020; Yu et al. 2020). There is a significant increase in the prevalence of atrophy, A $\beta$ - and non-A $\beta$  pathologies with advancing age, with one or more pathologies evident in many individuals over the age of 60 and in nearly all individuals over the age of 80 (Fjell et al. 2014; Ossenkoppele et al. 2015; White et al. 2016; Spina et al. 2021). Therefore with increasing age, the association between pathological changes and cognitive decline becomes more complex. Additionally, there are many different approaches that are used to measure neurodegenerative changes and to define biomarker abnormalities (Mattsson-Carlgrén et al. 2020). However, it is still unclear how these different measures are related and how they influence the prediction of clinical progression.

### *Grey matter networks*

Normal cognitive functioning requires efficient information transfer between neuronal populations (Palop and Mucke 2016), and disruptions in brain networks have shown to contribute to cognitive dysfunction in many neurological disorders, including AD (Yu et al. 2021). The accumulation of A $\beta$  plaques and neurofibrillary tangles can disrupt neuronal connectivity, resulting in a loss of neuronal network integrity. Therefore, AD can be regarded as a disconnection syndrome (Selkoe 2002; Delbeuck et al. 2003; Edwards 2019).

Brain networks can be constructed through multiple neuroimaging techniques (e.g., sMRI, DTI, fMRI). The focus of this thesis is only on structural MRI networks whose nodes and edges (i.e. connections) are defined by structural covariance correlations of morphological information such as cortical thickness and/or volume. The organisation of connections in such grey matter networks can be quantified using graph theoretical metrics such as path length, clustering coefficient, and the small-world coefficient. These measures are indicative of how efficiently information is processed in a network. As compared to healthy individuals, AD brain networks show a loss of small world organisation, indicative of a more random network topology (Pievani et al. 2014; Stam 2014). The loss of integrity of grey matter networks has been associated with biomarkers of A $\beta$  pathology in previous studies (Tijms et al. 2016; ten Kate et al. 2018; Voevodskaya et al. 2018). This suggests that changes in grey matter network topology occur in the presence of amyloid already in individuals with normal cognition. How tau pathology may contribute to the grey matter network alterations in AD is yet unclear. As elevated tau burden is thought to be more closely related to synaptic function and atrophy, than A $\beta$  plaques

(la Joie et al. 2020; Coomans et al. 2021; Iaccarino et al. 2021), tau pathology may contribute to impaired network organisation in AD.

Furthermore, growing evidence suggests that disruptions in grey matter networks may be a sensitive early marker of disease progression, and have been associated with clinical progression to mild cognitive impairment or dementia and an increased risk of cognitive decline in pre-dementia patients (Pereira et al. 2016; Dicks et al. 2018; Tijms et al. 2018; Verfaillie et al. 2018). As a consequence, grey matter network graph theory measures may serve as an early prognostic biomarker for subsequent disease progression. However, to identify individuals at risk for cognitive decline in the future, findings at the group level must be translated to subject-level applications.

### *Cortical myelin*

Grey matter is composed predominantly of neuronal cell bodies and dendrites, but also includes myelinated axons. This insulating sheath that surrounds neuronal axons, is vulnerable to AD pathology and deteriorates with neuronal and axonal degeneration (Bartzokis 2011; Dean et al. 2017). Myelin integrity is considered essential for efficient neuronal communication by fine-tuning conduction speed and synchronization, thereby affecting brain connectivity (Nave and Werner 2014; Timmler and Simons 2019).

According to Glasser and van Essen (2011), the ratio of T1-weighted and T2-weighted images can be used as a proxy measure of myelin content in grey matter. The contrast in T1-w and T2-w images is to a large extent driven by myelin, and by calculating the ratio between these images, the shared field inhomogeneities in the images are reduced and the contrast for myelin content is enhanced. Ongoing research has shown close spatial

correspondence of the T1w/T2w ratio with cyto- and myeloarchitecture, regional gene expression, synaptic density, and other connectivity measures such as DTI (Ganzetti et al. 2015; Shafee et al. 2015; Huntenburg et al. 2017; Nieuwenhuys and Broere 2017; Burt et al. 2018; Ritchie et al. 2018; Fulcher et al. 2019). More advanced sequences such as the myelin water fraction (MWF) or quantitative magnetization transfer (qMT) can be considered more direct measures of myelin (Heath et al. 2018), but the T1w/T2w ratio has the advantage that it relies on standard sequences with short scan times, and might therefore be more suitable for clinical practice. To date, the ratio of T1-w/T2w images has not been investigated in AD patients and could serve as a promising measure of brain connectivity disruptions in AD.

### **Conclusion**

With the rapid development of biomarkers for neurodegenerative diseases, we are now able to ask questions and provide answers about the interrelationships between specific biomarkers and their association with cognitive decline and progression to dementia. Such knowledge is essential for the development of effective treatment strategies for Alzheimer's disease. Furthermore, it is crucial for identifying individuals at an early disease stage at high risk of progression, which could assist in the selection of the right participants for disease-modifying clinical trials.

### **Thesis aims**

The aim of this thesis is to improve understanding of the complex interrelationships between markers of AD pathology (i.e. amyloid and tau markers), structural brain changes (including measures of neuronal injury and brain network alterations), and their association with cognitive decline and clinical progression across different stages of AD.



Three specific objectives are addressed in this thesis:

1. Improve understanding of the direct and indirect effects of amyloid pathology and different measures of neurodegeneration on future cognitive decline in individuals with normal cognition (Ch. 2, 3).
2. Understand how grey matter networks and myelin proxy measures change in relation to key pathological proteins in Alzheimer's disease (Ch. 4, 5).
3. Test whether grey matter network measures, alone or combined with other prognostic biomarkers, can identify individuals with prodromal Alzheimer's disease that will show rapid clinical decline (Ch. 6).

### **Thesis outline**

In **chapter 2** we examined the relationship between abnormal A $\beta$  and cognitive decline in cognitively normal individuals over the age of 90 and the extent to which such effects are mediated by cortical atrophy.

In **chapter 3** we compared different neurodegeneration markers and determined their predictive value for clinical progression in individuals with subjective cognitive decline.

In **chapter 4** we examined the relationship between tau deposition and alterations in whole-brain and regional grey matter networks in individuals across the AD spectrum.

In **chapter 5** we compared T1-w/T2-w ratio values between individuals with normal cognition and patients with AD dementia, and assessed to what extent neuronal injury, white matter hyperintensities, and cognitive functioning contributed to alterations in T1-w/T2-w values.

In **chapter 6** we explored whether grey matter networks can be used to identify individuals with prodromal AD who will progress rapidly.

### References

- Bartzokis G. 2011. Alzheimer's disease as homeostatic responses to age-related myelin breakdown. *Neurobiology of Aging*. 32:1341–1371.
- Bilgel M, An Y, Helpfrey J, Elkins W, Gomez G, Wong DF, Davatzikos C, Ferrucci L, Resnick SM. 2018. Effects of amyloid pathology and neurodegeneration on cognitive change in cognitively normal adults. *Brain*. 141:2475–2485.
- Bobinski M, de Leon MJ, Wegiel J, DeSanti S, Convit A, saint Louis LA, Rusinek H, Wisniewski HM. 1999. The histological validation of post mortem magnetic resonance imaging-determined hippocampal volume in Alzheimer's disease. *Neuroscience*. 95:721–725.
- Burt JB, Demirtaş M, Eckner WJ, Navejar NM, Ji JL, Martin WJ, Bernacchia A, Anticevic A, Murray JD. 2018. Hierarchy of transcriptomic specialization across human cortex captured by structural neuroimaging topography. *Nature Neuroscience*. 21:1251–1259.
- Busche MA, Hyman BT. 2020. Synergy between amyloid- $\beta$  and tau in Alzheimer's disease. *Nature Neuroscience*. 23:1183–1193.
- Coomans EM, Schoonhoven DN, Tuncel H, Verfaillie SCJ, Wolters EE, Boellaard R, Ossenkuppele R, den Braber A, Scheper W, Schober P, Sweeney SP, Ryan JM, Schuit RC, Windhorst AD, Barkhof F, Scheltens P, Golla SS v, Hillebrand A, Gouw AA, van Berckel BNM. 2021. In vivo tau pathology is associated with synaptic loss and altered synaptic function. *Alzheimer's Research & Therapy*. 13:35.
- Dean DC, Hurley SA, Kecskemeti SR, O'Grady JP, Canda C, Davenport-Sis NJ, Carlsson CM, Zetterberg H, Blennow K, Asthana S, Sager MA, Johnson SC, Alexander AL, Bendlin BB. 2017. Association of Amyloid Pathology With Myelin Alteration in Preclinical Alzheimer Disease. *JAMA Neurology*. 74:41.
- Delbeuck X, van der Linden M, Collette F. 2003. Alzheimer's Disease as a Disconnection Syndrome? *Neuropsychol Rev*. 13:79–92.
- den Heijer T, van der Lijn F, Koudstaal PJ, Hofman A, van der Lugt A, Krestin GP, Niessen WJ, Breteler MMB. 2010. A 10-year follow-up of hippocampal volume on magnetic resonance imaging in early dementia and cognitive decline. *Brain*. 133:1163–1172.
- Dickerson BC, Wolk DA. 2012. MRI cortical thickness biomarker predicts AD-like CSF and cognitive decline in normal adults. *Neurology*. 78:84–90.
- Dicks E, Tijms BM, ten Kate M, Gouw AA, Benedictus MR, Teunissen CE, Barkhof F, Scheltens P, van der Flier WM. 2018. Gray matter network measures are associated with cognitive decline in mild cognitive impairment. *Neurobiology of Aging*. 61:198–206.

- Edwards FA. 2019. A Unifying Hypothesis for Alzheimer's Disease: From Plaques to Neurodegeneration. *Trends in Neurosciences*. 42:310–322.
- Elobeid A, Libard S, Leino M, Popova SN, Alafuzoff I. 2016. Altered Proteins in the Aging Brain. *Journal of Neuropathology and Experimental Neurology*. 75:316–325.
- Fjell AM, McEvoy L, Holland D, Dale AM, Walhovd KB. 2014. What is normal in normal aging? Effects of aging, amyloid and Alzheimer's disease on the cerebral cortex and the hippocampus. *Progress in Neurobiology*. 117:20–40.
- Flores R, Wisse LEM, Das SR, Xie L, McMillan CT, Trojanowski JQ, Robinson JL, Grossman M, Lee E, Irwin DJ, Yushkevich PA, Wolk DA. 2020. Contribution of mixed pathology to medial temporal lobe atrophy in Alzheimer's disease. *Alzheimer's & Dementia*. 16:843–852.
- Frisoni GB, Fox NC, Jack CR, Scheltens P, Thompson PM. 2010. The clinical use of structural MRI in Alzheimer disease. *Nature Reviews Neurology*. 6:67–77.
- Fulcher BD, Murray JD, Zerbi V, Wang X-J. 2019. Multimodal gradients across mouse cortex. *Proceedings of the National Academy of Sciences*. 116:4689–4695.
- Ganzetti M, Wenderoth N, Mantini D. 2015. Whole brain myelin mapping using T1- and T2-weighted MR imaging data. *Frontiers in Human Neuroscience*. 8:917–928.
- Glasser MF, van Essen DC. 2011. Mapping Human Cortical Areas In Vivo Based on Myelin Content as Revealed by T1- and T2-Weighted MRI. *Journal of Neuroscience*. 31:11597–11616.
- Hansson O. 2021. Biomarkers for neurodegenerative diseases. *Nature Medicine*. 18:698–705.
- Heath F, Hurley SA, Johansen-Berg H, Sampaio-Baptista C. 2018. Advances in noninvasive myelin imaging. *Developmental Neurobiology*. 78:136–151.
- Huntenburg JM, Bazin PL, Goulas A, Tardif CL, Villringer A, Margulies DS. 2017. A Systematic Relationship Between Functional Connectivity and Intracortical Myelin in the Human Cerebral Cortex. *Cereb Cortex*. 27:981–997.
- Iaccarino L, la Joie R, Edwards L, Strom A, Schonhaut DR, Ossenkoppele R, Pham J, Mellinger T, Janabi M, Baker SL, Soleimani-Meigooni D, Rosen HJ, Miller BL, Jagust WJ, Rabinovici GD. 2021. Spatial Relationships between Molecular Pathology and Neurodegeneration in the Alzheimer's Disease Continuum. *Cerebral Cortex*. 31:1–14.
- Jack CR, Bennett DA, Blennow K, Carrillo MC, Dunn B, Haeberlein SB, Holtzman DM, Jagust W, Jessen F, Karlawish J, Liu E, Molinuevo JL, Montine T, Phelps C, Rankin KP, Rowe CC, Scheltens P, Siemers E, Snyder HM, Sperling R, Elliott C, Masliah E, Ryan L, Silverberg N. 2018. NIA-AA Research Framework: Toward a biological definition of Alzheimer's disease. *Alzheimer's and Dementia*. 14:535–562.

- Jack CR, Knopman DS, Jagust WJ, Petersen RC, Weiner MW, Aisen PS, Shaw LM, Vemuri P, Wiste HJ, Weigand SD, Lesnick TG, Pankratz VS, Donohue MC, Trojanowski JQ. 2013. Tracking pathophysiological processes in Alzheimer's disease: an updated hypothetical model of dynamic biomarkers. *The Lancet Neurology*. 12:207–216.
- Josephs KA, Dickson DW, Tosakulwong N, Weigand SD, Murray ME, Petrucelli L, Liesinger AM, Senjem ML, Sychalla AJ, Knopman DS, Parisi JE, Petersen RC, Jack CR, Whitwell JL. 2017. Rates of hippocampal atrophy and presence of post-mortem TDP-43 in patients with Alzheimer's disease: a longitudinal retrospective study. *The Lancet Neurology*. 16:917–924.
- la Joie R, Visani A v., Baker SL, Brown JA, Bourakova V, Cha J, Chaudhary K, Edwards L, Iaccarino L, Janabi M, Lesman-Segev OH, Miller ZA, Perry DC, O'Neil JP, Pham J, Rojas JC, Rosen HJ, Seeley WW, Tsai RM, Miller BL, Jagust WJ, Rabinovici GD. 2020. Prospective longitudinal atrophy in Alzheimer's disease correlates with the intensity and topography of baseline tau-PET. *Science Translational Medicine*. 12:eaau5732.
- Mattsson-Carlgren N, Leuzy A, Janelidze S, Palmqvist S, Stomrud E, Strandberg O, Smith R, Hansson O. 2020. The implications of different approaches to define AT(N) in Alzheimer disease. *Neurology*. 94:e2233–e2244.
- McKhann G, Drachman D, Folstein M, Katzman R, Price D, Stadlan EM. 1984. Clinical diagnosis of Alzheimer's disease: Report of the NINCDS-ADRDA Work Group\* under the auspices of Department of Health and Human Services Task Force on Alzheimer's Disease. *Neurology*. 34:939–939.
- McKhann GM, Knopman DS, Chertkow H, Hyman BT, Jack CR, Kawas CH, Klunk WE, Koroshetz WJ, Manly JJ, Mayeux R, Mohs RC, Morris JC, Rossor MN, Scheltens P, Carrillo MC, Thies B, Weintraub S, Phelps CH. 2011. The diagnosis of dementia due to Alzheimer's disease: Recommendations from the National Institute on Aging-Alzheimer's Association workgroups on diagnostic guidelines for Alzheimer's disease. *Alzheimer's & Dementia*. 7:263–269.
- Mormino EC, Betensky RA, Hedden T, Schultz AP, Amariglio RE, Rentz DM, Johnson KA, Sperling RA. 2014. Synergistic Effect of  $\beta$ -Amyloid and Neurodegeneration on Cognitive Decline in Clinically Normal Individuals. *JAMA Neurology*. 71:1379.
- Nave K-A, Werner HB. 2014. Myelination of the Nervous System: Mechanisms and Functions. *Annual Review of Cell and Developmental Biology*. 30:503–533.
- Nelson PT, Alafuzoff I, Bigio EH, Bouras C, Braak H, Cairns NJ, Castellani RJ, Crain BJ, Davies P, Tredici K del, Duyckaerts C, Frosch MP, Haroutunian V, Hof PR, Hulette CM, Hyman BT, Iwatsubo T, Jellinger KA, Jicha GA, Kövari E, Kukull WA, Leverenz JB, Love S, Mackenzie IR, Mann DM, Masliah E, McKee AC, Montine TJ, Morris JC, Schneider JA, Sonnen JA, Thal DR, Trojanowski JQ,

- Troncoso JC, Wisniewski T, Woltjer RL, Beach TG. 2012. Correlation of Alzheimer Disease Neuropathologic Changes With Cognitive Status: A Review of the Literature. *Journal of Neuropathology & Experimental Neurology*. 71:362–381.
- Nieuwenhuys R, Broere CAJ. 2017. A map of the human neocortex showing the estimated overall myelin content of the individual architectonic areas based on the studies of Adolf Hopf. *Brain Structure and Function*. 222:465–480.
- Ossenkoppele R, Jansen WJ, Rabinovici GD, Knol DL, van der Flier WM, van Berckel BNM, Scheltens P, Visser PJ, Verfaillie SCJ, Zwan MD, Adriaanse SM, Lammertsma AA, Barkhof F, Jagust WJ, Miller BL, Rosen HJ, Landau SM, Villemagne VL, Rowe CC, Lee DY, Na DL, Seo SW, Sarazin M, Roe CM, Sabri O, Barthel H, Koglin N, Hodges J, Leyton CE, Vandenberghe R, van Laere K, Drzezga A, Forster S, Grimmer T, Sánchez-Juan P, Carril JM, Mok V, Camus V, Klunk WE, Cohen AD, Meyer PT, Hellwig S, Newberg A, Frederiksen KS, Fleisher AS, Mintun MA, Wolk DA, Nordberg A, Rinne JO, Chételat G, Lleo A, Blesa R, Fortea J, Madsen K, Rodrigue KM, Brooks DJ. 2015. Prevalence of Amyloid PET Positivity in Dementia Syndromes. *JAMA*. 313:1939.
- Palop JJ, Mucke L. 2016. Network abnormalities and interneuron dysfunction in Alzheimer disease. *Nature Reviews Neuroscience*. 17:777–792.
- Pereira JB, Mijalkov M, Kakaei E, Mecocci P, Vellas B, Tsolaki M, Kłoszewska I, Soininen H, Spenger C, Lovestone S, Simmons A, Wahlund LO, Volpe G, Westman E. 2016. Disrupted Network Topology in Patients with Stable and Progressive Mild Cognitive Impairment and Alzheimer's Disease. *Cerebral Cortex*. 26:3476–3493.
- Pettigrew C, Soldan A, Zhu Y, Wang M, Moghekar A, Brown T, Miller M, Albert M. 2016. Cortical thickness in relation to clinical symptom onset in preclinical AD. *NeuroImage: Clinical*. 12:116–122.
- Pievani M, Filippini N, van den Heuvel MP, Cappa SF, Frisoni GB. 2014. Brain connectivity in neurodegenerative diseases - From phenotype to proteinopathy. *Nature Reviews Neurology*. 10:620–633.
- Ritchie J, Pantazatos SP, French L. 2018. Transcriptomic characterization of MRI contrast with focus on the T1-w/T2-w ratio in the cerebral cortex. *Neuroimage*. 174:504–517.
- Selkoe DJ. 2002. Alzheimer's Disease Is a Synaptic Failure. *Science*. 298:789–791.
- Selkoe DJ, Hardy J. 2016. The amyloid hypothesis of Alzheimer's disease at 25 years. *EMBO Molecular Medicine*. 8:595–608.
- Shafee R, Buckner RL, Fischl B. 2015. Gray matter myelination of 1555 human brains using partial volume corrected MRI images. *Neuroimage*. 105:473–485.
- Spina S, la Joie R, Petersen C, Nolan AL, Cuevas D, Cosme C, Hepker M, Hwang J-H, Miller ZA, Huang EJ, Karydas AM, Grant H, Boxer AL, Gorno-Tempini ML,

- Rosen HJ, Kramer JH, Miller BL, Seeley WW, Rabinovici GD, Grinberg LT. 2021. Comorbid neuropathological diagnoses in early versus late-onset Alzheimer's disease. *Brain*. 144:2186–2198.
- Stam CJ. 2014. Modern network science of neurological disorders. *Nature Reviews Neuroscience*. 15:683–695.
- ten Kate M, Barkhof F, Visser PJ, Teunissen CE, Scheltens P, van der Flier WM, Tijms BM. 2017. Amyloid-independent atrophy patterns predict time to progression to dementia in mild cognitive impairment. *Alzheimer's Research & Therapy*. 9:73.
- ten Kate M, Visser PJ, Bakardjian H, Barkhof F, Sikkes SAM, van der Flier WM, Scheltens P, Hampel H, Habert M-O, Dubois B, Tijms BM. 2018. Gray Matter Network Disruptions and Regional Amyloid Beta in Cognitively Normal Adults. *Frontiers in Aging Neuroscience*. 10:1–11.
- Tijms BM, Kate M ten, Wink AM, Visser PJ, Ecay M, Clerigue M, Estanga A, Garcia Sebastian M, Izagirre A, Villanua J, Martinez Lage P, van der Flier WM, Scheltens P, Sanz Arigita E, Barkhof F. 2016. Gray matter network disruptions and amyloid beta in cognitively normal adults. *Neurobiology of Aging*. 37:154–160.
- Tijms BM, ten Kate M, Gouw AA, Borta A, Verfaillie S, Teunissen CE, Scheltens P, Barkhof F, van der Flier WM. 2018. Gray matter networks and clinical progression in subjects with predementia Alzheimer's disease. *Neurobiology of Aging*. 61:75–81.
- Timmler S, Simons M. 2019. Grey matter myelination. *Glia*. 67:2063–2070.
- Tondelli M, Wilcock GK, Nichelli P, de Jager CA, Jenkinson M, Zamboni G. 2012. Structural MRI changes detectable up to ten years before clinical Alzheimer's disease. *Neurobiology of Aging*. 33:825.e25-825.e36.
- Verfaillie SCJ, Slot RE, Tijms BM, Bouwman F, Benedictus MR, Overbeek JM, Koene T, Vrenken H, Scheltens P, Barkhof F, van der Flier WM. 2018. Thinner cortex in patients with subjective cognitive decline is associated with steeper decline of memory. *Neurobiology of Aging*. 61:238–244.
- Verfaillie SCJ, Tijms B, Versteeg A, Benedictus MR, Bouwman FH, Scheltens P, Barkhof F, Vrenken H, van der Flier WM. 2016. Thinner temporal and parietal cortex is related to incident clinical progression to dementia in patients with subjective cognitive decline. *Alzheimer's and Dementia: Diagnosis, Assessment and Disease Monitoring*. 5:43–52.
- Voevodskaya O, Pereira JB, Volpe G, Lindberg O, Stomrud E, van Westen D, Westman E, Hansson O. 2018. Altered structural network organization in cognitively normal individuals with amyloid pathology. *Neurobiology of Aging*. 64:15–24.

- White LR, Edland SD, Hemmy LS, Montine KS, Zarow C, Sonnen JA, Uyehara-Lock JH, Gelber RP, Ross GW, Petrovitch H, Masaki KH, Lim KO, Launer LJ, Montine TJ. 2016. Neuropathologic comorbidity and cognitive impairment in the Nun and Honolulu-Asia Aging Studies. *Neurology*. 86:1000–1008.
- Wirth M, Villeneuve S, Haase CM, Madison CM, Oh H, Landau SM, Rabinovici GD, Jagust WJ. 2013. Associations Between Alzheimer Disease Biomarkers, Neurodegeneration, and Cognition in Cognitively Normal Older People. *JAMA Neurology*. 25:289–313.
- Yu L, Boyle PA, Dawe RJ, Bennett DA, Arfanakis K, Schneider JA. 2020. Contribution of TDP and hippocampal sclerosis to hippocampal volume loss in older-old persons. *Neurology*. 94:e142–e152.
- Yu M, Sporns O, Saykin AJ. 2021. The human connectome in Alzheimer disease — relationship to biomarkers and genetics. *Nature Reviews Neurology*. 17:545–563.





## CHAPTER 2

# **Amyloid- $\beta$ , cortical thickness, and subsequent cognitive decline in cognitively normal oldest-old**

Wiesje Pelkmans, Nienke Legdeur, Mara ten Kate, Frederik Barkhof, Maqsood M. Yaqub, Henne Holstege, Bart N. M. van Berckel, Philip Scheltens, Wiesje M. van der Flier, Pieter Jelle Visser, Betty M. Tijms

*Published in*  
*Annals of Clinical and Translational Neurology, 2021. 8(2) p.348–358. DOI:*  
*10.1002/acn3.51273*

## Abstract

**Objective:** To investigate the relationship between amyloid- $\beta$  ( $A\beta$ ) deposition and markers of brain structure on cognitive decline in oldest-old individuals with initial normal cognition.

**Methods:** We studied cognitive functioning in four domains at baseline and change over time in fifty-seven cognitively intact individuals from the EMIF-AD 90+ study. Predictors were  $A\beta$  status determined by [ $^{18}\text{F}$ ]-flutemetamol PET (normal =  $A\beta^-$  vs. abnormal =  $A\beta^+$ ), cortical thickness in 34 regions and hippocampal volume. Mediation analyses were performed to test whether effects of  $A\beta$  on cognitive decline were mediated by atrophy of specific anatomical brain areas.

**Results:** Subjects had a mean age of  $92.7 \pm 2.9$  years, of whom 19 (33%) were  $A\beta^+$ . Compared to  $A\beta^-$ ,  $A\beta^+$  individuals showed steeper decline on memory ( $\beta \pm \text{SE} = -0.26 \pm 0.09$ ), and processing speed ( $\beta \pm \text{SE} = -0.18 \pm 0.08$ ) performance over 1.5 years ( $p < .05$ ). Furthermore, medial and lateral temporal lobe atrophy was associated with steeper decline in memory and language across individuals. Mediation analyses revealed that part of the memory decline observed in  $A\beta^+$  individuals was mediated through parahippocampal atrophy.

**Interpretation:** These results show that  $A\beta$  abnormality even in the oldest old with initially normal cognition is not part of normal aging, but is associated with a decline in cognitive functioning. Other pathologies may also contribute to decline in the oldest old as cortical thickness predicted cognitive decline similarly in individuals with and without  $A\beta$  pathology.

## Introduction

Even though amyloid- $\beta$  ( $A\beta$ ) plaques are considered the pathological hallmark of Alzheimer's disease (AD; Montine et al. 2012; Jack et al. 2018),  $A\beta$  pathology is observed frequently in cognitively normal (CN) adults. Furthermore, post-mortem and *in vivo* studies have shown that the prevalence of abnormal  $A\beta$  in CN individuals increases with age from 16% at the age of 60, up to 44% of CNs in their 90's (Jansen et al. 2015; Elobeid et al. 2016), illustrative of the complex relationship of  $A\beta$  deposition with cognitive functioning. While previous studies have reported that  $A\beta$  pathology in CN individuals is related to subtle cognitive deficits (Visser et al. 2009; Hedden et al. 2013; Jansen et al. 2018), and an increased risk for cognitive decline and dementia (Vos et al. 2013; Donohue et al. 2017; Ebenau et al. 2020). The relationship of  $A\beta$  pathology and cognitive decline in the oldest-old, i.e. individuals of 90 years and older, is however less clear. Recent longitudinal studies in the oldest-old suggest a steeper cognitive decline in non-demented  $A\beta+$  compared to  $A\beta-$  individuals aged older than 90 (Kawas et al. 2013; Lopez et al. 2014; Zhao et al. 2018), although one study did not find such an association (Balasubramanian et al. 2012). Another driver of cognitive decline is cortical atrophy, in particular medial temporal lobe atrophy, which has been observed frequently in the oldest-old as well (Lopez et al. 2014; Zhao et al. 2018). Medial temporal lobe atrophy is considered a key feature of  $A\beta$  pathology, but in the oldest-old other causes of medial temporal lobe atrophy are common, such as hippocampal sclerosis, cerebrovascular disease, TDP-43 pathology, and aging-related tau astroglipathy (ARTAG; Kawas et al. 2015; Robinson et al. 2018). It still remains unclear how abnormal  $A\beta$  is related to cognitive decline in cognitively normal individuals over age 90 and to what extent such effects are mediated by cortical atrophy. In this study we investigated

if A $\beta$  pathology is associated with cognitive decline in CN oldest-old. Additionally, where this association was present, we further investigated whether the effect of A $\beta$  on cognitive decline was independent or mediated by cortical thickness.

### **Methods**

#### *Participants*

Individuals with normal cognition who underwent an amyloid positron emission tomography (PET) were selected from the Innovative Medicine Initiative European Medical Information Framework for AD (EMIF-AD) 90+ Study conducted at the Amsterdam University Medical Center (UMC). Individuals were recruited through general practitioners or via advertisements, see Legdeur et al. (2018) for detailed description of this cohort and overall study design. Normal cognition was defined as a Clinical Dementia Rating (CDR) score of zero, and a Mini-Mental State Examination (MMSE) score of  $\geq 26$ .

#### *MRI acquisition and processing*

3D-T1 weighted and 3D sagittal fluid-attenuated inversion recovery (FLAIR) images were acquired on a Philips 3T Achieva scanner using an 8-channel head coil and a sagittal turbo gradient-echo sequence (T1: 1.00 mm<sup>3</sup> isotropic voxels, repetition time (TR) = 7.9 ms, echo time (TE) = 4.5 ms, flip angle (FA) = 8 degrees; FLAIR: 1.12 mm<sup>3</sup> isotropic voxels, TR = 4800 ms, TE = 279 ms, and inversion time = 1650 ms). Cortical thickness was estimated from 3D T1 MRI using FreeSurfer (v5.3; <https://surfer.nmr.mgh.harvard.edu>). Non-brain tissue was removed, followed by transformation to MNI space, segmentation and creation of cortical surface meshes (Fischl 2012). The cortical thickness values were

summarized in anatomical regions according to the Desikan–Killiany atlas implemented in FreeSurfer. To reduce dimensionality of the data we averaged cortical thickness values for each brain region across hemispheres, resulting in 34 cortical regions of interest (ROIs). Hippocampal volume was obtained with FMRIB's Software Library (FSL) FIRST (v5.0.1), as reported previously in Patenaude et al. (2011). White matter hyperintensities (WMH) segmentation was performed using a previously established algorithm based on a three-level Gaussian mixture model to model healthy tissues and lesions (Sudre et al. 2015). Because of a skewed distribution, WMH volume was log transformed. Resulting images were visually checked for quality, and data from four subjects had to be excluded due to gross registration or segmentation errors.

### *Amyloid PET*

Dynamic [ $^{18}\text{F}$ ] flutemetamol amyloid-PET scans were performed on a Philips Ingenuity TF PET-MRI scanner (Philips Medical Systems, Cleveland, Ohio, USA). The tracer was produced by General Electric (GE) Healthcare at the Cyclotron Research Center of the University of Liège (Liège, Belgium). First, a 30 min dynamic emission scan was started simultaneously with a bolus intravenous injection of 185 MBq [ $^{18}\text{F}$ ] flutemetamol. The second part of the scan was performed from 90 to 110 min post injection. Immediately prior to each part of the PET scan a dedicated MR sequence was performed for attenuation correction. During scanning, the head was immobilized to reduce movement artifacts. Data from the two scan parts were coregistered and combined into a single 4D image using VINCI Software 2.56 (<https://vinci.sf.mpg.de>) and in-house built software for decay correction of the second part. Parametric nondisplaceable binding potential ( $\text{BP}_{\text{ND}}$ ) images were generated from the entire image set using the receptor

parametric mapping and cerebellar grey matter as reference tissue (Gunn et al. 1997; Wu and Carson 2002). Global cortical  $BP_{ND}$  was calculated as the volume weighted average  $BP_{ND}$  of 22 regions located within frontal, parietal, temporal, posterior cingulate, and medial temporal lobes (Tolboom et al. 2009). Dynamic  $BP_{ND}$  images were used for visual assessment of [ $^{18}F$ ] flutemetamol as negative ( $A\beta^-$ ) or positive ( $A\beta^+$ ) by the consensus of three readers, who had been trained according to the manufacturers image interpretation methodology and were blinded to the clinical and demographic data (Collij et al. 2019).

### *Neuropsychological assessment*

A trained neuropsychologist administered cognitive tests within the following cognitive domains: memory, language, processing speed, and executive functioning. For each cognitive domain, tests were combined into a composite score. For memory we included the CERAD 10 words test (delayed recall; Morris et al. 1989), the Wechsler Logical Memory Test (delayed recall; Wechsler et al. 2009), the Rey Complex Figure Test (delayed copy; Meyers et al. 1996), and the Visual Association Test A (Lindeboom et al. 2002). For language, we used the 2-minute Animal Fluency score (Zhao et al. 2013), and the Graded Naming Test (McKenna and Warrington 1980). For processing speed, we included the Digit Symbol Substitution Test from the Wechsler Adult Intelligence Scale-Revised (WAIS-R; Wechsler 1981), the Trail Making Test A (Reitan 1958), and the WAIS-III Digit span forward (Wilde and Strauss 2002). For executive functioning we included the Trail Making Test B (Reitan 1958), the WAIS-III Digit span backward (Wilde and Strauss 2002), Letter Fluency (one minute per letter, three letters; Zhao et al. 2013), and the Clock drawing test (Teunisse et al. 1991). For a subset ( $n = 43$ ; 75.4%), neuropsychological tests were repeated once circa 1.5 years

(1.0y – 2.8y) after baseline assessment. For each test we calculated Z-scores using the baseline mean and standard deviation of the total group. We created composite scores by averaging test Z-scores for each cognitive domain. Trail Making Test A & B scores were inverted so that for all cognitive tests lower scores indicated worse performance.

### *APOE genotyping*

For all participants, blood samples were collected for DNA analysis. DNA was extracted using the QIAamp® DNA Blood Mini Kit (QIAGEN GmbH, Hilden, Germany). Apolipoprotein e (APOE) genotype was determined using TaqMan assays (ThermoFisher Scientific, Foster City, CA, USA) on a QuantStudio-12 K-Flex system. We classified individuals as APOE ε4 carriers or non-carriers according to their genotype status at rs429358. For three participants, APOE data was missing.

### *Statistical analysis*

We compared demographical characteristics of the Aβ<sup>-</sup> and Aβ<sup>+</sup> groups using  $\chi^2$  tests for categorical variables and ANOVA for continuous variables. We ran four linear mixed models (LMM) with subject specific intercepts, and fixed slopes: Model 1 tested the effect of baseline Aβ status on cognitive decline with cognitive domain score as the outcome (*Model 1: Cognition ~ Time \* Aβ*). Model 2 tested the effect of Aβ status on cortical thickness of all FreeSurfer ROIs and on hippocampal volume (*Model 2: ROI ~ Aβ*). Model 3 tested the effect of cortical thickness and hippocampal volume on cognitive decline (*Model 3: Cognition ~ Time \* ROI*). Model 4 tested the combined the effects of Aβ pathology, cortical thickness, and their interactions with each other on cognitive decline (*Model 4: Cognition ~ Time \* ROI \* Aβ*). Interaction terms were removed when not significant ( $p > .05$ ). All models included sex,

education, WMH, and age as covariates, and for hippocampal volume, total intracranial volume was added as a covariate. LMM were corrected for multiple testing using a false discovery rate (FDR) procedure (Benjamini and Yekutieli 2001). Effects that did not survive FDR correction are shown as  $p_{uncorrected}$ .

When A $\beta$  status was significantly associated with both cognitive decline and thickness and/or volume in certain ROIs, we performed causal mediation analyses to assess whether the association between A $\beta$  status and cognitive decline was mediated by grey matter brain atrophy. Mediation analyses provides us with a better understanding of the complex pathways of A $\beta$  deposition towards cognitive decline. To estimate the average causal mediation effect three linear models were fitted: the first model has cognitive decline as the outcome of interest as the dependent variable and thickness/volume as predictor, while controlling for A $\beta$ ; the second model that has the mediator variable thickness/volume as the dependent variable and A $\beta$  status as predictor; the third model averages direct and indirect effects of A $\beta$  status on cognitive decline and are estimated based on the quasi-Bayesian Monte Carlo approximation (1000 simulations). Mediation analyses was performed only in individuals who had repeated assessment of cognitive function ( $n = 43$ ). Finally, we further investigated the effect of other factors known to be associated with cognitive decline, including APOE  $\epsilon 4$  genotype, education, and vascular damage. Statistical analyses were performed in R (v4.0.2) using the “lme4” package (v1.1), “mediation” package (v4.5; Tingley et al. 2014), and group estimates were obtained using the “emmeans” package (v1.5).



## Results

### Demographics

Participants ( $n = 57$ ) had an average age of 92.7 years, ranging from 88-102 years, were more often female (63%), and 33% had a visually rated abnormal amyloid PET scan (Table 1). The A $\beta$ + ( $n=19$ ) and A $\beta$ - ( $n=38$ ) groups did not differ in age, sex, APOE  $\epsilon$ 4 carriership, vascular burden, or years of education. Moreover, the two groups did not differ in availability of follow-up data, nor the time between test assessments. More years of education was associated with better performance on tests related to processing speed, executive functioning, and less steep decline in memory and executive functioning over time ( $p_{FDR}<.05$ ; Supplementary Table 3). Higher WMH volumes were associated with worse performance on language, processing speed, and faster decline on memory ( $p_{FDR}<.05$ ). No association between age, sex, or APOE  $\epsilon$ 4 carriership and cognitive performance or cognitive decline was observed.

**Table 1. Subject characteristics according to A $\beta$  status.**

	A $\beta$ - ( $n = 38$ )	A $\beta$ + ( $n = 19$ )	Total ( $n = 57$ )	<i>p</i> -value
Sex, f (%)	23 (60.5)	13 (68.4)	36 (63.2)	.771
Age, (y)	92.51 (3.13)	93.00 (2.56)	92.67 (2.94)	.554
Education, (y)	12.78 (4.53)	11.50 (4.30)	12.35 (4.46)	.312
A $\beta$ load (BPND)	0.15 (0.12)	0.56 (0.28)	0.29 (0.27)	<.001*
APOE $\epsilon$ 4 carrier (%)	2 (5.7)	3 (16.7)	5 (9.4)	.426
WMH volume	9.59 (0.89)	9.71 (0.94)	9.63 (0.90)	.635
T0 – T1 difference, (y)	1.57 (0.57)	1.82 (0.64)	1.66 (0.60)	.191
T1 availability (%)	27 (71.1)	16 (84.2)	43 (75.4)	.446
Deceased at T1 (%)	10 (26.3)	2 (10.5)	12 (21.1)	.301

Data are presented as mean (SD), or n (%). A $\beta$  = amyloid- $\beta$ ; BPND = nondisplaceable binding potential; APOE = apolipoprotein e; WMH = White matter hyperintensities (log); T0 = baseline; T1 = follow-up;  $p<0.05$ .

### *Associations of amyloid status and cortical thickness with cognitive decline*

First, we tested the effects of A $\beta$  status on cognitive decline over time (Model 1). At baseline, A $\beta$ + individuals tended to show worse performance on memory and language, although this did not reach significance (Fig. 1). Over time, A $\beta$ + individuals showed steeper decline in memory ( $\beta \pm SE = -0.26 \pm 0.09$ ), and processing speed ( $\beta \pm SE = -0.18 \pm 0.08$ ) than A $\beta$ - individuals ( $p_{uncorrected} < .05$ ; Fig. 1). Also, a steeper decline in language performance ( $\beta \pm SE = -0.15 \pm 0.08$ ) was observed at trend level (Supplementary Table 1a).

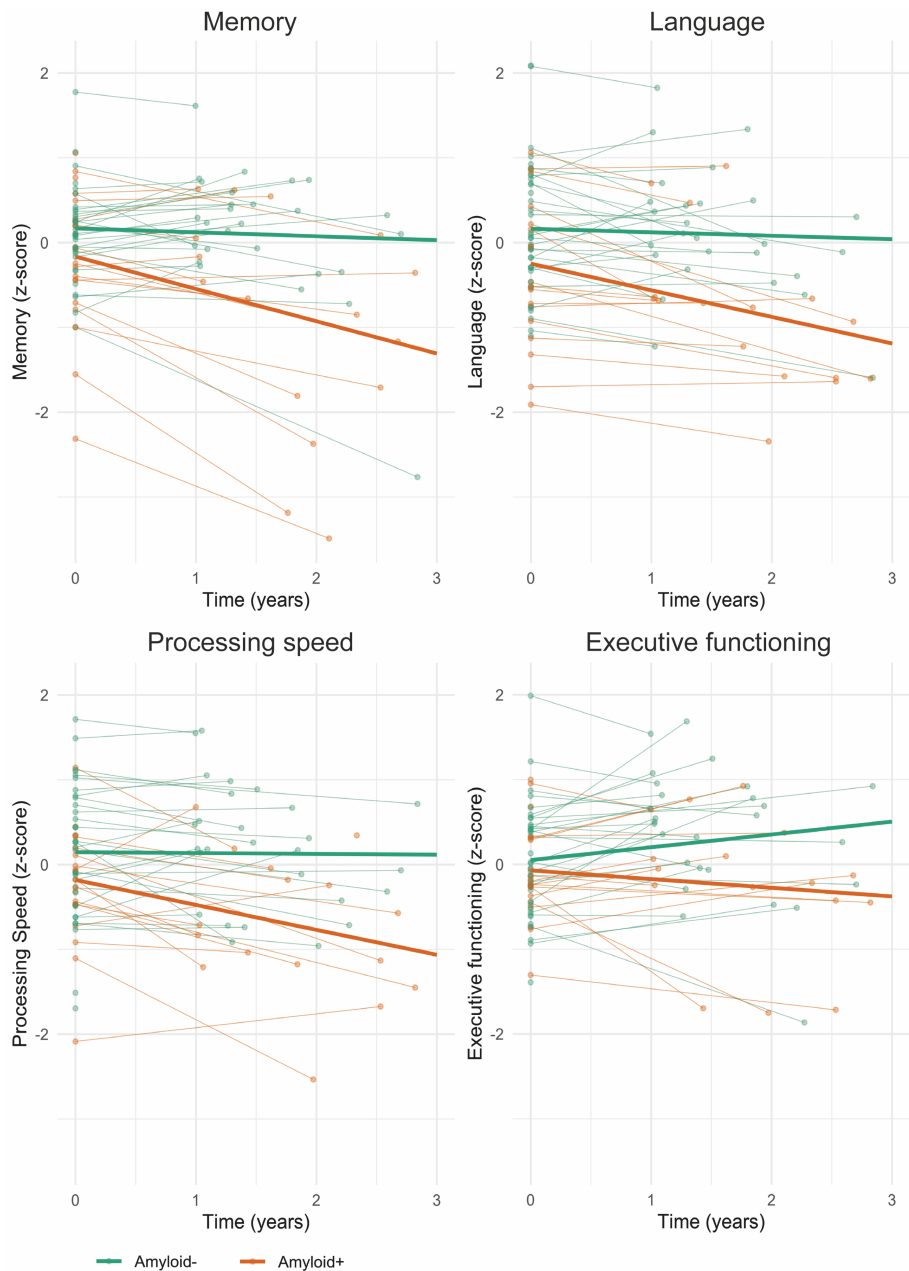


**Figure 1. Cognitive performance over time in relation to A $\beta$  status.**

Spaghetti plots showing individual longitudinal change on memory, language, processing speed, and executive performance according to A $\beta$  status (Amyloid- is normal A $\beta$ ; Amyloid+ is abnormal A $\beta$ ). All scores were z-scored and for processing speed and executive functioning inverted such that lower scores indicate worse impairment.

Next, we tested effects of A $\beta$  status on cortical thickness (Model 2). Individuals with A $\beta$ + showed thinner parahippocampal cortex and a thinner medial orbitofrontal cortex compared to A $\beta$ - individuals ( $p_{uncorrected} < .05$ ; Fig. 2). Hippocampal volume did not differ between A $\beta$ - and A $\beta$ + individuals (Supplementary Table 1c). Then we studied effects of cortical thickness on cognitive decline over time (Model 3). A thinner cortex in predominantly anterior cingulate and multiple lateral temporal regions, including the entorhinal, parahippocampal, fusiform, and superior temporal cortex, was associated with a steeper decline in memory ( $p_{FDR} < .05$ ; Fig. 3), with no interaction effects of A $\beta$  status. In addition, smaller hippocampal volume was associated with worse memory and processing speed performance at baseline and a faster decline in memory over time ( $p_{uncorrected} < .05$ ), independent of A $\beta$  status. Moreover, thinner superior frontal and lateral temporal regions, including the fusiform, inferior and superior temporal, posterior cingulate, and supramarginal cortex, were associated with a steeper decline in language performance ( $p_{uncorrected} < .05$ ), of which only the posterior cingulate cortex survived the correction for multiple comparisons. Additionally, a few cortical regions showed that thicker cortex was associated with a steeper decline in executive functioning ( $p_{uncorrected} < .05$ ; Fig. 3).

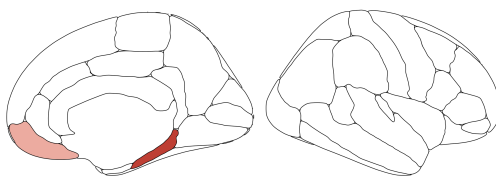


**Figure 2. Amyloid associations with regional cortical thickness.** Betas are provided for regions with thinner cortex in abnormal A $\beta$  individuals compared to normal A $\beta$  individuals at  $p_{uncorrected} < .05$ .

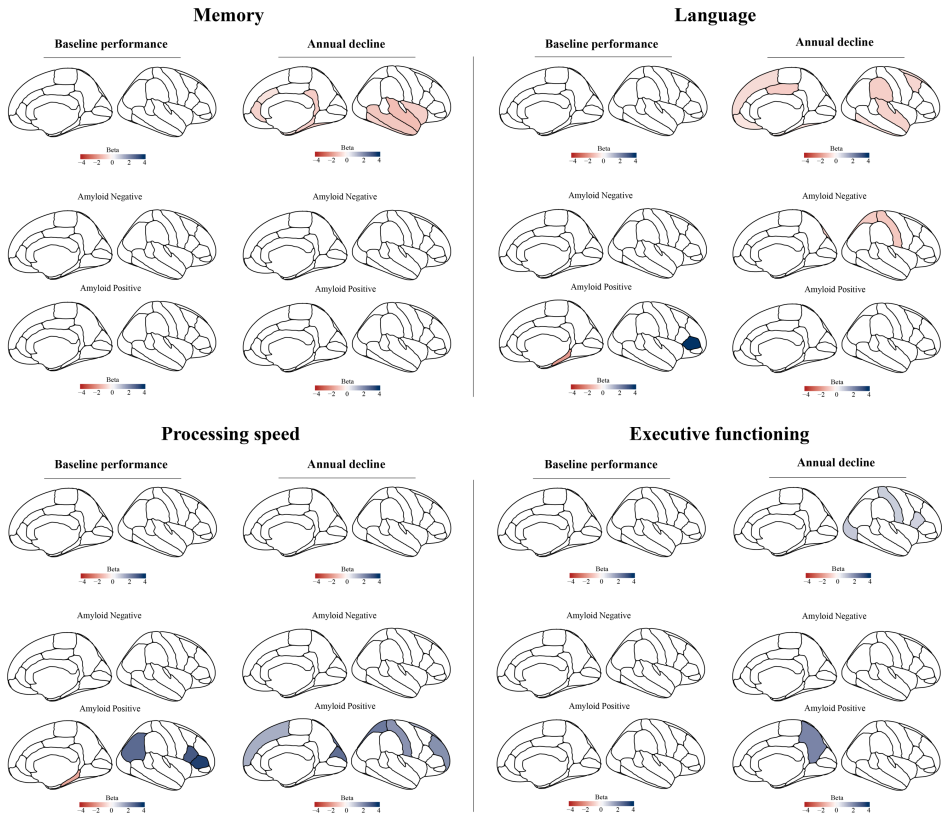


**Figure 3. Associations of cortical thickness with baseline and decline in cognitive functioning, by A $\beta$  status.** Effect of cortical thickness on baseline (left) and annual change (right) on memory, language, processing speed, and executive functioning across all subjects and by A $\beta$  status. **Top left:** thinner caudal\* and rostral\* anterior cingulate, entorhinal\*, fusiform\*, inferior, superior\* and middle\* temporal, insula\*, isthmus cingulate, parahippocampal\*, and temporal pole\* was associated with a faster decline in memory. **Top right:** thinner caudal middle frontal, entorhinal, fusiform, inferior and superior temporal, medial orbitofrontal, posterior cingulate\*, superior frontal, and supramarginal cortex was associated with faster decline in language. A $\beta$ + individuals with thinner pars triangularis and parahippocampal cortex showed worse language performance compared to A $\beta$ - individuals. A $\beta$ - individuals with thinner postcentral and a superior parietal cortex showed faster decline in language performance compared to A $\beta$ + individuals. **Bottom left:** A $\beta$ + individuals with thinner parahippocampal and a thicker inferior parietal, pars triangularis, pars opercularis showed worse processing speed performance compared to A $\beta$ - individuals. A $\beta$ + individuals with thicker cuneus, frontal pole, postcentral, rostral middle frontal, superior frontal, and superior parietal cortex showed a faster decline on processing speed compared to A $\beta$ - individuals. **Bottom right:** thicker lateral occipital, pars opercularis, and postcentral regions were associated with faster decline in executive functioning. A $\beta$ + individuals with thicker precuneus showed a faster decline in executive functioning compared to A $\beta$ - individuals. Beta estimates in red indicate thinner cortex is associated with steeper decline on cognitive test

score, blue indicates a thicker cortex is associated with steeper decline on cognitive test score. Data are presented for regions significant with an uncorrected  $p$ -value  $< 0.05$ . \*Indicates region significant at  $p_{\text{FDR}} < 0.05$ .

Finally, we examined the interactions of A $\beta$  status and brain structure measures on the rate of cognitive decline (Model 4). A $\beta$ + individuals with a thinner parahippocampal and a thicker pars triangularis ( $\beta \pm \text{SE} = 1.90 \pm 0.91$ ;  $\beta \pm \text{SE} = 4.04 \pm 1.87$ ;  $p_{\text{uncorrected}} < .05$ ; Fig. 3) showed worse language performance. While also thinner postcentral and superior parietal cortex ( $\beta \pm \text{SE} = 1.01 \pm 0.37$ ;  $\beta \pm \text{SE} = 0.94 \pm 0.36$ ;  $p_{\text{uncorrected}} < .05$ ) was associated with faster language decline in A $\beta$ - individuals. Furthermore, we observed that thicker cortex in occipital and parietal regions was associated with slower processing speed and steeper decline over time in A $\beta$ + individuals ( $p_{\text{uncorrected}} < .05$ ; Fig. 3; see supplementary Table 1 for full LMM results). We repeated all analyses excluding  $n = 12$  individuals that passed away before the second neuropsychological assessment took place, and observed overall largely similar results (see supplementary Table 2).

### *Mediation analyses*

Next, we investigated whether the effect of A $\beta$  pathology on cognitive performance was mediated by cortical thickness (indirect effect) or not (independent effect) for cortical regions that were associated with abnormal A $\beta$  (i.e., parahippocampal gyrus and medial orbitofrontal cortex). Memory decline associated with A $\beta$ + was fully mediated by parahippocampal thinning (36.4%;  $p < .05$ ; Fig. 4). Decline in language performance associated with A $\beta$ + was partially mediated by parahippocampal thinning (21.6%;  $p < .05$ ), and partially independent (78.4%  $p < .05$ ) after controlling for the presence of parahippocampal atrophy. The effect of A $\beta$  on decline in processing speed, and executive functioning were independent of

parahippocampal thickness. Moreover,  $A\beta$  associated cognitive decline was independent of medial orbitofrontal thickness for all cognitive domains ( $p < .05$ ; Fig. 4).

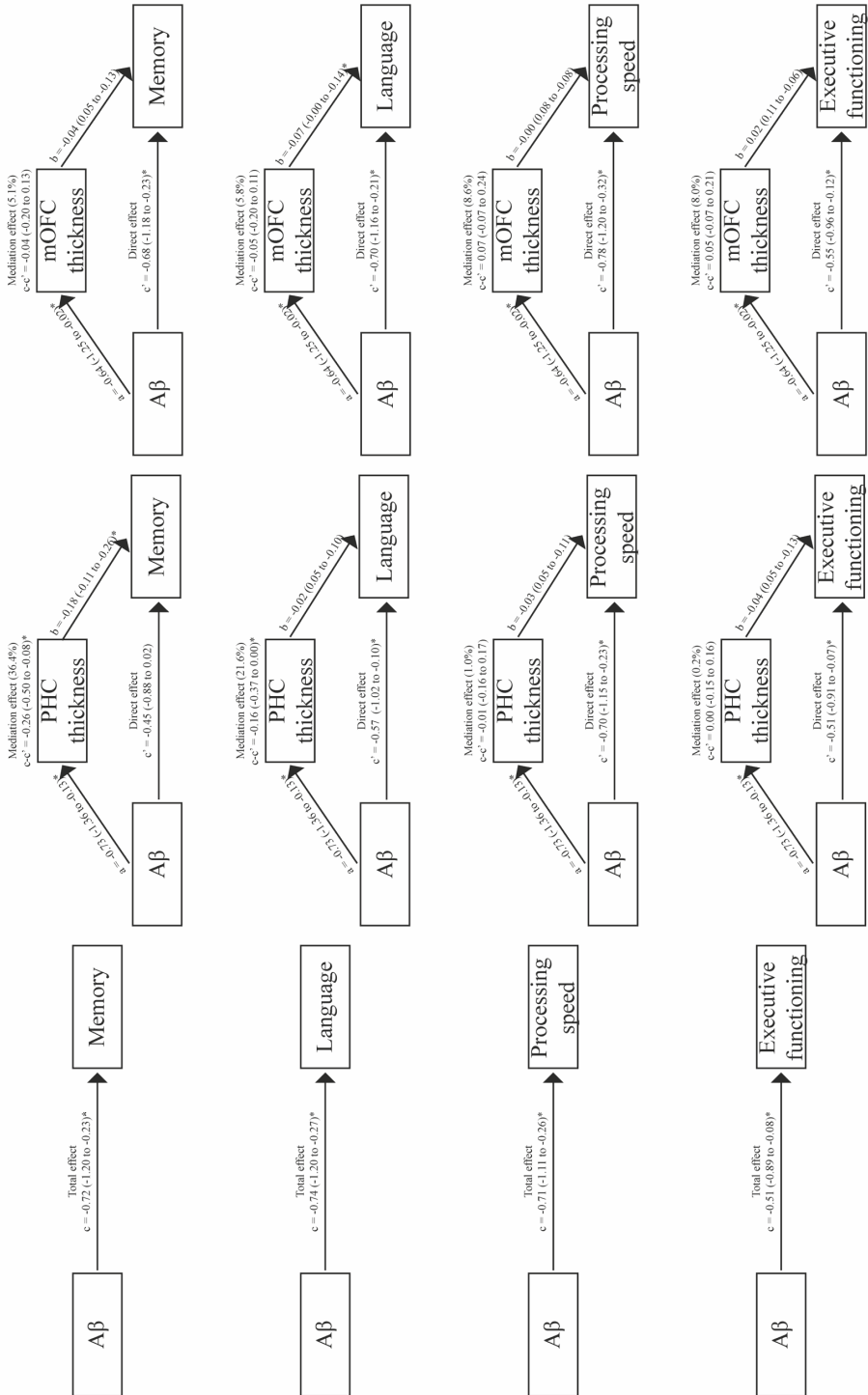




**Figure 4. Mediation analysis showing how cortical thinning mediates the effect of A $\beta$  on longitudinal decline in cognitive functioning.** The total effect of A $\beta$  on memory, language, processing speed, and executive functioning over time (left). Mediation effect of A $\beta$  through PHC thickness on memory, language, processing speed, and executive functioning over time (middle). Mediation effect of A $\beta$  through mOFC thickness on memory, language, processing speed, and executive functioning over time (right). The figure shows regression coefficients with a 95% confidence interval. a, the effect of A $\beta$  on cortical thickness; b, the effect of cortical thickness on cognitive decline when controlling for A $\beta$ ; c, the total effect of A $\beta$  on cognitive decline (without controlling for mediation effects); c', the direct effect of A $\beta$  on cognitive decline when adjusting for mediation; c-c', the mediation effect. \* =  $p < .05$ ; A $\beta$  = amyloid-beta; PHC = parahippocampal cortex; mOFC = medial orbitofrontal cortex.

## Discussion

In this study of oldest-old with initially intact cognition, we found that abnormal A $\beta$  was associated with steeper decline in memory and processing speed performance over 1.5 years. Our findings support the notion that both A $\beta$  pathology and brain atrophy have detrimental effects on cognitive functioning among cognitively normal individuals that are separate from normal ageing. These results suggest that A $\beta$  abnormality is indicative of a neurodegenerative process, that also in the oldest-old with apparent high reserve and maintenance mechanisms lead to cognitive decline. In addition, non-A $\beta$  pathologies may also contribute to decline in the oldest-old as a thinner medial and lateral temporal cortex was related to subsequent decline in memory and language irrespective of A $\beta$  pathology, indicating that other, possibly A $\beta$  independent pathological processes might also be involved in cognitive decline in the oldest-old.

Numerous studies have reported on the role of A $\beta$  pathology in very early cognitive decline (Petersen et al. 2016; Bilgel et al. 2018; Clark et al. 2018), and we further extend on those findings by showing that the detrimental effect of A $\beta$  is also present in nonagenarians with initially intact cognition. Our baseline results are in line with other cross-sectional data showing only a subtle effect of A $\beta$  pathology in preclinical AD on cognition

(Hedden et al. 2013; Jansen et al. 2018; Legdeur, Tijms, et al. 2019), consistent with the hypothesis that changes in cognition occur relatively late in the AD pathophysiological cascade. Over time, the differences between A $\beta$ + and A $\beta$ - individuals became larger, as the A $\beta$ + subjects showed steeper decline on memory as reported previously (Storandt et al. 2009; Snitz et al. 2013), and also in the processing speed domain.

Furthermore, at baseline A $\beta$ + individuals showed thinner cortex in parahippocampal and orbitofrontal regions compared to A $\beta$ -, consistent with other work in CN individuals demonstrating a relationship between A $\beta$  and reduced grey matter (Becker et al. 2011; Doré et al. 2013; Doherty et al. 2015; van Bergen et al. 2018). However, while previously hippocampal atrophy has been closely related to memory functioning and shown to be a strong and early predictor of conversion to dementia (Mormino et al. 2009; Huijbers et al. 2015; Legdeur, Visser, et al. 2019), we observed no differences between A $\beta$ + and A $\beta$ - individuals in hippocampal volume. Possibly, other pathological factors, such as hippocampal sclerosis, TDP-43 pathology, ARTAG, argyrophilic grain disease (AGD), primary age-related tauopathy (PART), and cerebrovascular disease, may contribute to atrophy in these regions, which at old ages become increasingly more common (Beach et al. 2012; Kawas et al. 2015; Robinson et al. 2018).

Such pathologies may also explain our observation that thinner medial and lateral temporal cortex was associated with subsequent decline in memory and language regardless of A $\beta$  status. Associations of decreased grey matter volume in temporal, frontal, and parietal regions with progression to dementia have been demonstrated in individuals without A $\beta$  (Verfaillie et al. 2016; ten Kate et al. 2017). Selective sparing of these cortical regions, most notably the anterior cingulate cortex and medial temporal lobe, is frequently reported in superagers compared to age-matched

controls and has been associated with resilience to cognitive decline (Harrison et al. 2018; Arenaza-Urquijo et al. 2019; de Godoy et al. 2020). Whether the oldest-old with good cognitive health in the present study are protected by relatively preserved cortical regions is unknown from the present analyses without a control group, however the anterior cingulate and medial temporal thickness were still negatively associated with cognition.

Mediation analyses indicated that cortical regions that were associated with abnormal A $\beta$  (i.e., parahippocampal gyrus and medial orbitofrontal cortex) partly mediated the effects of A $\beta$  on downstream memory and language decline. A $\beta$  no longer had a significant association with memory performance over time when parahippocampal thickness was included in the mediation model, supporting that the structural integrity of the parahippocampal gyrus is important for memory functioning (Köhler et al. 1998; Ward et al. 2014). A finding that might be related to the commonly observed neurofibrillary tangle pathology in the medial temporal lobe in CN adults (Braak and Braak 1991). No significant mediation of cortical thickness was observed for the other cognitive domains, indicative of a direct effect of A $\beta$  pathology on cognitive decline.

Another finding we observed, which did not survive correction for multiple comparisons, was that thicker parietal cortices in A $\beta$ + individuals were associated steeper decline in processing speed. This finding was unexpected, as usually cortical thinning is a sign of neuronal loss. It is unclear what such thicker cortex may reflect. Possibly, as this effect was only observed in abnormal A $\beta$ , it might reflect a tissue reactive response to A $\beta$  pathology, as previous studies have shown a positive correlation of microglial activation and A $\beta$  deposition (Meyer-Luehmann et al. 2008). Microglial activation in preclinical disease stages has been associated with

initially preserved or increased brain volume (Hamelin et al. 2016; Femminella et al. 2019). Still, it has to be noted that the number of A $\beta$ + subjects in this study was small, and requires replication in larger samples. Further repeated MRI studies are needed to investigate whether these brain areas may show thinning at a later point in time.

Furthermore, we investigated the influence of APOE genotype on cognitive decline, which is considered the major genetic risk factor for sporadic AD (Corder et al. 1993). Carriership of the  $\epsilon$ 4 allele has been associated with the presence and lower age of onset of A $\beta$  deposits, and A $\beta$ -associated cognitive decline (Jansen et al. 2015; Yamazaki et al. 2019). The underrepresentation of  $\epsilon$ 4-carriers in our sample (9.4%), might have contributed to the intact cognition at a very high age in these individuals, and to the absence of an association between APOE $\epsilon$ 4 carriership and cognitive decline as well. An interesting next step may lie in investigating factors associated with cognitive resilience among the oldest-old who are APOE  $\epsilon$ 4 carriers.

There are some limitations to our study. Subjects only underwent an MRI and PET scan at baseline, and cognitive decline was based on cognitive assessments at two time points on average 1.5 years apart. Future studies with longer follow-up will aid in determining the temporal ordering of the changes in brain structure and cognitive impairments. Also, the relatively small number of individuals with abnormal amyloid might have resulted in limited statistical power to detect differences that are expected to be subtle in individuals who have initially intact cognition, which is also reflected by the notion that only a few relationships survived correction for multiple testing, and uncorrected results should be interpreted with caution. Furthermore, information on tau levels was unavailable in our sample, and so, it remains unknown to what extent effects of A $\beta$  on cortical thinning and

cognitive decline was influenced by tau pathology. Previous studies suggest that the presence of abnormal tau biomarkers, the other pathological hallmark of AD, is related to worse cognitive functioning in the presence of A $\beta$  (Vos et al. 2013), and increases with age (Elobeid et al. 2016; Lowe et al. 2018). Therefore, future studies measuring tau pathology using CSF or PET in this age group could contribute to a better understanding of the complex A $\beta$  and tau interaction, and their associations with cognition. Strengths of our study include the extensive phenotyping of a longitudinal cohort of oldest-old individuals with maintained cognitive health.

In conclusion, our findings contribute to our understanding of the role of A $\beta$  deposition on cognitive decline in the oldest-old, and suggest that also at very high ages A $\beta$  abnormality is not benign.

### **Acknowledgements**

This work has received support from the EU/EFPIA Innovative Medicines Initiative Joint Undertaking (EMIF grant No. 115372) and received kind sponsoring of the PET-tracer [ $^{18}\text{F}$ ]flutemetamol from GE Healthcare.

## References

- Arenaza-Urquijo EM, Przybelski SA, Lesnick TL, Graff-Radford J, Machulda MM, Knopman DS, Schwarz CG, Lowe VJ, Mielke MM, Petersen RC, Jack CR, Vemuri P. 2019. The metabolic brain signature of cognitive resilience in the 80+: beyond Alzheimer pathologies. *Brain*. 142:1134–1147.
- Balasubramanian AB, Kawas CH, Peltz CB, Brookmeyer R, Corrada MM. 2012. Alzheimer disease pathology and longitudinal cognitive performance in the oldest-old with no dementia. *Neurology*. 79:915–921.
- Beach TG, Monsell SE, Phillips LE, Kukull W. 2012. Accuracy of the Clinical Diagnosis of Alzheimer Disease at National Institute on Aging Alzheimer Disease Centers, 2005–2010. *Journal of Neuropathology & Experimental Neurology*. 71:266–273.
- Becker JA, Hedden T, Carmasin J, Maye J, Rentz DM, Putcha D, Fischl B, Greve DN, Marshall GA, Salloway S, Marks D, Buckner RL, Sperling RA, Johnson KA. 2011. Amyloid- $\beta$  associated cortical thinning in clinically normal elderly. *Annals of Neurology*. 69:1032–1042.
- Benjamini Y, Yekutieli D. 2001. The control of the false discovery rate in multiple testing under dependency. *The Annals of Statistics*. 29:1165–1188.
- Bilgel M, An Y, Hephrey J, Elkins W, Gomez G, Wong DF, Davatzikos C, Ferrucci L, Resnick SM. 2018. Effects of amyloid pathology and neurodegeneration on cognitive change in cognitively normal adults. *Brain*. 141:2475–2485.
- Braak H, Braak E. 1991. Neuropathological staging of Alzheimer-related changes. *Acta Neuropathologica*. 82:239–259.
- Clark LR, Berman SE, Norton D, Kosciak RL, Jonaitis E, Blennow K, Bendlin BB, Asthana S, Johnson SC, Zetterberg H, Carlsson CM. 2018. Age-accelerated cognitive decline in asymptomatic adults with CSF  $\beta$ -amyloid. *Neurology*. 90:e1306–e1315.
- Collij LE, Konijnenberg E, Reimand J, Kate M ten, Braber A den, Alves IL, Zwan M, Yaqub M, van Assema DME, Wink AM, Lammertsma AA, Scheltens P, Visser PJ, Barkhof F, van Berckel BNM. 2019. Assessing Amyloid Pathology in Cognitively Normal Subjects Using 18 F-Flutemetamol PET: Comparing Visual Reads and Quantitative Methods. *Journal of Nuclear Medicine*. 60:541–547.
- Corder EH, Saunders AM, Strittmatter WJ, Schmechel DE, Gaskell PC, Small GW, Roses AD, Haines JL, Pericak-Vance MA. 1993. Gene Dose of Apolipoprotein E Type 4 Allele and the Risk of Alzheimer ' s Disease in Late Onset Families. *Science* (1979). 261:921–923.
- de Godoy LL, Alves CAPF, Saavedra JSM, Studart-Neto A, Nitrini R, da Costa Leite C, Bisdas S. 2020. Understanding brain resilience in superagers: a systematic review. *Neuroradiology*.

- Doherty BM, Schultz SA, Oh JM, Kosciak RL, Dowling NM, Barnhart TE, Murali D, Gallagher CL, Carlsson CM, Bendlin BB, LaRue A, Hermann BP, Rowley HA, Asthana S, Sager MA, Christian BT, Johnson SC, Okonkwo OC. 2015. Amyloid burden, cortical thickness, and cognitive function in the Wisconsin Registry for Alzheimer's Prevention. *Alzheimer's & Dementia: Diagnosis, Assessment & Disease Monitoring*. 1:160–169.
- Donohue MC, Sperling RA, Petersen R, Sun CK, Weiner M, Aisen PS. 2017. Association between elevated brain amyloid and subsequent cognitive decline among cognitively normal persons. *JAMA - Journal of the American Medical Association*. 317:2305–2316.
- Doré V, Villemagne VL, Bourgeat P, Fripp J, Acosta O, Chetelat G, Zhou L, Martins R, Ellis KA, Masters CL, Ames D, Salvado O, Rowe CC. 2013. Cross-sectional and Longitudinal Analysis of the Relationship Between A $\beta$  Deposition, Cortical Thickness, and Memory in Cognitively Unimpaired Individuals and in Alzheimer Disease. *JAMA Neurology*. 70:903.
- Ebenau JL, Timmers T, Wesselman LMP, Verberk IMW, Verfaillie SCJ, Slot RER, van Harten AC, Teunissen CE, Barkhof F, van den Bosch KA, van Leeuwenstijn M, Tomassen J, Braber A den, Visser PJ, Prins ND, Sikkes SAM, Scheltens P, van Berckel BNM, van der Flier WM. 2020. ATN classification and clinical progression in subjective cognitive decline. *Neurology*. 95:e46–e58.
- Elobeid A, Libard S, Leino M, Popova SN, Alafuzoff I. 2016. Altered Proteins in the Aging Brain. *Journal of Neuropathology and Experimental Neurology*. 75:316–325.
- Femminella GD, Dani M, Wood M, Fan Z, Calsolaro V, Atkinson R, Edginton T, Hinz R, Brooks DJ, Edison P. 2019. Microglial activation in early Alzheimer trajectory is associated with higher gray matter volume. *Neurology*. 92:e1331–e1343.
- Fischl B. 2012. FreeSurfer. *Neuroimage*. 62:774–781.
- Gunn RN, Lammertsma AA, Hume SP, Cunningham VJ. 1997. Parametric Imaging of Ligand-Receptor Binding in PET Using a Simplified Reference Region Model. *Neuroimage*. 6:279–287.
- Hamelin L, Lagarde J, Dorothée G, Leroy C, Labit M, Comley RA, de Souza LC, Corne H, Dauphinot L, Bertoux M, Dubois B, Gervais P, Colliot O, Potier MC, Bottlaender M, Sarazin M. 2016. Early and protective microglial activation in Alzheimer's disease: a prospective study using 18 F-DPA-714 PET imaging. *Brain*. 139:1252–1264.
- Harrison TM, Maass A, Baker SL, Jagust WJ. 2018. Brain morphology, cognition, and  $\beta$ -amyloid in older adults with superior memory performance. *Neurobiology of Aging*. 67:162–170.
- Hedden T, Oh H, Younger AP, Patel TA. 2013. Meta-analysis of amyloid-cognition relations in cognitively normal older adults. *Neurology*. 80:1341–1348.

- Huijbers W, Mormino EC, Schultz AP, Wigman S, Ward AM, Larvie M, Amariglio RE, Marshall GA, Rentz DM, Johnson KA, Sperling RA. 2015. Amyloid- $\beta$  deposition in mild cognitive impairment is associated with increased hippocampal activity, atrophy and clinical progression. *Brain*. 138:1023–1035.
- Jack CR, Bennett DA, Blennow K, Carrillo MC, Dunn B, Haeberlein SB, Holtzman DM, Jagust W, Jessen F, Karlawish J, Liu E, Molinuevo JL, Montine T, Phelps C, Rankin KP, Rowe CC, Scheltens P, Siemers E, Snyder HM, Sperling R, Elliott C, Masliah E, Ryan L, Silverberg N. 2018. NIA-AA Research Framework: Toward a biological definition of Alzheimer's disease. *Alzheimer's and Dementia*. 14:535–562.
- Jansen WJ, Ossenkuppele R, Knol DL, Tijms BM, Scheltens P, Verhey FRJJ, Visser PJ, Aalten P, Aarsland D, Alcolea D, Alexander M, Almdahl IS, Arnold SE, Baldeiras II, Barthel H, van Berckel BNMM, Bibeau K, Blennow K, Brooks DJ, van Buchem MA, Camus V, Cavedo E, Chen K, Chetelat G, Cohen AD, Drzezga A, Engelborghs S, Fagan AM, Fladby T, Fleisher AS, van der Flier WM, Ford L, Forster S, Fortea J, Foskett N, Frederiksen KS, Freund-Levi Y, Frisoni GB, Froelich L, Gabryelewicz T, Gill KD, Gkatzima O, Gomez-Tortosa E, Gordon MF, Grimmer T, Hampel H, Hausner L, Hellwig S, Herukka S-KK, Hildebrandt H, Ishihara L, Ivanoiu A, Jagust WJ, Johannsen P, Kandimalla R, Kapaki E, Klimkowicz-Mrowiec A, Klunk WE, Kohler S, Koglin N, Kornhuber J, Kramberger MG, Van Laere K, Landau SM, Lee DY, de Leon M, Lisetti V, Lleo A, Madsen K, Maier W, Marcusson J, Mattsson N, De Mendonca A, Meulenbroek O, Meyer PT, Mintun MA, Mok V, Molinuevo JLJL, Møllergård HM, Morris JC, Mroczko B, Van der Mussele S, Na DL, Newberg A, Nordberg A, Nordlund A, Novak GP, Paraskevas GP, Parnetti L, Perera G, Peters O, Popp J, Prabhakar S, Rabinovici GD, Ramakers IHGBGB, Rami L, De Oliveira CR, Rinne JO, Rodrigue KM, Rodriguez-Rodriguez E, Roe CM, Rot U, Rowe CC, Ruther E, Sabri O, Sanchez-Juan PP, Santana I, Sarazin M, Schroder J, Schutte C, Seo SW, Soetewey F, Soininen H, Spuru L, Struyfs H, Teunissen CE, Tsolaki M, Vandenberghe R, Verbeek MM, Villemagne VL, Vos SJB, van Waalwijk van Doorn LJCC, Waldemar G, Wallin AKA, Wallin AKA, Wiltfang J, Wolke DA, Zboch M, Zetterberg H, Förster S, Fortea J, Foskett N, Frederiksen KS, Freund-Levi Y, Frisoni GB, Froelich L, Gabryelewicz T, Gill KD, Gkatzima O, Gómez-Tortosa E, Gordon MF, Grimmer T, Hampel H, Hausner L, Hellwig S, Herukka S-KK, Hildebrandt H, Ishihara L, Ivanoiu A, Jagust WJ, Johannsen P, Kandimalla R, Kapaki E, Klimkowicz-Mrowiec A, Klunk WE, Köhler S, Koglin N, Kornhuber J, Kramberger MG, Van Laere K, Landau SM, Lee DY, de Leon M, Lisetti V, Lleo A, Madsen K, Maier W, Marcusson J, Mattsson N, de Mendonça A, Meulenbroek O, Meyer PT, Mintun MA, Mok V, Molinuevo JLJL, Møllergård HM, Morris JC, Mroczko B, Van der Mussele S, Na DL, Newberg A, Nordberg A, Nordlund A, Novak GP, Paraskevas GP, Parnetti L, Perera G, Peters O, Popp J, Prabhakar S,



- Rabinovici GD, Ramakers IHGBGB, Rami L, Resende de Oliveira C, Rinne JO, Rodrigue KM, Rodríguez-Rodríguez E, Roe CM, Rot U, Rowe CC, Rütther E, Sabri O, Sanchez-Juan PP, Santana I, Sarazin M, Schröder J, Schütte C, Seo SW, Soetewey F, Soininen H, Spuru L, Struyfs H, Teunissen CE, Tsolaki M, Vandenberghe R, Verbeek MM, Villemagne VL, Vos SJB, van Waalwijk van Doorn LJCC, Waldemar G, Wallin ÅK, Wallin ÅK, Wiltfang J, Wolk DA, Zboch M, Zetterberg H. 2015. Prevalence of cerebral amyloid pathology in persons without dementia: A meta-analysis. *JAMA - Journal of the American Medical Association*. 313:1924–1938.
- Jansen WJ, Ossenkoppele R, Tijms BM, Fagan AM, Hansson O, Klunk WE, van der Flier WM, Villemagne VL, Frisoni GB, Fleisher AS, Lleó A, Mintun MA, Wallin A, Engelborghs S, Na DL, Chételat G, Molinuevo JL, Landau SM, Mattsson N, Kornhuber J, Sabri O, Rowe CC, Parnetti L, Popp J, Fladby T, Jagust WJ, Aalten P, Lee DY, Vandenberghe R, Resende de Oliveira C, Kapaki E, Froelich L, Ivanoiu A, Gabryelewicz T, Verbeek MM, Sanchez-Juan P, Hildebrandt H, Camus V, Zboch M, Brooks DJ, Drzezga A, Rinne JO, Newberg A, de Mendonça A, Sarazin M, Rabinovici GD, Madsen K, Kramberger MG, Nordberg A, Mok V, Mroczko B, Wolk DA, Meyer PT, Tsolaki M, Scheltens P, Verhey FRJ, Visser PJ, Aarsland D, Alcolea D, Alexander M, Almdahl IS, Arnold SE, Baldeiras I, Barthel H, van Berckel BNM, Blennow K, van Buchem MA, Cavado E, Chen K, Chipi E, Cohen AD, Förster S, Fortea J, Frederiksen KS, Freund-Levi Y, Gkatzima O, Gordon MF, Grimmer T, Hampel H, Hausner L, Hellwig S, Herukka S-K, Johannsen P, Klimkowicz-Mrowiec A, Köhler S, Koglin N, van Laere K, de Leon M, Lisetti V, Maier W, Marcusson J, Meulenbroek O, Møllergård HM, Morris JC, Nordlund A, Novak GP, Paraskevas GP, Perera G, Peters O, Ramakers IHGB, Rami L, Rodríguez-Rodríguez E, Roe CM, Rot U, Rütther E, Santana I, Schröder J, Seo SW, Soininen H, Spuru L, Stomrud E, Struyfs H, Teunissen CE, Vos SJB, van Waalwijk van Doorn LJC, Waldemar G, Wallin ÅK, Wiltfang J, Zetterberg H. 2018. Association of Cerebral Amyloid- $\beta$  Aggregation With Cognitive Functioning in Persons Without Dementia. *JAMA Psychiatry*. 75:84.
- Kawas CH, Greenia DE, Bullain SS, Clark CM, Pontecorvo MJ, Joshi AD, Corrada MM. 2013. Amyloid imaging and cognitive decline in nondemented oldest-old: The 90+ Study. *Alzheimer's and Dementia*. 9:199–203.
- Kawas CH, Kim RC, Sonnen JA, Bullain SS, Trieu T, Corrada MM. 2015. Multiple pathologies are common and related to dementia in the oldest-old: The 90 + Study. *Neurology*. 85:535–542.
- Köhler S, Black SE, Sinden M, Szekely C, Kidron D, Parker JL, Foster JK, Moscovitch M, Wincour G, Szalai JP, Bronskill MJ. 1998. Memory impairments associated with hippocampal versus parahippocampal-gyru atrophy: an MR volumetry study in Alzheimer's disease. *Neuropsychologia*. 36:901–904.

- Legdeur N, Badissi M, Carter SF, de Crom S, van de Kreeke A, Vreeswijk R, Trappenburg MC, Oudega ML, Koek HL, van Campen JP, Keijsers CJPW, Amadi C, Hinz R, Gordon MF, Novak G, Podhorna J, Serné E, Verbraak F, Yaqub M, Hillebrand A, Griffa A, Pendleton N, Kramer SE, Teunissen CE, Lammertsma A, Barkhof F, van Berckel BNM, Scheltens P, Muller M, Maier AB, Herholz K, Visser PJ. 2018. Resilience to cognitive impairment in the oldest-old: design of the EMIF-AD 90+ study. *BMC Geriatrics*. 18:289.
- Legdeur N, Tijms BM, Konijnenberg E, den Braber A, ten Kate M, Sudre CH, Tomassen J, Badissi M, Yaqub M, Barkhof F, van Berckel BN, Boomsma DI, Scheltens P, Holstege H, Maier AB, Visser PJ, N L, BM T, E K, den Braber A, M TK, CH S, J T, M B, M Y, F B, van Berckel BN, DI B, PJ V. 2019. Associations of Brain Pathology Cognitive and Physical Markers With Age in Cognitively Normal Individuals Aged 60–102 Years. *The Journals of Gerontology: Series A*. XX:1–9.
- Legdeur N, Visser PJ, Woodworth DC, Muller M, Fletcher E, Maillard P, Scheltens P, DeCarli C, Kawas CH, Corrada MM. 2019. White Matter Hyperintensities and Hippocampal Atrophy in Relation to Cognition: The 90+ Study. *J Am Geriatr Soc*. 67:1827–1834.
- Lindeboom J, Schmand B, Tulner L, Walstra G, Jonker C. 2002. Visual association test to detect early dementia of the Alzheimer type. *Journal of Neurology Neurosurgery and Psychiatry*. 73:126–133.
- Lopez OL, Klunk WE, Mathis C, Coleman RL, Price J, Becker JT, Aizenstein HJ, Snitz B, Cohen A, Ikonovic M, McDade E, DeKosky ST, Weissfeld L, Kuller LH. 2014. Amyloid, neurodegeneration, and small vessel disease as predictors of dementia in the oldest-old. *Neurology*. 83:1804–1811.
- Lowe VJ, Wiste HJ, Senjem ML, Weigand SD, Therneau TM, Boeve BF, Josephs KA, Fang P, Pandey MK, Murray ME, Kantarci K, Jones DT, Vemuri P, Graff-Radford J, Schwarz CG, Machulda MM, Mielke MM, Roberts RO, Knopman DS, Petersen RC, Jack CR. 2018. Widespread brain tau and its association with ageing, Braak stage and Alzheimer's dementia. *Brain*. 141:271–287.
- McKenna P, Warrington EK. 1980. Testing for nominal dysphasia. *Journal of Neurology, Neurosurgery and Psychiatry*. 43:781–788.
- Meyer-Luehmann M, Spires-Jones TL, Prada C, Garcia-Alloza M, de Calignon A, Rozkalne A, Koenigsknecht-Talboo J, Holtzman DM, Bacskai BJ, Hyman BT. 2008. Rapid appearance and local toxicity of amyloid- $\beta$  plaques in a mouse model of Alzheimer's disease. *Nature*. 451:720–724.
- Meyers JE, Bayless JD, Meyers KR. 1996. Rey complex figure: memory error patterns and functional abilities. *Applied Neuropsychology*. 3:89–92.
- Montine TJ, Phelps CH, Beach TG, Bigio EH, Cairns NJ, Dickson DW, Duyckaerts C, Frosch MP, Masliah E, Mirra SS, Nelson PT, Schneider JA, Thal DR, Trojanowski JQ, Vinters H V, Hyman BT. 2012. National Institute on Aging-

- Alzheimer's Association guidelines for the neuropathologic assessment of Alzheimer's disease: a practical approach. *Acta Neuropathologica*. 123:1–11.
- Mormino EC, Kluth JT, Madison CM, Rabinovici GD, Baker SL, Miller BL, Koeppe RA, Mathis CA, Weiner MW, Jagust WJ. 2009. Episodic memory loss is related to hippocampal-mediated  $\beta$ -amyloid deposition in elderly subjects. *Brain*. 132:1310–1323.
- Morris JC, Heyman A, Mohs RC, Hughes JP, van Belle G, Fillenbaum G, Mellits ED, Clark C. 1989. The Consortium to Establish a Registry for Alzheimer's Disease (CERAD). Part I. Clinical and neuropsychological assessment of Alzheimer's disease. *Neurology*. 39:1159–1165.
- Patenaude B, Smith SM, Kennedy DN, Jenkinson M. 2011. A Bayesian model of shape and appearance for subcortical brain segmentation. *Neuroimage*. 56:907–922.
- Petersen RC, Wiste HJ, Weigand SD, Rocca WA, Roberts RO, Mielke MM, Lowe VJ, Knopman DS, Pankratz VS, Machulda MM, Geda YE, Jack CR. 2016. Association of Elevated Amyloid Levels With Cognition and Biomarkers in Cognitively Normal People From the Community. *JAMA Neurology*. 73:85.
- Reitan RM. 1958. Validity of the trail making test as an indicator of organic brain damage. *Perceptual and Motor Skills*. 8:271–276.
- Robinson JL, Corrada MM, Kovacs GG, Dominique M, Caswell C, Xie SX, Lee VMY, Kawas CH, Trojanowski JQ. 2018. Non-Alzheimer's contributions to dementia and cognitive resilience in The 90+ Study. *Acta Neuropathologica*. 136:377–388.
- Snitz BE, Weissfeld LA, Lopez OL, Kuller LH, Saxton J, Singhbahu DM, Klunk WE, Mathis CA, Price JC, Ives DG, Cohen AD, McDade E, DeKosky ST. 2013. Cognitive trajectories associated with  $\beta$ -amyloid deposition in the oldest-old without dementia. *Neurology*. 80:1378–1384.
- Storandt M, Mintun MA, Head D, Morris JC. 2009. Cognitive Decline and Brain Volume Loss as Signatures of Cerebral Amyloid- $\beta$  Peptide Deposition Identified With Pittsburgh Compound B. *Archives of Neurology*. 66:1476–1481.
- Sudre CH, Cardoso MJ, Bouvy WH, Biessels GJ, Barnes J, Ourselin S. 2015. Bayesian Model Selection for Pathological Neuroimaging Data Applied to White Matter Lesion Segmentation. *IEEE Transactions on Medical Imaging*. 34:2079–2102.
- ten Kate M, Barkhof F, Visser PJ, Teunissen CE, Scheltens P, van der Flier WM, Tijms BM. 2017. Amyloid-independent atrophy patterns predict time to progression to dementia in mild cognitive impairment. *Alzheimer's Research & Therapy*. 9:73.
- Teunisse S, Derix MMA, Crevel H van. 1991. Assessing the Severity of Dementia. *Arch Neurol*. 48:274–277.

- Tingley D, Yamamoto T, Hirose K, Keele L, Imai K. 2014. mediation : R Package for Causal Mediation Analysis. *Journal of Statistical Software*. 59:1–38.
- Tolboom N, Yaqub M, van der Flier WM, Boellaard R, Luurtsema G, Windhorst AD, Barkhof F, Scheltens P, Lammertsma AA, Van Berckel BNM. 2009. Detection of Alzheimer Pathology In Vivo Using Both 11C-PIB and 18F-FDDNP PET. *Journal of Nuclear Medicine*. 50:191–197.
- van Bergen JMG, Li X, Quevenco FC, Gietl AF, Treyer V, Leh SE, Meyer R, Buck A, Kaufmann PA, Nitsch RM, van Zijl PCM, Hock C, Unschuld PG. 2018. Low cortical iron and high entorhinal cortex volume promote cognitive functioning in the oldest-old. *Neurobiology of Aging*. 64:68–75.
- Verfaillie SCJ, Tijms B, Versteeg A, Benedictus MR, Bouwman FH, Scheltens P, Barkhof F, Vrenken H, van der Flier WM. 2016. Thinner temporal and parietal cortex is related to incident clinical progression to dementia in patients with subjective cognitive decline. *Alzheimer's and Dementia: Diagnosis, Assessment and Disease Monitoring*. 5:43–52.
- Visser PJ, Verhey F, Knol DL, Scheltens P, Wahlund L-O, Freund-Levi Y, Tsolaki M, Minthon L, Wallin ÅK, Hampel H, Bürger K, Pirttila T, Soininen H, Rikkert MO, Verbeek MM, Spuru L, Blennow K. 2009. Prevalence and prognostic value of CSF markers of Alzheimer's disease pathology in patients with subjective cognitive impairment or mild cognitive impairment in the DESCRIPA study: a prospective cohort study. *The Lancet Neurology*. 8:619–627.
- Vos SJ, Xiong C, Visser PJ, Jasielec MS, Hassenstab J, Grant EA, Cairns NJ, Morris JC, Holtzman DM, Fagan AM. 2013. Preclinical Alzheimer's disease and its outcome: a longitudinal cohort study. *The Lancet Neurology*. 12:957–965.
- Ward AM, Schultz AP, Huijbers W, Van Dijk KRA, Hedden T, Sperling RA. 2014. The parahippocampal gyrus links the default-mode cortical network with the medial temporal lobe memory system. *Human Brain Mapping*. 35:1061–1073.
- Wechsler D. 1981. *Manual for the Wechsler Adult Intelligence Scale - Revised*, Psychological Corporation.
- Wechsler D, Holdnack J, Drozdick L. 2009. *Wechsler Memory Scale: Fourth Edition Technical and Interpretive Manual*. San Antonio: Pearson.
- Wilde N, Strauss E. 2002. Functional equivalence of WAIS-III/WMS-III digit and spatial span under forward and backward recall conditions. *Clin Neuropsychol*. 16:322–330.
- Wu Y, Carson RE. 2002. Noise Reduction in the Simplified Reference Tissue Model for Neuroreceptor Functional Imaging. *Journal of Cerebral Blood Flow & Metabolism*. 22:1440–1452.
- Yamazaki Y, Zhao N, Caulfield TR, Liu C-CC, Bu G. 2019. Apolipoprotein E and Alzheimer disease: pathobiology and targeting strategies. *Nature Reviews Neurology*. 15:501–518.

Zhao Q, Guo Q, Hong Z. 2013. Clustering and switching during a semantic verbal fluency test contribute to differential diagnosis of cognitive impairment. *Neuroscience Bulletin*. 29:75–82.

Zhao Y, Tudorascu DL, Lopez OL, Cohen AD, Mathis CA, Aizenstein HJ, Price JC, Kuller LH, Kamboh MI, DeKosky ST, Klunk WE, Snitz BE. 2018. Amyloid  $\beta$  Deposition and Suspected Non-Alzheimer Pathophysiology and Cognitive Decline Patterns for 12 Years in Oldest Old Participants Without Dementia. *JAMA Neurology*. 75:88.

## Supplementary material

Supplementary Table 1a. Baseline and annual change effect of A $\beta$  status on cognitive functioning.

Fixed effects	Memory			Language			Processing Speed			Executive Function		
	<i>beta (se)</i>	<i>p</i>	<i>pFDR</i>	<i>beta (se)</i>	<i>p</i>	<i>pFDR</i>	<i>beta (se)</i>	<i>p</i>	<i>pFDR</i>	<i>beta (se)</i>	<i>p</i>	<i>pFDR</i>
A $\beta$ status	-0.37 (0.22)	.090	.180	-0.37 (0.21)	.083	.180	-0.21 (0.18)	.255	.340	-0.02 (0.17)	.883	.088
Time	-0.06 (0.06)	.320	.320	-0.09 (0.05)	.089	.293	-0.07 (0.05)	.219	.293	0.08 (0.06)	.199	.293
A $\beta$ status X time	<b>-0.26 (0.09)</b>	<b>.007</b>	<b>.029</b>	-0.15 (0.08)	.059	.079	-0.18 (0.08)	<b>.042</b>	<b>.079</b>	-0.14 (0.09)	.137	.137

Neuropsychological tests were Z-transformed and averaged for each cognitive domain. Linear mixed models were adjusted for age, education, WMH, and sex. Significant results ( $p < .05$ ) are indicated in bold. A $\beta$  = Amyloid-beta; SF = standard error.

**Supplementary Table 1b. Cortical thickness (mm) according to amyloid status.**

Brain Region	A $\beta$ -, n = 38		A $\beta$ +, n = 19		p	p FDR
	Mean (SE)	95% CI	Mean (SE)	95% CI		
Banks of the superior temporal sulcus	2.30 (0.02)	2.26 - 2.34	2.27 (0.03)	2.22 - 2.32	0.203	0.953
Caudal anterior cingulate	2.58 (0.04)	2.50 - 2.67	2.57 (0.06)	2.45 - 2.69	0.933	0.953
Caudal middle frontal	2.33 (0.02)	2.29 - 2.38	2.33 (0.03)	2.27 - 2.40	0.915	0.953
Cuneus	1.75 (0.02)	1.71 - 1.79	1.73 (0.03)	1.68 - 1.79	0.527	0.953
Entorhinal	2.97 (0.06)	2.84 - 3.09	2.90 (0.09)	2.72 - 3.08	0.431	0.953
Frontal pole	2.69 (0.05)	2.59 - 2.78	2.64 (0.07)	2.50 - 2.77	0.531	0.953
Fusiform	2.43 (0.02)	2.39 - 2.48	2.38 (0.03)	2.31 - 2.44	0.146	0.953
Inferior parietal	2.21 (0.02)	2.17 - 2.26	2.21 (0.03)	2.15 - 2.27	0.868	0.953
Inferior temporal	2.49 (0.03)	2.44 - 2.55	2.49 (0.04)	2.42 - 2.57	0.920	0.953
Insula	2.76 (0.03)	2.70 - 2.81	2.76 (0.04)	2.68 - 2.84	0.953	0.953
Isthmus cingulate	2.06 (0.02)	2.02 - 2.10	2.07 (0.03)	2.02 - 2.12	0.699	0.953
Lateral occipital	1.95 (0.02)	1.91 - 1.99	1.95 (0.03)	1.89 - 2.01	0.952	0.953
Lateral orbitofrontal	2.41 (0.02)	2.36 - 2.46	2.37 (0.03)	2.30 - 2.44	0.311	0.953
Lingual	1.80 (0.02)	1.77 - 1.83	1.81 (0.02)	1.76 - 1.85	0.910	0.953
Medial orbitofrontal	2.21 (0.02)	2.16 - 2.25	2.13 (0.03)	2.07 - 2.19	<b>0.042</b>	0.721
Middle temporal	2.61 (0.02)	2.56 - 2.66	2.60 (0.04)	2.53 - 2.67	0.759	0.953
Paracentral	2.22 (0.02)	2.17 - 2.27	2.25 (0.03)	2.18 - 2.32	0.564	0.953
Parahippocampal	2.47 (0.04)	2.39 - 2.54	2.28 (0.05)	2.18 - 2.38	<b>0.005</b>	0.157
Pars opercularis	2.39 (0.02)	2.34 - 2.43	2.38 (0.03)	2.31 - 2.44	0.802	0.953
Pars orbitalis	2.50 (0.04)	2.43 - 2.58	2.50 (0.05)	2.40 - 2.61	0.879	0.953
Pars triangularis	2.28 (0.02)	2.23 - 2.32	2.27 (0.03)	2.20 - 2.34	0.660	0.953
Pericalcarine	1.55 (0.02)	1.51 - 1.58	1.54 (0.02)	1.49 - 1.58	0.583	0.953
Postcentral	1.94 (0.02)	1.90 - 1.97	1.90 (0.03)	1.85 - 1.96	0.365	0.953
Posterior cingulate	2.32 (0.02)	2.27 - 2.36	2.31 (0.03)	2.25 - 2.37	0.895	0.953
Precentral	2.30 (0.02)	2.26 - 2.35	2.31 (0.03)	2.25 - 2.37	0.939	0.953
Precuneus	2.14 (0.02)	2.10 - 2.18	2.13 (0.03)	2.07 - 2.19	0.681	0.953
Rostral anterior cingulate	2.68 (0.03)	2.62 - 2.75	2.61 (0.05)	2.51 - 2.70	0.181	0.953
Rostral middle frontal	2.24 (0.03)	2.19 - 2.29	2.23 (0.04)	2.15 - 2.31	0.761	0.953
Superior frontal	2.45 (0.03)	2.40 - 2.50	2.45 (0.04)	2.38 - 2.52	0.904	0.953
Superior parietal	2.00 (0.02)	1.95 - 2.04	2.00 (0.03)	1.93 - 2.06	0.902	0.953
Superior temporal	2.45 (0.02)	2.40 - 2.49	2.42 (0.03)	2.36 - 2.48	0.333	0.953
Supramarginal	2.28 (0.02)	2.24 - 2.32	2.28 (0.03)	2.22 - 2.33	0.809	0.953
Temporal pole	3.39 (0.05)	3.30 - 3.48	3.44 (0.07)	3.31 - 3.57	0.578	0.953
Transverse temporal	2.19 (0.03)	2.13 - 2.25	2.17 (0.04)	2.08 - 2.25	0.673	0.953

Group differences in cortical thickness by one-way ANOVA adjusted for age, education, WMH, and sex. Average cortical thickness for both left and right hemisphere. Significant results (p<.05) are indicated in bold. A $\beta$  = amyloid- $\beta$ ; SE = standard error; CI = confidence interval.

**Supplementary Table 1c. Hippocampal volume according to amyloid status.**

	A $\beta$ -, n = 38		A $\beta$ +, n = 19		P
	Mean (SE)	95% CI	Mean (SE)	95% CI	
Hippocampal volume, mm <sup>3</sup>	3026 (62)	2902 - 3151	2998 (85)	2828 - 3168	.667

Group difference in hippocampal volume by one-way ANOVA, adjusted for intracranial volume, education, WMH, age and sex. A $\beta$  = amyloid- $\beta$ ; SE = standard error; CI = confidence interval.

Supplementary Table 1d. Associations of cortical thickness with baseline and decline on memory performance by Aβ status.

Region	THK		Time X THK		THK X Aβ		Time X THK X Aβ		Time X THK in Aβ-		Time X THK in Aβ+	
	beta(se)	p	beta(se)	p	beta(se)	p	F	p	beta(se)	p	beta(se)	p
Banks of the superior temporal sulcus	0.63 (1.01)	.533	0.28 (0.49)	.561	.795		2.18	1.47	.986	-0.61 (0.53)	.258	.548
Caudal anterior cingulate	0.43 (0.42)	.308	0.49 (0.18)	.009	.035		0.04	.848	.986	0.41 (0.26)	.128	.423
Caudal middle frontal	1.30 (0.80)	.110	0.563	0.27 (0.47)	.558	.795	0.17	1.684	.986	-0.34 (0.52)	.524	.712
Cuneus	0.43 (0.96)	.654	.830	0.05 (0.53)	.929	.958	2.93 (1.92)	.133	.752	0.16 (0.688)	.986	.545
Entorhinal	0.58 (0.27)	.032	.378	0.43 (0.10)	<0.001	.002	0.36 (0.55)	.517	.765	0.34 (0.11)	.005	.057
Frontal pole	0.24 (0.39)	.540	.799	0.31 (0.16)	.061	.174	0.73 (0.79)	.365	.765	0.00 (0.952)	.986	.18
Fusiform	1.14 (0.76)	.139	.563	0.96 (0.32)	.005	.027	2.69 (1.71)	.120	.752	0.60 (0.44)	.986	.135
Inferior parietal	0.68 (0.87)	.437	.743	0.04 (0.42)	.929	.958	1.61 (1.77)	.368	.765	0.14 (0.713)	.986	.403
Inferior temporal	0.86 (0.69)	.217	.564	0.83 (0.33)	.016	.053	1.12 (1.42)	.433	.765	0.14 (0.714)	.986	.403
Insula	0.58 (0.62)	.356	.672	0.86 (0.22)	<0.001	.002	2.02 (1.27)	.117	.752	0.78 (0.383)	.986	.010
Isthmus cingulate	0.41 (0.99)	.684	.831	0.93 (0.43)	.036	.110	2.05 (1.88)	.281	.765	0.06 (0.813)	.986	.127
Lateral occipital	0.45 (0.89)	.614	.830	0.50 (0.48)	.304	.608	1.94 (1.77)	.278	.765	0.01 (0.939)	.986	.712
Lateral orbitofrontal	-0.05 (0.77)	.944	.944	0.54 (0.35)	.127	.332	2.67 (1.65)	.112	.752	0.10 (0.754)	.986	.745
Lingual	0.28 (1.21)	.816	.882	0.19 (0.62)	.760	.892	1.34 (2.57)	.604	.765	0.03 (0.71)	.967	.967
Medial orbitofrontal	0.36 (0.82)	.659	.830	0.28 (0.30)	.359	.642	1.03 (1.65)	.534	.765	0.10 (0.754)	.986	.745
Middle temporal	1.77 (0.68)	.012	.378	1.03 (0.37)	.007	.030	0.80 (1.38)	.564	.765	0.86 (0.358)	.986	.065
Paracentral	0.67 (0.76)	.385	.689	-0.50 (0.33)	.144	.351	-0.833 (1.61)	.608	.765	0.09 (0.769)	.986	.051
Parahippocampal	0.92 (0.42)	.033	.378	0.84 (0.16)	<0.001	<0.001	1.54 (0.88)	.086	.752	0.44 (0.512)	.986	0.73
Pars opercularis	0.49 (0.85)	.571	.809	-0.13 (0.39)	.739	.892	-0.15 (1.80)	.936	.951	0.35 (0.559)	.986	0.69
Pars orbitalis	0.14 (0.52)	.791	.882	-0.04 (0.25)	.874	.958	1.22 (1.08)	.265	.765	0.83 (0.366)	.986	0.32
Parstriangularis	0.09 (0.82)	.911	.939	0.22 (0.43)	.616	.838	0.89 (2.04)	.665	.779	0.00 (0.986)	.986	-0.18
Percalcarine	1.15 (1.17)	.329	.658	0.80 (0.61)	.194	.440	1.66 (2.61)	.527	.765	0.07 (0.790)	.986	0.66
Postcentral	1.29 (0.98)	.193	.563	-0.12 (0.44)	.790	.895	0.27 (2.36)	.910	.951	0.00 (0.946)	.986	-0.41
Posterior cingulate	0.19 (0.87)	.830	.882	0.00 (0.37)	.995	.995	0.81 (1.83)	.660	.779	0.67 (0.416)	.986	0.22
Precentral	0.97 (0.90)	.283	.642	-0.17 (0.42)	.688	.866	-0.12 (1.91)	.951	.951	0.36 (0.551)	.986	-0.67
Precuneus	1.12 (0.86)	.199	.563	-0.33 (0.43)	.443	.700	1.43 (2.03)	.483	.765	0.30 (0.260)	.986	-0.41
Rostral anterior cingulate	0.62 (0.51)	.232	.564	0.78 (0.20)	<0.001	.002	1.89 (1.01)	.067	.752	0.79 (0.378)	.986	0.55
Rostral middle frontal	0.50 (0.71)	.485	.784	0.31 (0.41)	.453	.700	1.60 (1.69)	.349	.765	0.04 (0.845)	.986	-0.16
Superior frontal	1.00 (0.74)	.182	.563	0.39 (0.39)	.323	.610	1.59 (1.56)	.311	.765	0.90 (0.175)	.986	-0.45
Superior parietal	1.27 (0.81)	.124	.563	-0.39 (0.44)	.390	.664	0.67 (1.82)	.716	.812	0.13 (0.723)	.986	-0.69
Supramarginal	1.53 (0.84)	.074	.563	1.19 (0.41)	.006	.028	1.13 (1.73)	.518	.765	0.96 (0.332)	.986	0.55
Supramarginal	1.38 (0.97)	.161	.563	0.54 (0.50)	.278	.592	2.42 (2.09)	.252	.765	0.32 (0.604)	.986	0.17
Temporal pole	0.52 (0.38)	.180	.563	0.59 (0.13)	<0.001	.001	0.59 (0.69)	.398	.765	0.27 (0.404)	.986	0.62
Transverse temporal	0.17 (0.64)	.789	.882	0.13 (0.28)	.644	.842	0.99 (1.32)	.458	.765	0.00 (0.965)	.986	0.00

Supplementary Table 1e. Associations of hippocampal volume with baseline and decline on memory performance by Aβ status.

Region	THK		Time X THK		THK X Aβ		Time X THK X Aβ		Time X THK in Aβ-		Time X THK in Aβ+	
	beta(se)	p	beta(se)	p	beta(se)	p	F	p	beta(se)	p	beta(se)	p
Hippocampus	0.00067 (0.00043)	.029	0.00027 (0.00014)	.053	-0.00015 (0.00057)	.792	2.70	.109	0.00003 (0.00020)	.899	0.00044 (0.00016)	.015

Data are represented as β (SE) as estimated by linear mixed models. Intracranial volume, sex, education, WMH, and age were included as covariates. Interaction terms were removed when not significant. Time in years; volume in mm3. A positive beta estimate indicates the effect of a smaller volume, whereas a negative beta indicates the effect of a larger volume. Significant results (p<.05) are indicated in bold. Aβ = amyloid-beta; SE = standard error; THK = thickness.



Supplementary Table 1f. Associations of cortical thickness with baseline and decline on language performance by Aβ status.

Region	Language (n observations = 100)																	
	THK		Time X THK		THK X Aβ		Time X THK X Aβ		Time X THK in Aβ-		Time X THK in Aβ+							
	beta(se)	p	beta(se)	p	beta(se)	p	beta(se)	p	beta(se)	p	beta(se)	p						
Banks of the superior temporal sulcus	0.19 (0.96)	.840	.938	0.63 (0.38)	1.06	.212	-1.97 (1.85)	.292	.910	0.00	.960	.960	0.41 (0.48)	.407	.498	0.37 (0.67)	.587	.950
Caudal anterior cingulate	0.36 (0.41)	.381	.938	0.19 (0.15)	.219	.310	-0.57 (0.82)	.486	.979	0.69	.410	.656	0.01 (0.25)	.953	.982	0.28 (0.18)	.148	.950
Caudal middle frontal	0.26 (0.78)	.740	.938	0.74 (0.36)	.046	.156	-0.90 (1.81)	.619	.979	1.54	.222	.617	0.83 (0.45)	.076	.198	-0.08 (0.66)	.911	.971
Cuneus	-0.24 (0.91)	.789	.938	-0.14 (0.43)	.746	.793	0.17 (1.88)	.926	.979	0.68	.415	.656	-0.15 (0.58)	.797	.847	-0.87 (0.62)	.181	.950
Entorhinal	0.32 (0.27)	.240	.938	0.21 (0.09)	.032	.156	-0.16 (0.38)	.786	.979	0.16	.692	.767	0.22 (0.11)	.056	.196	0.14 (0.17)	.434	.950
Frontal pole	0.10 (0.38)	.793	.938	0.12 (0.13)	.378	.476	-0.48 (0.78)	.541	.979	1.70	.200	.617	0.20 (0.18)	.261	.385	-0.15 (0.19)	.460	.950
Fusiform	-0.32 (0.76)	.680	.938	0.61 (0.27)	.028	.156	0.07 (1.76)	.967	.979	0.81	.373	.656	0.63 (0.33)	.069	.196	0.05 (0.53)	.933	.971
Inferior parietal	-0.49 (0.83)	.555	.938	0.48 (0.33)	.159	.234	-1.62 (1.71)	.348	.910	1.14	.291	.656	0.58 (0.42)	.177	.342	-0.15 (0.55)	.787	.950
Inferior temporal	0.07 (0.68)	.914	.942	0.60 (0.27)	.031	.156	-0.49 (1.42)	.733	.979	0.83	.367	.656	0.76 (0.38)	.059	.196	0.26 (0.38)	.516	.950
Insula	0.37 (0.61)	.547	.938	0.29 (0.20)	.152	.234	1.88 (1.28)	.147	.910	0.36	.552	.757	0.29 (0.24)	.229	.358	0.05 (0.42)	.900	.971
Isthmus cingulate	-1.17 (0.95)	.223	.938	0.56 (0.36)	.122	.214	2.22 (1.82)	.230	.910	2.38	.131	.509	0.81 (0.41)	.058	.196	-0.39 (0.64)	.554	.950
Lateral occipital	-0.55 (0.85)	.523	.938	0.06 (0.39)	.877	.904	0.78 (1.72)	.654	.979	0.24	.623	.757	0.00 (0.59)	.999	.999	-0.41 (0.50)	.427	.950
Lateral orbitofrontal	-0.29 (0.73)	.699	.938	0.43 (0.28)	.126	.214	0.25 (1.65)	.881	.979	0.15	.699	.767	0.32 (0.35)	.365	.478	0.08 (0.58)	.887	.971
Lingual	-1.58 (1.13)	.168	.938	0.38 (0.50)	.444	.510	0.96 (2.44)	.696	.979	3.25	.079	.507	0.90 (0.62)	.161	.342	-0.88 (0.74)	.254	.950
Medial orbitofrontal	0.55 (0.77)	.481	.938	0.47 (0.23)	.045	.156	-0.16 (1.60)	.920	.979	0.31	.582	.757	0.47 (0.37)	.219	.358	0.22 (0.38)	.574	.950
Middle temporal	1.03 (0.70)	.148	.938	0.45 (0.31)	.155	.234	-0.86 (1.43)	.548	.979	3.02	.090	.507	0.78 (0.40)	.061	.196	-0.32 (0.48)	.513	.950
Paracentral	-0.62 (0.73)	.400	.938	0.45 (0.26)	.098	.212	-1.06 (1.56)	.500	.979	2.46	.124	.509	0.69 (0.33)	.043	.196	-0.10 (0.42)	.805	.971
Parahippocampal	1.12 (0.43)	.012	.420	0.14 (0.16)	.394	.478	1.90 (0.91)	.042	.710	2.33	.135	.509	0.23 (0.22)	.311	.423	-0.29 (0.24)	.250	.950
Pars opercularis	-0.13 (0.81)	.872	.938	0.59 (0.30)	.057	.162	-2.84 (1.72)	.104	.910	0.08	.780	.829	0.37 (0.45)	.424	.498	0.55 (0.41)	.204	.950
Pars orbitalis	-0.18 (0.49)	.713	.938	0.14 (0.20)	.486	.533	-1.49 (1.05)	.163	.910	0.02	.891	.918	0.08 (0.24)	.743	.842	0.02 (0.38)	.956	.971
Pars triangularis	0.12 (0.78)	.883	.938	0.40 (0.34)	.250	.326	-1.04 (1.87)	.035	.710	0.83	.368	.656	0.32 (0.38)	.414	.498	-0.54 (0.88)	.548	.950
Percalcarine	0.21 (1.13)	.851	.938	-0.01 (0.50)	.980	.980	1.83 (2.55)	.475	.979	1.57	.218	.617	0.17 (0.57)	.773	.847	-1.20 (0.97)	.236	.950
Postcentral	-0.05 (0.93)	.960	.960	0.74 (0.33)	.032	.156	-2.18 (2.22)	.330	.910	4.56	.039	.441	1.01 (0.37)	.011	.196	-0.67 (0.67)	.335	.950
Posterior cingulate	-0.98 (0.82)	.238	.938	0.92 (0.26)	.001	.032	-0.12 (1.77)	.945	.979	0.35	.557	.757	1.06 (0.42)	.019	.196	0.76 (0.31)	.027	.915
Precentral	-0.72 (0.85)	.401	.938	0.26 (0.34)	.450	.510	-0.38 (1.83)	.837	.979	4.98	.031	.441	0.55 (0.40)	.181	.342	-0.94 (0.54)	.098	.950
Precuneus	-0.35 (0.83)	.671	.938	0.56 (0.34)	.103	.212	-1.99 (1.96)	.313	.910	1.14	.292	.656	0.58 (0.37)	.131	.298	-0.31 (0.79)	.701	.971
Rostral anterior cingulate	0.37 (0.51)	.474	.938	0.34 (0.18)	.066	.173	0.03 (1.04)	.979	.979	0.25	.620	.757	0.29 (0.23)	.214	.358	0.06 (0.38)	.877	.971
Rostral middle frontal	0.25 (0.68)	.714	.938	0.50 (0.32)	.125	.214	-1.89 (1.63)	.251	.910	0.74	.394	.656	0.49 (0.40)	.232	.358	-0.20 (0.63)	.754	.971
Superior frontal	0.20 (0.72)	.679	.938	0.64 (0.30)	.040	.156	-0.93 (1.56)	.555	.979	1.45	.236	.617	0.78 (0.41)	.066	.196	-0.02 (0.51)	.971	.971
Superior parietal	0.20 (0.78)	.795	.938	0.59 (0.35)	.095	.212	-1.97 (1.73)	.260	.910	6.35	.016	.441	0.94 (0.36)	.015	.196	-0.97 (0.68)	.176	.950
Superior temporal	0.26 (0.85)	.760	.938	0.79 (0.34)	.025	.156	-0.73 (1.76)	.680	.979	0.65	.425	.656	0.89 (0.50)	.085	.206	0.25 (0.59)	.679	.971
Supramarginal	-0.33 (0.95)	.728	.938	0.85 (0.38)	.032	.156	-1.02 (2.11)	.629	.979	3.66	.063	.507	1.06 (0.45)	.026	.196	-0.65 (0.79)	.427	.950
Supramarginal	0.39 (0.38)	.316	.938	0.24 (0.12)	.057	.162	0.04 (0.71)	.954	.979	0.18	.671	.767	0.32 (0.15)	.044	.196	0.20 (0.20)	.330	.950
Transverse temporal	-0.76 (0.60)	.208	.938	0.26 (0.22)	.243	.326	-1.27 (1.24)	.309	.910	0.43	.514	.757	0.38 (0.35)	.284	.403	0.04 (0.30)	.904	.971

Data are represented as β (SE) as estimated by linear mixed models. Sex, education, WMH, and age were included as covariates. Interaction terms were removed when not significant. Time in years; cortical thickness in mm. A positive beta estimate indicates the effect of cortical thinning, whereas a negative beta indicates the effect of a thicker cortical region. Significant results (p<.05) are indicated in bold. Aβ = amyloid-beta; SE = standard error; THK = thickness.

Supplementary Table 1g. Associations of hippocampal volume with baseline and decline on language performance by Aβ status.

Region	Language (n observations = 100)											
	THK		Time X THK		THK X Aβ		ne X THK X		Time X THK in Aβ-		Time X THK in Aβ+	
	beta(se)	p	beta(se)	p	beta(se)	p	F	p	beta(se)	p	beta(se)	p
Hippocampus 0.000007 (0.00030)	.827	.000009 (0.00012)	.422	-0.00043 (0.00061)	.480	0.40	.529	0.00002 (0.00018)	.933	0.00015 (0.00014)	.825	

Data are represented as β (SE) as estimated by linear mixed models. Intracranial volume, sex, education, WMH, and age were included as covariates. Interaction terms were removed when not significant. Time in years; volume in mm<sup>3</sup>. A positive beta estimate indicates the effect of a smaller volume, whereas a negative beta indicates the effect of a larger volume. Significant results (p<.05) are indicated in bold. Aβ = amyloid-beta; SE = standard error; THK = thickness.

Supplementary Table 1b. Associations of cortical thickness with baseline and decline on processing speed performance by Aβ status.

Region	Processing Speed (n observations = 99)																	
	THK		Time X THK		THK X Aβ		Time X THK X Aβ		Time X THK in Aβ-		Time X THK in Aβ+							
	beta(se)	p	beta(se)	p	beta(se)	p	F	p	beta(se)	p	beta(se)	p						
Banks of the superior temporal sulcus	-0.58 (0.81)	.476	.705	0.60 (0.42)	.157	.982	-1.87 (1.55)	.232	.608	1.55	.219	.466	0.72 (0.39)	.076	.995	-0.44 (1.02)	.670	.727
Caudal anterior cingulate	-0.20 (0.35)	.574	.750	0.31 (0.17)	.069	.982	-0.85 (0.70)	.231	.608	0.61	.441	.537	0.12 (0.21)	.569	.995	0.44 (0.29)	1.45	.403
Caudal middle frontal	-0.63 (0.66)	.339	.607	0.29 (0.41)	.481	.982	-0.76 (1.53)	.621	.760	1.64	.207	.466	0.36 (0.40)	.377	.995	-0.63 (0.98)	.532	.670
Cuneus	-0.95 (0.75)	.217	.574	-0.59 (0.46)	.204	.982	0.22 (1.52)	.885	.912	10.72	.002	.072	0.20 (0.49)	.692	.995	-2.67 (0.72)	.002	.077
Entorhinal	0.28 (0.24)	.231	.574	0.03 (0.11)	.811	.982	-0.17 (0.52)	.745	.845	0.03	.863	.863	-0.01 (0.10)	.935	.995	0.07 (0.27)	.814	.814
Frontal pole	-0.55 (0.31)	.086	.574	-0.07 (0.15)	.651	.982	0.31 (0.64)	.626	.760	9.06	.004	.075	0.19 (0.16)	.243	.995	-0.66 (0.24)	.015	.216
Fusiform	-0.15 (0.66)	.817	.885	0.07 (0.31)	.829	.982	-1.05 (1.51)	.489	.742	2.22	1.44	.407	0.15 (0.29)	.610	.995	-1.07 (0.78)	.189	.427
Inferior parietal	-1.13 (0.68)	.103	.574	0.01 (0.38)	.987	.987	-2.78 (1.37)	.046	.348	0.79	.378	.537	0.04 (0.37)	.910	.995	-0.86 (0.81)	.301	.521
Inferior temporal	-0.39 (0.58)	.504	.714	0.09 (0.31)	.760	.982	-1.23 (1.21)	.313	.648	1.14	.708	.730	0.07 (0.34)	.840	.995	-0.14 (0.58)	.808	.814
Insula	-0.45 (0.52)	.397	.675	0.17 (0.22)	.447	.982	0.72 (1.10)	.518	.742	1.10	.300	.518	-0.07 (0.20)	.747	.995	0.61 (0.63)	.344	.521
Isthmus cingulate	-1.50 (0.78)	.060	.574	-0.05 (0.41)	.901	.982	0.64 (1.58)	.686	.805	4.41	.525	.576	0.00 (0.37)	.995	.995	-0.96 (1.02)	.362	.521
Lateral occipital	-1.21 (0.69)	.084	.574	-0.64 (0.42)	.135	.982	-0.42 (1.39)	.817	.896	0.68	.415	.537	-0.42 (0.50)	.400	.995	-1.25 (0.69)	.090	.307
Lateral orbitofrontal	-0.44 (0.62)	.477	.705	-0.13 (0.31)	.687	.982	-1.20 (1.36)	.381	.648	0.65	.423	.537	-0.28 (0.30)	.360	.995	-0.84 (0.83)	.327	.521
Lingual	-1.25 (0.95)	.194	.574	-0.34 (0.56)	.546	.982	-3.82 (1.99)	.058	.348	1.65	.206	.466	0.17 (0.55)	.760	.995	-1.63 (1.12)	.166	.403
Medial orbitofrontal	-0.15 (0.66)	.820	.885	0.03 (0.27)	.915	.982	0.13 (1.36)	.925	.925	0.87	.357	.537	-0.06 (0.33)	.844	.995	-0.57 (0.55)	.320	.521
Middle temporal	-0.13 (0.62)	.833	.885	0.08 (0.35)	.825	.982	-0.85 (1.27)	.506	.742	0.83	.367	.537	0.16 (0.36)	.648	.995	-0.53 (0.73)	.476	.647
Paracentral	-0.31 (0.61)	.613	.772	-0.28 (0.30)	.343	.982	-1.24 (1.32)	.349	.648	2.31	1.36	.407	-0.03 (0.30)	.922	.995	-0.85 (0.57)	.161	.403
Parahippocampal	0.56 (0.38)	.149	.574	0.17 (0.17)	.334	.982	1.64 (0.81)	.047	.348	1.08	.305	.518	0.18 (0.19)	.354	.995	-0.17 (0.39)	.668	.727
Pars opercularis	-0.85 (0.68)	.217	.574	0.34 (0.34)	.325	.982	-3.12 (1.43)	.033	.348	0.35	.557	.592	0.01 (0.39)	.985	.995	0.28 (0.64)	.665	.727
Pars orbitalis	-0.46 (0.41)	.273	.574	0.02 (0.22)	.940	.982	-1.66 (0.87)	.061	.348	0.75	.392	.537	0.05 (0.20)	.806	.995	-0.53 (0.57)	.368	.521
Pars triangularis	-0.90 (0.64)	.165	.574	-0.25 (0.38)	.505	.982	-3.70 (1.49)	.016	.348	1.15	.290	.518	-0.39 (0.33)	.243	.995	-1.68 (1.28)	.209	.427
Percalcarine	-0.57 (0.95)	.550	.749	-0.09 (0.55)	.873	.982	-1.14 (2.15)	.598	.760	0.60	.442	.537	-0.06 (0.49)	.896	.995	-1.03 (1.50)	.504	.659
Postcentral	-0.03 (0.80)	.971	.984	-0.16 (0.38)	.681	.982	-2.43 (1.86)	.196	.608	6.35	.016	.133	0.15 (0.35)	.673	.995	-1.97 (0.88)	.043	.250
Posterior cingulate	-1.33 (0.68)	.055	.574	0.52 (0.32)	.105	.982	-1.34 (1.48)	.368	.648	2.24	1.42	.407	-0.09 (0.40)	.829	.995	0.85 (0.50)	.115	.355
Precentral	-0.77 (0.72)	.287	.574	-0.04 (0.37)	.925	.982	-1.61 (1.53)	.295	.648	5.73	.021	.143	0.34 (0.35)	.335	.995	-1.48 (0.78)	.078	.307
Precuneus	-0.77 (0.69)	.270	.574	-0.02 (0.39)	.953	.982	-2.26 (1.59)	.159	.608	5.10	.029	.163	0.18 (0.33)	.594	.995	-2.16 (1.11)	.067	.307
Rostral anterior cingulate	-0.14 (0.44)	.747	.885	0.15 (0.20)	.473	.982	-0.77 (0.89)	.524	.742	0.43	.513	.576	0.04 (0.20)	.842	.995	-0.23 (0.56)	.684	.727
Rostral middle frontal	-0.58 (0.57)	.318	.601	-0.19 (0.37)	.616	.982	-1.77 (1.33)	.188	.608	4.66	.036	.168	0.01 (0.35)	.986	.995	-1.98 (0.85)	.033	.250
Superior frontal	-0.71 (0.60)	.242	.574	-0.27 (0.35)	.447	.982	-0.22 (1.28)	.865	.912	4.51	.040	.168	-0.01 (0.37)	.976	.995	-1.45 (0.65)	.044	.250
Superior parietal	-0.49 (0.66)	.459	.705	-0.35 (0.40)	.403	.982	-1.77 (1.43)	.219	.608	7.07	.011	.123	0.08 (0.35)	.825	.995	-2.49 (0.95)	.019	.216
Superior temporal	-0.01 (0.73)	.984	.984	0.11 (0.39)	.772	.982	-1.46 (1.53)	.344	.648	0.44	.512	.576	-0.10 (0.43)	.823	.995	-0.46 (0.89)	.615	.727
Supramarginal	-0.99 (0.79)	.216	.574	0.07 (0.44)	.879	.982	-1.85 (1.73)	.288	.648	2.88	.097	.366	0.10 (0.42)	.821	.995	-1.50 (1.14)	.213	.427
Temporal pole	0.08 (0.33)	.815	.885	0.04 (0.14)	.775	.982	-0.32 (0.63)	.613	.760	1.35	.252	.503	-0.04 (0.14)	.790	.995	0.28 (0.30)	.367	.521
Transverse temporal	-0.61 (0.50)	.227	.574	-0.32 (0.24)	.187	.982	-1.48 (1.01)	.150	.608	1.93	.172	.451	-0.04 (0.29)	.894	.995	-0.73 (0.40)	.089	.307

Supplementary Table 11. Associations of hippocampal volume with baseline and decline on processing speed performance by Aβ status.

Region	Processing Speed (n observations = 99)											
	THK		Time X THK		THK X Aβ		Time X THK X Aβ		Time X THK in Aβ-		Time X THK in Aβ+	
	beta(se)	p	beta(se)	p	beta(se)	p	F	p	beta(se)	p	beta(se)	p
Hippocampus	0.00049 (0.00024)	.049	-0.00013 (0.00013)	.309	-0.00054 (0.00048)	.267	0.28	.601	-0.00020 (0.00015)	.185	-0.00049 (0.00022)	.825

Data are represented as β (SE) as estimated by linear mixed models. Intracranial volume, sex, education, WMH, and age were included as covariates. Interaction terms were removed when not significant. Time in years; volume in mm<sup>3</sup>. A positive beta estimate indicates the effect of a smaller volume, whereas a negative beta indicates the effect of a larger volume. Significant results (p<.05) are indicated in bold. Aβ = amyloid-beta; SE = standard error; THK = thickness.

Supplementary Table 1j. Associations of cortical thickness with baseline and decline on executive functioning performance by Aβ status.

Region	Executive Functioning (n observations = 100)																	
	THK		Time X THK		THK X Aβ		Time X THK X Aβ		Time X THK in Aβ+									
	beta(se)	p	beta(se)	p	beta(se)	p	F	p	beta(se)	p								
Banks of the superior temporal sulcus	-0.38 (0.74)	.607	.898	0.25 (0.47)	.599	.385	-0.92 (1.46)	.529	.957	3.57	.065	.694	0.64 (0.54)	.245	.757	-1.22 (0.86)	.176	.578
Caudal anterior cingulate	-0.19 (0.32)	.553	.898	-0.14 (0.18)	.461	.873	-0.44 (0.66)	.500	.957	0.23	.633	.933	-0.29 (0.27)	.288	.800	-0.03 (0.28)	.909	.966
Caudal middle frontal	-0.07 (0.60)	.906	.986	0.03 (0.45)	.944	.975	0.13 (1.46)	.932	.957	0.33	.571	.933	-0.02 (0.55)	.965	1.00	-0.34 (0.89)	.709	.931
Cuneus	-0.78 (0.69)	.260	.898	-0.45 (0.51)	.379	.873	0.08 (1.47)	.957	.975	3.17	.082	.694	0.04 (0.65)	.953	1.00	-1.80 (0.75)	.029	.464
Entorhinal	0.00 (0.22)	.986	.986	-0.03 (0.12)	.814	.975	0.33 (0.49)	.500	.957	0.48	.492	.933	-0.09 (0.13)	.489	.843	0.07 (0.25)	.767	.931
Frontal pole	-0.44 (0.29)	.131	.898	-0.04 (0.16)	.818	.975	-0.05 (0.61)	.936	.957	0.12	.733	.933	-0.15 (0.21)	.471	.843	-0.08 (0.27)	.781	.931
Fusiform	0.14 (0.59)	.814	.986	0.20 (0.34)	.565	.873	-1.19 (1.39)	.396	.957	2.04	.160	.933	0.37 (0.39)	.359	.843	-0.82 (0.71)	.266	.692
Inferior parietal	-0.50 (0.62)	.422	.898	-0.61 (0.40)	.135	.764	-1.35 (1.32)	.311	.957	0.65	.423	.933	-0.51 (0.49)	.306	.800	-1.12 (0.68)	.117	.496
Inferior temporal	-0.30 (0.53)	.565	.898	0.01 (0.34)	.965	.975	-1.52 (1.12)	.180	.957	0.00	.961	.993	-0.05 (0.46)	.918	1.00	0.01 (0.55)	.986	1.00
Insula	-0.41 (0.47)	.393	.898	0.11 (0.25)	.649	.919	0.37 (1.04)	.726	.957	1.66	.205	.933	-0.13 (0.27)	.631	.959	0.73 (0.55)	.204	.578
Isthmus cingulate	-0.60 (0.73)	.412	.898	0.43 (0.43)	.331	.873	-0.43 (1.49)	.775	.957	0.39	.537	.933	0.21 (0.49)	.677	.959	0.68 (0.95)	.487	.919
Lateral occipital	-0.73 (0.63)	.249	.898	-0.92 (0.45)	.044	.520	-0.67 (1.32)	.613	.957	0.15	.701	.933	-0.84 (0.66)	.210	.757	-1.20 (0.58)	.055	.464
Lateral orbitofrontal	-0.93 (0.54)	.091	.898	-0.10 (0.34)	.767	.975	-0.94 (1.25)	.454	.957	0.70	.408	.933	-0.51 (0.39)	.198	.757	0.20 (0.79)	.799	.931
Lingual	-0.60 (0.87)	.490	.898	-0.47 (0.60)	.438	.873	-0.52 (1.94)	.790	.957	4.15	.047	.694	0.42 (0.72)	.566	.916	-1.93 (0.92)	.051	.464
Medial orbitofrontal	-0.43 (0.60)	.471	.898	-0.03 (0.29)	.906	.975	0.26 (1.25)	.837	.957	1.60	.212	.933	-0.74 (0.41)	.085	.757	0.11 (0.53)	.841	.931
Middle temporal	0.20 (0.56)	.723	.946	-0.22 (0.38)	.564	.873	-0.53 (1.19)	.661	.957	0.01	.926	.993	-0.38 (0.47)	.423	.843	-0.18 (0.66)	.782	.931
Paracentral	-0.34 (0.56)	.545	.898	0.01 (0.33)	.969	.975	-0.49 (1.26)	.699	.957	0.39	.538	.933	0.13 (0.40)	.748	.978	-0.22 (0.56)	.699	.931
Parahippocampal	0.05 (0.35)	.894	.986	0.26 (0.19)	.180	.765	0.68 (0.78)	.384	.957	0.11	.741	.933	0.12 (0.25)	.653	.959	0.16 (0.35)	.650	.931
Pars opercularis	-0.51 (0.60)	.399	.898	-0.76 (0.36)	.042	.520	0.17 (1.33)	.899	.957	0.05	.827	.970	-0.85 (0.50)	.100	.757	-1.01 (0.54)	.849	.931
Pars orbitalis	-0.24 (0.37)	.521	.898	-0.25 (0.24)	.301	.873	-1.24 (0.83)	.138	.957	0.19	.667	.933	-0.37 (0.26)	.162	.757	-0.10 (0.54)	.849	.931
Pars triangularis	-0.93 (0.57)	.108	.898	-0.58 (0.41)	.161	.765	-2.08 (1.44)	.153	.957	0.28	.602	.933	-0.74 (0.42)	.090	.757	-1.27 (1.20)	.305	.692
Pericalcarine	-0.81 (0.86)	.349	.898	-0.02 (0.61)	.975	.975	0.43 (2.01)	.830	.957	0.14	.707	.933	0.00 (0.65)	.996	1.00	-0.30 (1.36)	.830	.931
Postcentral	0.02 (0.71)	.980	.986	-0.84 (0.41)	.046	.520	-0.84 (1.78)	.638	.957	0.46	.501	.933	-0.86 (0.45)	.068	.757	-1.48 (0.84)	.097	.496
Posterior cingulate	-0.09 (0.63)	.888	.986	-0.26 (0.36)	.477	.873	-0.34 (1.40)	.809	.957	0.85	.362	.933	0.12 (0.54)	.820	1.00	-0.49 (0.49)	.339	.720
Precentral	-0.35 (0.65)	.595	.898	0.32 (0.40)	.428	.873	-1.09 (1.47)	.463	.957	0.55	.460	.933	0.40 (0.46)	.396	.843	-0.16 (0.78)	.843	.931
Precuneus	-0.17 (0.63)	.787	.986	-0.06 (0.42)	.889	.975	-0.85 (1.53)	.583	.957	7.01	.011	.375	0.30 (0.44)	.496	.843	-2.25 (2.00)	.023	.464
Rostral anterior cingulate	-0.33 (0.39)	.406	.898	0.14 (0.23)	.544	.873	-0.26 (0.83)	.758	.957	0.00	.991	.993	-0.02 (0.27)	.932	1.00	0.00 (0.52)	1.00	1.00
Rostral middle frontal	-0.59 (0.51)	.255	.898	-0.59 (0.39)	.133	.764	-0.71 (1.26)	.573	.957	0.46	.501	.933	-0.70 (0.45)	.130	.757	-1.31 (0.77)	.108	.496
Superior frontal	-0.53 (0.54)	.334	.898	-0.39 (0.38)	.315	.873	-0.16 (1.20)	.897	.957	0.05	.825	.970	-0.70 (0.48)	.157	.757	-0.54 (0.69)	.444	.888
Superior parietal	-0.31 (0.60)	.601	.898	-0.36 (0.43)	.410	.873	-1.10 (1.39)	.433	.957	1.40	.242	.933	-0.17 (0.47)	.714	.971	-1.26 (0.91)	.186	.578
Superior temporal	-0.25 (0.67)	.706	.946	-0.25 (0.42)	.552	.873	-1.63 (1.41)	.250	.957	0.02	.877	.993	0.00 (0.58)	1.00	1.00	0.17 (0.81)	.834	.931
Supramarginal	-0.56 (0.72)	.445	.898	-0.35 (0.49)	.478	.873	-1.11 (1.64)	.501	.957	0.61	.438	.933	-0.44 (0.57)	.446	.843	-1.25 (1.11)	.285	.692
Temporal pole	0.01 (0.30)	.965	.986	-0.01 (0.16)	.941	.975	-0.30 (0.59)	.614	.941	0.30	.584	.933	-0.04 (0.19)	.852	1.00	0.13 (0.28)	.659	.931
Transverse temporal	-0.18 (0.46)	.687	.946	-0.49 (0.27)	.070	.591	-1.09 (0.97)	.267	.957	0.00	.993	.993	-0.48 (0.39)	.228	.757	-0.55 (0.40)	.191	.578

Data are represented as β (SE) as estimated by linear mixed models. Sex, education, WMH, and age were included as covariates. Interaction terms were removed when not significant. Time in years; cortical thickness in mm. A positive beta estimate indicates the effect of cortical thinning, whereas a negative beta indicates the effect of a thicker cortical region. Significant results (p<.05) are indicated in bold. Aβ = amyloid-beta; SE = standard error; THK = thickness.

Supplementary Table 1k. Associations of hippocampal volume with baseline and decline on executive functioning performance by Aβ status.

Region	Executive Functioning (n observations = 100)											
	THK		Time X THK		THK X Aβ		Time X THK X Aβ		Time X THK in Aβ+			
	beta(se)	p	beta(se)	p	beta(se)	p	F	p	beta(se)	p		
Hippocampus	0.0007 (0.0022)	.748	-0.0010 (0.0014)	.494	-0.0045 (0.0046)	.326	0.09	.770	-0.0016 (0.00021)	.443	-0.0009 (0.00021)	.677

Data are represented as β (SE) as estimated by linear mixed models. Intracranial volume, sex, education, WMH, and age were included as covariates. Interaction terms were removed when not significant. Time in years; volume in mm3. A positive beta estimate indicates the effect of a smaller volume, whereas a negative beta indicates the effect of a larger volume. Significant results (p<.05) are indicated in bold. Aβ = amyloid-beta; SE = standard error; THK = thickness.

**Supplementary Table 2a. Baseline and annual change effect of A $\beta$  status on cognitive functioning in a subset without terminal decline.**

Fixed effects	Memory			Language			Processing Speed			Executive Function		
	beta (se)	p	pFDR	beta (se)	p	pFDR	beta (se)	p	pFDR	beta (se)	p	pFDR
A $\beta$ status	-0.38 (0.25)	.136	.181	-0.46 (0.25)	.072	.181	-0.36 (0.22)	.111	.181	-0.16 (0.21)	.454	.454
Time	-0.05 (0.06)	.380	.379	-0.09 (0.05)	.102	.368	-0.08 (0.06)	.184	.368	0.07 (0.07)	.326	.379
A $\beta$ status X time	-0.23 (0.09)	<b>.011</b>	<b>.043</b>	-0.15 (0.08)	.060	.097	-0.16 (0.09)	<b>.073</b>	<b>.097</b>	-0.12 (0.10)	.254	.254

Individuals that might have suffered from terminal decline were removed (n=43). Neuropsychological tests were Z-transformed and averaged for each cognitive domain. Linear mixed models were adjusted for age, education, WMH, and sex. Significant results ( $p < .05$ ) are indicated in bold. A $\beta$  = Amyloid-beta; SE = standard error.

**Supplementary Table 2b. Cortical thickness (mm) according to amyloid status in a subset without terminal decline.**

Brain region	A $\beta$ -, n = 27		A $\beta$ +, n = 16		p	pFDR
	Mean (SE)	95% CI	Mean (SE)	95% CI		
Banks of the superior temporal sulcus	2.33 (0.02)	2.29 - 2.37	2.25 (0.02)	2.20 - 2.30	.089	.605
Caudal anterior cingulate	2.55 (0.05)	2.44 - 2.66	2.53 (0.07)	2.39 - 2.67	.803	.859
Caudal middle frontal	2.36 (0.03)	2.31 - 2.42	2.31 (0.03)	2.24 - 2.38	.327	.695
Cuneus	1.77 (0.02)	1.72 - 1.81	1.71 (0.03)	1.65 - 1.77	.250	.695
Entorhinal	2.96 (0.08)	2.80 - 3.13	2.93 (0.10)	2.73 - 3.14	.488	.695
Frontal pole	2.68 (0.06)	2.55 - 2.80	2.61 (0.08)	2.46 - 2.77	.558	.723
Fusiform	2.47 (0.03)	2.41 - 2.53	2.37 (0.04)	2.29 - 2.44	<b>.037</b>	.420
Inferior parietal	2.24 (0.03)	2.18 - 2.29	2.18 (0.03)	2.11 - 2.24	.315	.695
Inferior temporal	2.49 (0.03)	2.43 - 2.56	2.46 (0.04)	2.38 - 2.55	.617	.723
Insula	2.73 (0.04)	2.66 - 2.81	2.75 (0.05)	2.65 - 2.85	.808	.859
Isthmus cingulate	2.06 (0.03)	2.01 - 2.12	2.07 (0.03)	2.01 - 2.13	.991	.991
Lateral occipital	1.96 (0.02)	1.91 - 2.00	1.91 (0.03)	1.85 - 1.98	.379	.695
Lateral orbitofrontal	2.42 (0.03)	2.36 - 2.48	2.35 (0.04)	2.28 - 2.43	.131	.695
Lingual	1.82 (0.02)	1.78 - 1.86	1.79 (0.02)	1.75 - 1.84	.399	.695
Medial orbitofrontal	2.22 (0.03)	2.16 - 2.27	2.12 (0.04)	2.05 - 2.19	<b>.031</b>	.420
Middle temporal	2.61 (0.03)	2.55 - 2.67	2.57 (0.04)	2.49 - 2.64	.437	.695
Paracentral	2.23 (0.03)	2.17 - 2.29	2.22 (0.04)	2.15 - 2.29	.963	.991
Parahippocampal	2.45 (0.04)	2.37 - 2.54	2.29 (0.05)	2.19 - 2.40	<b>.011</b>	.383
Pars opercularis	2.40 (0.02)	2.36 - 2.45	2.34 (0.03)	2.28 - 2.40	.350	.695
Pars orbitalis	2.52 (0.04)	2.43 - 2.61	2.48 (0.05)	2.37 - 2.59	.609	.723
Pars triangularis	2.29 (0.03)	2.23 - 2.35	2.25 (0.04)	2.18 - 2.32	.407	.695
Pericalcarine	1.56 (0.02)	1.52 - 1.60	1.51 (0.02)	1.46 - 1.56	.176	.695
Postcentral	1.96 (0.02)	1.91 - 2.01	1.88 (0.03)	1.82 - 1.94	.171	.695
Posterior cingulate	2.33 (0.03)	2.27 - 2.38	2.28 (0.03)	2.21 - 2.35	.529	.720
Precentral	2.32 (0.02)	2.27 - 2.37	2.30 (0.03)	2.24 - 2.36	.591	.723
Precuneus	2.16 (0.02)	2.11 - 2.21	2.10 (0.03)	2.04 - 2.16	.243	.695
Rostral anterior cingulate	2.66 (0.04)	2.57 - 2.74	2.57 (0.05)	2.47 - 2.68	.079	.605
Rostral middle frontal	2.25 (0.03)	2.19 - 2.31	2.20 (0.04)	2.12 - 2.27	.476	.695
Superior frontal	2.47 (0.03)	2.40 - 2.53	2.42 (0.04)	2.34 - 2.50	.478	.695
Superior parietal	2.02 (0.03)	1.97 - 2.07	1.96 (0.03)	1.90 - 2.03	.491	.695
Superior temporal	2.46 (0.03)	2.40 - 2.51	2.40 (0.03)	2.34 - 2.47	.191	.695
Supramarginal	2.30 (0.02)	2.26 - 2.35	2.26 (0.03)	2.20 - 2.32	.266	.695
Temporal pole	3.40 (0.05)	3.30 - 3.51	3.43 (0.07)	3.30 - 3.57	.720	.816
Transverse temporal	2.21 (0.04)	2.14 - 2.29	2.16 (0.05)	2.07 - 2.25	.403	.695

Individuals that might have suffered from terminal decline were removed (n=43). Group differences in cortical thickness by one-way ANOVA, adjusted for age, education, WMH, and sex. Average cortical thickness for both left and right hemisphere. Significant results (p<.05) are indicated in bold. A $\beta$  = amyloid- $\beta$ ; SE = standard error; CI = confidence interval.

**Supplementary Table 2c. Hippocampal volume according to amyloid status in a subset without terminal decline.**

	A $\beta$ -, n = 27		A $\beta$ +, n = 16		P
	Mean (SE)	95% CI	Mean (SE)	95% CI	
Hippocampal volume, mm <sup>3</sup>	3052 (79)	2893 - 3212	3037 (92)	2850 - 3224	.999

Individuals that might have suffered from terminal decline were removed (n=43). Group difference in hippocampal volume by one-way ANOVA, adjusted for intracranial volume, age, education, WMH, and sex. A $\beta$  = amyloid- $\beta$ ; SE = standard error; CI = confidence interval.

Supplementary Table 2.d. Associations of cortical thickness with baseline and decline on memory performance by  $\beta$  status in a subset without terminal decline.

Region	THK		Time X THK		THK X $\beta$		Time X THK X $\beta$		Time X THK in $\beta^-$		Time X THK in $\beta^+$							
	beta(se)	p	beta(se)	p	beta(se)	p	F	p	beta(se)	p	beta(se)	p						
Banks of the superior temporal sulcus	0.91 (1.31)	.488	.820	0.26 (0.47)	.586	.829	2.48 (2.64)	.353	.975	2.66	1.11	.979	-0.59 (0.53)	.273	.580	0.99 (0.83)	.252	.636
Caudal anterior cingulate	0.24 (0.49)	.627	.820	0.45 (0.17)	.012	.051	0.71 (0.94)	.453	.975	0.14	7.08	.979	0.34 (0.26)	.207	.562	0.45 (0.21)	.055	.313
Caudal middle frontal	1.36 (1.00)	.178	.673	0.26 (0.45)	.575	.829	-1.31 (2.54)	.608	.999	0.33	5.70	.979	-0.29 (0.52)	.581	.791	0.26 (0.83)	.757	.968
Cuneus	-0.49 (1.19)	.679	.855	0.14 (0.51)	.792	.374	3.99 (2.27)	.067	.975	0.25	6.19	.979	-0.09 (0.63)	.889	.916	-0.60 (0.81)	.407	.968
Entorhinal	0.53 (0.30)	.088	.673	0.39 (0.10)	<0.001	.003	0.26 (0.60)	.668	.999	1.36	2.51	.979	0.31 (0.11)	.010	.119	0.54 (0.17)	.007	.077
Frontal pole	0.50 (0.42)	.246	.814	0.27 (0.15)	.088	.250	0.59 (0.85)	.488	.975	0.01	9.24	.981	0.16 (0.20)	.443	.722	0.16 (0.25)	.524	.968
Fusiform	1.13 (0.82)	.174	.673	0.87 (0.31)	.007	.041	1.72 (1.96)	.386	.975	0.63	4.32	.979	0.54 (0.36)	.151	.562	1.05 (0.62)	.111	.420
Inferior parietal	0.61 (1.05)	.568	.820	0.05 (0.41)	.905	.929	0.67 (2.38)	.779	.999	0.17	6.85	.979	-0.33 (0.47)	.496	.733	-0.03 (0.70)	.971	.986
Inferior temporal	1.14 (0.79)	.157	.673	0.74 (0.32)	.025	.085	0.27 (1.72)	.878	.999	0.26	6.14	.979	0.47 (0.44)	.296	.592	0.72 (0.46)	.138	.428
Insula	0.39 (0.70)	.586	.820	0.80 (0.21)	<0.001	.003	1.10 (1.43)	.448	.975	1.00	3.23	.979	0.60 (0.24)	.017	.147	1.08 (0.44)	.028	.236
Isthmus cingulate	0.75 (1.05)	.478	.820	0.84 (0.41)	.049	.152	0.87 (2.05)	.674	.999	0.12	7.28	.979	0.65 (0.45)	.164	.562	0.88 (0.77)	.272	.636
Lateral occipital	0.32 (1.15)	.781	.915	0.48 (0.47)	.310	.594	2.83 (2.32)	.229	.975	0.00	9.88	.988	0.28 (0.64)	.665	.837	0.20 (0.65)	.761	.968
Lateral orbitofrontal	0.08 (0.91)	.933	.961	0.50 (0.33)	.142	.372	2.92 (1.95)	.141	.975	0.07	7.95	.979	0.17 (0.38)	.662	.837	0.39 (0.74)	.604	.968
Lingual	-0.15 (1.52)	.924	.961	0.28 (0.60)	.644	.829	0.01 (3.37)	.998	.999	0.10	7.54	.979	0.21 (0.71)	.770	.846	-0.22 (0.47)	.823	.968
Medial orbitofrontal	0.76 (0.91)	.409	.820	0.27 (0.28)	.353	.632	1.34 (1.79)	.458	.975	0.09	7.66	.979	-0.03 (0.42)	.935	.935	-0.20 (0.48)	.681	.968
Middle temporal	1.87 (0.83)	.030	.664	0.92 (0.36)	.014	.051	-0.28 (1.89)	.883	.999	0.75	3.91	.979	0.56 (0.44)	.215	.562	1.08 (0.56)	.074	.313
Paracentral	0.47 (0.95)	.622	.820	-0.40 (0.32)	.229	.518	-1.99 (1.90)	.301	.975	0.31	5.83	.979	-0.65 (0.36)	.088	.497	-0.30 (0.53)	.579	.968
Parahippocampal	0.91 (0.53)	.094	.673	0.76 (0.15)	<0.001	<0.001	1.26 (1.05)	.239	.975	0.41	5.26	.979	0.63 (0.22)	.008	.119	0.83 (0.25)	.005	.077
Pars opercularis	0.76 (1.12)	.502	.820	-0.11 (0.38)	.773	.874	-2.55 (2.34)	.283	.975	0.59	4.46	.979	-0.64 (0.49)	.202	.562	-0.12 (0.56)	.826	.968
Pars orbitalis	0.44 (0.64)	.500	.820	-0.05 (0.24)	.833	.885	0.91 (1.27)	.480	.975	0.69	4.12	.979	-0.29 (0.25)	.264	.580	0.13 (0.48)	.790	.968
Pars triangularis	-0.01 (0.97)	.994	.994	0.21 (0.41)	.610	.829	0.02 (2.52)	.992	.999	0.00	9.55	.984	-0.12 (0.43)	.775	.846	-0.09 (1.11)	.937	.986
Pericalcarine	0.34 (1.44)	.813	.922	0.84 (0.59)	.163	.397	0.27 (3.79)	.944	.999	0.02	8.87	.979	0.71 (0.61)	.255	.580	0.35 (1.30)	.791	.968
Postcentral	1.63 (1.06)	.131	.673	-0.11 (0.42)	.797	.874	1.32 (2.68)	.625	.999	0.02	8.93	.979	-0.39 (0.44)	.383	.722	-0.38 (0.86)	.667	.968
Posterior cingulate	0.17 (0.98)	.862	.945	0.03 (0.36)	.929	.929	-0.28 (2.07)	.893	.999	0.30	5.86	.979	0.17 (0.51)	.735	.846	-0.24 (0.47)	.616	.968
Precentral	1.14 (1.12)	.314	.820	-0.18 (0.40)	.658	.829	2.24 (2.37)	.349	.975	0.72	4.03	.979	-0.66 (0.44)	.146	.562	0.04 (0.74)	.962	.986
Precuneus	0.96 (1.09)	.385	.820	-0.28 (0.42)	.499	.772	0.00 (2.69)	.999	.999	0.90	3.49	.979	-0.32 (0.42)	.456	.722	-1.31 (0.94)	.185	.524
Rosral anterior cingulate	0.19 (0.62)	.766	.915	0.74 (0.19)	<0.001	.003	1.95 (1.19)	.108	.975	0.78	3.82	.979	0.53 (0.24)	.034	.229	0.92 (0.42)	.045	.303
Rosral middle frontal	0.54 (0.94)	.566	.820	0.29 (0.40)	.474	.768	1.00 (2.26)	.661	.999	0.04	8.41	.979	-0.12 (0.45)	.796	.846	-0.01 (0.80)	.986	.986
Superior frontal	0.95 (0.87)	.282	.814	0.39 (0.38)	.315	.594	0.33 (1.93)	.867	.999	2.10	1.55	.979	-0.39 (0.47)	.420	.722	0.69 (0.62)	.081	.636
Superior parietal	1.42 (1.01)	.165	.673	-0.37 (0.43)	.389	.661	-0.41 (2.15)	.851	.999	0.20	6.60	.979	-0.62 (0.44)	.170	.562	-0.25 (0.90)	.784	.968
Superior temporal	2.02 (0.95)	.039	.664	1.05 (0.39)	.011	.051	-1.79 (2.20)	.420	.975	1.46	2.34	.979	0.36 (0.55)	.524	.742	1.34 (0.67)	.065	.313
Supramarginal	1.20 (1.11)	.287	.814	0.52 (0.48)	.281	.594	0.93 (2.63)	.725	.999	3.11	0.86	.979	-0.40 (0.54)	.467	.722	1.47 (0.94)	.138	.428
Temporal pole	0.31 (0.50)	.532	.820	0.55 (0.13)	<0.001	.002	0.60 (0.85)	.488	.975	0.20	6.60	.979	0.57 (0.14)	.000	.014	0.66 (0.19)	.003	.077
Transverse temporal	0.57 (0.74)	.444	.848	0.11 (0.27)	.696	.845	0.09 (1.56)	.954	.999	0.05	8.22	.979	-0.12 (0.38)	.746	.846	-0.03 (0.37)	.947	.986

Supplementary Table 2e. Associations of hippocampal volume with baseline and decline on memory performance by  $\beta$  status in a subset without terminal decline. Individuals that might have suffered from terminal decline were removed (n=43). Data are represented as  $\beta$  (SE) as estimated by linear mixed models. Sex, education, WMH, and age were included as covariates. Interaction terms were removed when not significant. Time in years; volume in mm<sup>3</sup>. A positive beta estimate indicates the effect of a larger volume. Significant results (p<.05) are indicated in bold.  $\beta$  = amyloid-beta; SE = standard error; THK = thickness.

Supplementary Table 2f. Associations of cortical thickness with baseline and decline on language performance by Aβ status in a subset without terminal decline.

Region	Language (n observations = 86)																	
	THK		Time X THK		THK X Aβ		Time X THK X Aβ		Time X THK in Aβ-		Time X THK in Aβ+							
	beta(se)	p	beta(se)	p	beta(se)	p	F	p	beta(se)	p	beta(se)	p						
Banks of the superior temporal sulcus	-0.26 (1.29)	.842	.968	0.70 (0.39)	.079	1.59	-3.86 (2.51)	1.32	.561	0.00	.947	.947	0.47 (0.50)	.348	.438	0.53 (0.69)	.456	1.00
Caudal anterior cingulate	0.17 (0.50)	.729	.968	0.19 (0.16)	.229	3.12	-0.65 (0.94)	.492	.812	0.74	.396	.722	0.01 (0.25)	.977	.977	0.04 (0.68)	.953	1.00
Caudal middle frontal	-0.10 (1.00)	.920	.968	0.81 (0.37)	.035	1.36	-2.39 (2.47)	.339	.720	1.25	.270	.706	0.90 (0.46)	.062	.231	0.04 (0.68)	.953	1.00
Cuneus	-0.96 (1.15)	.411	.838	-0.07 (0.44)	.878	9.33	0.63 (2.25)	.780	.829	0.90	.349	.722	0.03 (0.59)	.959	.977	-0.85 (0.64)	.203	.926
Entorhinal	0.49 (0.31)	.127	.838	0.19 (0.10)	.053	1.59	-0.35 (0.63)	.580	.822	0.07	.786	.835	0.19 (0.11)	.108	.262	0.14 (0.18)	.431	1.00
Frontal pole	-0.04 (0.43)	.929	.968	0.12 (0.13)	.368	4.47	-0.33 (0.85)	.704	.829	1.67	.204	.692	0.22 (0.19)	.259	.376	-0.16 (0.20)	.441	1.00
Fusiform	-0.07 (0.86)	.931	.968	0.58 (0.27)	.039	1.36	-0.98 (2.01)	.628	.829	0.56	.458	.742	0.60 (0.34)	.089	.253	0.10 (0.54)	.856	1.00
Inferior parietal	-0.84 (1.03)	.420	.838	0.52 (0.34)	.134	2.27	-3.70 (2.20)	.100	.561	0.69	.413	.722	0.59 (0.43)	.180	.322	0.02 (0.56)	.978	1.00
Inferior temporal	0.03 (0.82)	.968	.968	0.59 (0.28)	.038	1.36	-0.63 (1.77)	.725	.829	0.76	.389	.722	0.74 (0.39)	.073	.231	0.23 (0.40)	.566	1.00
Insula	0.26 (0.71)	.721	.968	0.28 (0.21)	.191	2.71	1.95 (1.44)	.182	.618	0.32	.577	.742	0.26 (0.24)	.288	.392	0.00 (0.43)	1.00	1.00
Isthmus cingulate	-0.89 (1.05)	.399	.838	0.51 (0.37)	.168	2.48	2.07 (2.03)	.315	.720	2.19	1.46	.618	0.78 (0.42)	.075	.231	-0.39 (0.65)	.562	1.00
Lateral occipital	-1.02 (1.11)	.364	.838	-0.03 (0.41)	.932	9.36	1.30 (2.24)	.565	.822	0.35	.560	.742	0.09 (0.61)	.891	.946	-0.44 (0.52)	.414	1.00
Lateral orbitofrontal	-1.19 (0.88)	.183	.838	0.48 (0.29)	.099	1.77	1.50 (1.89)	.432	.812	0.30	.590	.742	0.41 (0.36)	.260	.376	0.01 (0.60)	.982	1.00
Lingual	-2.18 (1.46)	.142	.838	0.42 (0.51)	.412	4.75	1.27 (3.15)	.688	.829	3.09	.087	.589	0.96 (0.64)	.147	.319	-0.78 (0.76)	.320	1.00
Medial orbitofrontal	0.21 (0.90)	.817	.968	0.50 (0.23)	.040	1.36	0.42 (1.76)	.811	.835	0.40	.529	.742	0.50 (0.38)	.197	.336	0.19 (0.39)	.651	1.00
Middle temporal	1.12 (0.89)	.215	.838	0.46 (0.32)	.164	2.48	-2.09 (1.95)	.289	.720	2.46	1.25	.606	0.75 (0.40)	.075	.231	-0.27 (0.50)	.601	1.00
Paracentral	-0.61 (0.93)	.520	.884	0.48 (0.27)	.087	1.65	-1.80 (1.84)	.335	.720	2.02	1.64	.618	0.70 (0.33)	.046	.231	-0.03 (0.43)	.944	1.00
Parahippocampal	1.32 (0.55)	.021	.726	0.12 (0.16)	.479	5.25	2.53 (1.05)	.020	.353	2.56	1.17	.606	0.22 (0.23)	.340	.438	-0.32 (0.25)	.218	.926
Pars opercularis	-1.13 (1.10)	.311	.838	0.67 (0.31)	.035	1.36	-5.12 (2.13)	.021	.353	0.18	.676	.742	0.42 (0.47)	.373	.453	0.66 (0.42)	.135	.926
Pars orbitalis	-0.96 (0.62)	.127	.838	0.20 (0.21)	.330	4.15	-0.82 (1.22)	.502	.812	0.06	.814	.838	0.13 (0.24)	.585	.663	0.04 (0.39)	.927	1.00
Pars triangularis	-1.15 (0.94)	.230	.838	0.52 (0.35)	.140	2.27	-4.67 (2.24)	.043	.491	0.71	.403	.722	0.45 (0.39)	.265	.376	-0.45 (0.90)	.627	1.00
Pericalcarine	-0.35 (1.42)	.808	.968	0.04 (0.52)	.936	9.36	1.08 (3.67)	.771	.829	1.51	.226	.698	0.25 (0.59)	.678	.744	-1.30 (1.01)	.217	.926
Postcentral	0.15 (1.06)	.887	.968	0.75 (0.34)	.033	1.36	-3.89 (2.49)	.126	.561	3.72	.061	.578	1.00 (0.38)	.014	.188	-0.56 (0.69)	.432	1.00
Posterior cingulate	-1.33 (0.95)	.172	.838	0.96 (0.27)	.001	.028	-1.36 (1.97)	.493	.812	0.23	.637	.742	1.06 (0.43)	.021	.188	0.81 (0.31)	.021	.729
Precentral	-0.67 (1.10)	.547	.886	0.28 (0.35)	.419	4.75	-0.82 (2.30)	.724	.829	4.33	.444	.578	0.58 (0.41)	.172	.322	-0.07 (0.56)	.138	.926
Preuncus	-0.78 (1.07)	.468	.838	0.64 (0.35)	.071	1.59	-4.42 (2.45)	.079	.561	0.65	.425	.722	0.65 (0.38)	.100	.262	-0.07 (0.81)	.931	1.00
Rosral anterior cingulate	0.19 (0.62)	.768	.968	0.34 (0.19)	.074	1.59	-0.13 (1.24)	.916	.916	0.20	.656	.742	0.29 (0.24)	.236	.376	0.09 (0.39)	.825	1.00
Rosral middle frontal	-0.70 (0.92)	.450	.838	0.60 (0.33)	.078	1.59	-2.46 (2.14)	.257	.720	0.70	.408	.722	0.59 (0.41)	.164	.322	-0.11 (0.65)	.866	1.00
Superior frontal	-0.84 (0.87)	.340	.838	0.70 (0.31)	.031	1.36	-1.32 (1.90)	.492	.812	1.34	.254	.706	0.82 (0.42)	.059	.231	0.05 (0.52)	.925	1.00
Superior parietal	0.08 (1.00)	.940	.968	0.66 (0.36)	.073	1.59	-2.62 (2.01)	.200	.620	6.08	.018	.188	1.01 (0.37)	.011	.188	-0.92 (0.70)	.208	.926
Superior temporal	0.75 (1.01)	.465	.838	0.76 (0.35)	.036	1.36	-3.30 (2.25)	.150	.565	0.37	.546	.742	0.75 (0.51)	.150	.319	0.26 (0.61)	.680	1.00
Supramarginal	-0.94 (1.11)	.403	.838	0.92 (0.39)	.024	1.36	-1.62 (2.57)	.533	.822	3.52	.068	.578	1.12 (0.46)	.022	.188	-0.55 (0.81)	.506	1.00
Supramarginal	0.14 (0.51)	.792	.968	0.25 (0.13)	.062	1.59	0.27 (0.89)	.762	.829	0.20	.161	.742	0.32 (0.16)	.052	.231	0.20 (0.20)	.345	1.00
Transverse temporal	-0.60 (0.73)	.413	.838	0.25 (0.23)	.284	3.71	2.37 (1.45)	.109	.561	0.24	.628	.742	0.29 (0.35)	.418	.491	0.05 (0.30)	.868	1.00

Individuals that might have suffered from terminal decline were removed (n=43). Data are represented as β (SE) as estimated by linear mixed models. Sex, education, WMH, and age were included as covariates. Interaction terms were removed when not significant. Time in years; cortical thickness in mm. A positive beta estimate indicates the effect of a smaller volume, whereas a negative beta indicates the effect of a thicker cortical region. Significant results (p<.05) are indicated in bold. Aβ = amyloid-beta; SE = standard error; THK = thickness.

Supplementary Table 2g. Associations of hippocampal volume with baseline and decline on language performance by Aβ status in a subset without terminal decline.

Region	Language (n observations = 86)											
	THK		Time X THK		THK X Aβ		Time X THK X Aβ		Time X THK in Aβ-		Time X THK in Aβ+	
	beta(se)	p	beta(se)	p	beta(se)	p	F	p	beta(se)	p	beta(se)	p
Hippocampus	0.00115 (0.00037)	.681	0.00009 (0.00012)	.440	-0.00103 (0.00073)	.166	0.33	.482	0.00001 (0.00019)	.949	0.00018 (0.00014)	.221

Individuals that might have suffered from terminal decline were removed (n=43). Data are represented as β (SE) as estimated by linear mixed models. Intracranial volume, sex and age were included as covariates. Interaction terms were removed when not significant. Time in years; volume in mm<sup>3</sup>. A positive beta estimate indicates the effect of a smaller volume, whereas a negative beta indicates the effect of a larger volume. Significant results (p<.05) are indicated in bold. Aβ = amyloid-beta; SE = standard error; THK = thickness.

Supplementary Table 2h. Associations of cortical thickness with baseline and decline on processing speed performance by Aβ status in a subset without terminal decline.

Region	Processing Speed (n observations = 85)																	
	THK		Time X THK		THK X Aβ		Time X THK X Aβ		Time X THK in Aβ+									
	beta(se)	p	beta(se)	p	beta(se)	p	F	p	beta(se)	p								
Banks of the superior temporal sulcus	-0.60 (0.113)	.598	.750	0.58 (0.045)	.203	.983	1.58 (2.22)	.480	.770	1.74	.195	.435	0.74 (0.40)	.074	.992	-0.48 (1.11)	.670	.735
Caudal anterior cingulate	-0.22 (0.44)	.218	.750	0.31 (0.18)	.088	.983	-0.76 (0.83)	.365	.770	0.62	.437	.551	-0.10 (0.21)	.632	.992	0.46 (0.31)	.171	.478
Caudal middle frontal	-0.94 (0.88)	.289	.468	0.33 (0.43)	.451	.983	-0.64 (1.6)	.767	.912	1.19	.281	.531	0.35 (0.41)	.396	.992	-0.54 (0.06)	.619	.702
Cuneus	-1.20 (0.99)	.232	.467	-0.63 (0.49)	.203	.983	1.27 (1.86)	.498	.770	11.38	.002	.057	0.27 (0.49)	.575	.992	-0.74 (0.29)	.004	.139
Entorhinal	0.39 (0.29)	.184	.467	0.00 (0.11)	.968	.983	-0.10 (0.59)	.869	.912	0.01	.911	.911	-0.03 (0.10)	.773	.992	0.20 (0.79)	.897	.897
Frontal pole	-0.53 (0.37)	.155	.467	-0.09 (0.15)	.558	.983	0.65 (0.72)	.367	.770	9.55	.004	.062	0.18 (0.16)	.269	.992	-0.70 (0.26)	.017	.284
Fusiform	-0.28 (0.77)	.713	.836	0.05 (0.33)	.868	.983	-0.26 (1.78)	.885	.912	2.92	.095	.324	0.20 (0.30)	.511	.992	-1.14 (0.82)	.191	.478
Inferior parietal	-1.45 (0.89)	.109	.467	-0.10 (0.40)	.983	.983	-5.93 (1.80)	.033	.351	3.36	.551	.585	0.00 (0.38)	.992	.992	-0.48 (0.88)	.592	.694
Inferior temporal	-0.43 (0.73)	.262	.750	0.10 (0.33)	.752	.983	-0.59 (1.56)	.710	.894	0.15	.703	.724	0.06 (0.35)	.861	.992	-0.15 (0.63)	.875	.840
Insula	-0.69 (0.62)	.270	.468	0.20 (0.23)	.395	.983	0.99 (1.27)	.438	.770	1.03	.316	.541	-0.04 (0.21)	.831	.992	0.62 (0.67)	.378	.612
Isthmus cingulate	-1.48 (0.89)	.105	.467	-0.14 (0.43)	.737	.983	1.27 (1.79)	.482	.770	0.69	.411	.541	-0.03 (0.37)	.932	.992	-1.07 (1.09)	.343	.584
Lateral occipital	-1.39 (0.94)	.146	.467	-0.64 (0.45)	.161	.983	0.32 (1.86)	.865	.912	0.78	.382	.541	-0.39 (0.51)	.453	.992	-1.22 (0.77)	.138	.469
Lateral orbitofrontal	-0.90 (0.77)	.251	.468	0.07 (0.33)	.835	.983	1.12 (1.66)	.944	.944	0.89	.352	.541	-0.20 (0.30)	.505	.992	-0.90 (0.90)	.337	.584
Lingual	-2.68 (1.24)	.036	.467	-0.17 (0.59)	.778	.983	-2.88 (2.58)	.270	.770	2.00	.164	.399	0.30 (0.56)	.601	.992	-1.40 (1.21)	.267	.566
Medial orbitofrontal	-0.11 (0.80)	.892	.954	0.02 (0.28)	.944	.983	1.19 (1.54)	.446	.770	0.94	.337	.541	-0.09 (0.33)	.788	.992	-0.59 (0.60)	.339	.584
Middle temporal	0.11 (0.83)	.898	.954	0.01 (0.38)	.970	.983	-1.61 (1.82)	.380	.770	0.48	.494	.563	0.08 (0.36)	.833	.992	-0.49 (0.81)	.556	.677
Paracentral	-0.57 (0.81)	.487	.719	-0.29 (0.31)	.351	.983	-0.86 (1.62)	.598	.884	2.05	.160	.399	-0.07 (0.30)	.821	.992	-0.86 (0.63)	.197	.478
Parahippocampal	0.85 (0.50)	.099	.467	0.12 (0.18)	.502	.983	2.49 (0.95)	.012	.197	1.66	.205	.435	0.18 (0.19)	.355	.992	-0.31 (0.41)	.467	.635
Pars opercularis	-1.53 (0.95)	.115	.467	0.44 (0.36)	.232	.983	-4.83 (1.81)	.011	.197	0.68	.414	.541	-0.02 (0.40)	.969	.992	0.59 (0.68)	.396	.613
Pars orbitalis	-0.69 (0.55)	.214	.467	0.04 (0.24)	.874	.983	-1.36 (1.06)	.206	.770	0.88	.353	.541	0.04 (0.20)	.853	.992	-0.51 (0.62)	.426	.629
Pars triangularis	-1.30 (0.81)	.115	.467	-0.22 (0.40)	.577	.983	-3.87 (1.84)	.041	.351	1.37	.248	.496	-0.38 (0.33)	.262	.992	-1.80 (1.37)	.213	.482
Percalcarine	-0.68 (1.25)	.586	.750	-0.12 (0.58)	.841	.983	2.78 (3.16)	.385	.770	0.39	.536	.585	-0.09 (0.49)	.858	.992	-0.99 (1.65)	.558	.677
Postcentral	0.09 (0.94)	.927	.955	-0.23 (0.40)	.574	.983	-2.75 (2.19)	.215	.770	5.34	.026	.179	0.06 (0.36)	.859	.992	-1.96 (0.96)	.062	.352
Posterior cingulate	-1.63 (0.82)	.054	.467	0.59 (0.33)	.084	.983	-1.77 (1.70)	.301	.770	2.57	.117	.363	-0.10 (0.40)	.806	.992	0.96 (0.54)	.099	.374
Precentral	-1.19 (0.95)	.218	.467	-0.02 (0.39)	.950	.983	-0.83 (1.97)	.676	.894	5.87	.020	.170	0.36 (0.35)	.312	.992	-1.53 (0.86)	.097	.374
Precuneus	-1.31 (0.93)	.166	.467	0.02 (0.41)	.952	.983	-3.38 (2.05)	.106	.723	3.56	.066	.281	0.20 (0.34)	.562	.992	-1.77 (1.42)	.167	.478
Rostral anterior cingulate	-0.28 (0.55)	.618	.750	0.15 (0.22)	.497	.983	0.43 (1.09)	.698	.894	0.47	.497	.563	0.06 (0.20)	.778	.992	-0.19 (0.62)	.767	.815
Rostral middle frontal	-1.09 (0.80)	.179	.467	-0.13 (0.39)	.733	.983	-1.33 (1.79)	.461	.770	4.66	.037	.202	0.03 (0.36)	.929	.992	-1.93 (0.93)	.058	.352
Superior frontal	-0.91 (0.75)	.233	.467	-0.30 (0.37)	.420	.983	0.25 (1.61)	.875	.912	4.44	.042	.202	-0.06 (0.38)	.884	.992	-1.51 (0.70)	.049	.352
Superior parietal	-0.62 (0.88)	.486	.719	-0.38 (0.42)	.369	.983	-1.71 (1.71)	.323	.770	6.49	.015	.166	0.02 (0.36)	.956	.992	-2.49 (1.03)	.029	.334
Superior temporal	0.00 (0.93)	.997	.997	0.09 (0.41)	.823	.983	-0.82 (2.11)	.700	.894	0.52	.474	.563	-0.13 (0.44)	.775	.992	-0.61 (0.97)	.539	.677
Supramarginal	-1.32 (0.97)	.179	.467	0.04 (0.47)	.930	.983	-1.55 (2.17)	.479	.770	2.97	.093	.324	0.06 (0.43)	.894	.992	-1.43 (1.28)	.291	.582
Temporal pole	-0.09 (0.45)	.852	.954	0.05 (0.15)	.716	.983	0.20 (0.80)	.809	.912	0.76	.389	.541	-0.02 (0.14)	.904	.992	0.25 (0.32)	.463	.635
Transverse temporal	-0.68 (0.63)	.283	.468	-0.36 (0.25)	.165	.983	-1.33 (1.23)	.286	.770	2.01	.164	.399	-0.10 (0.30)	.734	.992	-0.78 (0.42)	.087	.374

Individuals that might have suffered from terminal decline were removed (n=43). Data are represented as β (SE) as estimated by linear mixed models. Sex, education on WHM, and age were included as covariates. Interaction terms were removed when not significant. Time in years; cortical thickness in mm. A positive beta estimate indicates the effect of cortical thinning, whereas a negative beta indicates the effect of a thicker cortical region. Significant results (p<.05) are indicated in bold. Aβ = amyloid-beta; SE = standard error; THK = thickness.

Supplementary Table 2l. Associations of hippocampal volume with baseline and decline on processing speed performance by Aβ status in a subset without terminal decline.

Region	Processing Speed (n observations = 85)											
	THK		Time X THK		THK X Aβ		Time X THK X Aβ		Time X THK in Aβ+			
	beta(se)	p	beta(se)	p	beta(se)	p	F	p	beta(se)	p		
Hippocampus	0.00070 (0.00030)	.02	-0.00017 (0.00013)	.204	-0.00066 (0.00060)	.277	0.11	.642	-0.00023 (0.00015)	.153	-0.00009 (0.00024)	.708

Individuals that might have suffered from terminal decline were removed (n=43). Data are represented as β (SE) as estimated by linear mixed models. Intracranial volume, sex and age were included as covariates. Interaction terms were removed when not significant. Time in years; volume in mm3. A positive beta estimate indicates the effect of a smaller volume, whereas a negative beta indicates the effect of a larger volume. Significant results (p<.05) are indicated in bold. Aβ = amyloid-beta; SE = standard error; THK = thickness.



Supplementary Table 21. Associations of cortical thickness with baseline and decline on executive functioning performance by Aβ status in a subset without terminal decline.

Region	Executive Functioning (n observations = 86)															
	THK		Time X THK		THK X Aβ		Time X THK X Aβ		Time X THK in Aβ-		Time X THK in Aβ+					
	beta(se)	p	beta(se)	p	beta(se)	p	F	p	beta(se)	p	beta(se)	p				
Banks of the superior temporal sulcus	-0.21 (1.04)	.840	.985	0.23 (0.51)	.657	.885	3.91	.055	.466	0.73 (0.59)	.226	.730	-1.43 (0.96)	1.54	.569	
Caudal anterior cingulate	-0.05 (0.40)	.892	.996	-0.17 (0.20)	.400	.885	3.33	.069	.961	-0.36 (0.29)	.227	.730	-0.02 (0.31)	1.95	.986	
Caudal middle frontal	-0.27 (0.81)	.743	.985	0.11 (0.49)	.819	.898	0.32	.577	.961	0.06 (0.59)	.914	.953	-0.40 (0.99)	.693	.986	
Cuneus	-1.17 (0.90)	.202	.724	-0.43 (0.55)	.443	.885	1.25	(1.87)	.728	.921	4.43	.042	.466	0.30 (0.71)	.677	.918
Entorhinal	-0.01 (0.27)	.966	.996	-0.04 (0.13)	.751	.885	0.22	.639	.961	-0.10 (0.14)	.477	.810	0.07 (0.26)	.792	.442	
Frontal pole	-0.40 (0.34)	.247	.724	-0.06 (0.17)	.724	.885	0.28	(0.71)	.690	.921	0.01	.917	.810	-0.12 (0.29)	.685	.986
Fusiform	0.01 (0.70)	.994	.996	0.22 (0.37)	.544	.885	2.78	1.03	.702	0.48 (0.42)	.258	.730	-0.93 (0.75)	.238	.577	
Inferior parietal	-0.86 (0.81)	.291	.724	-0.56 (0.44)	.206	.885	1.53	(1.83)	.406	.921	0.40	.908	.810	-0.91 (0.78)	.256	.581
Inferior temporal	-0.21 (0.67)	.754	.985	-0.05 (0.37)	.890	.946	1.97	(1.46)	.184	.921	0.03	.865	.961	-0.11 (0.05)	.821	.918
Insula	-0.60 (0.57)	.293	.724	0.11 (0.27)	.679	.885	0.27	(1.24)	.831	.921	1.66	.205	.961	-0.18 (0.29)	.539	.873
Isthmus cingulate	-0.55 (0.84)	.511	.789	0.46 (0.47)	.335	.885	-0.41	(1.75)	.817	.921	0.25	.623	.961	0.24 (0.53)	.655	.918
Lateral occipital	-0.88 (0.86)	.314	.724	-0.97 (0.49)	.056	.834	0.19	(1.83)	.917	.921	0.44	.513	.961	-0.75 (0.72)	.306	.772
Lateral orbitofrontal	-1.06 (0.69)	.133	.724	-0.17 (0.37)	.642	.885	-0.84	(1.57)	.595	.921	0.46	.502	.961	-0.61 (0.42)	.158	.730
Lingual	-1.78 (1.16)	.132	.724	-0.19 (0.65)	.779	.885	0.49	(2.64)	.855	.921	4.72	.036	.466	0.77 (0.78)	.337	.772
Medial orbitofrontal	-0.08 (0.73)	.913	.996	-0.13 (0.31)	.674	.885	0.86	(1.46)	.558	.921	1.22	.277	.961	-0.86 (0.44)	.060	.730
Middle temporal	0.15 (0.75)	.840	.985	-0.23 (0.42)	.580	.885	-1.47	(1.73)	.399	.921	0.00	.958	.961	-0.38 (0.51)	.459	.810
Paracentral	-0.75 (0.74)	.320	.724	0.10 (0.36)	.781	.885	-0.17	(1.58)	.915	.921	0.60	.442	.961	0.24 (0.43)	.590	.911
Parahippocampal	0.45 (0.47)	.341	.724	0.20 (0.20)	.335	.885	0.59	(0.97)	.542	.921	0.06	.811	.961	0.06 (0.28)	.826	.918
Pars opercularis	-0.84 (0.85)	.328	.724	-0.76 (0.40)	.060	.834	-0.78	(1.81)	.667	.921	0.03	.874	.961	-0.90 (0.54)	.108	.730
Pars orbitalis	-0.36 (0.50)	.469	.769	-0.28 (0.26)	.283	.885	-1.05	(1.04)	.318	.921	0.06	.810	.961	-0.43 (0.28)	.135	.730
Pars triangularis	-1.15 (0.73)	.120	.724	-0.60 (0.44)	.185	.885	-2.36	(1.84)	.206	.921	0.40	.533	.961	-0.80 (0.46)	.090	.730
Pericalcarine	-1.67 (1.12)	.141	.724	0.29 (0.66)	.667	.885	-1.42	(3.02)	.641	.921	0.00	.961	.961	0.16 (0.70)	.818	.918
Postcentral	-0.21 (0.85)	.802	.985	-0.80 (0.44)	.074	.834	-1.00	(2.15)	.643	.921	0.45	.506	.961	-0.84 (0.48)	.095	.730
Posterior cingulate	0.00 (0.78)	.996	.996	-0.27 (0.39)	.494	.885	-0.86	(1.69)	.613	.921	0.63	.434	.961	0.05 (0.58)	.925	.953
Precentral	-0.80 (0.88)	.366	.733	0.47 (0.44)	.732	.885	-0.68	(1.96)	.732	.921	0.93	.340	.961	0.61 (0.50)	.232	.730
Precuneus	-0.62 (0.86)	.475	.769	0.00 (0.46)	.994	.994	-1.39	(2.10)	.509	.921	7.14	.011	.367	0.39 (0.48)	.421	.810
Rostral anterior cingulate	-0.37 (0.50)	.467	.769	0.11 (0.25)	.667	.885	-0.75	(1.04)	.477	.921	0.01	.907	.961	-0.07 (0.29)	.813	.918
Rostral middle frontal	-0.70 (0.72)	.337	.724	-0.62 (0.42)	.153	.885	-0.32	(1.77)	.857	.921	0.86	.359	.961	-0.70 (0.49)	.167	.730
Superior frontal	-1.01 (0.68)	.143	.724	-0.31 (0.42)	.464	.885	-0.15	(1.53)	.921	.921	0.00	.953	.961	-0.62 (0.52)	.246	.730
Superior parietal	-0.57 (0.80)	.473	.769	-0.31 (0.47)	.515	.885	-1.15	(1.72)	.508	.921	1.51	.226	.961	-0.11 (0.51)	.837	.918
Superior temporal	-0.47 (0.85)	.580	.857	0.27 (0.46)	.563	.885	-2.06	(1.95)	.296	.921	0.02	.900	.961	0.03 (0.63)	.959	.959
Supramarginal	-1.28 (0.88)	.150	.724	-0.19 (0.53)	.721	.885	-1.05	(2.08)	.618	.921	0.94	.338	.961	-0.28 (0.61)	.652	.918
Transverse pole	-0.11 (0.41)	.784	.985	-0.01 (0.17)	.967	.994	-0.32	(0.77)	.684	.921	0.18	.674	.961	-0.05 (0.20)	.791	.918
Transverse temporal	-0.57 (0.57)	.324	.724	-0.42 (0.29)	.150	.885	-0.49	(1.22)	.692	.921	0.11	.742	.961	-0.41 (0.42)	.341	.772

Individuals that might have suffered from terminal decline were removed (n=43). Data are represented as β (SE) as estimated by linear mixed models. Sex, education, WMH, and age were included as covariates. Interaction terms were removed when not significant. Time in years; volume in mm<sup>3</sup>. A positive beta estimate indicates the effect of a smaller volume, whereas a negative beta indicates the effect of a thicker cortical region. Significant results (p<.05) are indicated in bold. Aβ = amyloid-beta; SE = standard error; THK = thickness.

Supplementary Table 2k. Associations of hippocampal volume with baseline and decline on executive functioning performance by Aβ status in a subset without terminal decline.

Region	Executive Functioning (n observations = 86)											
	THK		Time X THK		THK X Aβ		Time X THK X Aβ		Time X THK in Aβ-		Time X THK in Aβ+	
	beta(se)	p	beta(se)	p	beta(se)	p	F	p	beta(se)	p	beta(se)	p
Hippocampus	0.000030 (0.00027)	.269	-0.00017 (0.00015)	.272	-0.00084 (0.00057)	.142	0.48	.593	-0.00025 (0.00022)	.261	-0.00008 (0.00021)	.713

Individuals that might have suffered from terminal decline were removed (n=43). Data are represented as β (SE) as estimated by linear mixed models. Intracranial volume, sex and age were included as covariates. Interaction terms were removed when not significant. Time in years; volume in mm<sup>3</sup>. A positive beta estimate indicates the effect of a smaller volume, whereas a negative beta indicates the effect of a larger volume. Significant results (p<.05) are indicated in bold. Aβ = amyloid-beta; SE = standard error; THK = thickness.

Supplementary Table 3. Baseline and annual change of other factors associated with cognitive functioning.

	Memory			Language			Processing Speed			Executive Function		
	beta (se)	p	pFDR	beta (se)	p	pFDR	beta (se)	p	pFDR	beta (se)	p	pFDR
Sex, f	-0.00 (0.23)	.999	.999	-0.27 (0.23)	.240	.481	-0.35 (0.21)	.105	.420	0.03 (0.20)	.870	.999
Age, y	0.02 (0.04)	.522	.522	-0.04 (0.04)	.274	.522	-0.04 (0.04)	.287	.522	-0.03 (0.03)	.439	.522
Education	0.01 (0.02)	.533	.533	0.04 (0.02)	.094	.126	0.09 (0.02)	<.0001	<.0001	0.06 (0.02)	<.001	.002
APOE ε4 carrier	-0.17 (0.36)	.643	.643	-0.41 (0.37)	.273	.613	-0.38 (0.36)	.306	.613	-0.20 (0.31)	.532	.643
WMH volume	-0.16 (0.12)	.169	.169	-0.41 (0.11)	.001	.002	-0.31 (0.11)	.007	.014	-0.20 (0.10)	.054	.072
Sex X time	0.06 (0.10)	.568	.568	-0.05 (0.08)	.540	.568	-0.13 (0.09)	.162	.568	-0.10 (0.10)	.310	.568
Age X time	-0.04 (0.02)	.064	.255	0.00 (0.02)	.849	.849	-0.01 (0.02)	.534	.712	-0.03 (0.02)	.231	.462
Education X time	0.01 (0.02)	.009	.038	-0.01 (0.01)	.294	.392	0.00 (0.01)	.825	.825	0.02 (0.01)	.022	.043
APOE ε4 carrier X time	0.07 (0.15)	.658	.878	0.07 (0.12)	.558	.878	0.25 (0.15)	.107	.429	0.02 (0.15)	.885	.885
WMH volume X time	-0.18 (0.05)	.002	.007	-0.00 (0.05)	.981	.981	-0.05 (0.05)	.346	.462	-0.10 (0.06)	.091	.182

Neuropsychological tests were Z-transformed and averaged for each cognitive domain. Significant results ( $p < .05$ ) are indicated in bold. SE = standard error; f = female; y = years; APOE = apolipoprotein e genotype; WMH = White matter hyperintensities (log).





## CHAPTER 3

# **Association of CSF, blood, and imaging markers of neurodegeneration with clinical progression in people with subjective cognitive decline**

Jarith L. Ebenau, Wiesje Pelkmans, Inge M.W. Verberk, Sander C.J. Verfaillie, Karlijn A. van den Bosch, Mardou van Leeuwenstijn, Lyduine E. Collij, Philip Scheltens, Niels D. Prins, Frederik Barkhof, Bart N.M. van Berckel, Charlotte E. Teunissen, Wiesje M. van der Flier

*Published in*

*Neurology, 2022. 98(13) p.1315-1326.*

*DOI:10.1212/WNL.000000000200035*

## Abstract

**Background and Objectives:** Multiple biomarkers have been suggested to measure neurodegeneration (N) in the AT(N) framework, leading to inconsistencies between studies. We investigated the association of five N biomarkers with clinical progression and cognitive decline in individuals with subjective cognitive decline (SCD).

**Methods:** We included individuals with SCD from the Amsterdam Dementia Cohort and SCIENCE project, a longitudinal cohort study (follow-up  $4\pm 3$ y). We used the following N biomarkers: CSF total (t)-tau, medial temporal atrophy visual rating on MRI, hippocampal volume (HV), serum neurofilament light (NfL) and serum glial fibrillary acidic protein (GFAP). We determined correlations between biomarkers. We assessed associations between N biomarkers and clinical progression to mild cognitive impairment or dementia (Cox regression), and MMSE over time (linear mixed models). Models included age and sex, CSF A $\beta$  (A), and CSF p-tau (T) as covariates, in addition to the N biomarker.

**Result:** We included 401 individuals ( $61\pm 9$ y, 42%F, MMSE $28\pm 2$ , vascular comorbidities 8-19%). N biomarkers were modestly to moderately correlated (range  $r$  -0.28 – 0.58). Serum NfL and GFAP correlated most strongly ( $r$  0.58,  $p<0.01$ ). T-tau was strongly correlated with p-tau ( $r$  0.89,  $p<0.01$ ), although these biomarkers supposedly represent separate biomarker groups. All N biomarkers individually predicted clinical progression, but only HV, NfL and GFAP added predictive value beyond A $\beta$  and p-tau (HR 1.52 (95%CI 1.11-2.09); 1.51 (1.05-2.17); 1.50 (1.04-2.15)). T-tau, HV and GFAP individually predicted MMSE slope (range beta -0.17 – -0.11,  $p<0.05$ ), but only HV remained associated beyond A $\beta$  and p-tau (beta -0.13 (SE 0.04),  $p<0.05$ ).

**Discussion:** In cognitively unimpaired elderly, correlations between different N biomarkers were only moderate, indicating they reflect different aspects of neurodegeneration and should not be used interchangeably. T-tau was strongly associated with p-tau (T), which makes it less desirable to use as measure for N. HV, NfL and GFAP predicted clinical progression beyond A and T. Our results do not allow to choose one most suitable biomarker for N, but illustrate the added prognostic value of N beyond A and T.

### **Introduction**

In recent years, there has been a major change in the definition of Alzheimer's disease (AD). Formerly, the core criteria of AD diagnosis were based on clinical symptoms (McKhann et al. 2011). In 2018, a research framework has been put forward by the NIA-AA in which every individual is classified based on specific biomarkers in the AT(N) classification (Jack et al. 2018). In this framework, the term 'Alzheimer's disease' refers to the presence of abnormal amyloid-beta accumulation and neurofibrillary tau tangles, i.e. 'A', measured by CSF A $\beta$  or amyloid PET, and 'T', measured by CSF phosphorylated tau (p-tau) or tau PET. The AT(N) construct is independent of the cognitive stage of the individual, which makes it possible to identify AD in cognitively normal individuals.

The 'N' in the AT(N) classification represents neurodegeneration. Neurodegeneration can have many different causes and is not specific for AD. Therefore, neurodegenerative markers are not necessary for the diagnosis, but rather have been suggested to provide pathologic staging information and predictive value. Proposed biomarkers of N include atrophy on MRI, hypometabolism on fluorodeoxyglucose (FDG) PET or CSF total tau (t-tau; Jack et al. 2018). In addition, blood-based biomarkers are now available and have been suggested as non-invasive alternative markers for N (Jack et al. 2018; Rajan et al. 2020; Verberk et al. 2021).

Allowing different biomarkers as indicator of a biomarker group implies that they can be used interchangeably and measure the same pathological process. For the A and T biomarker group, this assumption holds fairly well, with moderate to high agreement and relatively high correlation coefficients between markers within A and T, respectively (Landau et al. 2013; Illán-Gala et al. 2018; la Joie et al. 2018). N biomarkers, however, are poorly correlated and show inadequate agreement



(Alexopoulos et al. 2014; Toledo et al. 2014; Jack et al. 2015; Vos et al. 2016; Illán-Gala et al. 2018). Furthermore, the fact that N biomarkers are suggested to provide staging information implies that individuals with a higher degree of neurodegeneration are assumed to deteriorate faster. However, there are only a few studies that directly compared different N biomarkers in their association with clinical progression or cognitive decline over time. Most are hampered by small sample sizes, and none have directly compared blood-based biomarkers to CSF and imaging biomarkers yet (Toledo et al. 2014; Ottoy et al. 2019; Yu et al. 2019; Guo et al. 2020; Mattsson-Carlgren et al. 2020).

It is difficult to determine which modality captures ‘neurodegeneration (N)’ most accurately, because there is no gold standard available. However, it should capture a different process than the accumulation of amyloid-beta (A) or fibrillary tau (T), as otherwise the addition of N would have no added value in the AT(N) classification. Furthermore, if different N biomarkers indeed capture the same process, correlations between N biomarkers should be higher than correlations between A and N, or T and N biomarkers. Finally, as N provides staging information, it should have some clinical correlate. In early disease stages especially, it is important to be able to accurately predict future deterioration, for both the individuals themselves and clinical trial recruitment, since these could still potentially benefit from disease modifying therapies.

Therefore, our aims were (1) to compare the different N biomarkers CSF total (t)-tau, medial temporal atrophy (MTA) visual rating on MRI, hippocampal volume (HV), serum neurofilament light (NfL) and serum glial fibrillary acidic protein (GFAP) to each other and to markers of A and T, and (2) to determine their predictive value for clinical progression and cognitive

decline beyond A and T, in a sample of cognitively normal individuals with subjective cognitive decline (SCD).

### **Methods**

#### *Study population*

We included 401 individuals with SCD from the Amsterdam Dementia Cohort (ADC) and SCIENCE project (Subjective Cognitive Impairment Cohort; Slot et al. 2018; van der Flier and Scheltens 2018). The SCIENCE project is a sub-study of ADC and prospectively follows individuals with SCD. Individuals were referred to our memory clinic because of cognitive complaints by their general physician, a geriatrist or a neurologist, and underwent an extensive diagnostic workup, including a physical, neurological and neuropsychological evaluation. In a multidisciplinary consensus meeting, all individuals received the label SCD when they performed within normal limits on a neuropsychological assessment, and criteria for mild cognitive impairment (MCI), dementia, or other neurological or psychiatric diseases that could potentially cause cognitive complaints, were not met.

At follow-up, diagnoses were re-evaluated as SCD, MCI, AD dementia or other types of dementia. Clinical progression was defined as progression from SCD to MCI or dementia. Inclusion criteria for the current study were baseline SCD diagnosis, availability of follow-up information ( $\geq 2$  diagnoses), availability of CSF, and availability of MRI and/or serum biomarkers within one year of diagnosis. MMSE was assessed annually and was used as longitudinal measure of global cognition. Education was rated using the Dutch Verhage system (Verhage and van der Werff 1964).

*Biomarkers*

We used all biomarkers both as continuous and dichotomous measures. We used CSF A $\beta$  (continuous and dichotomous, abnormal <813 pg/mL) or amyloid PET (dichotomous, visual assessment) as biomarker for A. When both amyloid PET and CSF A $\beta$  were available, the PET result was used. We used CSF p-tau (abnormal >52 pg/mL) as biomarker for T. We compared five different N biomarkers: CSF t-tau (abnormal >375 pg/mL), MTA score (abnormal  $\geq 1$ ), HV, serum NfL and serum GFAP. We used a cut-off value of  $\geq 1$  for MTA score instead of age-dependent cut-off values, to be consistent with thresholds for the other biomarkers, which are also age-independent (Rhodius-Meester et al. 2017). For HV, NfL and GFAP, no established cut-off values were available. Because of varying rates of N+ in literature (Ebenau et al. 2020; Mattsson-Carlgrén et al. 2020), we pragmatically took the 75th and 90th percentile for NfL and GFAP, and the 10th and 25th percentile for HV, which provides the reader with a range of possible effects sizes. Hence, for HV, NfL and GFAP, we chose two dichotomous definitions per biomarker. The following describe the procedures used to obtain these measures.

A lumbar puncture was performed between the L3/L4, L4/L5 or L5/S1 intervertebral space to obtain CSF, which was subsequently collected in polypropylene tubes (Teunissen et al. 2014). Levels of A $\beta$ <sub>1-42</sub>, tau phosphorylated threonine 181 (p-tau) and total tau were measured using sandwich ELISA's (Innotest beta-amyloid<sub>1-42</sub>, Innotest PhosphoTAU<sub>-181p</sub> and Innotest hTAU-Ag; (Duits et al. 2015). CSF A $\beta$  levels were corrected for the drift that occurred over the years (Tijms et al. 2018).

For 79 individuals, amyloid PET was performed using the tracers [<sup>18</sup>F]Florbetapir (n=13), [<sup>18</sup>F]Florbetaben (n=48), [<sup>18</sup>F]Flutemetamol (n=7) or [<sup>11</sup>C]-PIB (Pittsburgh compound-B, n=11). An intravenous cannula was used to administer the tracers. The following systems were used to acquire

the PET scans: Gemini TF PET-CT, Ingenuity TF PET-CT, and Ingenuity PET/MRI (Philips Healthcare, Best, The Netherlands). For [<sup>18</sup>F]Florbetaben and [<sup>18</sup>F]Flutemetamol imaging, a static scanning protocol was used, for [<sup>18</sup>F]Florbetapir and [<sup>11</sup>C]PIB imaging, a dynamic scanning protocol (Ossenkoppele et al. 2012; de Wilde et al. 2017; Zwan et al. 2017; Slot et al. 2018). A trained nuclear medicine physician visually rated all scans as 'positive' or 'negative', according to the radiotracer specific product guidelines.

Structural MRI 3D T1-weighted images (n=366 (89%)) were acquired as part of routine patient care from nine different systems. The acquisition parameters are described in the Supplementary Text 1. An experienced neuroradiologist reviewed all scans. T1-weighted images were used for visual rating of medial temporal lobe atrophy (MTA; range 0-4). Scores for the left and right sides were averaged (Scheltens et al. 1992). Hippocampal volume was estimated using FMRIB Software Library (FSL) FIRST (v5), as described previously by Patenaude et al. (2011). The FIRST algorithm first registers the 3D T1-weighted images to the Montreal Neurological Institute 152 template. Next, it uses a subcortical mask for segmentation based on shape models and voxel intensities to obtain hippocampal volumes. Hippocampal volumes were normalized for head size using the V-scaling factor from SIENAX (Smith et al. 2002), and left and right sides were averaged. All images were visually inspected for registration or segmentation errors.

Non-fasted serum samples (n=296 (72%)) were obtained through venipuncture and centrifuged on average within 2 hours from collection, at 1800g, 10 minutes at room temperature, before immediate storage at -80 °C until analysis. Serum GFAP and NfL levels were measured using the commercially available Simoa™ GFAP Discovery Kit (Quanterix) and the

Simoa™ NF-Light Advantage Kit (Quanterix) according to manufacturer's instructions and with on-board automated sample dilution (Verberk et al. 2021). All samples were measured in duplicates with good average intra-assay % coefficient of variation.

#### *Standard protocol approvals, registrations, and patient consents*

The research is conducted in accordance with ethical consent by VU University and the Helsinki Declaration of 1975. For all individuals included in the study, written informed consent was available.

#### *Statistics*

All analyses were performed in R version 4.0.3. We first used all biomarkers as continuous measures ( $A\beta$ , p-tau, t-tau, MTA, HV, NfL and GFAP). Since the AT(N) classification is based on dichotomous variables, we repeated all analyses with dichotomized biomarkers (A, T,  $N_{t\text{-tau}}$ ,  $N_{MTA}$ ,  $N_{HV25}$ ,  $N_{HV10}$ ,  $N_{NfL75}$ ,  $N_{NfL90}$ ,  $N_{GFAP75}$ ,  $N_{GFAP90}$ ). CSF p-tau, t-tau, serum NfL and GFAP were log transformed due to non-normality. For Cox proportional hazards models and linear mixed models, continuous predictors were transformed to z-scores for comparability of effect sizes, and HV was inverted, so that for all variables higher values indicates worse.

We first compared demographic and clinical variables between individuals that remained stable, and those that progressed to MCI or dementia during follow-up, using *t*-test, Mann-Whitney *U* test and chi-square where appropriate. To assess correlations between biomarkers, we used Pearson correlation analysis (CSF  $A\beta$ , p-tau and t-tau, MTA score, HV, and serum NfL and GFAP). We additionally used partial correlation to adjust for age and sex.

We then investigated the associations between biomarkers and clinical progression using Cox proportional hazards analyses, with progression to MCI or dementia as outcome. We ran four different models, with a cumulative number of predictors. We first ran analyses with continuous N biomarkers as single predictors (model 1). We then added age and sex as covariates (model 2). Then we added CSF A $\beta$  as covariate (model 3), and finally, also CSF p-tau (model 4). In models with MTA and HV, scanner type was additionally added as covariate. Separate analyses were performed for each of the N biomarkers t-tau, MTA, HV, NfL and GFAP. Finally, for exploration purposes, we combined multiple N biomarkers in one model, entering all N biomarkers that were significantly associated with the outcome in model 4, simultaneously.

Next, we investigated the relationship between the different N biomarkers and MMSE over time using linear mixed models. We ran four different models with a cumulative number of covariates, similar to the models described for the Cox analyses. We first used the N biomarker, time and N biomarker \* time as predictors (model 1). Next, we added age and sex as covariates (model 2). To account for the putative modifying effect of age and sex on rate of decline, we additionally added the interaction terms age \* time and sex \* time to model 2. Then we added CSF A $\beta$  and A $\beta$  \* time as covariates (model 3) and finally, also CSF p-tau and p-tau \* time (model 4). In models with MTA and HV, scanner type was additionally added as covariate. We included a random intercept and random slope.

We repeated the analyses with dichotomous N biomarkers. We visualized AT(N) distributions for different N biomarkers using bar graphs. We ran Cox proportional hazards models similarly to models with continuous N biomarkers, except dichotomized N biomarkers were used as predictors, as well as dichotomized A and T biomarkers when they were

added as covariates in models 3 and 4. We visualized the associations between N biomarkers and clinical progression to MCI or dementia using Kaplan Meier curves. All analyses were corrected for multiple testing using the false discovery rate (FDR). FDR corrected  $p$ -values  $<0.05$  were considered significant.

**Table 1.**  
**Demographics**

	<b>Stable</b> N=337 (84%)	<b>Progression</b> N=64 (16%)	<b>Total</b>
Age <sup>a</sup>	60±8.4	66±7.3	60.9±8.5*
Sex, female <sup>b</sup>	141 (42%)	26 (41%)	167 (42%)
Education <sup>c</sup>	6[5-6]	6[4-6]	6[5-6]
MMSE <sup>c</sup>	28.4±1.5	27.8±1.6	28.3±1.6*
APOE carriership <sup>b</sup>	115 (35%)	38 (61%)	153 (39%)*
Hypertension <sup>b</sup>	67 (20%)	11 (17%)	78 (19%)
Hypercholesterolemia <sup>b</sup>	30 (8.9%)	4 (6.2%)	34 (8.5%)
Diabetes Mellitus <sup>d</sup>	30 (8.9%)	1 (1.6%)	31 (7.7%)
BMI > 30 <sup>b</sup>	37 (14%)	5 (10%)	42 (13%)
CSF abeta <sup>a</sup>	1072.2±238	817.0±264.4	1031.5±259.5*
CSF p-tau <sup>c</sup>	46.5±20.2	67.8±33.8	49.9±24.2*
CSF t-tau <sup>c</sup>	278.1±165.1	501±358.4	313.7±223.2*
MTA score <sup>c</sup>	0[0-0.5]	0[0-1]	0[0-0.5]†
N available (%)	305 (90.5%)	59 (92.2%)	
HV <sup>a</sup>	4.8±0.6	4.5±0.5	4.7±0.6*
N available (%)	303 (89.9%)	58 (90.6%)	
Serum NFL <sup>c</sup>	10.2±5.6	14.3±5.7	10.9±5.8*
N available (%)	245 (72.7%)	51 (79.7%)	
Serum GFAP <sup>c</sup>	190.8±124.9	281.1±128.6	206.4±129.9*
N available (%)	245 (72.7%)	51 (79.7%)	
Total FU time <sup>c</sup>	3.6±2.7	4.5±3.2	3.8±2.8*
Time to diagnosis		3.0±2.9	
No. of visits <sup>c</sup>	2[2-3]	4[3-6]	3[2-4]*

Data are presented as mean±SD, N(%), or median[IQR]. Individuals are classified in the 'Progression' group if they showed clinical progression to mild cognitive impairment or dementia during follow-up. MRI was available for n=366, there were some missing values for MTA score (n=364) and HV (n=361) due to registration and segmentation errors. MMSE = mini-mental state examination, MTA = medial temporal atrophy, HV = hippocampal volume, NFL = neurofilament light, GFAP = glial fibrillary acidic protein. <sup>a</sup> t-test, <sup>b</sup> chi-square test, <sup>c</sup> Mann-Whitney U test, <sup>d</sup> Fisher's exact test, †  $p < .05$ , \* FDR corrected  $p < .05$ .



## Results

### *Baseline demographics*

The 401 individuals were on average  $61 \pm 9$  years old, 167(42%) were female, and 153(39%) were APOE  $\epsilon 4$  carriers (Table 1). At follow-up, 64(16%) individuals progressed to MCI or dementia (29(7%) to MCI, 23(6%) to AD dementia and 12(3%) to non-AD dementia). Individuals who progressed to MCI or dementia were on average older, had a lower baseline MMSE score and were more often APOE  $\epsilon 4$  carrier. Additionally, they had lower values for A $\beta$ , higher values for p-tau, t-tau, MTA, NfL and GFAP, and smaller hippocampal volume.

### *Correlations between N biomarkers*

The different N biomarkers were modestly to moderately correlated (range  $r$  -0.28 – 0.58, Figure 1A). Serum markers NfL and GFAP correlated most strongly ( $r$  0.58,  $p$  <0.01). P-tau and t-tau, representing different AT(N) biomarker groups (T and N respectively), were very strongly correlated ( $r$  0.89,  $p$  <0.01). Overall, the correlation coefficients between the different biomarkers for N were in a similar range as the correlation coefficients between the different biomarkers for N on the one hand, and biomarkers for A and T on the other hand ( $r$  -0.43 – 0.33, excluding the correlation between p-tau and t-tau). After adjusting for age and sex, drastically lower coefficients were observed (Figure 1B).

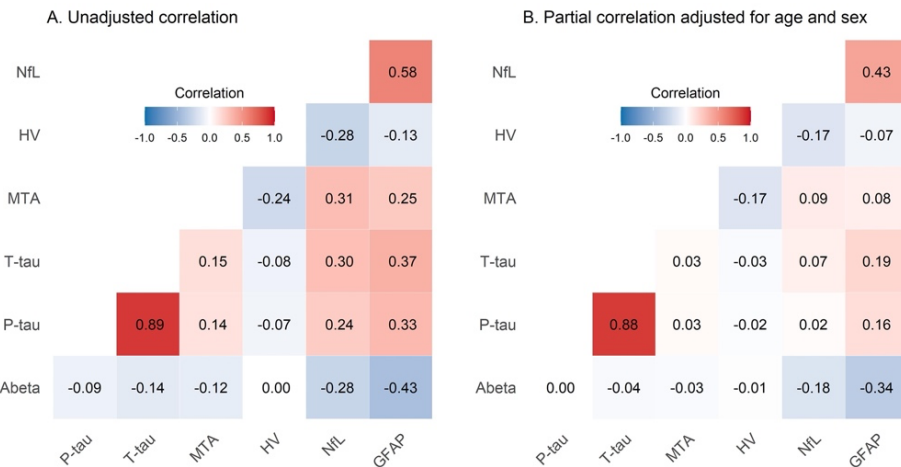


**Figure 1. Correlations between N biomarkers**

Heatmaps showing correlations between different biomarkers. A). Correlation coefficients (Pearson), B). Correlation coefficients (partial correlation, adjusted for age and sex). P-tau, t-tau, NfL and GFAP were log-transformed. MTA = medial temporal atrophy, HV = hippocampal volume, NfL = neurofilament light, GFAP = glial fibrillary acidic protein.

### *Risk of progression to MCI or dementia*

We investigated the predictive value of the different N biomarkers using Cox proportional hazards analyses. The mean follow-up duration was 3.8 years ( $\pm$  2.8 years). In uncorrected models, t-tau, MTA, HV, NfL and GFAP all predicted clinical progression to MCI or dementia (Table 2, model 1). After adding covariates in model 2 (age and sex), 3 (A $\beta$ , age and sex) and 4 (A $\beta$ , p-tau, age and sex), hazard ratios were attenuated. Model 4 showed that HV, NfL and GFAP added predictive value to A $\beta$  and p-tau. T-tau also predicted MCI or dementia in models 1 to 3, but was not entered in model 4 due to collinearity between t-tau and p-tau. In an additional explorative analysis, we added the three N markers HV, NfL and GFAP simultaneously in a model in addition to A $\beta$  and p-tau, since these biomarkers added predictive value in model 4. In this model, only HV remained significantly associated with clinical progression to MCI or dementia (HR 1.45 (SE 1.01 – 2.09)). The

associations for NfL (0.94 (0.56 – 1.59)) and GFAP (1.40 (0.86 – 2.29)) were attenuated (n=258 due to varying availability rates for N biomarkers).

Results of the analyses for complete cases only (n=256) were overall similar, although not all associations survived FDR correction (Sup. Table 1).

**Table 2.** Risk of MCI or dementia for continuous N biomarkers

Biomarker	n	Model 1	Model 2	Model 3	Model 4
T-tau	401	2.32 (1.86 - 2.88) <sup>ab</sup>	2.12 (1.67 - 2.70) <sup>ab</sup>	1.74 (1.36 - 2.23) <sup>ab</sup>	
A $\beta$				1.98 (1.50 - 2.63) <sup>ab</sup>	
P-tau					
MTA	364	1.34 (1.06 - 1.69) <sup>ab</sup>	1.02 (0.78 - 1.34)	0.97 (0.74 - 1.28)	1.00 (0.76 - 1.33)
A $\beta$				2.43 (1.79 - 3.31) <sup>ab</sup>	2.18 (1.60 - 2.96) <sup>ab</sup>
P-tau					1.42 (1.07 - 1.89) <sup>ab</sup>
HV	361	1.55 (1.17 - 2.07) <sup>ab</sup>	1.36 (0.99 - 1.87)	1.43 (1.06 - 1.95) <sup>ab</sup>	1.52 (1.11 - 2.09) <sup>ab</sup>
A $\beta$				2.58 (1.88 - 3.54) <sup>ab</sup>	2.25 (1.65 - 3.07) <sup>ab</sup>
P-tau					1.49 (1.14 - 1.94) <sup>ab</sup>
NfL	296	1.92 (1.51 - 2.46) <sup>ab</sup>	1.61 (1.18 - 2.21) <sup>ab</sup>	1.42 (1.00 - 2.01)	1.51 (1.05 - 2.17) <sup>ab</sup>
A $\beta$				2.24 (1.59 - 3.15) <sup>ab</sup>	1.96 (1.41 - 2.72) <sup>ab</sup>
P-tau					1.52 (1.14 - 2.03) <sup>ab</sup>
GFAP	296	2.40 (1.81 - 3.19) <sup>ab</sup>	2.03 (1.46 - 2.82) <sup>ab</sup>	1.58 (1.09 - 2.30) <sup>ab</sup>	1.50 (1.04 - 2.15) <sup>ab</sup>
A $\beta$				2.09 (1.46 - 3.00) <sup>ab</sup>	1.90 (1.34 - 2.68) <sup>ab</sup>
P-tau					1.44 (1.07 - 1.94) <sup>ab</sup>

Data shown are hazard ratio (95% confidence interval) as estimated by Cox proportional hazards analyses (outcome: clinical progression to mild cognitive impairment or dementia). Predictors: model 1: neurodegeneration biomarker; model 2: neurodegeneration biomarker, age and sex; model 3: A $\beta$ , neurodegeneration biomarker, age and sex; model 4: A $\beta$ , p-tau, neurodegeneration biomarker, age and sex. In models with MTA and HV, scanner type was additionally added as covariate. P-tau, t-tau, NfL and GFAP were log transformed, A $\beta$  and hippocampal volume were inverted, all biomarkers were z-transformed. MTA = medial temporal atrophy, HV = hippocampal volume, NfL = neurofilament light, GFAP = glial fibrillary acidic protein. T-tau was not entered in model 4 due to collinearity between t-tau and p-tau. <sup>a</sup> p < 0.05. <sup>b</sup> FDR corrected p < 0.05.

### *Cognitive decline over time*

We estimated change in MMSE over time using linear mixed models. In total, 1196 MMSE scores of 399 participants individuals were available, with missing values for two individuals (334  $\geq$  2 visits; range 1-17, median 3 visits). No associations between any N biomarkers and baseline MMSE scores were observed in our sample of cognitively normal elderly. Table 3 shows the results for the interaction between the N biomarkers and time,

which reflects the effect of each of the N biomarkers on MMSE slope. In both uncorrected models (model 1) and models corrected for age and sex (model 2), t-tau, HV and GFAP predicted MMSE slope. T-tau and HV also added predictive value to A $\beta$  (model 3), but only HV added predictive value beyond A $\beta$  and p-tau (model 8). Results were similar for analyses with complete cases (n=256, Sup. Table 2).

**Table 3. Risk of cognitive decline for continuous N biomarkers**

	<b>Model 1</b>	<b>Model 2</b>	<b>Model 3</b>	<b>Model 4</b>
Biomarker	Beta (SE)	Beta (SE)	Beta (SE)	Beta (SE)
T-tau	-0.17 (0.04) <sup>a,b</sup>	-0.15 (0.04) <sup>a,b</sup>	-0.14 (0.04) <sup>a,b</sup>	
A $\beta$			-0.11 (0.04) <sup>a,b</sup>	
P-tau				
MTA	-0.06 (0.04)	-0.04 (0.05)	-0.04 (0.05)	-0.04 (0.04)
A $\beta$			-0.14 (0.04) <sup>a,b</sup>	-0.12 (0.04) <sup>a,b</sup>
P-tau				-0.12 (0.04) <sup>a,b</sup>
HV	-0.11 (0.04) <sup>a,b</sup>	-0.13 (0.05) <sup>a,b</sup>	-0.13 (0.04) <sup>a,b</sup>	-0.13 (0.04) <sup>a,b</sup>
A $\beta$			-0.13 (0.04) <sup>a,b</sup>	-0.12 (0.04) <sup>a,b</sup>
P-tau				-0.11 (0.04) <sup>a,b</sup>
NfL	-0.06 (0.05)	-0.05 (0.06)	-0.01 (0.06)	-0.02 (0.06)
A $\beta$			-0.11 (0.05) <sup>a</sup>	-0.09 (0.05)
P-tau				-0.16 (0.05) <sup>a,b</sup>
GFAP	-0.15 (0.05) <sup>a,b</sup>	-0.14 (0.06) <sup>a,b</sup>	-0.11 (0.06)	-0.10 (0.06)
A $\beta$			-0.08 (0.05)	-0.06 (0.05)
P-tau				-0.16 (0.05) <sup>a,b</sup>

Results shown are beta (SE) as estimated by linear mixed models. Outcome is MMSE score. Predictors: model 5: neurodegeneration, time, neurodegeneration\*time; model 6: variables included in model 5, age, sex, age\*time and sex\*time; model 7: variables included in model 6, CSF A $\beta$  and A $\beta$ \*time; model 8: variables included in model 7, CSF p-tau and p-tau\*time). In models with MTA and HV, scanner type was additionally added as covariate. Betas represent the interaction between neurodegeneration biomarker and time, which corresponds to the cognitive slope. P-tau, t-tau, NfL and GFAP were log transformed, A $\beta$  and hippocampal volume were inverted, all biomarkers were z-transformed. MTA = medial temporal atrophy, HV = hippocampal volume, NfL = neurofilament light, GFAP = glial fibrillary acidic protein. T-tau was not entered in model 4 due to collinearity between t-tau and p-tau. <sup>a</sup> p < 0.05. <sup>b</sup> FDR corrected p < 0.05.

*Dichotomous N biomarkers*

The proportion of N+ individuals, and hence the distribution of AT(N) categories, strongly depended on the definition of N (Figure 2). Proportions of N+ varied between 10% ( $N_{HV10}$ ,  $N_{NFL90}$ ,  $N_{GFAP90}$ ), and 25% ( $N_{HV25}$ ,  $N_{NFL75}$ ,  $N_{GFAP75}$ ). For Nt-tau and NMTA, proportions of N+ were about 22%. N+ was more common in A- compared to A+ individuals for  $N_{MTA}$  or  $N_{HV}$ , and more common in A+ compared to A- individuals for  $N_{GFAP}$ . For  $N_{NFL}$  and  $N_{t-tau}$ , frequencies of N+ were similar between A+ and A-.

Cox proportional hazards analyses using dichotomous N biomarkers to predict clinical progression to MCI or dementia provided overall similar results to analyses with continuous biomarkers, for models 1 and 2 (Table 4). However, only  $N_{t-tau}$  and  $N_{HV25}$  added predictive value to A, and only  $N_{HV25}$  added value beyond A and T. Figure 3 visualizes the combined effect of A and N status for each N on risk of clinical progression in four-level variables (A-N-, A-N+, A+N-, A+N+).

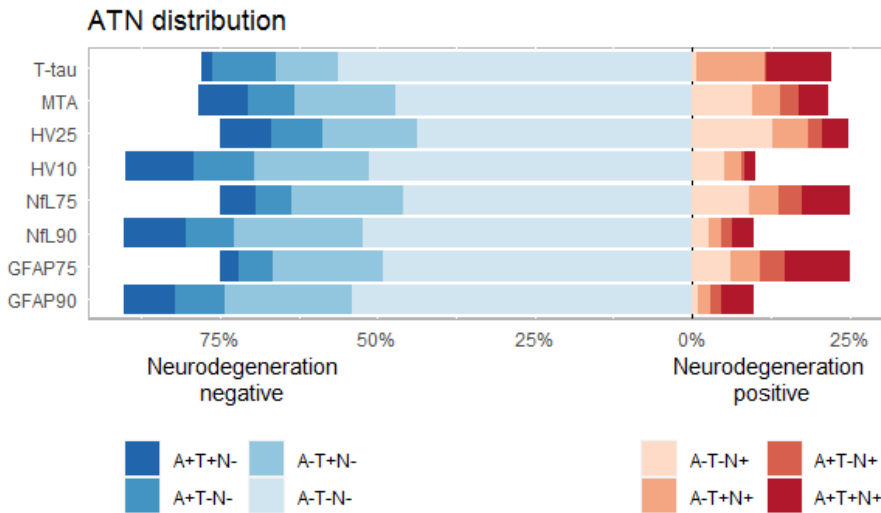


**Figure 2. Distribution of AT(N) profiles according to different definitions of neurodegeneration**

Distribution of AT(N) profiles for different definitions of neurodegeneration. MTA = medial temporal atrophy, HV 25 = hippocampal volume, threshold 25<sup>th</sup> percentile, HV 10 =

hippocampal volume, threshold 10<sup>th</sup> percentile, NfL 75 = neurofilament light, threshold 75<sup>th</sup> percentile, NfL 90 = neurofilament light, threshold 90<sup>th</sup> percentile, GFAP 75 = glial fibrillary acidic protein, threshold 75<sup>th</sup> percentile, GFAP 90 = glial fibrillary acidic protein, threshold 90<sup>th</sup> percentile.

**Table 4. Risk of MCI or dementia for dichotomous N biomarkers**

Biomarker	n	Model 1	Model 2	Model 3	Model 4
T-tau	401	4.95 (2.99 - 8.22) <sup>ab</sup>	3.68 (2.16 - 6.25) <sup>ab</sup>	2.47 (1.40 - 4.36) <sup>ab</sup>	#
MTA	364	1.74 (0.98 - 3.08)	0.90 (0.47 - 1.71)	0.84 (0.42 - 1.66)	0.85 (0.43 - 1.68)
HV 25 <sup>th</sup>	361	2.60 (1.49 - 4.54) <sup>ab</sup>	2.03 (1.13 - 3.67) <sup>ab</sup>	2.22 (1.22 - 4.04) <sup>ab</sup>	2.27 (1.24 - 4.16) <sup>ab</sup>
HV 10 <sup>th</sup>	361	1.94 (0.91 - 4.12)	1.31 (0.57 - 3.01)	1.89 (0.84 - 4.26)	1.96 (0.87 - 4.39)
NfL 75 <sup>th</sup>	296	3.50 (2.00 - 6.11) <sup>ab</sup>	1.98 (1.04 - 3.78) <sup>a</sup>	1.40 (0.73 - 2.68)	1.42 (0.74 - 2.71)
NfL 90 <sup>th</sup>	296	2.54 (1.30 - 4.96) <sup>ab</sup>	1.48 (0.72 - 3.04)	1.04 (0.51 - 2.11)	1.07 (0.53 - 2.17)
GFAP 75 <sup>th</sup>	296	4.01 (2.26 - 7.10) <sup>ab</sup>	2.32 (1.20 - 4.49) <sup>ab</sup>	1.10 (0.53 - 2.29)	1.03 (0.49 - 2.16)
GFAP 90 <sup>th</sup>	296	4.69 (2.52 - 8.74) <sup>ab</sup>	2.89 (1.48 - 5.66) <sup>ab</sup>	1.68 (0.86 - 3.27)	1.68 (0.87 - 3.25)

Data shown are hazard ratio (95% confidence interval) as estimated by Cox proportional hazards analyses (outcome: clinical progression to mild cognitive impairment or dementia). Predictors: model 1: dichotomized N biomarker; model 2: dichotomized N, age and sex; model 3: dichotomized A, N, age and sex; model 4: dichotomized A, T, N, age and sex. In models with MTA and HV, scanner type was additionally added as covariate. MTA = medial temporal atrophy, HV 25 = hippocampal volume, threshold 25<sup>th</sup> percentile, HV 10 = hippocampal volume, threshold 10<sup>th</sup> percentile, NfL 75 = neurofilament light, threshold 75<sup>th</sup> percentile, NfL 90 = neurofilament light, threshold 90<sup>th</sup> percentile, GFAP 75 = glial fibrillary acidic protein, threshold 75<sup>th</sup> percentile, GFAP 90 = glial fibrillary acidic protein, threshold 90<sup>th</sup> percentile. T-tau was not entered in model 4 due to collinearity between t-tau and p-tau. <sup>a</sup> p <0.05. <sup>b</sup> FDR corrected p <0.05.

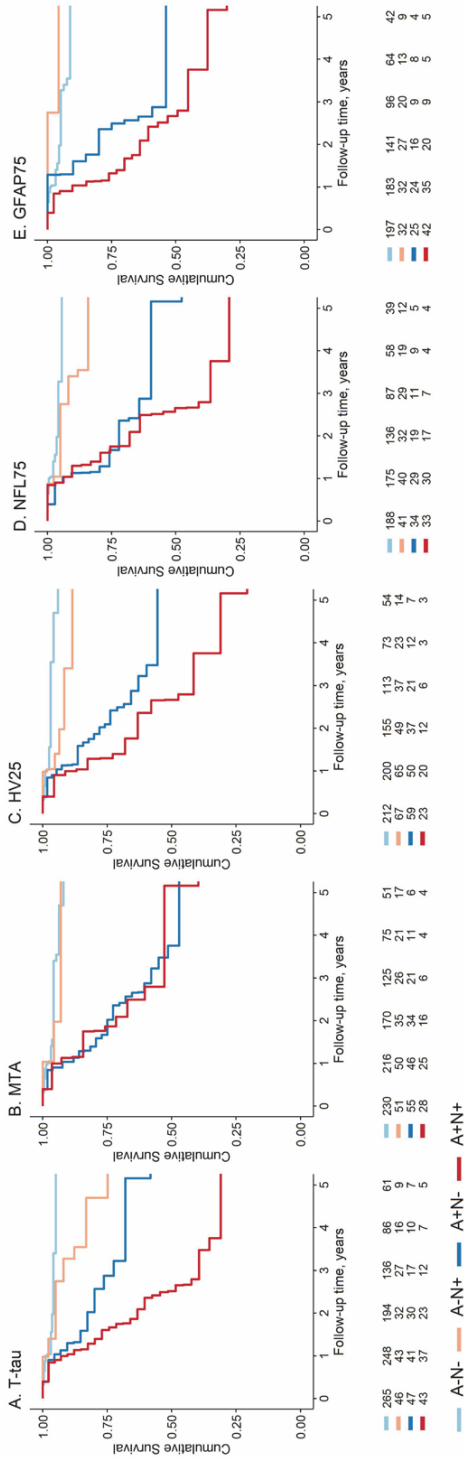


**Figure 3. Kaplan Meier curves visualizing clinical progression within AN classification.**

Kaplan Meier curves visualizing clinical progression to mild cognitive impairment or dementia for different definitions of neurodegeneration (A. T-tau, B. MTA, C. HV 25, D. NFL 75, E. GFAP 75). Survival is visualized by constructing a four-level variable of dichotomous amyloid and neurodegeneration status (A-N-, A-N+, A+N-, A+N+). MTA = medial temporal atrophy, HV 25 = hippocampal volume, threshold 25<sup>th</sup> percentile, NFL 75 = neurofilament light, threshold 75<sup>th</sup> percentile, GFAP 75 = glial fibrillary acidic protein, threshold 75<sup>th</sup> percentile.

### **Discussion**

In a sample of cognitively normal individuals with SCD, we found modest to moderate correlations and low concordance between the N biomarkers t-tau, MTA, HV, NfL and GFAP. N biomarkers HV, NfL and GFAP each predicted clinical progression, and had predictive value in addition to A $\beta$  and p-tau. Therefore, we recommend HV, NfL or GFAP as biomarkers for N. The tight correlation between t-tau and p-tau precludes the use of the former as a marker of a different biomarker category than the latter.

We extend on former observations that different markers of N are not necessarily closely correlated. The low correlation between N biomarkers likely contributes to the often discordant biomarker results in the AT(N) classification (Jack et al. 2015; Illán-Gala et al. 2018; Guo et al. 2020; Mattsson-Carlgrén et al. 2020). We add blood-based biomarkers to the comparison, showing similarly modest associations with the N biomarkers in other modalities, and also similarly strong associations with clinically relevant outcomes. Although at a population level, the overall qualitative pattern of biomarker frequencies remains rather stable regardless of the type of biomarkers used (Jack et al. 2015), it becomes problematic when researchers and clinicians treat the different N biomarkers as if they were identical. For prediction modelling at the individual patient level, the prognosis for an individual will vary considerably depending on the choice of N biomarker. The choice of N biomarker will also have an effect on the design of therapeutic trials, as well as the potential implementation of the AT(N) classification in the clinic. Studies investigating the AT(N) classification that use different definitions of their biomarkers, cannot be directly compared.

We found low to modest correlations and low concordance between different N biomarkers, which is largely in line with literature (Toledo et al.



2014; Gangishetti et al. 2018; Illán-Gala et al. 2018; Mattsson et al. 2019; Mattsson-Carlgren et al. 2020). One possible explanation for this is that although all N biomarkers capture a certain aspect of neurodegeneration, the underlying biological processes that lead to specific N biomarker abnormalities are far from identical. T-tau and NfL reflect the severity of neuroaxonal injury, atrophy on MRI reflects loss of the neuropil, and GFAP reflects astrocyte activity (Yang and Wang 2015; Zetterberg 2017; Jack et al. 2018; Khalil et al. 2018; Mattsson-Carlgren et al. 2020). Literature suggests these processes all have a different longitudinal trajectory, for example, NfL and t-tau abnormality likely precede HV abnormality and t-tau eventually reaches a plateau (Jack et al. 2013; McDade et al. 2018; Lleó et al. 2019; Palmqvist et al. 2019). This means correlations between N biomarkers of different processes are probably dependent on disease stage. However, MTA and HV were also poorly correlated, which is remarkable considering both HV and MTA aim to measure a similar process. We found a correlation coefficient of -0.24, which is relatively low and slightly lower than coefficients found in literature (range  $r$  -0.27 to -0.54; Clerx et al. 2013; Falgàs et al. 2019; Velickaite et al. 2020). This low correlation could be due to the fact that the MTA score is partly influenced by the volume of the surrounding CSF spaces, which means it reflects hippocampal atrophy as well as global and subcortical atrophy (Knoops et al. 2009). Furthermore, being cognitively normal, most individuals in our sample had an MTA score of 0, which reflects that the variability for this measure is probably too small to be a meaningful N biomarker in such a very early sample. In addition, the correlation coefficients between N biomarkers were in a similar range as the correlation coefficients between N biomarkers on the one hand, and A and T biomarkers on the other hand. This is in line with another study which found moderate correlations between biomarkers of different pathophysiological

categories (Illán-Gala et al. 2018). This implies that the underlying neurodegeneration processes are almost as different to each other, as they are different to processes underlying the A and T biomarker category. Overall, the low correlation coefficients illustrate that N biomarkers cannot be used interchangeably in the AT(N) classification.

We found that HV, NfL and GFAP predicted clinical progression, and HV predicted MMSE slope, beyond A $\beta$  and p-tau. Former studies that investigated the AT(N) classification often used only one biomarker for A, T and N respectively, and showed that overall, the AT(N) classification was associated with clinical progression and cognitive decline (Altomare et al. 2019; Burnham et al. 2019; Jack et al. 2019; Soldan et al. 2019; Ebenau et al. 2020; Grøntvedt et al. 2020). From these studies, the predictive value per individual biomarker cannot be discerned and thus cannot be used to choose the optimal N biomarker. Literature regarding the comparison between different N biomarkers is scarcer. There is, however, some support that HV is associated with cognitive decline and progression more strongly than t-tau (Ottoy et al. 2019; Yu et al. 2019; Guo et al. 2020). Although in our study, we found t-tau as individual biomarker also predicted clinical progression and cognitive decline, the high correlation with p-tau hampers the addition of t-tau to a model with A $\beta$  and p-tau, making it a less desirable biomarker to use in the AT(N) classification. NfL and GFAP have both been shown to be related to baseline cognition, cognitive decline and clinical progression as individual predictors, but have not yet been studied extensively in comparison to other N biomarkers (Mielke et al. 2019; de Wolf et al. 2020; Rajan et al. 2020; Teitsdottir et al. 2020). In a former study, we found GFAP was more strongly related to clinical progression and cognitive decline than NfL, which is in line with our current study (Verberk et al. 2021). We found both GFAP and NfL predicted clinical progression beyond A $\beta$  and p-tau, but

NfL was not associated with MMSE decline. A potential explanation for this difference in association is that NfL is a better marker for monitoring disease progression while its value does not lie in predicting future cognitive decline (Verberk et al. 2021). Differences could also be related to the fact that clinical progression to MCI or dementia is a binary outcome measure, while MMSE decline is a continuous measure with possibly a higher degree of measurement variation. Clinical progression might be a more sensitive measure with more clinical relevance. In contrast to NfL, GFAP was associated with MMSE decline, although associations were attenuated when additionally adjusting for A $\beta$  and/or p-tau. Of all N biomarkers we used, GFAP was associated most strongly with A $\beta$ , which could explain the attenuated estimates when A $\beta$  was added as covariate. MTA was not associated with clinical progression after correcting for covariates, nor with MMSE decline. Although we previously showed a dose response pattern with MTA as N (Ebenau et al. 2020), the small variability in MTA within cognitively normal individuals makes it too crude a measure to accurately predict decline. Overall, we show there is room for improved prediction beyond A $\beta$  and p-tau, using HV, NfL and GFAP as N biomarkers.

Limitations of the present study include that the list of N biomarkers examined is not exhaustive. For example, FDG-PET or other MRI atrophy measures have also been suggested as suitable N markers. Although the list of putative N biomarkers is long, we chose to use a variety of N biomarkers obtained by three different modalities that are widely used in literature, which makes our study relevant to the field. Another limitation is that the sample sizes somewhat differed for each N biomarker. This might have led to differences in outcome. However, when we repeated the analyses in the sample with complete data, results were similar, indicating their robustness (eTables 1 and 2). Furthermore, our sample consisted of individuals with

SCD presenting at a memory clinic, and the results might not be directly translatable to a community based setting or to other disease stages. Nonetheless, individuals with SCD can be considered an especially clinically relevant group, that might particularly benefit from the AT(N) classification system to grade their degree of underlying pathology. These are the individuals who present to a memory clinic because of worries about their cognition, and for this group AT(N) prediction modelling can make a relevant contribution. Another limitation is the lack of optimal cut-off values for HV, NfL and GFAP. Instead, we pragmatically used cut-off values obtaining a 10% and 25% N positivity rate, to provide a range of the true effect sizes. Additionally, we used continuous N biomarkers in all models. However, different cut-off values would probably have resulted in slightly different results. Last, we had a mean follow-up duration of 3.8 years and our sample had a relatively young age. Together, this could explain the low percentage of individuals with clinical progression to MCI or dementia, which limits the power to detect associations with N biomarkers. Furthermore, MMSE has a ceiling effect in cognitively normal individuals and perhaps our relatively short follow-up time hampered the finding of associations. Since all N biomarkers reflect different aspects of neurodegeneration, they could also have different associations with cognitive tests measuring specific cognitive domains. It would be interesting to investigate associations with other neuropsychological tests, but that is beyond the scope of this study since our aim was to assess the association between N biomarkers and disease progression in general. Strengths include the relatively large sample size of this well-defined cohort.

Concluding, correlations between different N biomarkers were low in a sample of cognitively normal individuals, indicating they may not reflect

the same underlying pathology. T-tau was strongly associated with p-tau, and thereby disqualified as measure for N in this context. Our results show HV, NfL and GFAP predicted clinical progression, and have added value beyond A $\beta$  and p-tau. However, our results do not allow to choose one most suitable biomarker for N.

### **Acknowledgements**

Research of the Alzheimer Center Amsterdam is part of the neurodegeneration research program of Amsterdam Neuroscience. The Alzheimer Center Amsterdam is supported by Stichting Alzheimer Nederland and Stichting VUmc fonds. The clinical database structure was developed with funding from Stichting Dioraphte. Jarith Ebenau is appointed at a research grant from Gieskes-Strijbis fonds. PET scans were funded by research grants from AVID and Piramal Neuroimaging. WF, NP, PS and CT are recipients of ABOARD, which is a public-private partnership receiving funding from ZonMW (#73305095007) and Health~Holland, Topsector Life Sciences & Health (PPP-allowance; #LSHM20106). Wiesje van der Flier holds the Pasman chair. Frederik Barkhof is supported by the NIHR biomedical research center at UCLH. Charlotte Teunissen is supported by the European Commission (Marie Curie International Training Network, JPND), the Dutch Research Council (ZonMW), The Weston Brain Institute, Alzheimer Netherlands.

### **Conflicts of interest**

J.L. Ebenau reports no disclosures relevant to the manuscript. W. Pelkmans reports no disclosures relevant to the manuscript. I.M.W. Verberk reports no disclosures relevant to the manuscript. S.C.J. Verfaillie reports no disclosures relevant to the manuscript. K.A. van den Bosch reports no

disclosures relevant to the manuscript. M. van Leeuwenstijn reports no disclosures relevant to the manuscript. L.E. Collij reports no disclosures relevant to the manuscript. P. Scheltens has acquired grant support (for the institution) from Biogen. In the past two years, he has received consultancy/speaker fees (paid to the institution) from Probiodrug Biogen, EIP Pharma, Merck AG. N.D. Prins reports consulting, advisory and speaker fees from Boehringer Ingelheim, Envivo, Janssen, Novartis, Probiodrug, Sanofi, Takeda, Kyowa Kirin Pharmaceutical Development, DSMB of AbbVie's M15-566, grants from Alzheimer Nederland (all paid directly to his institution) outside the submitted work. Dr. Prins is CEO and co-owner of the Brain Research Centre, Amsterdam, The Netherlands. F. Barkhof is a consultant for Biogen-Idec, Janssen Alzheimer Immunotherapy, Bayer-Schering, Merck-Serono, Roche, Novartis, Genzyme, and Sanofi-Aventis; has received sponsoring from European Commission-Horizon 2020, National Institute for Health Research-University College London Hospitals Biomedical Research Centre, Scottish Multiple Sclerosis Register, TEVA, Novartis, and Toshiba; and serves on the editorial boards of Radiology, Brain, Neuroradiology, Multiple Sclerosis Journal, and Neurology. B.N.M. van Berckel has received funding from ZonMW, the Netherlands Organization of Scientific Research, the Centre of Translational Molecular Imaging and Avid Radiopharmaceuticals. He has received funding from GE and IXICO. All funding is paid to his institution. C.E. Teunissen serves on the advisory board of Roche, performed contract research for Boehringer, Roche, Toyama Fujifilm, Esai and Probiodrug; obtained a grant with ADxNeurosciences, and received lecture fees from Biogen and Axon Neurosciences. W.M. van der Flier's research programs have been funded by ZonMW, the Netherlands Organization of Scientific Research, Alzheimer Nederland, Cardiovascular Onderzoek Nederland, Stichting Dioraphte, Gieskes-Strijbis fonds, Pasman

stichting, Boehringer Ingelheim, Life-MI, AVID, Biogen MA and Combinostics. All funding is paid to her institution.

## References

- Alexopoulos P, Kriett L, Haller B, Klupp E, Gray K, Grimmer T, Laskaris N, Förster S, Perneczky R, Kurz A, Drzezga A, Fellgiebel A, Yakushev I. 2014. Limited agreement between biomarkers of neuronal injury at different stages of Alzheimer's disease. *Alzheimer's & Dementia*. 10:684–689.
- Altomare D, de Wilde A, Ossenkoppele R, Pelkmans W, Bouwman F, Groot C, van Maurik I, Zwan M, Yaqub M, Barkhof F, van Berckel BN, Teunissen CE, Frisoni GB, Scheltens P, van der Flier WM. 2019. Applying the ATN scheme in a memory clinic population. *Neurology*. 93:e1635–e1646.
- Burnham SC, Coloma PM, Li Q-X, Collins S, Savage G, Laws S, Doecke J, Maruff P, Martins RN, Ames D, Rowe CC, Masters CL, Villemagne VL. 2019. Application of the NIA-AA Research Framework: Towards a Biological Definition of Alzheimer's Disease Using Cerebrospinal Fluid Biomarkers in the AIBL Study. *The Journal of Prevention of Alzheimer's Disease*. 6:1–8.
- Clerx L, van Rossum IA, Burns L, Knol DL, Scheltens P, Verhey F, Aalten P, Lapuerta P, van de Pol L, van Schijndel R, de Jong R, Barkhof F, Wolz R, Rueckert D, Bocchetta M, Tsolaki M, Nobili F, Wahlund L-O, Minthon L, Frölich L, Hampel H, Soininen H, Visser PJ. 2013. Measurements of medial temporal lobe atrophy for prediction of Alzheimer's disease in subjects with mild cognitive impairment. *Neurobiology of Aging*. 34:2003–2013.
- de Wilde A, van Maurik IS, Kunneman M, Bouwman F, Zwan M, Willemse EAJ, Biessels GJ, Minkman M, Pel R, Schoonenboom NSM, Smets EMA, Wattjes MP, Barkhof F, Stephens A, Lier EJ, Batrla-Utermann R, Scheltens P, Teunissen CE, van Berckel BNM, van der Flier WM. 2017. Alzheimer's biomarkers in daily practice (ABIDE) project: Rationale and design. *Alzheimer's & Dementia: Diagnosis, Assessment & Disease Monitoring*. 6:143–151.
- de Wolf F, Ghanbari M, Licher S, McRae-McKee K, Gras L, Weverling GJ, Wermeling P, Sedaghat S, Ikram MK, Waziry R, Koudstaal W, Klap J, Kostense S, Hofman A, Anderson R, Goudsmit J, Ikram MA. 2020. Plasma tau, neurofilament light chain and amyloid- $\beta$  levels and risk of dementia; a population-based cohort study. *Brain*. 143:1220–1232.
- Duits FH, Prins ND, Lemstra AW, Pijnenburg YAL, Bouwman FH, Teunissen CE, Scheltens P, Flier WM. 2015. Diagnostic impact of CSF biomarkers for Alzheimer's disease in a tertiary memory clinic. *Alzheimer's & Dementia*. 11:523–532.



- Ebenau JL, Timmers T, Wesselman LMP, Verberk IMW, Verfaillie SCJ, Slot RER, van Harten AC, Teunissen CE, Barkhof F, van den Bosch KA, van Leeuwenstijn M, Tomassen J, Braber A den, Visser PJ, Prins ND, Sikkes SAM, Scheltens P, van Berckel BNM, van der Flier WM. 2020. ATN classification and clinical progression in subjective cognitive decline. *Neurology*. 95:e46–e58.
- Falgàs N, Sánchez-Valle R, Bargalló N, Balasa M, Fernández-Villullas G, Bosch B, Olives J, Tort-Merino A, Antonell A, Muñoz-García C, León M, Grau O, Castellví M, Coll-Adrós N, Rami L, Redolfi A, Lladó A. 2019. Hippocampal atrophy has limited usefulness as a diagnostic biomarker on the early onset Alzheimer's disease patients: A comparison between visual and quantitative assessment. *NeuroImage: Clinical*. 23:101927.
- Gangishetti U, Christina Howell J, Perrin RJ, Louneva N, Watts KD, Kollhoff A, Grossman M, Wolk DA, Shaw LM, Morris JC, Trojanowski JQ, Fagan AM, Arnold SE, Hu WT. 2018. Non-beta-amyloid/tau cerebrospinal fluid markers inform staging and progression in Alzheimer's disease. *Alzheimer's Research & Therapy*. 10:98.
- Grøntvedt GR, Lauridsen C, Berge G, White LR, Salvesen Ø, Bråthen G, Sando SB. 2020. The Amyloid, Tau, and Neurodegeneration (A/T/N) Classification Applied to a Clinical Research Cohort with Long-Term Follow-Up. *Journal of Alzheimer's Disease*. 74:829–837.
- Guo Y, Li H, Tan L, Chen S, Yang Y, Ma Y, Zuo C, Dong Q, Tan L, Yu J. 2020. Discordant Alzheimer's neurodegenerative biomarkers and their clinical outcomes. *Annals of Clinical and Translational Neurology*. 7:1996–2009.
- Illán-Gala I, Pegueroles J, Montal V, Vilaplana E, Carmona-Iragui M, Alcolea D, Dickerson BC, Sánchez-Valle R, Leon MJ, Blesa R, Lleó A, Fortea J. 2018. Challenges associated with biomarker-based classification systems for Alzheimer's disease. *Alzheimer's & Dementia: Diagnosis, Assessment & Disease Monitoring*. 10:346–357.
- Jack CR, Bennett DA, Blennow K, Carrillo MC, Dunn B, Haeberlein SB, Holtzman DM, Jagust W, Jessen F, Karlawish J, Liu E, Molinuevo JL, Montine T, Phelps C, Rankin KP, Rowe CC, Scheltens P, Siemers E, Snyder HM, Sperling R, Elliott C, Masliah E, Ryan L, Silverberg N. 2018. NIA-AA Research Framework: Toward a biological definition of Alzheimer's disease. *Alzheimer's and Dementia*. 14:535–562.
- Jack CR, Knopman DS, Jagust WJ, Petersen RC, Weiner MW, Aisen PS, Shaw LM, Vemuri P, Wiste HJ, Weigand SD, Lesnick TG, Pankratz VS, Donohue MC, Trojanowski JQ. 2013. Tracking pathophysiological processes in Alzheimer's disease: an updated hypothetical model of dynamic biomarkers. *The Lancet Neurology*. 12:207–216.

- Jack CR, Wiste HJ, Therneau TM, Weigand SD, Knopman DS, Mielke MM, Lowe VJ, Vemuri P, Machulda MM, Schwarz CG, Gunter JL, Senjem ML, Graff-Radford J, Jones DT, Roberts RO, Rocca WA, Petersen RC. 2019. Associations of Amyloid, Tau, and Neurodegeneration Biomarker Profiles With Rates of Memory Decline Among Individuals Without Dementia. *JAMA*. 321:2316.
- Jack CR, Wiste HJ, Weigand SD, Knopman DS, Mielke MM, Vemuri P, Lowe V, Senjem ML, Gunter JL, Reyes D, Machulda MM, Roberts R, Petersen RC. 2015. Different definitions of neurodegeneration produce similar amyloid/neurodegeneration biomarker group findings. *Brain*. 138:3747–3759.
- Khalil M, Teunissen CE, Otto M, Piehl F, Sormani MP, Gattringer T, Barro C, Kappos L, Comabella M, Fazekas F, Petzold A, Blennow K, Zetterberg H, Kuhle J. 2018. Neurofilaments as biomarkers in neurological disorders. *Nature Reviews Neurology*. 14:577–589.
- Knoops AJG, van der Graaf Y, Appelman APA, Gerritsen L, Mali WPTM, Geerlings MI. 2009. Visual rating of the hippocampus in non-demented elders: Does it measure hippocampal atrophy or other indices of brain atrophy? The SMART-MR study. *Hippocampus*. 19:1115–1122.
- la Joie R, Bejanin A, Fagan AM, Ayakta N, Baker SL, Bourakova V, Boxer AL, Cha J, Karydas A, Jerome G, Maass A, Mensing A, Miller ZA, O'Neil JP, Pham J, Rosen HJ, Tsai R, Visani A v., Miller BL, Jagust WJ, Rabinovici GD. 2018. Associations between [ 18 F]AV1451 tau PET and CSF measures of tau pathology in a clinical sample. *Neurology*. 90:e282–e290.
- Landau SM, Lu M, Joshi AD, Pontecorvo M, Mintun MA, Trojanowski JQ, Shaw LM, Jagust WJ. 2013. Comparing positron emission tomography imaging and cerebrospinal fluid measurements of  $\beta$ -amyloid. *Annals of Neurology*. 74:826–836.
- Lleó A, Alcolea D, Martínez-Lage P, Scheltens P, Parnetti L, Poirier J, Simonsen AH, Verbeek MM, Rosa-Neto P, Slot RER, Tainta M, Izaguirre A, Reijs BLR, Farotti L, Tsolaki M, Vandenbergue R, Freund-Levi Y, Verhey FRJ, Clarimón J, Fortea J, Frolich L, Santana I, Molinuevo JL, Lehmann S, Visser PJ, Teunissen CE, Zetterberg H, Blennow K. 2019. Longitudinal cerebrospinal fluid biomarker trajectories along the Alzheimer's disease continuum in the BIOMARKAPD study. *Alzheimer's & Dementia*. 15:742–753.
- Mattsson N, Cullen NC, Andreasson U, Zetterberg H, Blennow K. 2019. Association Between Longitudinal Plasma Neurofilament Light and Neurodegeneration in Patients With Alzheimer Disease. *JAMA Neurology*. 76:791.

- Mattsson-Carlgrén N, Leuzy A, Janelidze S, Palmqvist S, Stomrud E, Strandberg O, Smith R, Hansson O. 2020. The implications of different approaches to define AT(N) in Alzheimer disease. *Neurology*. 94:e2233–e2244.
- McDade E, Wang G, Gordon BA, Hassenstab J, Benzinger TLS, Buckles V, Fagan AM, Holtzman DM, Cairns NJ, Goate AM, Marcus DS, Morris JC, Paumier K, Xiong C, Allegri R, Berman SB, Klunk W, Noble J, Ringman J, Ghetti B, Farlow M, Sperling RA, Chhatwal J, Salloway S, Graff-Radford NR, Schofield PR, Masters C, Rossor MN, Fox NC, Levin J, Jucker M, Bateman RJ. 2018. Longitudinal cognitive and biomarker changes in dominantly inherited Alzheimer disease. *Neurology*. 91:e1295–e1306.
- McKhann GM, Knopman DS, Chertkow H, Hyman BT, Jack CR, Kawas CH, Klunk WE, Koroshetz WJ, Manly JJ, Mayeux R, Mohs RC, Morris JC, Rossor MN, Scheltens P, Carrillo MC, Thies B, Weintraub S, Phelps CH. 2011. The diagnosis of dementia due to Alzheimer’s disease: Recommendations from the National Institute on Aging-Alzheimer’s Association workgroups on diagnostic guidelines for Alzheimer’s disease. *Alzheimer’s & Dementia*. 7:263–269.
- Mielke MM, Syrjanen JA, Blennow K, Zetterberg H, Vemuri P, Skoog I, Machulda MM, Kremers WK, Knopman DS, Jack C, Petersen RC, Kern S. 2019. Plasma and CSF neurofilament light: Relation to longitudinal neuroimaging and cognitive measures. *Neurology*. 93:e252–e260.
- Ossenkoppele R, Zwan MD, Tolboom N, van Assema DME, Adriaanse SF, Kloet RW, Boellaard R, Windhorst AD, Barkhof F, Lammertsma AA, Scheltens P, van der Flier WM, van Berckel BNM. 2012. Amyloid burden and metabolic function in early-onset Alzheimer’s disease: parietal lobe involvement. *Brain*. 135:2115–2125.
- Ottoy J, Niemantsverdriet E, Verhaeghe J, de Roeck E, Struyfs H, Somers C, Wyffels L, Ceysens S, van Mossevelde S, van den Bossche T, van Broeckhoven C, Ribbens A, Bjerke M, Stroobants S, Engelborghs S, Staelens S. 2019. Association of short-term cognitive decline and MCI-to-AD dementia conversion with CSF, MRI, amyloid- and 18F-FDG-PET imaging. *NeuroImage: Clinical*. 22:101771.
- Palmqvist S, Insel PS, Stomrud E, Janelidze S, Zetterberg H, Brix B, Eichenlaub U, Dage JL, Chai X, Blennow K, Mattsson N, Hansson O. 2019. Cerebrospinal fluid and plasma biomarker trajectories with increasing amyloid deposition in Alzheimer’s disease. *EMBO Molecular Medicine*. 11:1–13.
- Patenaude B, Smith SM, Kennedy DN, Jenkinson M. 2011. A Bayesian model of shape and appearance for subcortical brain segmentation. *NeuroImage*. 56:907–922.

- Rajan KB, Aggarwal NT, McAninch EA, Weuve J, Barnes LL, Wilson RS, DeCarli C, Evans DA. 2020. Remote Blood Biomarkers of Longitudinal Cognitive Outcomes in a Population Study. *Annals of Neurology*. 88:1065–1076.
- Rhodijs-Meester HFM, Benedictus MR, Wattjes MP, Barkhof F, Scheltens P, Muller M, van der Flier WM. 2017. MRI Visual Ratings of Brain Atrophy and White Matter Hyperintensities across the Spectrum of Cognitive Decline Are Differently Affected by Age and Diagnosis. *Frontiers in Aging Neuroscience*. 9:1–12.
- Scheltens P, Leys D, Barkhof F, Huglo D, Weinstein HC, Vermersch P, Kuiper M, Steinling M, Wolters EC, Valk J. 1992. Atrophy of medial temporal lobes on MRI in “probable” Alzheimer’s disease and normal ageing: diagnostic value and neuropsychological correlates. *J Neurol Neurosurg Psychiatry*. 55:967–972.
- Slot RER, Verfaillie SCJ, Overbeek JM, Timmers T, Wesselman LMP, Teunissen CE, Dols A, Bouwman FH, Prins ND, Barkhof F, Lammertsma AA, van Berckel BNM, Scheltens P, Sikkes SAM, van der Flier WM. 2018. Subjective Cognitive Impairment Cohort (SCIENCe): study design and first results. *Alzheimer’s Research & Therapy*. 10:76.
- Smith SM, Zhang Y, Jenkinson M, Chen J, Matthews PM, Federico A, de Stefano N. 2002. Accurate, Robust, and Automated Longitudinal and Cross-Sectional Brain Change Analysis. *Neuroimage*. 17:479–489.
- Soldan A, Pettigrew C, Fagan AM, Schindler SE, Moghekar A, Fowler C, Li Q-X, Collins SJ, Carlsson C, Asthana S, Masters CL, Johnson S, Morris JC, Albert M, Gross AL. 2019. ATN profiles among cognitively normal individuals and longitudinal cognitive outcomes. *Neurology*. 92:e1567–e1579.
- Teitsdottir UD, Jonsdottir MK, Lund SH, Darreh-Shori T, Snaedal J, Petersen PH. 2020. Association of glial and neuronal degeneration markers with Alzheimer’s disease cerebrospinal fluid profile and cognitive functions. *Alzheimer’s Research & Therapy*. 12:92.
- Teunissen CE, Tumani H, Engelborghs S, Mollenhauer B. 2014. Biobanking of CSF: International standardization to optimize biomarker development. *Clinical Biochemistry*. 47:288–292.
- Tijms BM, Willemse EAJ, Zwan MD, Mulder SD, Visser PJ, van Berckel BNM, van der Flier WM, Scheltens P, Teunissen CE. 2018. Unbiased approach to counteract upward drift in cerebrospinal fluid amyloid- $\beta$  1–42 analysis results. *Clinical Chemistry*. 64:576–585.

- Toledo JB, Weiner MW, Wolk DA, Da X, Chen K, Arnold SE, Jagust W, Jack C, Reiman EM, Davatzikos C, Shaw LM, Trojanowski JQ. 2014. Neuronal injury biomarkers and prognosis in ADNI subjects with normal cognition. *Acta Neuropathologica Communications*. 2:26.
- van der Flier WM, Scheltens P. 2018. Amsterdam Dementia Cohort: Performing Research to Optimize Care. *Journal of Alzheimer's Disease*. 62:1091–1111.
- Velickaite V, Ferreira D, Lind L, Ahlström H, Kilander L, Westman E, Larsson E. 2020. Visual rating versus volumetry of regional brain atrophy and longitudinal changes over a 5-year period in an elderly population. *Brain and Behavior*. 10:1–9.
- Verberk IMW, Laarhuis MB, van den Bosch KA, Ebenau JL, van Leeuwenstijn M, Prins ND, Scheltens P, Teunissen CE, van der Flier WM. 2021. Serum markers glial fibrillary acidic protein and neurofilament light for prognosis and monitoring in cognitively normal older people: a prospective memory clinic-based cohort study. *The Lancet Healthy Longevity*. 2:e87–e95.
- Verhage F, van der Werff J. 1964. An analysis of variance based on the Groninger intelligence test scores. *Ned Tijdschr Psychol*. 19:497–509.
- Vos SJB, Gordon BA, Su Y, Visser PJ, Holtzman DM, Morris JC, Fagan AM, Benzinger TLS. 2016. NIA-AA staging of preclinical Alzheimer disease: discordance and concordance of CSF and imaging biomarkers. *Neurobiology of Aging*. 44:1–8.
- Yang Z, Wang KKW. 2015. Glial fibrillary acidic protein: from intermediate filament assembly and gliosis to neurobiomarker. *Trends in Neurosciences*. 38:364–374.
- Yu J, Li J, Suckling J, Feng L, Pan A, Wang Y, Song B, Zhu S, Li D, Wang H, Tan C, Dong Q, Tan L, Mok V, Aisen PS, Weiner MM. 2019. Frequency and longitudinal clinical outcomes of Alzheimer's AT(N) biomarker profiles: A longitudinal study. *Alzheimer's & Dementia*. 15:1208–1217.
- Zetterberg H. 2017. Review: Tau in biofluids - relation to pathology, imaging and clinical features. *Neuropathology and Applied Neurobiology*. 43:194–199.
- Zwan MD, Bouwman FH, Konijnenberg E, van der Flier WM, Lammertsma AA, Verhey FRJ, Aalten P, van Berckel BNM, Scheltens P. 2017. Diagnostic impact of [18F]flutemetamol PET in early-onset dementia. *Alzheimer's Research & Therapy*. 9:2.

## Supplementary material

### Supplementary Text 1

The following acquisition parameters were used to acquire structure MRI 3D T1-weighted images: 1.5T Siemens Avanto (n=5): Magnetization prepared rapid acquisition gradient echo (MPRAGE), coronal plane, repetition time (TR) 2700 ms, echo time (TE) 5.2 ms, inversion time (TI) 950 ms, flip angle (FA) 8°, voxel size 1×1×1.5 mm<sup>3</sup>; 3T GE Discovery MR750 (n=9): FSPGR, sagittal plane, TR 7.8 ms, TE 3ms, FA 12°, voxel size 1 mm<sup>3</sup>; 1T Siemens Magnetom Impact (n=106): MPRAGE, coronal plane, TR 15 ms, TE 7 ms, TI 300 ms, FA 15°, voxel size 1×1×1.5 mm<sup>3</sup>; 3T Philips Ingenuity PET/MR system (n=47): sagittal turbo field echo (TFE), sagittal plane, TR 7 ms, TE 3 ms, FA 12°, voxel size 1×1×1 mm<sup>3</sup>; 1.5T GE SignaHDxt (n=8): sagittal fast spoiled gradient echo (FSPGR), sagittal plane, TR 12.4 ms, TE 5.17 ms, TI 450 ms, FA 12°, voxel size 0.98×0.98×1.5 mm<sup>3</sup>; 3T GE SignaHDxt (n=119): FSPGR, sagittal plane, TR 708 ms, TE 7 ms, FA 12°, voxel size 0.98×0.98×1 mm<sup>3</sup>; 1.5T Siemens Sonata (n=18): MPRAGE, coronal plane, TR 2700 ms, TE 3.97 ms, TI 950 ms, FA 8°, voxel size 1×1×1.5 mm<sup>3</sup>; Toshiba Titan 3T (n=53): sagittal fast field echo (FFE) sequence (TR = 9, TE = 3, TI = 800, FA = 7°, 1.00 x 1.00 x 1.00 mm voxels); 1.5T Siemens Vision (n=1): MPRAGE, coronal plane, TR 15 ms, TE 7 ms, FA 8°, voxel size 0.98×0.98×1.5 mm<sup>3</sup>.

**Supplementary Table 1. Risk of MCI or dementia for continuous N biomarkers for complete cases**

	<b>Model 1</b>	<b>Model 2</b>	<b>Model 3</b>	<b>Model 4</b>
<b>Biomarker</b>	<b>HR (95% CI)</b>	<b>HR (95% CI)</b>	<b>HR (95% CI)</b>	<b>HR (95% CI)</b>
T-tau	2.26 (1.74 - 2.94) <sup>ab</sup>	1.98 (1.47 - 2.67) <sup>ab</sup>	1.57 (1.16 - 2.11) <sup>ab</sup>	
MTA	1.53 (1.16 - 2.02) <sup>ab</sup>	1.18 (0.86 - 1.62)	1.00 (0.72 - 1.39)	1.01 (0.72 - 1.40)
HV	1.65 (1.18 - 2.30) <sup>ab</sup>	1.52 (1.06 - 2.18) <sup>ab</sup>	1.47 (1.04 - 2.07) <sup>ab</sup>	1.52 (1.06 - 2.16) <sup>ab</sup>
NfL	1.83 (1.40 - 2.39) <sup>ab</sup>	1.49 (1.04 - 2.13) <sup>ab</sup>	1.30 (0.86 - 1.94)	1.31 (0.87 - 1.98)
GFAP	2.47 (1.80 - 3.38) <sup>ab</sup>	2.08 (1.45 - 2.99) <sup>ab</sup>	1.49 (1.00 - 2.22) <sup>a</sup>	1.43 (0.96 - 2.12)

Data shown are hazard ratio (95% confidence interval) as estimated by Cox proportional hazards analyses (outcome: clinical progression to mild cognitive impairment or dementia). N = 256. Predictors included differed per model (model 1: neurodegeneration biomarker; model 2: neurodegeneration biomarker, age and sex; model 3: abeta, neurodegeneration biomarker, age and sex; model 4: abeta, p-tau, neurodegeneration biomarker, age and sex). In models with MTA and HV, scanner type was additionally added as covariate. P-tau, t-tau, NfL and GFAP were log transformed, abeta and hippocampal volume were inverted, all biomarkers were z-transformed. MTA = medial temporal atrophy, HV = hippocampal volume, NfL = neurofilament light, GFAP = glial fibrillary acidic protein. <sup>a</sup> p-value < 0.05. T-tau was not entered in model 4 due to collinearity between t-tau and p-tau. <sup>b</sup> FDR corrected p-value < 0.05.

**Supplementary Table 2. Risk of cognitive decline for continuous N biomarkers for complete cases**

	<b>Model 5</b>	<b>Model 6</b>	<b>Model 7</b>	<b>Model 8</b>
<b>Biomarker</b>	<b>Beta (SE)</b>	<b>Beta (SE)</b>	<b>Beta (SE)</b>	<b>Beta (SE)</b>
T-tau	-0.22 (0.04) <sup>ab</sup>	-0.22 (0.05) <sup>ab</sup>	-0.20 (0.05) <sup>ab</sup>	
MTA	-0.07 (0.06)	-0.06 (0.06)	-0.04 (0.06)	-0.03 (0.06)
HV	-0.15 (0.05) <sup>ab</sup>	-0.18 (0.05) <sup>ab</sup>	-0.17 (0.05) <sup>ab</sup>	-0.17 (0.05) <sup>ab</sup>
NfL	-0.09 (0.05)	-0.07 (0.06)	-0.04 (0.07)	-0.03 (0.06)
GFAP	-0.18 (0.05) <sup>ab</sup>	-0.17 (0.06) <sup>ab</sup>	-0.13 (0.06) <sup>a</sup>	-0.11 (0.06)

Results shown are beta (SE) as estimated by linear mixed models. Outcome is MMSE score. Predictors: model 5: neurodegeneration, time, neurodegeneration\*time; model 6: variables included in model 5, age, sex, age\*time and sex\*time; model 7: variables included in model 6, CSF abeta and abeta\*time; model 8: variables included in model 7, CSF p-tau and p-tau\*time). In models with MTA and HV, scanner type was additionally added as covariate. Betas represent the interaction between neurodegeneration biomarker and time, which corresponds to the cognitive slope. P-tau, t-tau, NfL and GFAP were log transformed, abeta and hippocampal volume were inverted, all biomarkers were z-transformed. MTA = medial temporal atrophy, HV = hippocampal volume, NfL = neurofilament light, GFAP = glial fibrillary acidic protein. T-tau was not entered in model 4 due to collinearity between t-tau and p-tau. <sup>a</sup> p-value < 0.05. <sup>b</sup> FDR corrected p-value < 0.05.







## CHAPTER 4

# **Tau-Related Grey Matter Network Breakdown Across the Alzheimer's Disease Continuum**

Wiesje Pelkmans, Rik Ossenkoppele, Ellen Dicks, Olof Strandberg, Frederik Barkhof, Betty M. Tijms, Joana B. Pereira, Oskar Hansson

*Published in*  
*Alzheimer's Research & Therapy, 2021. 13(138)*  
*DOI: 10.1186/s13195-021-00876-7*

### **Abstract**

**Background:** Changes in grey matter covariance networks have been reported in preclinical and clinical stages of Alzheimer's disease (AD), and have been associated with amyloid- $\beta$  ( $A\beta$ ) deposition and cognitive decline. However, the role of tau pathology on grey matter networks remains unclear. Based on previously reported associations between tau pathology, synaptic density and brain structural measures, tau-related connectivity changes across different stages of AD might be expected. We aimed to assess the relationship between tau aggregation and grey matter network alterations across the AD continuum.

**Methods:** We included 533 individuals (178  $A\beta$ -negative cognitively unimpaired (CU) subjects, 105  $A\beta$ -positive CU subjects, 122  $A\beta$ -positive patients with mild cognitive impairment, and 128 patients with AD dementia) from the BioFINDER-2 study. Single-subject grey matter networks were extracted from T1-weighted images and graph theory properties including degree, clustering coefficient, path length, and small world topology were calculated. Associations between tau positron emission tomography (PET) values and global and regional network measures were examined using linear regression models adjusted for age, sex, and total intracranial volume. Finally, we tested whether the association of tau pathology with cognitive performance was mediated by grey matter network disruptions.

**Results:** Across the whole sample, we found that higher tau load in the temporal meta-ROI was associated with significant changes in degree, clustering, path length, and small world values (all  $p < 0.001$ ), indicative of a less optimal network organisation. Already in CU  $A\beta$ -positive individuals associations between tau burden and lower clustering and path length were observed, whereas in advanced disease stages elevated tau pathology was

progressively associated with more brain network abnormalities. Moreover, the association between higher tau load and lower cognitive performance was only partly mediated (9.3 to 9.5%) through small world topology.

**Conclusions:** Our data suggest a close relationship between grey matter network disruptions and tau pathology in individuals with abnormal amyloid. This might reflect a reduced communication between neighbouring brain areas and an altered ability to integrate information from distributed brain regions with tau pathology, indicative of a more random network topology across different AD stages.

### **Introduction**

Alzheimer's disease (AD) is generally thought to start with the aggregation of amyloid- $\beta$  ( $A\beta$ ) in the brain, followed by deposition of neocortical tau pathology, synaptic dysfunction, atrophy, and cognitive decline (Selkoe and Hardy 2016; Jack et al. 2018; Scheltens et al. 2021). However, the sequence and interactions of the pathophysiological processes and structural brain changes that occur during this long pre-dementia period are not well understood. Given that brain network abnormalities can already be observed in pre-dementia stages and contribute to cognitive impairment in AD (Seeley et al. 2009; Jones et al. 2016; van den Heuvel and Sporns 2019), further clarification on the interrelations between brain connectivity with key pathological aggregates of AD could increase our understanding on the pathogenesis of AD.

One method to assess brain connectivity consists of measuring the similarity of cortical grey matter (GM) morphology, based on the notion that brain regions that engage in similar cognitive or behavioural processes tend to develop in a homologous way (Mechelli 2005; Alexander-Bloch, Giedd, et al. 2013; Evans 2013) through functional coactivation and/or axonal connectivity between brain regions (Gong et al. 2012; Alexander-Bloch, Raznahan, et al. 2013; Doucet et al. 2019). Previous studies have shown GM network disruptions in preclinical AD (Tijms et al. 2016; ten Kate et al. 2018; Verfaillie et al. 2018; Voevodskaya et al. 2018), mild cognitive impairment (Yao et al. 2010; Spreng and Turner 2013; Montembeault et al. 2016; Pereira et al. 2016; Dicks et al. 2018), and AD dementia (He et al. 2008; Seeley et al. 2009; Li et al. 2012; Tijms et al. 2013; Kim et al. 2016; John et al. 2017). Moreover, GM network disruptions have been related to increased  $A\beta$  pathology (Oh et al. 2011; Tijms et al. 2016; ten Kate et al. 2018; Voevodskaya et al. 2018), while influences of tau pathology on GM brain

networks remain unknown. Intraneuronal tau is thought to be more closely linked to synaptic function, brain integrity and clinical symptoms, than A $\beta$  plaques (Nelson et al. 2012; Menkes-Caspi et al. 2015; Ossenkoppele et al. 2016; Coomans et al. 2021). Therefore, we hypothesised that tau pathology may contribute to impaired network organization in AD.

In this study we tested whether tau deposition (measured with tau-positron emission tomography [PET]) was associated with GM network alterations (measured with structural magnetic resonance imaging [MRI]) in individuals across the AD spectrum, and whether these relationships were differentially linked with disease severity.

## Methods

### *Participants*

We included 533 individuals from the Swedish BioFINDER-2 study (NCT03174938) who underwent tau-PET, structural MRI, and lumbar puncture to determine cerebrospinal fluid (CSF) A $\beta_{42}$ /A $\beta_{40}$  levels as described previously (Leuzy et al. 2020). In the present study we included subjects > 50 years of age with an abnormal CSF A $\beta$  status, resulting in three groups along the AD continuum: A $\beta$ -positive cognitively unimpaired (CU) subjects (preclinical AD), A $\beta$ -positive patients with mild cognitive impairment (prodromal AD) and A $\beta$ -positive patients with AD dementia. Diagnosis was made according to clinical diagnostic criteria of the diagnostic and statistical manual of mental disorders (DSM)-5 (American Psychiatric Association 2013). In addition, an A $\beta$ -negative cognitively unimpaired control group was included.

All subjects underwent the Mini-Mental State Examination (MMSE; Folstein et al. 1983) and delayed word list recall test from the ADAS-Cog (Alzheimer's Disease Assessment Scale - Cognitive Subscale; Rosen et al.

1984) to assess global cognition and episodic memory, respectively. The inclusion and exclusion criteria of the BioFINDER-2 sub-cohorts are described in more detail in the Supplementary Methods section. All participants gave written informed consent to participate in the study. Ethical approval was given by the regional ethics committee at Lund University, Sweden. PET imaging procedures were approved by the Radiation protection committee at Skåne University Hospital and by the Swedish Medical Products Agency.

### *MRI Acquisition and Pre-processing*

T1-weighted images were acquired using a magnetization-prepared rapid gradient echo sequence on a 3T Siemens MAGNETOM Prisma scanner (Siemens Medical Solutions, Erlangen, Germany) using the following parameters: 178 slices, repetition time: 1950 ms, echo time: 3.4 ms, inversion time: 900 ms, flip angle: 9°, 1 mm isotropic voxels. All images were segmented into grey matter, white matter, and CSF using the Statistical Parametric Mapping (SPM12, <https://www.fil.ion.ucl.ac.uk/spm/software/spm12/>) running in MATLAB (v2019b). The segmented grey matter images were resliced to 2x2x2 mm isotropic voxels to reduce the dimensionality of the data. Then, the images were parcellated into 100 anatomical brain regions using the Automated Anatomical Labelling (AAL3) atlas (all thalamic nuclei combined; Rolls et al. 2020), which was warped from standard space to subject space using subject-specific inverse normalisation parameters. The quality of these steps was visually assessed and two subjects had to be excluded due to misalignment of the brain atlas with the GM image. Total intracranial volume (TIV) was computed as the sum of grey matter, white matter, and CSF volumes.



### *Single-Subject Grey Matter Networks*

Single-subject grey matter networks were extracted from the native grey matter images using an automated template-free approach that has been previously published ([https://github.com/bettytijms/Single\\_Subject\\_Grey\\_Matter\\_Networks](https://github.com/bettytijms/Single_Subject_Grey_Matter_Networks); Tijms et al. 2012). For each subject, the grey matter network was built as a set of nodes connected by edges. The nodes were defined as cubes of 3 x 3 x 3 voxels (6x6x6 mm<sup>3</sup>), which size was chosen based on 2 factors: (I) the minimum spatial resolution needed to still capture cortical folding has shown to be 3 mm [38], (II) and the practical computational limitations that exist with large matrices. These cubes keep the 3D structure of the cortex intact, and thereby contain information on grey matter intensity as well as spatial information between the voxels. In order to find the maximum correlation value with a target cube using Pearson correlation coefficients, each cube was rotated by an angle with multiples of 45° over all axes, contributing to all positive connections. Self-connections were set to zero. The resulting similarity matrix containing all pairwise correlations was binarized using a threshold that reduced the chance of spurious correlations in the network to 5%. This corresponded to a significance level of  $p < 0.05$  corrected for multiple comparisons using a permutation-based procedure (Noble 2009). The presence of an edge was indicated when the correlation between each pair of nodes exceeds this threshold. For regional network analyses, the corresponding atlas label for each cube was determined, this enabled averaging the GM network values and volume across nodes that were labelled according to that atlas region. A total of four subjects had to be excluded due to network calculation failure.

### *Network Properties*

Global and regional measures were calculated for each individual GM network. To assess global network properties the following measures were computed: network size (the total number of nodes in the network), degree (the number of edges), connectivity density (the ratio of existing connections to the maximum number of possible connections), clustering coefficient (the fraction of a node's neighbours that are also neighbours of each other), and path length (shortest path length between all pairs of nodes in the network). To normalise the network properties to random networks, we divided the average clustering coefficient and path length values by those values of five randomised reference networks of identical size and degree distribution, resulting in  $\gamma$  and  $\lambda$ , respectively (Maslov and Sneppen 2002). The ratio of  $\gamma$  to  $\lambda$ , is defined as the small-world coefficient  $\sigma$  (Humphries and Gurney 2008), indicative of the optimal balance between information segregation and integration. To assess regional network properties, the degree, clustering coefficient, and path length were also calculated for each atlas brain area, i.e., region of interest (ROI). All network measures were computed with functions from the Brain Connectivity Toolbox (<https://sites.google.com/site/bctnet/>; Bullmore and Sporns 2009), modified for large scale networks.

### *PET Acquisition and Pre-processing*

Tau-PET imaging was conducted 70–90 min after injection of  $365 \pm 20$  MBq [ $^{18}\text{F}$ ]RO948 on digital GE Discovery MI scanners (General Electric Medical Systems; Yap et al. 2021). Low-dose CT scans were performed immediately prior to the PET scans for attenuation correction. PET data was reconstructed using VPFX-S (ordered subset expectation maximization with time-of-flight and point spread function corrections) with 6 iterations and

17 subsets with 3 mm smoothing, standard Z filter, and 25.6-cm field of view with a  $256 \times 256$  matrix. After list-mode data was binned into 4x5-min time frames, PET images were motion corrected (rigid transformation using AFNI, 3dvolreg; Cox J.S. 1996), summed, and co-registered to their corresponding T1-weighted MR images. Standardized uptake value ratio (SUVR) images were created using the inferior cerebellar cortex as a reference region (Leuzy et al. 2020). We calculated PET data both corrected and uncorrected for partial volume errors. Partial volume correction (PVC) was performed using the geometric transfer matrix method, as described in Rousset et al. (1998), PVC findings are available in the supplementary results section (Sup. Figure 1,2, Sup. Table2).

To investigate the associations between tau pathology and network changes across different AD pathological stages, four composite regions were created based on the Braak staging scheme for neurofibrillary tangle pathology (Braak and Braak 1991), adapted to PET space by Cho et al. (2016). These included the following brain regions as defined by the AAL atlas (see Supplementary Methods 2 for details), and cover stage I-II (hippocampal formation), stage III-IV (fusiform, amygdala, cingulate and inferior and middle temporal cortices), and stage V-VI (widespread neocortical areas including the orbitofrontal, superior, middle and inferior frontal, precentral, paracentral, postcentral, precuneus, inferior and superior parietal, supramarginal, superior temporal, medial and lateral occipital cortices). In addition, a tau temporal meta-ROI capturing stages I to IV was calculated using the volume weighted average of the corresponding regions (Ossenkoppele et al. 2018).

### *CSF Collection and Analysis*

CSF samples were obtained with a lumbar puncture and collected into 5 ml LoBind polypropylene tubes handled according to the Alzheimer's Association Flow Chart for lumbar puncture (Blennow et al. 2010). Concentrations of  $A\beta_{42}$  and  $A\beta_{40}$  were quantified using enzyme-linked immunosorbent assays (ELISAs; INNOTEST, Fujirebio). Amyloid-status was determined using the  $A\beta_{42}/A\beta_{40}$  ratio with a cut-off of  $<0.089$  as defined abnormal in clinical practice at the Sahlgrenska University Hospital, Mölndal, Sweden (Leuzy et al. 2020).

### *Statistical Analyses*

Comparisons of demographical and clinical characteristics between groups were performed using chi-squared tests for categorical variables and one-way ANOVA for continuous variables.

To analyse the relationship between tau-PET (predictor) and global network measures (outcome), we used linear regression models adjusted for age, sex, and TIV (all models), and connectivity density (for path length, clustering,  $\gamma$ ,  $\lambda$ , and  $\sigma$ ), since higher-order measures have shown to depend on the number of nodes and edges in the network (van Wijk et al. 2010). The association between tau-PET and global network measures was first tested across the whole sample, and then repeated within diagnostic groups with the interaction term group. Additionally, CSF  $A\beta_{42}/A\beta_{40}$  was added to the linear regression model to test for an interaction effect CSF  $A\beta_{42}/A\beta_{40} * \tau$  on GM network changes. Z-scores for the network properties were calculated using the  $A\beta$ -negative control group mean and standard deviation, to aid comparisons of effect sizes between network properties.

We further investigated the relationship of tau pathology with GM network disruptions at the local level across all AAL areas. Regional analyses

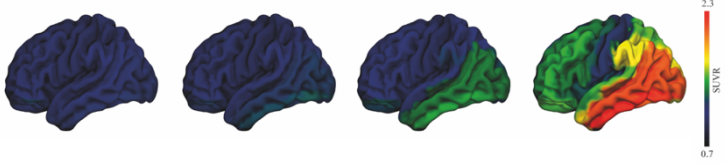
were adjusted for age, sex, TIV, local GM volume, and for clustering and path length also local degree. For global network analyses, we applied a threshold of  $p < 0.05$ , corrected for multiple comparisons using the false discovery rate (FDR) correction method. For local network analyses, we adjusted for multiple testing using a Bonferroni correction ( $p < 0.05$ ).

Finally, we performed mediation analyses using the Mediation package (Tingley et al. 2014), to assess whether the association of tau pathology with cognitive performance was mediated by GM network disruptions. For these exploratory analyses we assessed the small world coefficient only, as it indicates how randomly organized the network is, and it can be considered a summary measure of both  $\gamma$  and  $\lambda$ . Analyses were performed using R (v4.0.2.) and visualized using Surf Ice (v2).

## Results

### *Participants*

In total 178 A $\beta$ -negative CU controls, 105 preclinical AD, 122 prodromal AD, and 128 AD dementia patients were included in the present study (mean age =  $70.5 \pm 9.3$  years; Table 1). Control subjects were younger and had a lower prevalence of apolipoprotein E (*APOE*)  $\epsilon 4$  than the other groups. As expected, lower MMSE scores, lower hippocampal volume, and higher tau-PET SUVR values were observed in the prodromal AD and AD dementia groups compared to the CU subjects.

**Table 1. Subject characteristics**


	<b>Control</b>	<b>Preclinical AD</b>	<b>Prodromal AD</b>	<b>AD dementia</b>
	<i>n</i> =178	<i>n</i> =105	<i>n</i> =122	<i>n</i> =128
Age, (y)	66.1 (10.3) <sup>b,c,d</sup>	71.8 (9.3) <sup>a</sup>	72.0 (7.2) <sup>a</sup>	74.1 (6.8) <sup>a</sup>
Sex, f	103 (58%) <sup>c</sup>	56 (53%)	55 (45%) <sup>a</sup>	71 (55%)
Education (y)	12.6 (3.3)	12.3 (3.5)	12.7 (4.5)	12.1 (4.4)
MMSE	29.1 (1.1) <sup>c,d</sup>	28.8 (1.3) <sup>c,d</sup>	27.0 (1.9) <sup>a,b,d</sup>	20.0 (4.4) <sup>a,b,c</sup>
<i>APOEε4</i> carrier	60 (34%) <sup>b,c,d</sup>	65 (62%) <sup>a</sup>	83 (69%) <sup>a</sup>	91 (71%) <sup>a</sup>
Hippocampal vol.	7.5 (1.4) <sup>b,c,d</sup>	7.0 (1.4) <sup>a,c,d</sup>	6.1 (1.4) <sup>a,b,d</sup>	5.0 (1.1) <sup>a,b,c</sup>
Tau-PET	1.09 (0.08) <sup>c,d</sup>	1.14 (0.15) <sup>c,d</sup>	1.24 (0.26) <sup>a,c,d</sup>	1.72 (0.43) <sup>a,b,c</sup>

Data are presented as mean  $\pm$  SD, or n (%); Tau-PET is SUVR in Meta-ROI; Hippocampal volume is in cm<sup>3</sup>; AD, Alzheimer's disease; F, female; MMSE, Mini Mental State Examination (0–30); ApoE, Apolipoprotein; SUVR, Standardized uptake value ratio; ApoE 2 missings; *a* significantly different than control; *b* significantly different than preclinical AD; *c* significantly different than prodromal AD; *d* significantly different than AD dementia at *p*<0.05; Surfaceplots display mean [18F]RO948 SUVR images.

### *Single-Subject Grey Matter Networks*

Networks had an average size of 6976 nodes (sd=664) and an average connectivity density of 16% (sd=1) across all participants (Table 2). We observed that all grey matter network metrics showed lower values indicative of increased network abnormalities with advancing disease severity (Table 2). Differences between A $\beta$ -negative controls and preclinical AD subjects were subtle and higher-order network differences lost significance after adjusting for covariates, including age. Compared to A $\beta$ -negative controls, prodromal AD subjects showed lower clustering, path length,  $\gamma$ ,  $\lambda$ , and small world coefficient values. Similar changes were observed in AD dementia, with in addition lower network size and degree compared to controls. In addition, all higher-order metrics were significantly lower in AD dementia compared to prodromal AD and significantly lower in prodromal AD compared to preclinical AD.

Table 2. Summary of global network measures

	Control <i>n</i> =178	Preclinical AD <i>n</i> =105	Prodromal AD <i>n</i> =122	AD dementia <i>n</i> =128
Network size	7171.15 (671.92) <sup>d</sup>	7007.46 (672.18) <sup>d</sup>	6987.52 (612.17) <sup>d</sup>	6666.01 (581.66) <sup>ab,c</sup>
Degree	1193.11 (148.21) <sup>d</sup>	1159.10 (139.57) <sup>d</sup>	1140.61 (133.61) <sup>d</sup>	1072.01 (138.78) <sup>ab,c</sup>
Connectivity density	16.61 (0.98)	16.53 (1.07)	16.30 (0.92)	16.06 (1.27)
Clustering coefficient	0.46 (0.02) <sup>cd</sup>	0.46 (0.02) <sup>cd</sup>	0.45 (0.02) <sup>ab,d</sup>	0.44 (0.02) <sup>ab,c</sup>
Path length	1.98 (0.03) <sup>cd</sup>	1.97 (0.03) <sup>cd</sup>	1.96 (0.03) <sup>ab,d</sup>	1.96 (0.03) <sup>ab,c</sup>
Gamma	1.58 (0.11) <sup>cd</sup>	1.54 (0.12) <sup>cd</sup>	1.50 (0.09) <sup>ab,d</sup>	1.43 (0.09) <sup>ab,c</sup>
Lambda	1.08 (0.01) <sup>cd</sup>	1.07 (0.02) <sup>cd</sup>	1.07 (0.01) <sup>ab,d</sup>	1.06 (0.01) <sup>ab,c</sup>
Small world coefficient	1.47 (0.08) <sup>cd</sup>	1.43 (0.09) <sup>cd</sup>	1.40 (0.07) <sup>ab,d</sup>	1.35 (0.07) <sup>ab,c</sup>

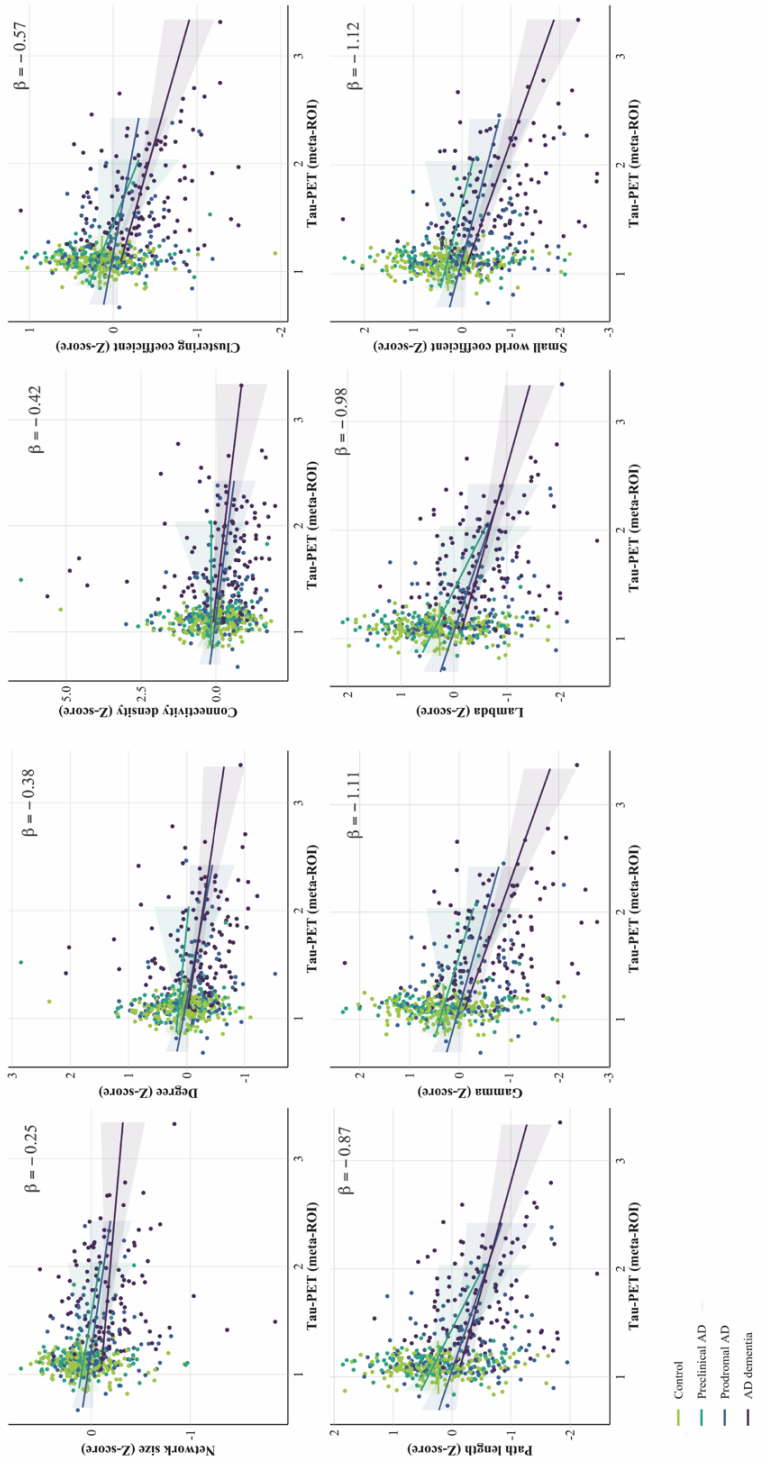
Data are presented as mean  $\pm$  SD; AD, Alzheimer's disease; gamma is normalised clustering; lambda is normalised path length  
*a* significantly different than control; *b* significantly different than preclinical AD; *c* significantly different than prodromal  
AD; *d* significantly different than AD dementia at *p* < 0.05 when adjusting for age, sex, TIV, and connectivity density  
(clustering, path length,  $\gamma$ ,  $\lambda$ , small world-only).

Table 3. Associations between global network measures and tau-PET

Network property	Whole sample	Control	Preclinical AD	Prodromal AD	AD dementia
Network size	<b>-0.25 (0.03)</b> <sup>***</sup>	0.14 (0.26)	-0.22 (0.18)	-0.17 (0.10)	-0.08 (0.06)
Degree	<b>-0.38 (0.06)</b> <sup>***</sup>	-0.37 (0.46)	-0.22 (0.31)	-0.36 (0.17)	<b>-0.26 (0.10)</b> <sup>*</sup>
Connectivity density	<b>-0.42 (0.13)</b> <sup>**</sup>	-1.03 (0.97)	-0.04 (0.66)	-0.48 (0.35)	-0.42 (0.21)
Clustering coefficient	<b>-0.57 (0.05)</b> <sup>***</sup>	-0.24 (0.38)	<b>-0.58 (0.26)</b> <sup>*</sup>	-0.26 (0.14)	<b>-0.34 (0.08)</b> <sup>***</sup>
Path length	<b>-0.87 (0.08)</b> <sup>***</sup>	-0.25 (0.62)	<b>-1.04 (0.42)</b> <sup>*</sup>	<b>-0.65 (0.23)</b> <sup>**</sup>	<b>-0.47 (0.14)</b> <sup>**</sup>
Gamma	<b>-1.11 (0.09)</b> <sup>***</sup>	-0.23 (0.71)	-0.79 (0.48)	<b>-0.65 (0.26)</b> <sup>*</sup>	<b>-0.72 (0.16)</b> <sup>***</sup>
Lambda	<b>-0.98 (0.09)</b> <sup>***</sup>	-0.29 (0.69)	<b>-1.15 (0.47)</b> <sup>*</sup>	<b>-0.72 (0.25)</b> <sup>**</sup>	<b>-0.53 (0.15)</b> <sup>**</sup>
Small world coefficient	<b>-1.12 (0.10)</b> <sup>***</sup>	-0.21 (0.73)	-0.70 (0.49)	<b>-0.63 (0.27)</b> <sup>*</sup>	<b>-0.75 (0.16)</b> <sup>***</sup>

Data are presented as  $\beta$  (SE); Network measures are Z transformed; gamma is normalized clustering; lambda is normalized path length; SUVR values in temporal meta-ROI; Model is adjusted for age, sex, TIV, and connectivity density (clustering, path length,  $\gamma$ ,  $\lambda$ , small world-only). \* *p* < 0.05, \*\* *p* < 0.01, \*\*\* *p* < 0.001, FDR corrected.





**Figure 1.** Scatterplots of the relation between tau-PET SUVR values and global grey matter network measures by disease stage. Standardised beta estimates are displayed for significant relationships across all participants adjusting for age, sex, TIV, and connectivity density (clustering, path length,  $\gamma$ ,  $\lambda$ , small world-only).

*Relationship between Tau Pathology and Global Grey Matter Network Measures*

Across the whole sample, higher tau-PET values in the temporal meta-ROI were associated with lower values in all network properties (range  $\beta = -0.25$  to  $\beta = -1.12$ ; Figure 1; Table 3), showing strongest associations for  $\gamma$  and small world values. We observed similar relationships between GM network measures and tau signal in early (i.e., stage I/II) and late (i.e., stage V/VI) tau accumulation regions (Supplementary Results Table 1).

When repeating the analyses stratified by diagnostic group, we found more significant associations between tau-PET and network measures with increasing disease severity: In preclinical AD, higher tau-PET values in the meta-ROI was associated with lower clustering values ( $\beta \pm SE$ ;  $-0.58 \pm 0.26$ ), path length ( $-1.04 \pm 0.24$ ), and  $\lambda$  values ( $-1.15 \pm 0.47$ ; all  $p < .05$ ; Figure 1; Table 3). In prodromal AD, higher tau-PET retention was related to lower path length ( $-0.65 \pm 0.23$ ),  $\gamma$  ( $-0.65 \pm 0.26$ ),  $\lambda$  ( $-0.72 \pm 0.25$ ), and small world coefficient values ( $-0.63 \pm 0.27$ ). In AD dementia, higher tau PET signal in the temporal meta-ROI was associated with lower degree ( $-0.26 \pm 0.10$ ), clustering ( $-0.34 \pm 0.08$ ), path length ( $-0.47 \pm 0.14$ ),  $\gamma$  ( $-0.72 \pm 0.16$ ),  $\lambda$  ( $-0.53 \pm 0.15$ ), and small world coefficient values ( $-0.75 \pm 0.16$ ). No association between tau-PET values and global network measures was observed in A $\beta$ -negative controls. Moreover, no group interaction effects were observed, indicating that the *strength* of the association between GM network measures and tau pathology did not differ significantly between disease stage.

When repeating the same analysis using the three ROIs specific for different tau stages, no association was observed between tau-PET values in the hippocampal formation (Braak I/II) and global network properties in preclinical AD participants (Supplementary Results Table 1), suggesting that

using the tau-PET signal in the temporal meta-ROI is more suitable in relation to network measures than early tau-accumulation regions. Tau pathology in limbic (Braak III-IV) and neocortical (Braak V-VI) areas correlated with decreased degree, clustering, path length,  $\gamma$ ,  $\lambda$ , and small world coefficient values in prodromal and AD dementia subjects (Supplementary Results Table 1). Moreover, we observed similar relationships between GM network measures and tau signal when repeating the analyses without the  $A\beta$ -negative control group (Supplementary Results Table 3). Furthermore, there were no significant interactions between tau pathology and  $A\beta_{42}/A\beta_{40}$  ratio values on GM network measures, suggesting that the associations between GM network alterations and tau pathology in  $A\beta$  positive individuals cannot be explained by CSF  $A\beta$  levels (Supplementary Results Table 3).

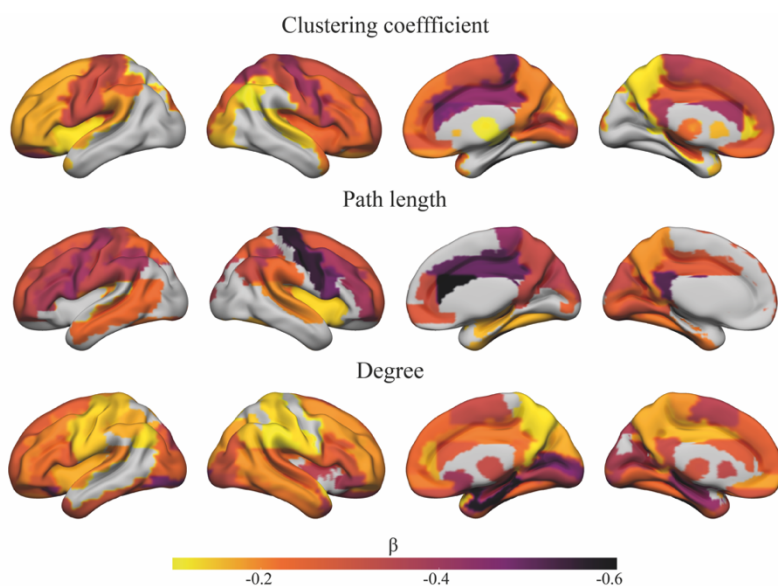


**Figure 2.** Surface plots of standardised  $\beta$  values of the relationship between tau-PET and local clustering, path length, and degree in participants with abnormal  $A\beta$ . Data are presented for regions with a significant correlation at  $p_{\text{Bonferroni}} < .05$  adjusted for age, sex, TIV, local degree, and local GM volume.

### *Relationship between Tau Pathology and Regional Grey Matter Network Measures*

Next, we examined the relationship between tau burden in the temporal meta-ROI with network measures at a local level in subjects on the AD continuum to assess a region-dependent effect. We observed different anatomical patterns of associations for each network measure. Lower clustering values were associated with higher tau-PET SUVR values in widespread brain areas, showing the strongest associations in the precentral cortex, cingulate gyri, and frontal lobe (all  $p_{\text{bonferroni}} < 0.05$ ; Figure 2). Associations between lower path length values and higher tau-PET retention were strongest in the cingulate gyri, precentral cortex, and inferior frontal cortex. Regions characterized by a lower degree showed also widespread associations with tau, which was most pronounced in the hippocampus, parahippocampus, amygdala, medial occipital cortex and calcarine cortex (Figure 2).

### *Associations with Cognitive Performance*

We performed an exploratory analysis of the relationship of tau-pathology and small world topology with cognitive performance. Both higher tau-PET retention ( $\beta \pm \text{SE}$ ;  $-8.6 \pm 0.37$ ;  $5.30 \pm 0.34$ ) and lower small world values ( $\beta \pm \text{SE}$ ;  $2.14 \pm 0.19$ ;  $-1.23 \pm 0.15$ ) were significantly related to lower MMSE scores and more errors on the ADAS-Cog delayed word recall, respectively ( $p < 0.05$ ; Figure 3). Moreover, small world values remained significant when controlling for tau-SUVR values. Mediation analysis revealed that lower MMSE scores and more recall errors associated with tau pathology were partially mediated by decreased small world values (9.3% to 9.5%), but were mostly independent after controlling for the effect of small world coefficient.

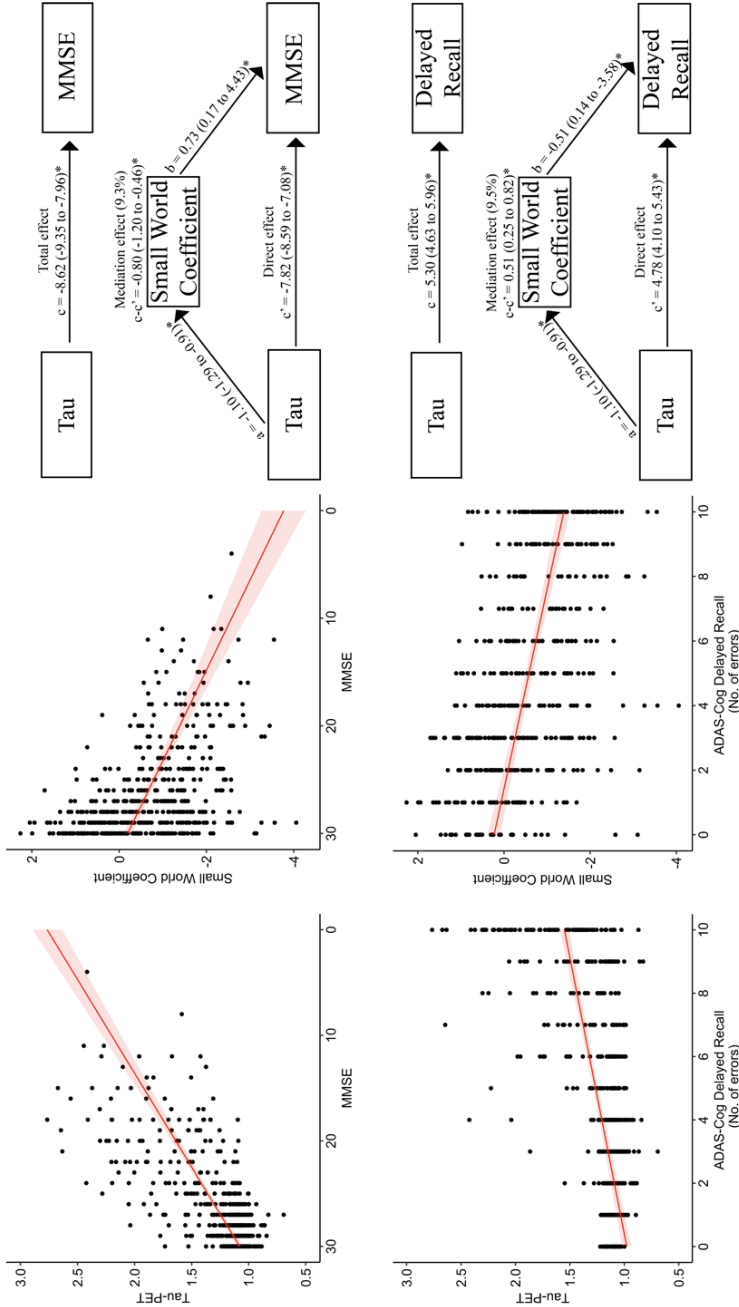


**Figure 3.** MMSE and ADAS-Cog delayed recall performance in relation to Tau-PET and Small world coefficient. Scatterplot showing the association of tau-PET SUVr values in the temporal meta-ROI and standardised grey matter network small world values with MMSE scores (top), and the ADAS-Cog delayed recall (bottom). Mediation analysis showing how small world topology mediates the effect of tau pathology on cognitive performance (right). Regression coefficients with a 95% confidence interval are displayed. (a) The effect of tau load on small world topology; (b) The effect of small world topology on cognitive performance when controlling for tau; (c). The total effect of tau on cognition (without controlling for mediation effects); (c'). The direct effect of tau pathology on cognition when adjusting for mediation; (c-c'). The mediation effect. \* $p < 0.05$ .

### **Discussion**

In a large well-phenotyped cohort, we observed that higher tau-PET retention is related to greater GM network disruptions in individuals across the AD continuum. More advanced tau-related GM network abnormalities were observed with increasing disease severity. These findings suggest that tau pathology is associated with a reduced communication between neighbouring brain areas and an altered ability to integrate information from distributed brain regions indicative of a more random network topology across different AD stages.

Our results show a close relationship between GM network disruptions and tau pathology in individuals with abnormal amyloid. With increasing disease severity, we observed a greater tau load, as well as a greater number of abnormal GM network measures. As a result, the association of more network abnormalities with increased tau-PET retention may be largely based on differences in disease stage. Furthermore, when stratifying the analyses for diagnostic groups, we observed that distinct network measures were sensitive to different aspects and severity of neurodegeneration. Specifically, already in preclinical AD increased tau-PET signal was associated with network alterations showing lower clustering, lower path length values and normalised path length  $\lambda$ . These associations were absent in CU individuals with normal amyloid, indicating that the presence of A $\beta$  might significantly alter tau-related GM connectivity. These findings are in line with prior studies showing deterioration in network properties in preclinical AD (ten Kate et al. 2018; Verfaillie et al. 2018; Dicks et al. 2020). In prodromal AD more network measures became abnormal with increasing tau pathology, additionally including changes in normalised clustering  $\gamma$ , and small world topology. In AD dementia patients nearly all network metrics were abnormal, suggesting that with pronounced

neurodegeneration GM networks exhibit significant topological alterations, which is in line with previous studies in AD dementia (He et al. 2008; Tijms et al. 2013; Pereira et al. 2016). Overall, these findings may indicate that higher tau burden is associated with a higher dissimilarity (i.e., asynchronous atrophy) between neighbouring areas, and increased similarity between distant brain areas as a result of progression of atrophy across the cortex, producing an increase in randomly connected nodes. Suggestive of an increasingly random network and reduction in small world organisation with disease progression (Bullmore and Sporns 2009; van den Heuvel and Sporns 2019).

When characterising the spatial associations of tau pathology and GM network changes, tau deposition appeared to be widespread and strongly associated with lower clustering and path length in several regions of the default-mode network including the medial prefrontal cortex, precuneus, and anterior and posterior cingulate cortex. These findings may be related to early amyloid accumulating regions (Buckner et al. 2005; Palmqvist et al. 2017). We see that it is in these regions that clustering and path length further relates to tau, while also, more unexpectedly, in late tau accumulating regions such as the sensory-motor cortex and occipital lobe, strong associations of lower clustering and path length with tau were observed. Similar regional associations of GM network decline over time have been observed in individuals in presymptomatic stages of familial AD (Vermunt et al. 2020). For lower degree, most strong correlations were observed in the medial temporal lobe, a region considered to be the tau epicentre where neurofibrillary tangles originate (Braak and Braak 1991), suggestive of less connections in the medial temporal lobe with increasing tau-PET signal.

Previous studies have related alterations in GM networks with abnormal amyloid aggregation in cognitively unimpaired individuals (Oh et al. 2011; Tijms et al. 2016; ten Kate et al. 2018; Voevodskaya et al. 2018), indicating that structural changes in GM networks are an early event in the pathophysiology of AD. Moreover, the presence of A $\beta$  is hypothesized to increase the accumulation of tau outside of the medial temporal lobe (Price and Morris 1999; Jack et al. 2019; Baek et al. 2020), which may further accelerate network decline. As pathological tau shows reduced ability to stabilize microtubules, contributing to impaired axonal transport (Menkes-Caspi et al. 2015; Coomans et al. 2021), this may lead to further synaptic loss and neurodegeneration, resulting in substantial network damage and impaired cognition (Nelson et al. 2012; Ossenkoppele et al. 2016; Schultz et al. 2017; Pereira et al. 2020). As reflected by our work showing that both increased tau pathology and a more random GM network topology were associated with worse performance on a global cognition and episodic memory test. Both factors showed an independent contribution to worse cognitive performance, while mediation analyses also indicated that small world topology partly mediated the effect of tau pathology on cognition.

### **Limitations**

There are some limitations to our study. Firstly, this a cross-sectional study that assumes three clinical stages of disease progression, future longitudinal studies are needed to determine the temporal ordering in tau pathology and associated brain network changes more accurately. Secondly, for uniformity reasons ROIs for both regional tau quantification and network topology calculation were created according to the AAL atlas. Unfortunately, the entorhinal cortex is not available as a separate region in this brain atlas, hence in the current study stage I/II refers to the hippocampus and



parahippocampus which includes the entorhinal cortex. This may have attenuated some of the results, but when testing the accuracy of the temporal meta-ROI in the AAL atlas with the Desikan-Killiany atlas, we observed a correlation of  $R=0.99$ , rendering such effects likely to be minimal. Thirdly, since tau abnormalities are closely related to  $A\beta$  pathology, it is difficult to know how specific the observed GM network alterations are to tau pathology. Strengths of our study includes the large number of well characterised participants. Moreover, the multimodal approach of combining structural MRI and tau-PET imaging aids in understanding fundamental questions in the AD pathophysiology.

### **Conclusions**

We found that GM network disruptions in AD are strongly linked with tau burden, already in an early disease stage when cognition is within the normal range, and becomes increasingly random with clinical progression. These findings provide more insight into the pathophysiological processes that contribute to brain network alterations in AD. An interesting future approach might lie in further investigating the prognostic value of GM single-subject networks in predicting cognitive decline, and whether it can be implemented in clinical practise.

### **Ethics approval and consent to participate**

All participants gave written informed consent to participate in the study. Ethical approval was given by the regional ethics committee at Lund University, Sweden. PET imaging procedures were approved by the Radiation protection committee at Skåne University Hospital and by the Swedish Medical Products Agency.

### **Availability of data and materials**

Anonymised study data for the primary analyses presented in this report are available on request from any qualified investigator for purposes of replicating the results.

### **Competing interests**

RO is an associate editor at Alzheimer's Research & Therapy. FB is a consultant to Biogen Idec, Merck-Serono, Novartis, Roche, IXICO Ltd, GeNeuro, and Combinostics. He received grants for Amyloid imaging for the Prevention of Alzheimer Disease (Innovative Medicines Initiative), European Progression Of Neurological Disease (H2020), UK Multiple Sclerosis Society, Dutch Multiple Sclerosis Society, National Institute Health Research University College London Biomedical Research Centre. OH has acquired research support (for the institution) from AVID Radiopharmaceuticals, Biogen, Eli Lilly, Eisai, GE Healthcare, Pfizer, and Roche. In the past 2 years, he has received consultancy/speaker fees from AC Immune, Alzpath, Biogen, Cerveau and Roche.

### **Funding**

The BioFINDER study was supported by the Swedish Research Council (2016-00906), the Knut and Alice Wallenberg foundation (2017-0383), the Marianne and Marcus Wallenberg foundation (2015.0125), the Strategic Research Area MultiPark (Multidisciplinary Research in Parkinson's disease) at Lund University, the Swedish Alzheimer Foundation (AF-939932), the Swedish Brain Foundation (FO2019-0326), The Parkinson foundation of Sweden (1280/20), the Skåne University Hospital Foundation (2020-0000028), Regionalt Forskningsstöd (2020-0314) and the Swedish federal government under the ALF agreement (2018-Projekt0279). The

precursor of  $^{18}\text{F}$ -RO948 was provided by Roche. ED is supported by Race Against Dementia (<https://www.raceagainstdementia.com/>). FB is supported by the NIHR biomedical research centre at UCLH. JBP is supported by the Swedish Research Council, Alzheimerfonden, Stratneuro, Center for Medical Innovation, Stohnes and Gamla Tjänarinnor. The funding sources had no role in the design and conduct of the study; in the collection, analysis, interpretation of the data; or in the preparation, review, or approval of the manuscript.

### **Authors' contributions**

WP, RO, JP, OH contributed to study concept and design. WP analysed the data. WP, RO, ED, OS, FB, BT, JP and OH interpreted the data and revised the manuscript for intellectual content. All authors approved the final manuscript.

### **Acknowledgements**

The authors kindly thank all participants for their contribution.

## References

- Alexander-Bloch A, Giedd JN, Bullmore E. 2013. Imaging structural co-variance between human brain regions. *Nature Reviews Neuroscience*. 14:322–336.
- Alexander-Bloch A, Raznahan A, Bullmore E, Giedd J. 2013. The Convergence of Maturational Change and Structural Covariance in Human Cortical Networks. *Journal of Neuroscience*. 33:2889–2899.
- American Psychiatric Association. 2013. *Diagnostic and Statistical Manual of Mental Disorders*, Arlington. American Psychiatric Association.
- Baek M seok, Cho H, Lee HS, Choi JY, Lee JH, Ryu YH, Lee MS, Lyoo CH. 2020. Temporal trajectories of in vivo tau and amyloid- $\beta$  accumulation in Alzheimer's disease. *European Journal of Nuclear Medicine and Molecular Imaging*. 47:2879–2886.
- Blennow K, Hampel H, Weiner M, Zetterberg H. 2010. Cerebrospinal fluid and plasma biomarkers in Alzheimer disease. *Nature Reviews Neurology*. 6:131–144.
- Braak H, Braak E. 1991. Neuropathological staging of Alzheimer-related changes. *Acta Neuropathologica*. 82:239–259.
- Buckner RL, Snyder AZ, Shannon BJ, Larossa G, Sachs R, Fotenos AF, Sheline YI, Klunk WE, Mathis CA, Morris JC, Mintun MA. 2005. Molecular, Structural, and Functional Characterization of Alzheimer's Disease: Evidence for a Relationship between Default Activity, Amyloid, and Memory. *Journal of Neuroscience*. 25:7709–7717.
- Bullmore E, Sporns O. 2009. Complex brain networks : graph theoretical analysis of structural and functional systems. *Nature Reviews Neurology*. 10:186–198.
- Cho H, Choi JY, Hwang MS, Kim YJ, Lee HM, Lee HS, Lee JH, Ryu YH, Lee MS, Lyoo CH. 2016. In vivo cortical spreading pattern of tau and amyloid in the Alzheimer disease spectrum. *Annals of Neurology*. 80:247–258.
- Coomans EM, Schoonhoven DN, Tuncel H, Verfaillie SCJ, Wolters EE, Boellaard R, Ossenkuppele R, den Braber A, Scheper W, Schober P, Sweeney SP, Ryan JM, Schuit RC, Windhorst AD, Barkhof F, Scheltens P, Golla SS v, Hillebrand A, Gouw AA, van Berckel BNM. 2021. In vivo tau pathology is associated with synaptic loss and altered synaptic function. *Alzheimer's Research & Therapy*. 13:35.
- Cox J.S. RW; H. 1996. AFNI: Software for analysis and visualization of functional magnetic resonance neuroimages. *Computers and Biomedical Research*. 29:162–173.
- Dicks E, Tijms BM, ten Kate M, Gouw AA, Benedictus MR, Teunissen CE, Barkhof F, Scheltens P, van der Flier WM. 2018. Gray matter network measures are associated with cognitive decline in mild cognitive impairment. *Neurobiology of Aging*. 61:198–206.

- Dicks E, Vermunt L, van der Flier WM, Barkhof F, Scheltens P, Tijms BM. 2020. Grey matter network trajectories across the Alzheimer's disease continuum and relation to cognition. *Brain Communications*. 2:1–15.
- Doucet GE, Moser DA, Rodrigue A, Bassett DS, Glahn DC, Frangou S. 2019. Person-Based Brain Morphometric Similarity is Heritable and Correlates With Biological Features. *Cerebral Cortex*. 29:852–862.
- Evans AC. 2013. Networks of anatomical covariance. *Neuroimage*. 80:489–504.
- Folstein MF, Robins LN, Helzer JE. 1983. The Mini-Mental State Examination. *Arch Gen Psychiatry*. 40:812.
- Gong G, He Y, Chen ZJ, Evans AC. 2012. Convergence and divergence of thickness correlations with diffusion connections across the human cerebral cortex. *Neuroimage*. 59:1239–1248.
- He Y, Chen Z, Evans A. 2008. Structural Insights into Aberrant Topological Patterns of Large-Scale Cortical Networks in Alzheimer's Disease. *Journal of Neuroscience*. 28:4756–4766.
- Humphries MD, Gurney K. 2008. Network 'Small-World-Ness': A Quantitative Method for Determining Canonical Network Equivalence. *PLoS ONE*. 3:e0002051.
- Jack CR, Bennett DA, Blennow K, Carrillo MC, Dunn B, Haeberlein SB, Holtzman DM, Jagust W, Jessen F, Karlawish J, Liu E, Molinuevo JL, Montine T, Phelps C, Rankin KP, Rowe CC, Scheltens P, Siemers E, Snyder HM, Sperling R, Elliott C, Masliah E, Ryan L, Silverberg N. 2018. NIA-AA Research Framework: Toward a biological definition of Alzheimer's disease. *Alzheimer's and Dementia*. 14:535–562.
- Jack CR, Wiste HJ, Botha H, Weigand SD, Therneau TM, Knopman DS, Graff-Radford J, Jones DT, Ferman TJ, Boeve BF, Kantarci K, Lowe VJ, Vemuri P, Mielke MM, Fields JA, Machulda MM, Schwarz CG, Senjem ML, Gunter JL, Petersen RC. 2019. The bivariate distribution of amyloid- $\beta$  and tau: relationship with established neurocognitive clinical syndromes. *Brain*. 142:3230–3242.
- John M, Ikuta T, Ferbinteanu J. 2017. Graph analysis of structural brain networks in Alzheimer's disease: beyond small world properties. *Brain Structure and Function*. 222:923–942.
- Jones DT, Knopman DS, Gunter JL, Graff-Radford J, Vemuri P, Boeve BF, Petersen RC, Weiner MW, Jack CR. 2016. Cascading network failure across the Alzheimer's disease spectrum. *Brain*. 139:547–562.
- Kim H-J, Shin J-H, Han CE, Kim HJ, Na DL, Seo SW, Seong J-K. 2016. Using Individualized Brain Network for Analyzing Structural Covariance of the Cerebral Cortex in Alzheimer's Patients. *Frontiers in Neuroscience*. 10:1–11.
- Kiselev VG, Hahn KR, Auer DP. 2003. Is the brain cortex a fractal? *Neuroimage*. 20:1765–1774.

- Leuzy A, Smith R, Ossenkoppele R, Santillo A, Borroni E, Klein G, Ohlsson T, Jögi J, Palmqvist S, Mattsson-Carlgrén N, Strandberg O, Stomrud E, Hansson O. 2020. Diagnostic Performance of RO948 F 18 Tau Positron Emission Tomography in the Differentiation of Alzheimer Disease From Other Neurodegenerative Disorders. *JAMA Neurology*. 77:955.
- Li Y, Wang Y, Wu G, Shi F, Zhou L, Lin W, Shen D. 2012. Discriminant analysis of longitudinal cortical thickness changes in Alzheimer's disease using dynamic and network features. *Neurobiology of Aging*. 33:427.e15-427.e30.
- Maslov S, Sneppen K. 2002. Specificity and Stability in Topology of Protein Networks. *Science* (1979). 296:910–913.
- Mechelli A. 2005. Structural Covariance in the Human Cortex. *Journal of Neuroscience*. 25:8303–8310.
- Menkes-Caspi N, Yamin HG, Kellner V, Spires-Jones TL, Cohen D, Stern EA. 2015. Pathological Tau Disrupts Ongoing Network Activity. *Neuron*. 85:959–966.
- Montembeault M, Rouleau I, Provost J-S, Brambati SM. 2016. Altered Gray Matter Structural Covariance Networks in Early Stages of Alzheimer's Disease. *Cerebral Cortex*. 26:2650–2662.
- Nelson PT, Alafuzoff I, Bigio EH, Bouras C, Braak H, Cairns NJ, Castellani RJ, Crain BJ, Davies P, Tredici K del, Duyckaerts C, Frosch MP, Haroutunian V, Hof PR, Hulette CM, Hyman BT, Iwatsubo T, Jellinger KA, Jicha GA, Kövari E, Kukull WA, Leverenz JB, Love S, Mackenzie IR, Mann DM, Masliah E, McKee AC, Montine TJ, Morris JC, Schneider JA, Sonnen JA, Thal DR, Trojanowski JQ, Troncoso JC, Wisniewski T, Woltjer RL, Beach TG. 2012. Correlation of Alzheimer Disease Neuropathologic Changes With Cognitive Status: A Review of the Literature. *Journal of Neuropathology & Experimental Neurology*. 71:362–381.
- Noble WS. 2009. How does multiple testing correction work? *Nature Biotechnology*. 27:1135–1137.
- Oh H, Mormino EC, Madison C, Hayenga A, Smiljic A, Jagust WJ. 2011.  $\beta$ -Amyloid affects frontal and posterior brain networks in normal aging. *Neuroimage*. 54:1887–1895.
- Ossenkoppele R, Rabinovici GD, Smith R, Cho H, Scholl M, Strandberg O, Palmqvist S, Mattsson N, Janelidze S, Santillo A, Ohlsson T, Jögi J, Tsai R, la Joie R, Kramer J, Boxer AL, Gorno-Tempini ML, Miller BL, Choi JY, Ryu YH, Lyoo CH, Hansson O. 2018. Discriminative accuracy of [18F]flortaucipir positron emission tomography for Alzheimer disease vs other neurodegenerative disorders. *JAMA - Journal of the American Medical Association*. 320:1151–1162.
- Ossenkoppele R, Schonhaut DR, Schöll M, Lockhart SN, Ayakta N, Baker SL, O'Neil JP, Janabi M, Lazaris A, Cantwell A, Vogel J, Santos M, Miller ZA, Bettcher BM, Vessel KA, Kramer JH, Gorno-Tempini ML, Miller BL, Jagust WJ, Rabinovici

- GD. 2016. Tau PET patterns mirror clinical and neuroanatomical variability in Alzheimer's disease. *Brain*. 139:1551–1567.
- Palmqvist S, Schöll M, Strandberg O, Mattsson N, Stomrud E, Zetterberg H, Blennow K, Landau S, Jagust W, Hansson O. 2017. Earliest accumulation of  $\beta$ -amyloid occurs within the default-mode network and concurrently affects brain connectivity. *Nature Communications*. 8:1214.
- Pereira JB, Janelidze S, Ossenkoppele R, Kvartsberg H, Brinkmalm A, Mattsson-Carlgrén N, Stomrud E, Smith R, Zetterberg H, Blennow K, Hansson O. 2020. Untangling the association of amyloid- $\beta$  and tau with synaptic and axonal loss in Alzheimer's disease. *Brain*. 144:1–15.
- Pereira JB, Mijalkov M, Kakaei E, Mecocci P, Vellas B, Tsolaki M, Kloszewska I, Soininen H, Spenger C, Lovestone S, Simmons A, Wahlund LO, Volpe G, Westman E. 2016. Disrupted Network Topology in Patients with Stable and Progressive Mild Cognitive Impairment and Alzheimer's Disease. *Cerebral Cortex*. 26:3476–3493.
- Price JL, Morris JC. 1999. Tangles and Plaques in Nondemented Aging and Preclinical" Alzheimer's Disease. *Annals of Neurology*. 45:358–368.
- Rolls ET, Huang C-C, Lin C-P, Feng J, Joliot M. 2020. Automated anatomical labelling atlas 3. *Neuroimage*. 206:116189.
- Rosen WG, Mohs RC, Davis KL. 1984. A new rating scale for Alzheimer's disease. *American Journal of Psychiatry*. 141:1356–1364.
- Rousset OG, Ma Y, Evans AC. 1998. Correction for partial volume effects in PET: principle and validation. *Journal of Nuclear Medicine*. 39:904–911.
- Scheltens P, de Strooper B, Kivipelto M, Holstege H, Chételat G, Teunissen CE, Cummings J, van der Flier WM. 2021. Alzheimer's disease. *The Lancet*. 397:1577–1590.
- Schultz AP, Chhatwal JP, Hedden T, Mormino EC, Hanseeuw BJ, Sepulcre J, Huijbers W, LaPoint M, Buckley RF, Johnson KA, Sperling RA. 2017. Phases of Hyperconnectivity and Hypoconnectivity in the Default Mode and Salience Networks Track with Amyloid and Tau in Clinically Normal Individuals. *The Journal of Neuroscience*. 37:4323–4331.
- Seeley WW, Crawford RK, Zhou J, Miller BL, Greicius MD, Michael D. 2009. Neurodegenerative Diseases Target Large-Scale Human Brain Networks. *Neuron*. 62:42–52.
- Selkoe DJ, Hardy J. 2016. The amyloid hypothesis of Alzheimer's disease at 25 years. *EMBO Molecular Medicine*. 8:595–608.
- Spreng RN, Turner GR. 2013. Structural Covariance of the Default Network in Healthy and Pathological Aging. *Journal of Neuroscience*. 33:15226–15234.
- ten Kate M, Visser PJ, Bakardjian H, Barkhof F, Sikkens SAM, van der Flier WM, Scheltens P, Hampel H, Habert M-O, Dubois B, Tijms BM. 2018. Gray Matter

- Network Disruptions and Regional Amyloid Beta in Cognitively Normal Adults. *Frontiers in Aging Neuroscience*. 10:1–11.
- Tijms BM, Kate M ten, Wink AM, Visser PJ, Ecay M, Clerigue M, Estanga A, Garcia Sebastian M, Izagirre A, Villanua J, Martinez Lage P, van der Flier WM, Scheltens P, Sanz Arigita E, Barkhof F. 2016. Gray matter network disruptions and amyloid beta in cognitively normal adults. *Neurobiology of Aging*. 37:154–160.
- Tijms BM, Möller C, Vrenken H, Wink AM, de Haan W, van der Flier WM, Stam CJ, Scheltens P, Barkhof F. 2013. Single-Subject Grey Matter Graphs in Alzheimer's Disease. *PLoS ONE*. 8:e58921.
- Tijms BM, Seris P, Willshaw DJ, Lawrie SM. 2012. Similarity-based extraction of individual networks from gray matter MRI scans. *Cerebral Cortex*. 22:1530–1541.
- Tingley D, Yamamoto T, Hirose K, Keele L, Imai K. 2014. mediation : R Package for Causal Mediation Analysis. *Journal of Statistical Software*. 59:1–38.
- van den Heuvel MP, Sporns O. 2019. A cross-disorder connectome landscape of brain dysconnectivity. *Nature Reviews Neuroscience*. 20:435–446.
- van Wijk BCM, Stam CJ, Daffertshofer A. 2010. Comparing Brain Networks of Different Size and Connectivity Density Using Graph Theory. *PLoS ONE*. 5:e13701.
- Verfaillie SCJ, Slot RER, Dicks E, Prins ND, Overbeek JM, Teunissen CE, Scheltens P, Barkhof F, van der Flier WM, Tijms BM. 2018. A more randomly organized grey matter network is associated with deteriorating language and global cognition in individuals with subjective cognitive decline. *Human Brain Mapping*. 39:3143–3151.
- Vermunt L, Dicks E, Wang G, Dincer A, Flores S, Keefe SJ, Berman SB, Cash DM, Chhatwal JP, Cruchaga C, Fox NC, Ghetti B, Graff-Radford NR, Hassenstab J, Karch CM, Laske C, Levin J, Masters CL, McDade E, Mori H, Morris JC, Noble JM, Perrin RJ, Schofield PR, Xiong C, Scheltens P, Visser PJ, Bateman RJ, Benzinger TLS, Tijms BM, Gordon BA, Allegri R, Amtashar F, Benzinger T, Berman S, Bodge C, Brandon S, Brooks W, Buck J, Buckles V, Chea S, Chrem P, Chui H, Cinco J, Jack C, D'Mello M, Donahue T, Douglas J, Edigo N, Erekin-Taner N, Fagan A, Farlow M, Farrar A, Feldman H, Flynn G, Fox N, Franklin E, Fujii H, Gant C, Gardener S, Ghetti B, Goate A, Goldman J, Gordon B, Gray J, Gurney J, Hassenstab J, Hirohara M, Holtzman D, Hornbeck R, DiBari SH, Ikeuchi T, Ikonovic S, Jerome G, Jucker M, Kasuga K, Kawarabayashi T, Klunk W, Koeppe R, Kuder-Buletta E, Laske C, Levin J, Marcus D, Martins R, Mason NS, Maue-Dreyfus D, McDade E, Montoya L, Mori H, Nagamatsu A, Neimeyer K, Noble J, Norton J, Perrin R, Raichle M, Ringman J, Roh JH, Schofield P, Shimada H, Shiroto T, Shoji M, Sigurdson W, Sohrabi H, Sparks P, Suzuki K, Swisher L, Taddei K, Wang J, Wang P, Weiner M, Wolfsberger M,



- Xiong C, Xu X. 2020. Single-subject grey matter network trajectories over the disease course of autosomal dominant Alzheimer's disease. *Brain Communications*. 2:1–14.
- Voevodskaya O, Pereira JB, Volpe G, Lindberg O, Stomrud E, van Westen D, Westman E, Hansson O. 2018. Altered structural network organization in cognitively normal individuals with amyloid pathology. *Neurobiology of Aging*. 64:15–24.
- Yao Z, Zhang Y, Lin L, Zhou Y, Xu C, Jiang T. 2010. Abnormal cortical networks in mild cognitive impairment and alzheimer's disease. *PLoS Computational Biology*. 6:e1001006.
- Yap SY, Frias B, Wren MC, Schöll M, Fox NC, Årstad E, Lashley T, Sander K. 2021. Discriminatory ability of next-generation tau PET tracers for Alzheimer's disease. *Brain*.

## Supplementary material

### Supplementary methods 1. Inclusion and exclusion criteria for the Swedish BioFINDER 2 study

The BioFINDER-2 study enrolls participants in five sub-cohorts; Cohort A and B includes neurologically and cognitively healthy controls. The inclusion criteria are: i) ages 40-65 years (cohort A) and ages 66-100 years (cohort B); ii) absence of cognitive symptoms as assessed by a physician with special interest in cognitive disorders; iii) MMSE score 27-30 (A) or 26-30 (cohort B) at screening visit; iv) do not fulfil the criteria for MCI or any dementia according to DSM-5 (American Psychiatric Association 2013); v) fluent in Swedish. The recruitment process of cohorts A and B is designed to build two study populations with 50% *APOE*  $\epsilon$ 4 carriers in each.

Cohort C comprises participants with subjective cognitive deficits (SCD) or minor neurocognitive impairment (MCI) (the latter according to DSM-5 (American Psychiatric Association 2013)). Inclusion criteria are: i) Age 40-100 years; ii) referred to the memory clinics due to cognitive symptoms; iii) MMSE score of 24 – 30 points; iv) does not fulfil the criteria for any dementia (major neurocognitive disorder) according to DSM-5 (American Psychiatric Association 2013), v) fluent in Swedish. In accordance with the research framework by the National Institute on Aging-Alzheimer's Association (Jack et al. 2018), study participants with SCD were analysed together with the cognitively healthy participants (and combined in the cognitively unimpaired group). Participants were classified as having MCI if they performed worse than -1.5 SD in any cognitive domain according to age and education stratified test norms. The neuropsychological battery covered the domains attention/executive function (Trail Making Test A and B, Symbol Digit Modalities Test, and AQT), memory (10 word immediate and delayed recall from the Alzheimer's Disease Assessment Scale [ADAS]), verbal ability (verbal

fluency and the short version of the Boston Naming Test) and visuospatial function (incomplete letters and cube analysis from the Visual Object and Space Perception battery). Those that were not classified as MCI were considered to have SCD.

Cohort D consists of participants with dementia due to AD. Inclusion criteria are: i) Age 40-100 years; ii) referred to the memory clinics due to cognitive symptoms; iii) MMSE score of  $\geq 12$  points; iv) fulfil the DSM-5 criteria for dementia (major neurocognitive disorder) due to Alzheimer's disease (American Psychiatric Association 2013); v) fluent in Swedish. Cohort E covers other non-AD dementias and neurodegenerative disorders. Inclusion criteria are: i) Age 40-100 years; ii) fulfilment of criteria for dementia (major neurocognitive disorder) due to frontotemporal dementia (American Psychiatric Association 2013), Parkinson's disease with dementia, dementia with Lewy Bodies or vascular dementia (American Psychiatric Association 2013), alternatively the criteria for Parkinson's disease (Gelb et al. 1999), progressive supranuclear palsy (Höglinger et al. 2017), multiple system atrophy (Gilman et al. 2008), or semantic variant primary progressive aphasia (Gorno-Tempini et al. 2011); iii) fluent in Swedish.

Exclusion criteria for all sub-cohorts are: i) significant unstable systemic illness that makes it difficult to participate in the study; ii) current significant alcohol or substance misuse; iii) refusing lumbar puncture, MRI or PET.

## Supplementary references

- American Psychiatric Association. 2013. Diagnostic and Statistical Manual of Mental Disorders, Arlington. American Psychiatric Association.
- Gelb DJ, Oliver E, Gilman S. 1999. Diagnostic Criteria for Parkinson Disease. *Archives of Neurology*. 56:33.
- Gilman S, Wenning GK, Low PA, Brooks DJ, Mathias CJ, Trojanowski JQ, Wood NW, Colosimo C, Dürr A, Fowler CJ, Kaufmann H, Klockgether T, Lees A, Poewe W, Quinn N, Revesz T, Robertson D, Sandroni P, Seppi K, Vidailhet M. 2008. Second consensus statement on the diagnosis of multiple system atrophy. *Neurology*. 71:670–676.
- Gorno-Tempini ML, Hillis AE, Weintraub S, Kertesz A, Mendez M, Cappa SF, Ogar JM, Rohrer JD, Black S, Boeve BF, Manes F, Dronkers NF, Vandenberghe R, Rascovsky K, Patterson K, Miller BL, Knopman DS, Hodges JR, Mesulam MM, Grossman M. 2011. Classification of primary progressive aphasia and its variants. *Neurology*. 76:1006–1014.
- Höglinger GU, Respondek G, Stamelou M, Kurz C, Josephs KA, Lang AE, Mollenhauer B, Müller U, Nilsson C, Whitwell JL, Arzberger T, Englund E, Gelpi E, Giese A, Irwin DJ, Meissner WG, Pantelyat A, Rajput A, van Swieten JC, Troakes C, Antonini A, Bhatia KP, Bordelon Y, Compta Y, Corvol J-C, Colosimo C, Dickson DW, Dodel R, Ferguson L, Grossman M, Kassubek J, Krismer F, Levin J, Lorenzl S, Morris HR, Nestor P, Oertel WH, Poewe W, Rabinovici G, Rowe JB, Schellenberg GD, Seppi K, van Eimeren T, Wenning GK, Boxer AL, Golbe LI, Litvan I. 2017. Clinical diagnosis of progressive supranuclear palsy: The movement disorder society criteria. *Movement Disorders*. 32:853–864.
- Jack CR, Bennett DA, Blennow K, Carrillo MC, Dunn B, Haeberlein SB, Holtzman DM, Jagust W, Jessen F, Karlawish J, Liu E, Molinuevo JL, Montine T, Phelps C, Rankin KP, Rowe CC, Scheltens P, Siemers E, Snyder HM, Sperling R, Elliott C, Masliah E, Ryan L, Silverberg N. 2018. NIA-AA Research Framework: Toward a biological definition of Alzheimer’s disease. *Alzheimer’s and Dementia*. 14:535–562.

**Supplementary Methods 2. AAL atlas ROIs included in Braak staging**

Braak stage	AAL-derived ROIs
I	Parahippocampal gyrus (includes the entorhinal cortex)
II	Hippocampus
III	Amygdala; lingual gyrus; fusiform gyrus
IV	Inferior temporal gyrus; middle temporal gyrus; temporal pole; thalamus; anterior, middle, posterior cingulate; insula
V	Frontal cortex; parietal cortex; occipital cortex; superior temporal gyrus; precuneus; nucleus accumbens; caudate nucleus; putamen
VI	Precentral gyrus; postcentral gyrus; paracentral gyrus; cuneus; supplementary motor area; calcarine fissure

**Sup. Table 1a. Associations between global network measures and tau SUVR values in Braak I-II**

Network property	Whole sample	Control	Preclinical AD	Prodromal AD	AD dementia
Network size	<b>-0.21 (0.04)</b> ***	0.29 (0.16)	0.01 (0.16)	-0.05 (0.09)	0.03 (0.08)
Degree	<b>-0.41 (0.07)</b> ***	-0.03 (0.29)	-0.10 (0.29)	-0.28 (0.16)	-0.36 (0.15)
Connectivity density	<b>-0.53 (0.15)</b> ***	-0.54 (0.61)	0.25 (0.61)	-0.49 (0.33)	<b>-0.81 (0.31)</b> *
Clustering coefficient	<b>-0.50 (0.06)</b> ***	0.16 (0.24)	-0.22 (0.24)	0.12 (0.14)	-0.25 (0.13)
Path length	<b>-0.76 (0.10)</b> ***	0.34 (0.40)	-0.52 (0.40)	0.06 (0.22)	-0.30 (0.21)
Gamma	<b>-1.01 (0.12)</b> ***	0.41 (0.46)	-0.23 (0.46)	0.02 (0.25)	<b>-0.67 (0.24)</b> *
Lambda	<b>-0.85 (0.12)</b> ***	0.37 (0.45)	-0.58 (0.45)	0.07 (0.25)	-0.34 (0.23)
Small world coefficient	<b>-1.03 (0.12)</b> ***	0.42 (0.47)	-0.15 (0.47)	0.01 (0.26)	<b>-0.72 (0.24)</b> *

Data are presented as  $\beta$  (SE). Network measures are Z transformed. SUVR values in Braak I-II. Model is adjusted for age, sex, TIV, and connectivity density (clustering, path length,  $\gamma$ ,  $\lambda$ , small world-only). \* $p < 0.05$ , \*\* $p < 0.01$ , \*\*\* $p < 0.001$ , FDR corrected.

**Sup. Table 1b. Associations between global network measures and tau SUVR values in Braak III-IV**

Network property	Whole sample	Control	Preclinical AD	Prodromal AD	AD dementia
Network size	<b>-0.25 (0.03)</b> ***	0.08 (0.27)	-0.23 (0.17)	-0.17 (0.09)	-0.08 (0.05)
Degree	<b>-0.37 (0.06)</b> ***	-0.43 (0.47)	-0.24 (0.31)	-0.35 (0.16)	<b>-0.25 (0.10)</b> *
Connectivity density	<b>-0.41 (0.12)</b> **	-1.07 (1.00)	-0.07 (0.65)	-0.46 (0.39)	-0.39 (0.20)
Clustering coefficient	<b>-0.56 (0.05)</b> ***	-0.34 (0.39)	<b>-0.60 (0.25)</b> *	<b>-0.29 (0.14)</b> *	<b>-0.33 (0.08)</b> ***
Path length	<b>-0.85 (0.08)</b> ***	-0.40 (0.64)	<b>-1.05 (0.41)</b> *	<b>-0.70 (0.22)</b> **	<b>-0.45 (0.13)</b> **
Gamma	<b>-1.09 (0.09)</b> ***	-0.41 (0.73)	-0.81 (0.47)	<b>-0.69 (0.26)</b> *	<b>-0.70 (0.15)</b> ***
Lambda	<b>-0.96 (0.09)</b> ***	-0.45 (0.71)	<b>-1.17 (0.46)</b> *	<b>-0.78 (0.25)</b> **	<b>-0.51 (0.15)</b> **
Small world coefficient	<b>-1.10 (0.09)</b> ***	-0.38 (0.75)	-0.73 (0.49)	<b>-0.67 (0.26)</b> *	<b>-0.73 (0.15)</b> ***

Data are presented as  $\beta$  (SE). Network measures are Z transformed. SUVR values in tau Braak III-IV. Model is adjusted for age, sex, TIV, and connectivity density (clustering, path length,  $\gamma$ ,  $\lambda$ , small world-only). \* $p < 0.05$ , \*\* $p < 0.01$ , \*\*\* $p < 0.001$ , FDR corrected.

**Sup. Table 1c. Associations between global network measures and tau SUVR values in Braak V-VI**

Network property	Whole sample	Control	Preclinical AD	Prodromal AD	AD dementia
Network size	<b>-0.35 (0.05)</b> ***	-0.16 (0.27)	-0.25 (0.25)	-0.18 (0.13)	<b>-0.18 (0.07)</b> *
Degree	<b>-0.53 (0.08)</b> ***	0.17 (0.47)	-0.01 (0.43)	-0.25 (0.23)	<b>-0.52 (0.12)</b> ***
Connectivity density	<b>-0.60 (0.17)</b> ***	0.60 (0.99)	0.50 (0.91)	-0.24 (0.50)	<b>-0.84 (0.25)</b> **
Clustering coefficient	<b>-0.75 (0.07)</b> ***	-0.43 (0.39)	<b>-0.80 (0.36)</b> *	<b>-0.44 (0.19)</b> *	<b>-0.42 (0.10)</b> ***
Path length	<b>-1.16 (0.11)</b> ***	-0.59 (0.64)	<b>-1.40 (0.59)</b> *	<b>-1.12 (0.32)</b> ***	<b>-0.60 (0.16)</b> ***
Gamma	<b>-1.49 (0.13)</b> ***	-0.91 (0.73)	-1.14 (0.67)	<b>-1.08 (0.36)</b> **	<b>-0.92 (0.19)</b> ***
Lambda	<b>-1.30 (0.13)</b> ***	-0.67 (0.71)	<b>-1.55 (0.65)</b> *	<b>-1.24 (0.35)</b> ***	<b>-0.68 (0.18)</b> ***
Small world coefficient	<b>-1.51 (0.13)</b> ***	-0.94 (0.75)	-1.05 (0.68)	<b>-1.04 (0.37)</b> *	<b>-0.96 (0.19)</b> ***

Data are presented as  $\beta$  (SE). Network measures are Z transformed. SUVR values in tau Braak V-VI. Model is adjusted for age, sex, TIV, and connectivity density (clustering, path length,  $\gamma$ ,  $\lambda$ , small world-only). \* $p < 0.05$ , \*\* $p < 0.01$ , \*\*\* $p < 0.001$ , FDR corrected.

**Supplementary Table 2. Associations between global network measures and tau SUVR PVC**

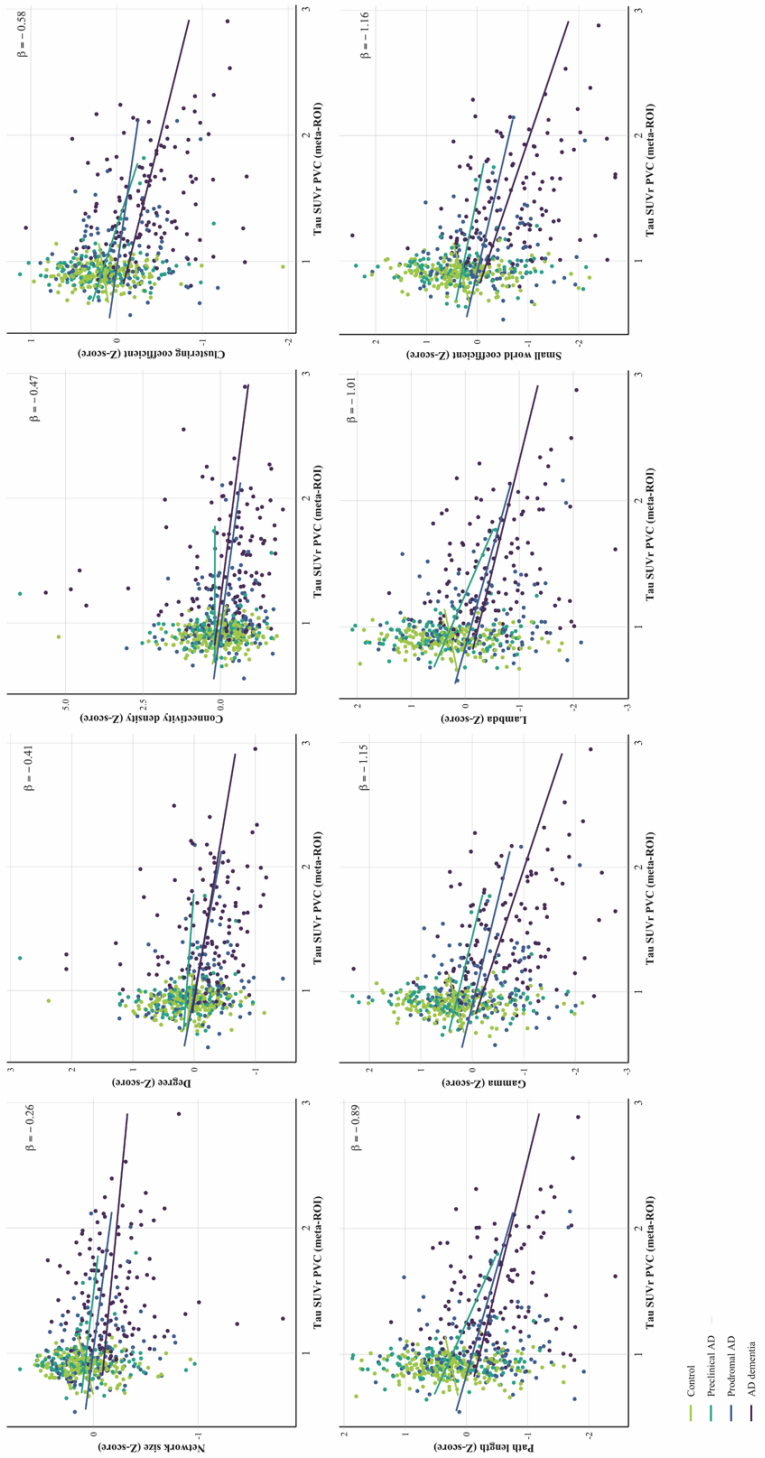
Network property	Whole sample	Control	Preclinical AD	Prodromal AD	AD dementia
Network size	<b>-0.26 (0.04)</b> ***	0.27 (0.27)	-0.17 (0.19)	-0.16 (0.10)	-0.09 (0.06)
Degree	<b>-0.41 (0.06)</b> ***	-0.27 (0.47)	-0.18 (0.33)	-0.39 (0.18)	<b>-0.32 (0.11)</b> *
Connectivity density	<b>-0.47 (0.13)</b> ***	-0.99 (0.99)	-0.01 (0.70)	-0.55 (0.38)	-0.52 (0.23)
Clustering coefficient	<b>-0.58 (0.05)</b> ***	-0.13 (0.39)	-0.54 (0.27)	-0.23 (0.15)	<b>-0.34 (0.09)</b> ***
Path length	<b>-0.89 (0.09)</b> ***	0.27 (0.64)	<b>-1.01 (0.45)</b> *	<b>-0.62 (0.25)</b> *	<b>-0.47 (0.15)</b> **
Gamma	<b>-1.15 (0.10)</b> ***	0.44 (0.73)	-0.71 (0.51)	-0.63 (0.28)	<b>-0.76 (0.17)</b> ***
Lambda	<b>-1.01 (0.10)</b> ***	0.29 (0.69)	<b>-1.11 (0.50)</b> *	<b>-0.69 (0.27)</b> *	<b>-0.54 (0.16)</b> **
Small world coefficient	<b>-1.16 (0.11)</b> ***	0.47 (0.74)	-0.61 (0.52)	-0.62 (0.29)	<b>-0.80 (0.17)</b> ***

Data are presented as  $\beta$  (SE). Network measures are Z transformed. SUVR values in tau meta-ROI of Braak I-IV with PVC. Model is adjusted for age, sex, TIV, and connectivity density (clustering, path length,  $\gamma$ ,  $\lambda$ , small world-only). \* $p < 0.05$ , \*\* $p < 0.01$ , \*\*\* $p < 0.001$ , FDR corrected.

**Supplementary table 3. Associations between global network measures and tau-PET in A $\beta$ + subjects**

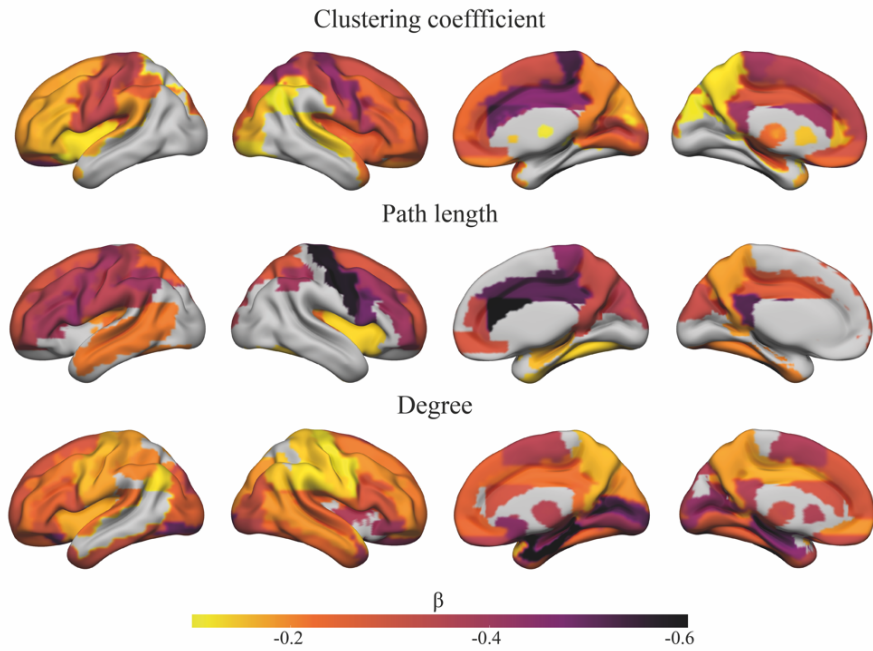
Network property	All A $\beta$ +	Preclinical AD	Prodromal AD	AD dementia	Tau * A $\beta$ 42/A $\beta$ 40
Network size	<b>-0.24 (0.04)</b> ***	-0.25 (0.19)	-0.18 (0.10)	-0.07 (0.06)	-0.36 (0.27)
Degree	<b>-0.38 (0.07)</b> ***	-0.29 (0.32)	-0.37 (0.17)	-0.24 (0.10)	0.50 (0.47)
Connectivity density	<b>-0.44 (0.14)</b> **	-0.14 (0.70)	-0.48 (0.37)	-0.38 (0.23)	1.64 (1.00)
Clustering coefficient	<b>-0.53 (0.06)</b> ***	<b>-0.61 (0.27)</b> *	-0.27 (0.15)	<b>-0.34 (0.09)</b> ***	0.28 (0.41)
Path length	<b>-0.80 (0.09)</b> ***	<b>-1.09 (0.43)</b> *	<b>-0.66 (0.23)</b> **	<b>-0.45 (0.14)</b> **	0.23 (0.65)
Gamma	<b>-1.02 (0.10)</b> ***	-0.86 (0.50)	<b>-0.66 (0.27)</b> *	<b>-0.70 (0.16)</b> ***	0.37 (0.74)
Lambda	<b>-0.90 (0.10)</b> ***	<b>-1.12 (0.48)</b> *	<b>-0.73 (0.26)</b> **	<b>-0.50 (0.16)</b> **	0.26 (0.72)
Small world coefficient	<b>-1.03 (0.11)</b> ***	-0.79 (0.51)	<b>-0.64 (0.27)</b> *	<b>-0.72 (0.17)</b> ***	0.41 (0.76)

Data are presented as  $\beta$  (SE). Network measures are Z transformed; gamma is normalized clustering; lambda is normalized path length; SUVR values in temporal meta-ROI; Model is adjusted for age, sex, TIV, and connectivity density (clustering, path length,  $\gamma$ ,  $\lambda$ , small world-only); Interaction effect of tau-PET with continuous CSF A $\beta$ 42/A $\beta$ 40 ratios in A $\beta$ + individuals; \* $p < 0.05$ , \*\* $p < 0.01$ , \*\*\* $p < 0.001$ , FDR corrected.



**Supplementary Figure 1.** Scatterplots of the relation between tau SUVR with PVC and global grey matter network measures by disease stage. Standardised beta estimates are displayed for significant relationships across all participants adjusting for age, sex, TIV, and connectivity density.





**Supplementary Figure 2.** Surface plots of standardised  $\beta$  values of the relationship between tau SUVR with PVC and local clustering, path length, and degree in participants with abnormal A $\beta$ . Data are presented for regions with a significant correlation at  $p_{\text{Bonferroni}} < .05$  adjusted for age, sex, TIV, local degree, and local GM volume.



## CHAPTER 5

# **Grey matter T1-w/T2-w ratios are higher in Alzheimer's disease**

Wiesje Pelkmans, Ellen Dicks, Frederik Barkhof, Hugo Vrenken,  
Philip Scheltens, Wiesje M. van der Flier and Betty M. Tijms

*Published in  
Human Brain Mapping, 2019. 40(13) p.3900-3909.*

*DOI:10.1002/hbm.24638*

*\*Recognised as one of the most read papers in HBM in 2018-2019*

## **Abstract**

Myelin determines the conduction of neuronal signals along axonal connections in networks of the brain. Loss of myelin integrity in neuronal circuits might result in cognitive decline in Alzheimer's disease (AD). Recently, the ratio of T1-weighted by T2-weighted MRI has been used as a proxy for myelin content in grey matter of the cortex. With this approach we investigated whether AD dementia patients show lower cortical myelin content (i.e. a lower T1-w/T2-w ratio value). We selected structural T1-w and T2-w MR images of 293 AD patients and 172 participants with normal cognition (NC). T1-w/T2-w ratios were computed for the whole brain and within 90 AAL atlas regions using SPM12, compared between groups and correlated with the neuronal injury marker tau in CSF and MMSE. In contrast to our hypothesis, AD patients showed higher whole brain T1-w/T2-w ratios than NC, and regionally in 31 anatomical areas ( $p < .0005$ ;  $d = .21$  to  $.48$ ), predominantly in the inferior parietal lobule, angular gyrus, anterior cingulate, and precuneus. Regional higher T1w-/T2-w values were associated with higher CSF tau concentrations ( $p < .0005$ ;  $r = .16$  to  $.22$ ) and worse MMSE scores ( $p < .0005$ ;  $r = -.16$  to  $-.21$ ). These higher T1-w/T2-w values in AD seem to contradict previous pathological findings of demyelination and dysconnectivity in AD. Future research should further investigate the biological processes reflected by increases in T1-w/T2-w values.

## Introduction

Alzheimer's disease (AD), the most common cause of dementia, is characterized by a progressive decline in cognition and is one of the major public health challenges of the 21<sup>st</sup> century (Scheltens et al. 2016). AD is pathologically defined by  $\beta$ -amyloid (A $\beta$ ) neuritic plaques, tau neurofibrillary tangles, and is associated with neuronal, axonal, and synaptic degeneration (Braak and Braak 1991; Selkoe 2002). Myelin, the insulating sheath surrounding neuronal axons, is vulnerable to AD pathology while it is essential for efficient neuronal communication by fine-tuning conduction speed and synchronization, thereby affecting brain connectivity (Nave and Werner 2014; Timmler and Simons 2019). A failure in cerebral connectivity has been shown to interfere with healthy cognitive functioning (Pievani et al. 2014; Fornito et al. 2015).

In recent years, several proxy measures of myelin content have been proposed, including quantitative magnetic resonance imaging (MRI) techniques such as myelin water fraction (MWF) (Laule et al. 2007) and quantitative susceptibility mapping (QSM) (de Rochefort et al. 2008). Moreover, diffusion tensor imaging (DTI) has been used extensively to measure the myelin integrity of large axonal fibre bundles over long distance white matter (WM) networks, which are disrupted in AD (Chua et al. 2008; Gao et al. 2014).

An alternative approach of determining regional variation in cortical myelin content, the ratio of the signal intensity of the T1-weighted (T1-w) and T2-weighted (T2-w) image, has been proposed (Glasser and van Essen 2011). The T1-w/T2-w technique was developed to parcellate the cerebral cortex from patterns of cortical myelination, and have shown to closely correspond with histological measures of myeloarchitecture (Glasser and van Essen 2011; Nieuwenhuys and Broere 2017). Compared to other

quantitative MRI contrasts, this technique has the advantage that images can be acquired during routine clinical MR examinations, with high signal-to-noise, and without complex modelling of the MR signal (Heath et al. 2018). Along the life-span, the T1-w/T2-w myelin shows an inverted U curve (Grydeland et al. 2013, 2019; Shafee et al. 2015), following the maturation of cortical regions throughout life. In addition, higher T1-w/T2-w ratios have been associated with greater performance stability during a processing speed task (Grydeland et al. 2013). In disorders with a strong demyelinating component such as multiple sclerosis (MS), the T1-w/T2-w ratio is lowered in pathologically vulnerable regions (Beer et al. 2016; Nakamura et al. 2017; Righart et al. 2017). However, recent studies have raised controversy on the interpretation of the T1-w/T2-w ratio, showing that this measure may also reflect tissue microstructure other than myelin, such as axon and dendrite density or iron content (van Rooden et al. 2014; Arshad et al. 2017; Righart et al. 2017; Uddin et al. 2018). Because disrupted brain connectivity is an important feature of AD (Pievani et al. 2014; Fornito et al. 2015; Dicks et al. 2018), an intracortical reduction of myelin content in AD could be hypothesized. But also other pathological factors associated with AD might lead to intracortical tissue changes. To better understand what this myelin proxy in AD reflects, we compared T1-w/T2-w ratio values between older adults with normal cognition and patients with AD-type dementia for the whole brain and on a regional level. We further investigated the influence of factors that are associated with AD, including cerebrospinal fluid (CSF) total-tau protein concentration, white matter hyperintensities (WMH), and global cognitive functioning that may contribute to alterations in T1-w/T2-w values.

## Methods

### *Participants*

Individuals with normal cognition (NC) and with AD dementia who had T1-weighted and T2-weighted structural MRI were selected from the Amsterdam Dementia Cohort (Van Der Flier et al. 2014; Van Der Flier and Scheltens 2018). Probable AD dementia was diagnosed according to NIA-AA criteria with evidence of abnormal levels of A $\beta$  protein (McKhann et al. 2011). Individuals with NC were required to have normal CSF A $\beta_{1-42}$  levels. Participants were excluded if younger than 40 years old or if the MRI was acquired more than 3 months after clinical diagnosis. All data was collected as part of routine dementia screening.

### *CSF biomarkers*

Collection of CSF by lumbar puncture for all subjects was performed as described previously (Van Der Flier et al. 2014). A $\beta_{1-42}$ , phosphorylated tau (p-tau), and total tau protein concentrations were measured using InnoTest sandwich ELISAs (Innogenetics, Fujirebio, Ghent, Belgium). The cut-off for abnormal drift-corrected CSF A $\beta_{1-42}$  was set at < 813 ng/L (Tijms et al. 2018), at > 375 ng/L for CSF total tau and at > 52 ng/L for p-tau (Mulder et al. 2010).

### *MRI acquisition*

Structural T1-weighted and T2-weighted images were acquired as part of routine patient care from a single scanner (3T GE MR750). The following parameters for T1 were used: 3D-FSPGR, sagittal plane, TR 7.8 ms, TE 3 ms, FA 12°, voxel size 1 mm<sup>3</sup>, 5.06 min; for T2: 2D-TSE, axial plane, TR 8340 ms, TE 20.7 ms, FA 90°, voxel size 0.5×0.5×3 mm<sup>3</sup>, 3.35 min. To determine WMH, we additionally analysed 3D-fluid attenuation inversion recovery (FLAIR)

images, acquired in a sagittal plane, with TR 8000 ms, TE 126.6 ms, FA 90°, voxel size 1 mm<sup>3</sup>, 5.48 min.

### *MRI processing*

T1-w and T2-w images were converted to Nifti format and analysed using a similar method as proposed by (Glasser and van Essen 2011). The origin was manually set to the anterior commissure. The T2-weighted image was rigidly registered with a 4<sup>th</sup> degree B-Spline interpolation to the T1-weighted image using Statistical Parametric Mapping Software version 12 (SPM12; Functional Imaging Laboratory, University College London, London, UK) running in Matlab 7.12 (MathWorks, Natick, MA). The SPM12 segmentation function allowed for bias field correction of both images, as well as tissue segmentation of the T1-w images into CSF, GM and WM tissue probability maps. For validation purposes, we conducted analyses without field bias correction for the T1-w and T2-w images as well, obtaining similar results but with less discriminative power to detect differences in intracortical microstructure (Supplementary material Table 2). The data presented here refer to the T1-w/T2-w images with bias correction. For each subject, 90 cortical areas were identified with the automated anatomical labelling (AAL) atlas (Tzourio-Mazoyer et al. 2002), using the SPM normalize function with inverted deformation fields to warp the AAL atlas to Montreal Neurological Institute (MNI) space. Interpolation was set to nearest neighbour. The atlases were masked using subject-specific masks covering voxels with a GM probability >.3. The T1-weighted image was then divided by the T2-weighted image and masked with the GM mask to obtain T1-w/T2-w ratios within 90 regions of the AAL atlas (Figure 1). On the FLAIR sequence, WMH were assessed using the Fazekas scale (Fazekas et al. 1987) (0 = none; 1 = punctuate; 2 = early confluent; and 3 = confluent) and



dichotomized into absent (0-1) or present (2-3). All images were visually inspected for segmentation or warping errors; none had to be excluded.

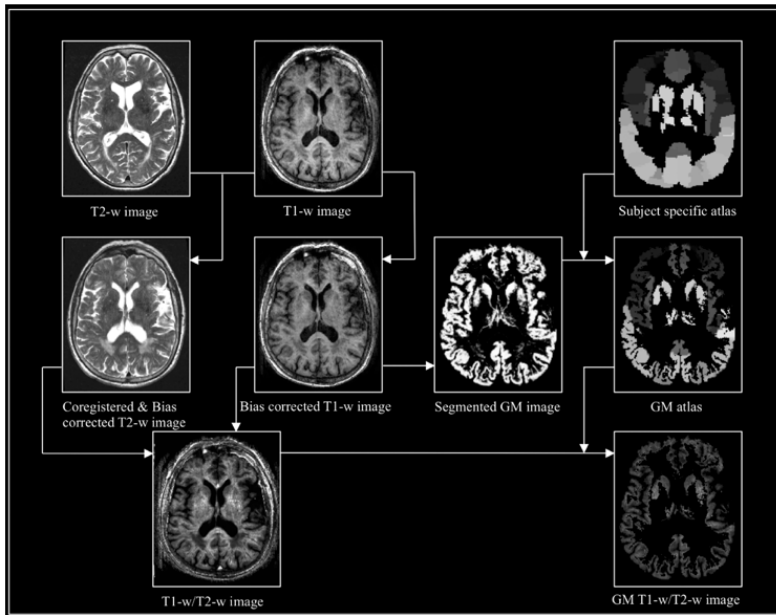


**Figure 1. Flow diagram of pre-processing steps to generate T1-w/T2-w images.** Workflow of T1-w/T2-w image data processing using SPM12, including registration of the T2-w image to the T1w-w image, bias correction of both images, segmentation, warping of the standard AAL atlas to a subject specific atlas. Finally, the T1-w/T2-w image is calculated as the ratio of T1-w and T2-w images and masked with a GM mask.

### *Statistical analysis*

Demographic and biomarker data of the diagnostic groups were compared using two-sample *t*-tests for continuous data or chi-square tests for categorical data. We used general linear models (GLM) to test whether AD patients had globally (i.e. whole cortex) significantly different T1-w/T2-w ratios compared to the NC group. This analysis was adjusted for sex and age as the T1-w/T2-w ratio has previously shown to vary as a function of age. This model was repeated for regional T1-w/T2-w values using Bonferroni

correction for multiple comparisons (i.e.  $p$  value of  $<0.0005$  for 90 AAL regions,  $0.05/90$ ), and for analysis of individual T1-w and T2-w images as well.

To gain further insight into the biological underpinnings of the T1-w/T2-w ratio, we further studied the influence of factors known to be associated with AD, i.e. WMH, tau & MMSE, on T1-w/T2-w values. We used GLM, adjusted for age and sex, to investigate whether WMH severity has an effect on the T1-w/T2-w ratio by comparing T1-w/T2-w ratio values between individuals with WMH, defined as having a Fazekas score 2 to 3, to individuals without pronounced WMH (Fazekas 0-1).

Next, we computed a linear regression analysis of CSF total tau concentration and mean T1-w/T2-w ratio values for all AAL regions using all subjects and for each group separately. Previous studies have shown that total tau and p-tau concentrations are highly correlated (Mulder et al. 2010), therefore we chose to analyse the relationship of T1-w/T2-w ratios with total-tau protein only, rather than also p-tau. Furthermore, the correlation of the whole cortex and regional T1-w/T2-w ratio and global cognitive performance score, as measured by the Mini Mental State Examination (MMSE) was calculated. All statistical analyses were performed in R (version 3.5.1), and brain images were visualized with Surf Ice (version 10.14).

## Results

### *Demographic and clinical data*

We included 293 AD and 172 NC subjects. AD patients had higher tau levels than controls, were on average older, more likely to be female, and showed more vascular brain damage, lower total GM volume and total WM volume compared to NC participants (Table 1). The average anatomical distribution of T1-w/T2-w values across the cortex in NC participants was qualitatively

similar to myelin maps previously reported (Glasser and Van Essen 2011; Supplementary material Figure 1). Consistent with their results we observed high T1-w/T2-w values in sensory motor regions and visual cortex. The lowest T1-w/T2-w values are located in the temporal (pole), anterior cingulate cortex and frontal areas corresponding with their findings as well.

**Table 1. Demographic and clinical characteristics according to diagnostic group**

	NC (n = 172)	AD (n = 293)	Total (n = 465)
Sex, F	69 (40%)	159 (54%)*	228 (49%)
Age	59.0 ± 7.3	66.0 ± 7.7*	63.4 ± 8.3
MMSE score	28.3 ± 1.7	20.2 ± 5.0*	23.2 ± 5.7
CSF Aβ <sub>1-42</sub>	1138.7 ± 178.9	620.9 ± 98.0*	812.5 ± 283.7
CSF t-tau	229.1 ± 88.4	713.8 ± 466.9*	534.5 ± 441.6
CSF p-tau	42.8 ± 15.0	90.1 ± 43.1*	72.6 ± 42.2
Vascular damage	11 (6%)	71 (24%)*	82 (18%)
Grey matter volume	659.8 ± 66.9	552.4 ± 63.1*	592.2 ± 82.8
White matter volume	452.3 ± 52.0	415.9 ± 58.2*	429.4 ± 58.6
Cerebrospinal fluid	369.0 ± 78.7	486.3 ± 88.0*	443.0 ± 101.9

Data are presented as mean ± SD, or n (%). NC, Normal Cognition; AD, Alzheimer's Disease; F, Female; Age in years; MMSE, Mini Mental State Examination (0-30); CSF, Cerebrospinal fluid, CSF in ng/L; Vascular damage defined as Fazekas ≥ 2; Volume in mm<sup>3</sup>; (\* =  $p < 0.05$ ).

#### *Altered intracortical T1-w/T2-w ratios in AD*

Average whole cortex T1-w/T2-w values were higher in AD compared to NC [NC:  $EMM = 1.004$ ,  $SE = .009$ ; AD:  $EMM = 1.038$ ,  $SE = .007$ ;  $F(1, 464) = 8.33$ ,  $d = .15$ ,  $p < .01$ ] (Estimated marginal means (EMM); standard error (SE); Figure 2). At regional level stronger effects were found, with multiple brain regions showing higher T1-w/T2-w values in AD (Figure 3). The largest differences were observed in the anterior cingulate, inferior parietal lobule,

supramarginal gyrus, angular gyrus, precuneus, and superior temporal gyrus (range  $d = .21$  to  $d = .48$ ;  $p < .0005$  to  $p < .00000001$ ; Supplementary Table 1). No regions with significantly lower values were observed in AD.

Comparisons of individual images between diagnostic groups resulted in no significant differences in T1-w image intensity. However uncorrected results showed a trend of higher T1-w image intensity in AD patients in the inferior parietal lobule, angular gyrus, precuneus, and superior parietal lobule. T2-w images showed significantly lower intensities in the anterior cingulate in the AD group compared to NC ( $p < .0005$ ; Figure 4). And a trend towards lower T2-w image intensity in AD patients in the inferior parietal lobule, precuneus, hippocampus and insula. Moreover, to exclude possible age or sex effects, the main analysis was re-run using a subset ( $n=50$ ) of age- and sex-matched individuals. Obtaining similar results, albeit less significant (Supplementary table 3).

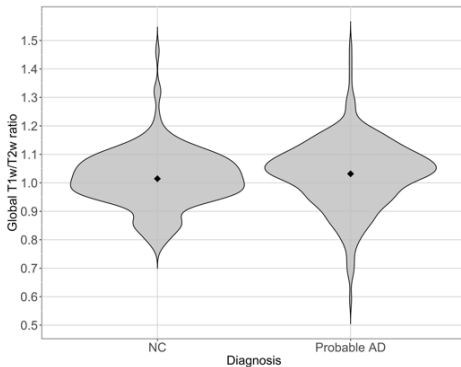


**Figure 2. Violin plot representation of mean T1-w/T2-w ratio values in all GM regions for AD and NC.** Global, i.e. whole brain, average T1-w/T2-w ratios are significantly higher in AD compared to CN subjects, adjusted for age, and sex. NC ( $n=172$ ): EMM = 1.004, SE = .009; AD ( $n=293$ ): EMM = 1.038, SE = .007;  $F(1, 464)=8.326$ ,  $d = .15$ ,  $p < .005$ . Note: plot created with raw data (without covariates).

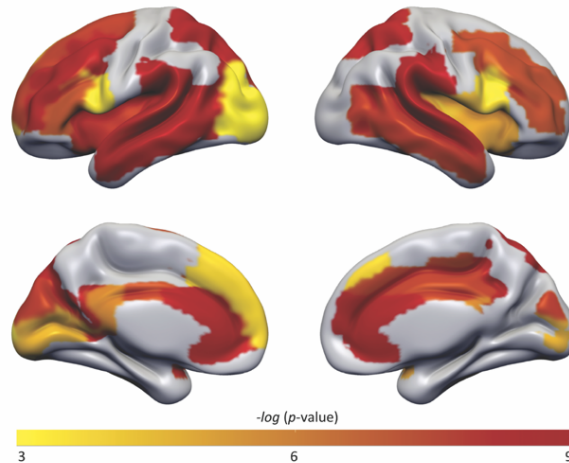


**Figure 3. P-value map of AAL regions with significant different T1-w/T2-w ratios between AD and NC subjects.** Higher T1-w/T2-w ratio values were found widespread in AD, in particular in AD-related regions: Superior & Middle Frontal Gyrus; Inferior Frontal Gyrus Pars Opercularis & Triangularis; Rolandic Operculum; Insula; Anterior, Mid & Posterior Cingulate Gyrus; Calcarine; Cuneus; Middle Occipital Gyrus; Superior & Inferior Parietal Lobule; Supramarginal Gyrus; Angular Gyrus; Precuneus; Superior & Middle Temporal Gyrus. All analyses were adjusted for multiple comparisons showing a moderate (Yellow  $p < .0005$ ) to highly (Red  $p < .000000001$ ) significance scale.

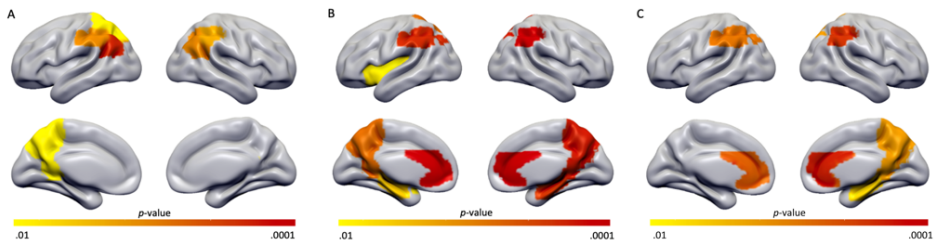


**Figure 4. P-value map of AAL regions with different T1-w images, T2-w images and 1/T2-w images between AD and NC subjects.** Figures shown are uncorrected for multiple comparisons to give insight into the pattern of regions that differed between groups at a trend level. A) Surface plot shows a trend of higher T1-w image intensity in AD patients in the inferior parietal lobule, angular gyrus, precuneus, and superior parietal lobule. B) T2-w images had significantly lower intensities in the anterior cingulate in the AD group. And showed a trend towards lower T2-w image intensity in AD patients in the inferior parietal lobule, precuneus, hippocampus and insula. C) Surface plot shows a trend of higher 1/T2-w image intensity in AD patients in the anterior cingulate gyrus, inferior parietal lobule, hippocampus, and precuneus. Displayed are regions with a p-value scale of (Yellow  $p < .01$ ) to (Red  $p < .0001$ ).

### *Association of T1-w/T2-w ratio values with other AD markers*

There was no significant difference between the group with WMH and the group without WMH in T1-w/T2-w values, regional or whole brain [ $F(1, 463) = .92, p = .34, d = .004$ ]. Next, the effect of the neuronal injury marker tau on the mean global T1-w/T2-w ratio was explored. The regression analysis indicated that T1-w/T2-w ratios across the whole cortex increased with higher tau concentrations in CSF ( $r = .11, p < .01$ ; Figure 5a). These associations were specific for the AD group (AD:  $r = .12, p < .05$ ; CN:  $r = -.07, p = .40$ ) and located in mostly frontal and parietal regions with significant correlation values ranging from  $r = .16$  to  $.22$  (all  $p < .0005$ ; Figure 5b), and remained when adjusting for age and sex. Note that we did not investigate the relationship of CSF A $\beta$  levels and T1-w/T2-w ratio as the diagnostic groups already reflect this association, because CN and AD subjects were selected based on their amyloid status. We further analysed the mean whole cortex correlation between T1-w/T2-w ratio and MMSE scores which was  $r = -.08$ , with p-value = .08 (AD:  $r = -.05, p = .34$ ; CN:  $r = .08, p = .34$ ). Which implies that worse global cognitive functioning correlated with higher T1-w/T2-w ratios at a trend level (Figure 5c), and regionally stronger associations were observed, which remained when adjusting for age and sex, mostly in temporal, cingulate and parietal brain areas (range  $r = -.16$  to  $r = -.21$ , all  $p < .0005$ ; Figure 5d).

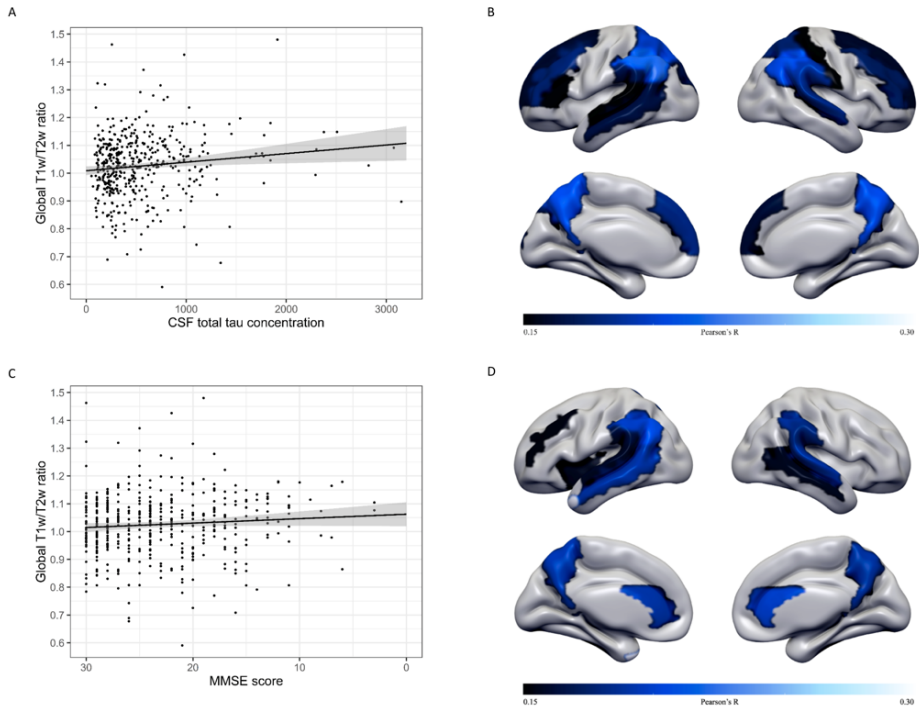


**Figure 5. Association of T1-w/T2-w ratio values with other AD markers. A)** Global T1-w/T2-w ratio as a function of tau. Scatterplot showing an association of higher T1-w/T2-w ratios with abnormal CSF tau concentrations in the total sample. Regression line in black, the 95% CI in shaded grey. **B)** Surface map showing regional associations of CSF total tau concentration with T1-w/T2-w values. Higher tau concentrations are associated with higher T1-w/T2-w ratios in the Superior & Middle Frontal Gyrus, Pars Triangularis, Medial Frontal Gyrus, Superior Occipital, Postcentral Gyrus, Superior & Inferior Parietal Lobule, Supramarginal Gyrus, Angular Gyrus, Precuneus, and Superior Temporal Gyrus across all subjects (Range  $r = .15$  to  $r = .22$ ;  $p = .0005$  to  $p = .000001$ ). **C)** Global T1-w/T2-w ratio as a function of MMSE score. Scatterplot showing the relation between global T1-w/T2-w ratios according to MMSE score in the total sample. Regression line in black, the 95% CI in shaded grey. **D)** Surface map showing regional associations of MMSE scores with T1-w/T2-w values. Lower MMSE scores are associated with higher T1-w/T2-w ratios in the Middle Frontal Gyrus, Insula, Anterior Cingulate Gyrus, Inferior Parietal Lobule, Supramarginal Gyrus, Angular Gyrus, Precuneus, Superior & Middle Temporal Gyrus across all subjects (Range  $r = .15$  to  $r = .21$ ;  $p = .0005$  to  $p = .000008$ ).

## Discussion

The main finding of our study was that T1-w/T2-w ratio values were higher in AD compared to controls, which was contrary to our expectation. These changes tended to be most pronounced in anatomical areas known to be affected in AD such as the interior parietal lobule and precuneus, and were associated with higher levels of the neuronal injury marker tau and worse cognition.

Previous studies have suggested that myelin is the predominant source of MR contrast in T1-weighted and T2-weighted images (Eickhoff et al. 2005; Laule et al. 2007; Bock et al. 2009; Wallace et al. 2016), and by using the ratio of these images the contrast sensitivity to detect myelin content is increased further due to attenuation of the shared intensity biases (Glasser and van Essen 2011). Although, other studies have questioned the sensitivity of the T1-w/T2-w ratio for myelin content, and argued that it is likely not the only factor contributing to the T1-w/T2-w image (Arshad et al. 2017; Righart et al. 2017; Uddin et al. 2018). Still, it has been shown that T1-w/T2-w ratio differentiates between high and low myelinated cortex as determined by myelin proteolipid protein staining (Nakamura et al. 2017). Also in our study, we observed no indication that our T1-w/T2-w map differed from those previously reported in NC, with high T1-w/T2-w values in regions such as the basal ganglia, thalamus, and paracentral lobule (Ganzetti et al. 2015) and low T1-w/T2-w ratios in the insula, anterior cingulate, hippocampus, medial orbitofrontal gyrus and temporal pole (Fischl et al. 2004; Glasser et al. 2014), suggesting it correlates well with cortical myelination.

To the best of our knowledge, this technique has not been applied in AD dementia before, however, a previous study showed that higher T1-w/T2-w values correlated with amyloid beta deposition on positron-



emission tomography (PET) in individuals with normal cognition (Yasuno et al. 2017). Our observation of higher T1-w/T2-w seems in line with that study. The authors found higher regional T1-w/T2-w ratios in the frontal cortex and anterior cingulate in subjects with high PiB binding compared to subjects with low PiB binding and suggested that microstructural alterations induced by amyloid beta could be detected with the T1-w/T2-w ratio. In our study the higher T1-w/T2-w ratio in AD also seem to be regionally specific, showing the highest T1-w/T2-w ratios in AD patients in the angular gyrus, inferior parietal lobule, precuneus, anterior cingulate, supramarginal gyrus, and superior temporal gyrus. These high T1-w/T2-w regions overlap with areas known be involved in AD, and have been associated with the 'default mode network', a set of brain areas that shows high functional correlations when a person is not performing a task. In particular, these regions seem most vulnerable for early amyloid depositions and decreased functional connectivity in AD (Buckner 2005; Palmqvist et al. 2017). Additionally, this corresponds with numerous studies showing that particularly late-myelinating, i.e. temporal and frontal, intracortical fibres seem particularly prone to lose myelin (Thal et al. 2002; Bartzokis et al. 2004; Brettschneider et al. 2015; Jucker and Walker 2018). The sensory and motor regions, i.e. early-myelinating, showed little difference in T1-w/T2-w ratio between AD and NC individuals. These regions are known to have a relative sparing of AD pathology until late disease stages (Bartzokis et al. 2007). Although the relationships were not strong, our findings showed an association of higher T1-w/T2-w ratios in mostly frontal and parietal areas with increased tau pathology, and higher T1-w/T2-w ratios in mainly temporal areas with a decline in global cognitive functioning, suggesting that the cortical changes detected by the

T1-w/T2-w ratio show a regional vulnerability and an association with pathology.

Additionally, we analysed the intensity measures derived from the T1-w and T2-w images separately. GM T1-w images did not show significant differences in intensity between NC and AD groups. However, T2-w images had significantly lower intensities in the anterior cingulate and inferior parietal lobule in the AD group compared to NC. Therefore, the group difference in T1-w/T2-w ratios seems to be predominantly driven by the overall lower T2-w signal in AD patients. A finding that might be related to increased A $\beta$  protein concentrations, which are known to decrease the T2-w signal (Imon et al. 1995). When applying the ratio of T1-w by T2-w images, it greatly improves the sensitivity to detect subtle differences, then using single modalities separately.

However, it remains unclear what biological substrate higher T1-w/T2-w values reflect. Disorders with a strong demyelinating component such as MS, have consistently showed lower T1-w/T2-w values in pathologically vulnerable regions (Beer et al. 2016; Nakamura et al. 2017; Righart et al. 2017). Additionally, lowered T1-w/T2-w ratios in several brain regions in schizophrenia (Ganzetti et al. 2015; Iwatani et al. 2015) and bipolar disorder patients (Ishida et al. 2017) have been identified. Recent transcriptomic studies have further observed correlations of the T1-w/T2-w intensity in the cortex with expression of genes associated with cortical microcircuit specialization and myelin (Burt et al. 2018; Ritchie et al. 2018).

In contrast, recently a study with Parkinson disease patients showed a higher T1-w/T2-w ratio in the substantia nigra pars compacta compared to controls (Du et al. 2018). Also in Huntington disease, higher T1-w/T2-w ratios in several cortical regions including the insula, ventrolateral frontal cortex, and medial temporal pole were found (C. D. Rowley et al., 2018). This

incongruency suggests that in AD either demyelination does not occur, or the T1-w/T2-w ratio measures something different rather than myelin content. Still, structural imaging and histological studies have reported a disruption in WM integrity in AD (Bartzokis et al. 2004; Carmichael et al. 2010; Nir et al. 2013; Rowley et al. 2013; Filley and Fields 2016). For example, more white matter hyperintensities have been related to an increased risk of dementia and cognitive deficits, independently of vascular risk factors and stroke in the AD continuum (DeBette et al. 2010; Nir et al. 2013; Gordon et al. 2015). Cortical demyelination in the context of AD has been demonstrated also in the medial temporal lobe and lingual gyri using the magnetization transfer ratio in mild cognitive impairment patients (Carmeli et al. 2013). Moreover, focal demyelination of the cortical grey matter has been reported around A $\beta$  plaques, suggesting a vulnerability of myelin to A $\beta$  toxicity (Mitew et al. 2010). Therefore, we consider it unlikely that no demyelination occurs in AD.

Another possibility is remyelination (Peters 2009), which has also been suggested by a recent study by Bulk et al. (2018). Using a combined post mortem T2\*w MRI with histology, the authors showed an unexpected increase in cortical myelin staining in late stage AD. The increase in myelin density did show a more disorganized cortical myelin architecture compared to controls. Furthermore, Van Duijn et al. (2017) also found increased myelin protein labelling in regions affected severely by A $\beta$  and tau pathology. Possibly, adequate intracortical myelin plasticity may initially compensate for the subcortical transmission delays along WM subcortical fibres, but eventually during the disease course significant intracortical oligodendrocyte deficits develop. Note however, that Bulk et al. (2018), and multiple other studies (Connor et al. 1992; Zecca et al. 2004; Ward et al. 2014; Ayton et al. 2019), also demonstrated increased iron accumulation in

AD. T2-w sequences are known to be highly sensitive to iron deposits, and so the T1-w/T2-w ratio may reflect the presence of both processes (Dusek et al. 2013). Because there is a strong colocalization of myelin and iron in the cortex (Quintana et al. 2006; Fukunaga et al. 2010; Stüber et al. 2014), this would imply that even though iron may contribute to the T1-w/T2-w signal, the T1-w/T2-w signal would still mainly (directly and indirectly) reflect the underlying myeloarchitecture. However in pathological conditions such as AD, the relationship of myelin and iron may be altered, for instance by loss of oligodendrocytes or iron rich depositions around A $\beta$  plaques (Hare et al. 2013). There is also evidence that brain regions originally low in iron content, such as the frontal and temporal lobe, appear to be most vulnerable to iron dyshomeostasis and are susceptible to amyloid pathology (Hallgren and Sourander 1958; Connor et al. 1992). In other words, there appears to be a synergy of iron and  $\beta$ -amyloid toxicity in specific brain regions that overlap with regions we observed to show high T1-w/T2-w ratios in AD. Further research should further investigate this question using a combined PET and MR approach. To summarize, the T1-w/T2-w ratio is likely to be influenced by other microstructural factors than myelin and does not seem suited as a measure for disrupted cortical myelination in diseased cohorts. Rather, more studies are needed to measure these other pathological processes at the same time in AD to further understand what T1-w/T2-w changes in AD reflect.

There are some limitations to our study. Since data was collected in clinical setting, our analysis was not identical to the original approach of Glasser and van Essen (2011), including different acquisition parameters, i.e. isotropic voxels for both images versus non-isotropic voxels for T2-w images in our study. As a consequence, our analyses may be more prone to partial volume effects. In order to study possible contamination from non-

GM tissue classes, we repeated analyses in a subset of individuals including only voxels with increasing GM probabilities and the use of an eroded GM mask. Findings were consistent to the main analyses, suggesting that our results cannot simply be explained by differences in partial volume effects (Supplementary Figure 2 & 3). Furthermore, as we used a volumetric approach, we are unable to exclude the possibility that cortical layering patterns may have influenced the T1-w/T2-w ratio. Future studies should compare volumetric approaches with e.g., a surface-based registration that might better account for each person's cortical folding pattern (Fischl et al. 1999). Moreover, the differences in T1-w/T2-w ratio between AD and NC individuals are highly significant, however the effect sizes are too small to be of clinical significance. Another limitation is that we have no pathological data available to further study whether T1-w/T2-w corresponds to myelin in the same individuals: future research should take confounding effects such as iron and inflammation into account and histologically quantify the T1-w/T2-w in healthy and pathological tissue. Alongside this, the large sample size, the use of the same scanning protocol for all subjects, and the use of AD biomarkers strengthens our study.

In conclusion, our findings of higher T1-w/T2-w values in AD suggest that this measure may not (only) reflect myelin content. Currently the T1-w/T2-w ratio is used frequently across various populations to characterize myelin. Our results suggest that this measure should be interpreted with caution in particular in disease populations and further validation and characterization of the T1-w/T2-w ratio and its neurobiological origin in AD is necessary for correct interpretation.

## **Acknowledgments**

Research of the VUmc Alzheimer Center is part of the neurodegeneration research program of Amsterdam Neuroscience ([www.amsterdamresearch.org](http://www.amsterdamresearch.org)). The VUmc Alzheimer Center is supported by Stichting Alzheimer Nederland and Stichting VUmc fonds. The clinical database structure was developed with funding from Stichting Dioraphte. I wish to thank Dr. Steenwijk for his valuable advice on this project.

## **Disclosures**

W. Pelkmans and E. Dicks report no disclosures. F. Barkhof is a consultant for Biogen-Idec, Janssen Alzheimer Immunotherapy, Bayer-Schering, Merck-Serono, Roche, Novartis, Genzyme, and Sanofi-Aventis; has received sponsoring from European Commission–Horizon 2020, National Institute for Health Research–University College London Hospitals Biomedical Research Centre, Scottish Multiple Sclerosis Register, TEVA, Novartis, and Toshiba; is supported by the University College London Hospitals NHS Foundation Trust Biomedical Research Center; and serves on the editorial boards of *Radiology*, *Brain*, *Neuroradiology*, *Multiple Sclerosis Journal*, and *Neurology*. H. Vrenken reports no disclosures. P. Scheltens has acquired grant support (for the institution) from BiogenGE Healthcare, Danone Research, Piramal, and Merck. In the past 2 years, he has received consultancy/speaker fees (paid to the institution) from Lilly, GE Healthcare, Novartis, Sanofi, Nutricia, Probiobdrug, Biogen, Roche, Avraham, and EIP Pharma, Merck AG. W. M. van der Flier's research programs have been funded by ZonMW, the Netherlands Organization of Scientific Research, Seventh European Framework Programme, Alzheimer Nederland, Cardiovascular Onderzoek Nederland, Stichting Dioraphte, Gieskes-Strijbis fonds, Boehringer Ingelheim, Piramal Imaging, Roche BV, Janssen Stellar,

Biogen MA and Combinostics. All funding is paid to her institution. B. M. Tijms declares that she is supported by the ZonMW Memorabel '(Grant number #73305056)'.

### References

- Arshad M, Stanley JA, Raz N. 2017. Test-retest reliability and concurrent validity of in vivo myelin content indices: Myelin water fraction and calibrated T1w/T2w image ratio. *Human Brain Mapping*. 38:1780–1790.
- Ayton S, Wang Y, Diouf I, Schneider JA, Brockman J, Morris MC, Bush AI. 2019. Brain iron is associated with accelerated cognitive decline in people with Alzheimer pathology. *Molecular Psychiatry*.
- Bartzokis G, Lu PH, Mintz J. 2007. Human brain myelination and amyloid beta deposition in Alzheimer's disease. *Alzheimers Dement*. 3:122–125.
- Bartzokis G, Sultzer D, Lu PH, Nuechterlein KH, Mintz J, Cummings JL. 2004. Heterogeneous age-related breakdown of white matter structural integrity: Implications for cortical “disconnection” in aging and Alzheimer's disease. *Neurobiology of Aging*. 25:843–851.
- Beer A, Biberacher V, Schmidt P, Righart R, Buck D, Berthele A, Kirschke J, Zimmer C, Hemmer B, Mühlau M. 2016. Tissue damage within normal appearing white matter in early multiple sclerosis: assessment by the ratio of T1- and T2-weighted MR image intensity. *Journal of Neurology*. 263:1495–1502.
- Bock NA, Kocharyan A, Liu J V., Silva AC. 2009. Visualizing the entire cortical myelination pattern in marmosets with magnetic resonance imaging. *Journal of Neuroscience Methods*. 185:15–22.
- Braak H, Braak E. 1991. Neuropathological staging of Alzheimer-related changes. *Acta Neuropathologica*. 82:239–259.
- Brettschneider J, Del Tredici K, Lee VMY, Trojanowski JQ. 2015. Spreading of pathology in neurodegenerative diseases: A focus on human studies. *Nature Reviews Neuroscience*. 16:109–120.
- Buckner RL. 2005. Molecular, Structural, and Functional Characterization of Alzheimer's Disease: Evidence for a Relationship between Default Activity, Amyloid, and Memory. *Journal of Neuroscience*. 25:7709–7717.
- Bulk M, Abdelmoula WM, Nabuurs RJA, van der Graaf LM, Mulders CWH, Mulder AA, Jost CR, Koster AJ, van Buchem MA, Natté R, Dijkstra J, van der Weerd L. 2018. Postmortem MRI and histology demonstrate differential iron accumulation and cortical myelin organization in early- and late-onset Alzheimer's disease. *Neurobiology of Aging*. 62:231–242.
- Burt JB, Demirtaş M, Eckner WJ, Navejar NM, Ji JL, Martin WJ, Bernacchia A, Anticevic A, Murray JD. 2018. Hierarchy of transcriptomic specialization across human cortex captured by structural neuroimaging topography. *Nature Neuroscience*. 21:1251–1259.
- Carmeli C, Donati A, Antille V, Viceic D, Ghika J, von Gunten A, Clarke S, Meuli R, Frackowiak RS, Knyazeva MG. 2013. Demyelination in Mild Cognitive Impairment Suggests Progression Path to Alzheimer's Disease. *PLoS ONE*. 8:e72759.



- Carmichael O, Schwarz C, Drucker D, Fletcher E, Harvey D, Beckett L, Jack CR, Weiner M, DeCarli C. 2010. Longitudinal changes in white matter disease and cognition in the first year of the Alzheimer disease neuroimaging initiative. *Archives of Neurology*. 67:1370–1378.
- Chua TC, Wen W, Slavin MJ, Sachdev PS. 2008. Diffusion tensor imaging in mild cognitive impairment and Alzheimer's disease: A review. *Current Opinion in Neurology*. 21:83–92.
- Connor JR, Snyder BS, Beard JL, Fine RE, Mufson EJ. 1992. Regional distribution of iron and iron-regulatory proteins in the brain in aging and Alzheimer's disease. *JNeurosciRes*. 31:327–335.
- de Rochefort L, Brown R, Prince MR, Wang Y. 2008. Quantitative MR susceptibility mapping using piece-wise constant regularized inversion of the magnetic field. *Magnetic Resonance in Medicine*. 60:1003–1009.
- Debette S, Beiser A, Decarli C, Au R, Himali JJ, Kelly-Hayes M, Romero JR, Kase CS, Wolf PA, Seshadri S. 2010. Association of MRI markers of vascular brain injury with incident stroke, mild cognitive impairment, dementia, and mortality: The framingham offspring study. *Stroke*. 41:600–606.
- Dicks E, Tijms BM, ten Kate M, Gouw AA, Benedictus MR, Teunissen CE, Barkhof F, Scheltens P, van der Flier WM. 2018. Gray matter network measures are associated with cognitive decline in mild cognitive impairment. *Neurobiology of Aging*. 61:198–206.
- Du G, Lewis MM, Sica C, Kong L, Huang X. 2018. Magnetic resonance T1w/T2w ratio: A parsimonious marker for Parkinson disease. *Annals of Neurology*. 85:1–9.
- Dusek P, Dezortova M, Wuerfel J. 2013. Imaging of Iron. In: *International Review of Neurobiology*. 1st ed. Elsevier Inc. p. 195–239.
- Eickhoff S, Walters NB, Schleicher A, Kril J, Egan GF, Zilles K, Watson JDG, Amunts K. 2005. High-resolution MRI reflects myeloarchitecture and cytoarchitecture of human cerebral cortex. *Human Brain Mapping*. 24:206–215.
- Fazekas F, Chawluk JB, Alavi A. 1987. MR signal abnormalities at 1.5 T in Alzheimer's dementia and normal aging. *American Journal of Neuroradiology*. 8:421–426.
- Filley CM, Fields RD. 2016. White matter and cognition: making the connection. *Journal of Neurophysiology*. 116:2093–2104.
- Fischl B, Salat DH, Van Der Kouwe AJW, Makris N, Ségonne F, Quinn BT, Dale AM. 2004. Sequence-independent segmentation of magnetic resonance images. *NeuroImage*. 23:S69–S84.
- Fischl B, Sereno MI, Dale AM. 1999. Cortical Surface-Based Analysis. II: Inflation, Flattening, and a Surface-Based Coordinate System. *NeuroImage*. 207:195–207.
- Fornito A, Zalesky A, Breakspear M. 2015. The connectomics of brain disorders. *Nature Reviews Neuroscience*. 16:159–172.
- Fukunaga M, Li T-Q, van Gelderen P, de Zwart JA, Shmueli K, Yao B, Lee J, Maric D, Aronova MA, Zhang G, Leapman RD, Schenck JF, Merkle H, Duyn JH. 2010. Layer-specific

- variation of iron content in cerebral cortex as a source of MRI contrast. *Proceedings of the National Academy of Sciences*. 107:3834–3839.
- Ganzetti M, Wenderoth N, Mantini D. 2015. Mapping pathological changes in brain structure by combining T1- and T2-weighted MR imaging data. *Neuroradiology*. 57:917–928.
- Gao J, Cheung RTF, Chan YS, Chu LW, Mak HKF, Lee TMC. 2014. The relevance of short-range fibers to cognitive efficiency and brain activation in aging and dementia. *PLoS ONE*. 9:e90307.
- Glasser MF, Goyal MS, Preuss TM, Raichle ME, van Essen DC. 2014. Trends and properties of human cerebral cortex: Correlations with cortical myelin content. *Neuroimage*. 93:165–175.
- Glasser MF, van Essen DC. 2011. Mapping Human Cortical Areas In Vivo Based on Myelin Content as Revealed by T1- and T2-Weighted MRI. *Journal of Neuroscience*. 31:11597–11616.
- Gordon BA, Najmi S, Hsu P, Roe CM, Morris JC, Benzinger TLS. 2015. The effects of white matter hyperintensities and amyloid deposition on Alzheimer dementia. *NeuroImage: Clinical*. 8:246–252.
- Grydeland H, Vértes PE, Váša F, Romero-García R, Whitaker K, Alexander-Bloch AF, Bjørnerud A, Patel AX, Sederevičius D, Tamnes CK, Westlye LT, White SR, Walhovd KB, Fjell AM, Bullmore ET. 2019. Waves of maturation and senescence in micro-structural MRI markers of human cortical myelination over the lifespan. *Cerebral Cortex*. 29:1369–1381.
- Grydeland H, Walhovd KB, Tamnes CK, Westlye LT, Fjell AM. 2013. Intracortical Myelin Links with Performance Variability across the Human Lifespan: Results from T1- and T2-Weighted MRI Myelin Mapping and Diffusion Tensor Imaging. *Journal of Neuroscience*. 33:18618–18630.
- Hallgren B, Sourander P. 1958. THE EFFECT OF AGE ON THE NON-HAEMIN IRON IN THE HUMAN BRAIN. *Journal of Neurochemistry*. 3:41–51.
- Hare D, Ayton S, Bush A, Lei P. 2013. A delicate balance: Iron metabolism and diseases of the brain. *Frontiers in Aging Neuroscience*. 5:1–19.
- Heath F, Hurley SA, Johansen-Berg H, Sampaio-Baptista C. 2018. Advances in noninvasive myelin imaging. *Developmental Neurobiology*. 78:136–151.
- Imon Y, Yamaguchi S, Yamamura Y, Tsuji S, Kajima T, Ito K, Nakamura S. 1995. Low intensity areas observed on T2-weighted magnetic resonance imaging of the cerebral cortex in various neurological diseases. *Journal of the Neurological Sciences*. 134:27–32.
- Ishida T, Donishi T, Iwatani J, Yamada S, Takahashi S, Ukai S, Shinosaki K, Terada M, Kaneoke Y. 2017. Elucidating the aberrant brain regions in bipolar disorder using T1-weighted/T2-weighted magnetic resonance ratio images. *Psychiatry Research: Neuroimaging*. 263:76–84.

- Iwatani J, Ishida T, Donishi T, Ukai S, Shinosaki K, Terada M, Kaneoke Y. 2015. Use of T1-weighted/T2-weighted magnetic resonance ratio images to elucidate changes in the schizophrenic brain. *Brain and Behavior*. 5:1–14.
- Jucker M, Walker LC. 2018. Propagation and spread of pathogenic protein assemblies in neurodegenerative diseases. *Nature Neuroscience*. 21:1341–1349.
- Laule C, Vavasour IM, Kolind SH, Li DKB, Traboulsee TL, Moore GRW, MacKay AL. 2007. Magnetic resonance imaging of myelin. *Neurotherapeutics : the journal of the American Society for Experimental NeuroTherapeutics*. 4:460–484.
- McKhann GM, Knopman DS, Chertkow H, Hyman BT, Jack CR, Kawas CH, Klunk WE, Koroshetz WJ, Manly JJ, Mayeux R, Mohs RC, Morris JC, Rossor MN, Scheltens P, Carrillo MC, Thies B, Weintraub S, Phelps CH. 2011. The diagnosis of dementia due to Alzheimer's disease: Recommendations from the National Institute on Aging-Alzheimer's Association workgroups on diagnostic guidelines for Alzheimer's disease. *Alzheimer's & Dementia*. 7:263–269.
- Mitew S, Kirkcaldie MTK, Halliday GM, Shepherd CE, Vickers JC, Dickson TC. 2010. Focal demyelination in Alzheimer's disease and transgenic mouse models. *Acta Neuropathologica*. 119:567–577.
- Mulder C, Verwey NA, van der Flier WM, Bouwman FH, Kok A, van Elk EJ, Scheltens P, Blankenstein MA. 2010. Amyloid- $\beta$ (1-42), total tau, and phosphorylated tau as cerebrospinal fluid biomarkers for the diagnosis of Alzheimer disease. *Clinical Chemistry*. 56:248–253.
- Nakamura K, Chen JT, Ontaneda D, Fox RJ, Trapp BD. 2017. T1-/T2-weighted ratio differs in demyelinated cortex in multiple sclerosis. *Annals of Neurology*. 82:635–639.
- Nave K-A, Werner HB. 2014. Myelination of the Nervous System: Mechanisms and Functions. *Annual Review of Cell and Developmental Biology*. 30:503–533.
- Nieuwenhuys R, Broere CAJ. 2017. A map of the human neocortex showing the estimated overall myelin content of the individual architectonic areas based on the studies of Adolf Hopf. *Brain Structure and Function*. 222:465–480.
- Nir TM, Jahanshad N, Villalon-Reina JE, Toga AW, Jack CR, Weiner MW, Thompson PM. 2013. Effectiveness of regional DTI measures in distinguishing Alzheimer's disease, MCI, and normal aging. *NeuroImage: Clinical*. 3:180–195.
- Palmqvist S, Schöll M, Strandberg O, Mattsson N, Stomrud E, Zetterberg H, Blennow K, Landau S, Jagust W, Hansson O. 2017. Earliest accumulation of  $\beta$ -amyloid occurs within the default-mode network and concurrently affects brain connectivity. *Nature Communications*. 8:1214.
- Peters A. 2009. The effects of normal aging on myelinated nerve fibers in monkey central nervous system. *Frontiers in Neuroanatomy*. 3:1–10.
- Pievani M, Filippini N, van den Heuvel MP, Cappa SF, Frisoni GB. 2014. Brain connectivity in neurodegenerative diseases - From phenotype to proteinopathy. *Nature Reviews Neurology*. 10:620–633.

- Quintana C, Bellefqih S, Laval JY, Guerquin-Kern JL, Wu TD, Avila J, Ferrer I, Arranz R, Patiño C. 2006. Study of the localization of iron, ferritin, and hemosiderin in Alzheimer's disease hippocampus by analytical microscopy at the subcellular level. *Journal of Structural Biology*. 153:42–54.
- Righart R, Biberacher V, Jonkman LE, Klaver R, Schmidt P, Buck D, Berthele A, Kirschke JS, Zimmer C, Hemmer B, Geurts JGG, Mühlau M. 2017. Cortical pathology in multiple sclerosis detected by the T1/T2-weighted ratio from routine magnetic resonance imaging. *Annals of Neurology*. 82:519–529.
- Ritchie J, Pantazatos SP, French L. 2018. Transcriptomic characterization of MRI contrast with focus on the T1-w/T2-w ratio in the cerebral cortex. *Neuroimage*. 174:504–517.
- Rowley CD, Tabrizi SJ, Scahill RI, Leavitt BR, Roos RAC, Durr A, Bock NA. 2018. Altered Intracortical T1-Weighted/T2-Weighted Ratio Signal in Huntington's Disease. *Frontiers in Neuroscience*. 12:1–9.
- Rowley J, Fonov V, Wu O, Eskildsen SF, Schoemaker D, Wu L, Mohades S, Shin M, Sziklas V, Cheewakriengkrai L, Shmuel A, Dagher A, Gauthier S, Rosa-Neto P. 2013. White Matter Abnormalities and Structural Hippocampal Disconnections in Amnesic Mild Cognitive Impairment and Alzheimer's Disease. *PLoS ONE*. 8:e74776.
- Scheltens P, Blennow K, Breteler MMB, de Strooper B, Frisoni GB, Salloway S, Van der Flier WM. 2016. Alzheimer's disease. *The Lancet*. 388:505–517.
- Selkoe DJ. 2002. Alzheimer's Disease Is a Synaptic Failure. *Science* (1979). 298:789–791.
- Shafee R, Buckner RL, Fischl B. 2015. Gray matter myelination of 1555 human brains using partial volume corrected MRI images. *Neuroimage*. 105:473–485.
- Stüber C, Morawski M, Schäfer A, Labadie C, Wähnert M, Leuze C, Streicher M, Barapatre N, Reimann K, Geyer S, Spemann D, Turner R. 2014. Myelin and iron concentration in the human brain: A quantitative study of MRI contrast. *NeuroImage*. 93:95–106.
- Thal DR, Rüb U, Orantes M, Braak H. 2002. Phases of A $\beta$ -deposition in the human brain and its relevance for the development of AD. *Neurology*. 58:1791–1800.
- Tijms BM, Willems EAJ, Zwan MD, Mulder SD, Visser PJ, van Berckel BNM, van der Flier WM, Scheltens P, Teunissen CE. 2018. Unbiased approach to counteract upward drift in cerebrospinal fluid amyloid- $\beta$  1–42 analysis results. *Clinical Chemistry*. 64:576–585.
- Timmler S, Simons M. 2019. Grey matter myelination. *Glia*. 67:2063–2070.
- Tzourio-Mazoyer N, Landeau B, Papathanassiou D, Crivello F, Etard O, Delcroix N, Mazoyer B, Joliot M. 2002. Automated anatomical labeling of activations in SPM using a macroscopic anatomical parcellation of the MNI MRI single-subject brain. *Neuroimage*. 15:273–289.
- Uddin MN, Figley TD, Marrie RA, Figley CR. 2018. Can T1w/T2w ratio be used as a myelin-specific measure in subcortical structures? Comparisons between FSE-based T1w/T2w ratios, GRASE-based T1w/T2w ratios and multi-echo GRASE-based myelin water fractions. *NMR in Biomedicine*. 31:e3868.

- Van Der Flier WM, Pijnenburg YAL, Prins N, Lemstra AW, Bouwman FH, Teunissen CE, Van Berckel BNM, Stam CJ, Barkhof F, Visser PJ, Van Egmond E, Scheltens P. 2014. Optimizing patient care and research: The Amsterdam dementia cohort. *Journal of Alzheimer's Disease*. 41:313–327.
- Van Der Flier WM, Scheltens P. 2018. Amsterdam dementia cohort: Performing research to optimize care. *Journal of Alzheimer's Disease*. 62:1091–1111.
- Van Duijn S, Bulk M, Van Duinen SG, Nabuurs RJA, Van Buchem MA, Van Der Weerd L, Natté R. 2017. Cortical Iron Reflects Severity of Alzheimer's Disease. *Journal of Alzheimer's Disease*. 60:1533–1545.
- van Rooden S, Versluis MJ, Liem MK, Milles J, Maier AB, Oleksik AM, Webb AG, van Buchem MA, van der Grond J. 2014. Cortical phase changes in Alzheimer's disease at 7T MRI: A novel imaging marker. *Alzheimer's & Dementia*. 10:e19–e26.
- Wallace MN, Cronin MJ, Bowtell RW, Scott IS, Palmer AR, Gowland PA. 2016. Histological basis of laminar MRI patterns in high resolution images of fixed human auditory cortex. *Frontiers in Neuroscience*. 10:1–12.
- Ward RJ, Zucca FA, Duyn JH, Crichton RR, Zecca L. 2014. The role of iron in brain ageing and neurodegenerative disorders. *The Lancet Neurology*. 13:1045–1060.
- Yasuno F, Kazui H, Morita N, Kajimoto K, Ihara M, Taguchi A, Yamamoto A, Matsuoka K, Takahashi M, Nakagawara J, Iida H, Kishimoto T, Nagatsuka K. 2017. Use of T1-weighted/T2-weighted magnetic resonance ratio to elucidate changes due to amyloid  $\beta$  accumulation in cognitively normal subjects. *NeuroImage: Clinical*. 13:209–214.
- Zecca L, Youdim MBH, Riederer P, Connor JR, Crichton RR. 2004. Iron, brain ageing and neurodegenerative disorders. *Nature Reviews Neuroscience*. 5:863–873.

## Supplementary material

**Supplementary table 1. Table of mean T1-w/T2-w ratio values for all AAL brain regions compared between AD and NC subjects.**

AAL Region	Diagnosis	EMM	SE	F	d	p-value
1 Precentral Gyrus L	NC	1.08	.010	6.26	.10	.01266790
	AD	1.12	.007			
2 Precentral Gyrus R	NC	1.12	.010	3.25	.03	.07174438
	AD	1.14	.008			
3 Superior Frontal Gyrus L	NC	1.00	.009	15.07	.26	<b>.00011849</b>
	AD	1.05	.007			
4 Superior Frontal Gyrus R	NC	1.01	.009	11.41	.21	.00079088
	AD	1.05	.007			
5 Superior Orbital Frontal Gyrus L	NC	.98	.008	7.60	.17	.00607814
	AD	1.01	.006			
6 Superior Orbital Frontal Gyrus R	NC	.98	.008	6.95	.16	.00868921
	AD	1.01	.006			
7 Middle Frontal Gyrus L	NC	.98	.009	18.36	.35	<b>.00002227</b>
	AD	1.03	.007			
8 Middle Frontal Gyrus R	NC	.99	.009	14.64	.30	<b>.00014814</b>
	AD	1.04	.007			
9 Middle Orbital Frontal Gyrus L	NC	.95	.008	8.46	.20	.00380910
	AD	.98	.006			
10 Middle Orbital Frontal Gyrus R	NC	.96	.008	5.56	.13	.01882445
	AD	.99	.006			

11 Inferior Frontal Gyrus Pars Opercularis L	NC	.97	.009	12.37	.26	<b>.00047944</b>
	AD	1.01	.007			
12 Inferior Frontal Gyrus Pars Opercularis R	NC	.97	.009	12.47	.25	<b>.00045408</b>
	AD	1.01	.007			
13 Inferior Frontal Gyrus Pars Triangularis L	NC	.96	.009	14.39	.30	<b>.00016812</b>
	AD	1.01	.007			
14 Inferior Frontal Gyrus Pars Triangularis R	NC	.98	.009	11.53	.26	.00074575
	AD	1.02	.007			
15 Inferior Frontal Gyrus Pars Orbitalis L	NC	1.00	.009	7.50	.17	.00642322
	AD	1.03	.006			
16 Inferior Frontal Gyrus Pars Orbitalis R	NC	1.03	.009	4.40	.12	.03640697
	AD	1.05	.007			
17 Rolandic Operculum L	NC	.99	.010	10.58	.22	.00122432
	AD	1.03	.007			
18 Rolandic Operculum R	NC	.96	.009	12.90	.24	<b>.00036377</b>
	AD	1.01	.007			
19 Supplementary Motor Area L	NC	1.03	.010	4.86	.07	.02803077
	AD	1.06	.007			
20 Supplementary Motor Area R	NC	1.03	.010	5.85	.08	.01599272
	AD	1.05	.007			
21 Olfactory Cortex L	NC	.93	.009	5.63	.10	.01810567
	AD	.96	.006			
22 Olfactory Cortex R	NC	.93	.008	5.80	.13	.01643551

## Chapter 5

---

	AD	.95	.006			
23 Medial Frontal Gyrus L	NC	.96	.009	12.62	.29	<b>.00042139</b>
	AD	1.00	.007			
24 Medial Frontal Gyrus R	NC	.95	.009	10.22	.24	.00148292
	AD	.99	.007			
25 Medial Orbitofrontal Cortex L	NC	.91	.008	7.16	.19	.00773805
	AD	.93	.006			
26 Medial Orbitofrontal Cortex R	NC	.88	.008	8.04	.21	.00476612
	AD	.91	.006			
27 Gyrus Rectus L	NC	.93	.008	4.28	.12	.03907625
	AD	.95	.006			
28 Gyrus Rectus R	NC	.92	.008	4.75	.10	.02981004
	AD	.95	.006			
29 Insula L	NC	.85	.008	15.72	.34	<b>.00008521</b>
	AD	.89	.006			
30 Insula R	NC	.87	.008	13.07	.29	<b>.00033322</b>
	AD	.91	.006			
31 Anterior Cingulate Gyrus L	NC	.87	.009	19.43	.46	<b>.00001298</b>
	AD	.92	.006			
32 Anterior Cingulate Gyrus R	NC	.86	.009	23.57	.48	<b>.00000165</b>
	AD	.91	.006			
33 Midcingulate Area L	NC	.92	.009	10.50	.26	.00128381
	AD	.96	.007			
34 Midcingulate Area R	NC	.89	.009	15.07	.33	<b>.00011846</b>
	AD	.94	.006			
35 Posterior Cingulate Gyrus L	NC	1.04	.010	13.52	.25	<b>.00026328</b>
	AD	1.08	.007			



36 Posterior Cingulate Gyrus R	NC	1.05	.009	3.64	.04	.05690315
	AD	1.07	.007			
37 Hippocampus L	NC	.87	.008	1.58	.32	.20915277
	AD	.86	.006			
38 Hippocampus R	NC	.90	.008	4.07	.41	.04412484
	AD	.88	.006			
39 Parahippocampal Gyrus L	NC	.96	.009	.10	.16	.75176180
	AD	.97	.006			
40 Parahippocampal Gyrus R	NC	.96	.009	.00	.19	.94944799
	AD	.96	.006			
41 Amygdala L	NC	.98	.009	1.27	.07	.25958119
	AD	.99	.007			
42 Amygdala R	NC	.98	.009	1.82	.04	.17862583
	AD	1.00	.007			
43 Calcarine Sulcus L	NC	1.10	.010	12.97	.21	<b>.00035107</b>
	AD	1.15	.007			
44 Calcarine Sulcus R	NC	1.12	.010	9.86	.14	.00179885
	AD	1.16	.008			
45 Cuneus L	NC	1.04	.009	15.21	.23	<b>.00011040</b>
	AD	1.09	.007			
46 Cuneus R	NC	1.08	.010	9.76	.14	.00190088
	AD	1.12	.007			
47 Lingual Gyrus L	NC	1.08	.010	5.15	.08	.02372393
	AD	1.11	.007			
48 Lingual Gyrus R	NC	1.11	.010	1.97	.01	.16167314
	AD	1.13	.008			
49 Superior Occipital Gyrus L	NC	1.02	.010	10.02	.17	.00165187
	AD	1.06	.007			
50 Superior Occipital Gyrus R	NC	1.04	.010	5.85	.10	.01596634

## Chapter 5

---

	AD	1.07	.007			
51 Middle Occipital Gyrus L	NC	.99	.009	12.16	.22	.00053444
	AD	1.03	.007			
52 Middle Occipital Gyrus R	NC	.98	.009	8.69	.15	.00335976
	AD	1.02	.007			
53 Inferior Occipital Cortex L	NC	1.01	.009	4.94	.06	.02666731
	AD	1.04	.007			
54 Inferior Occipital Cortex R	NC	1.04	.009	.89	.06	.34534276
	AD	1.06	.007			
55 Fusiform Gyrus L	NC	.96	.009	5.26	.07	.02231508
	AD	.99	.007			
56 Fusiform Gyrus R	NC	.96	.009	2.30	.01	.13050923
	AD	.98	.006			
57 Postcentral Gyrus L	NC	1.09	.010	8.87	.17	.00305913
	AD	1.13	.008			
58 Postcentral Gyrus R	NC	1.08	.010	9.52	.17	.00216084
	AD	1.12	.008			
59 Superior Parietal Lobule L	NC	1.05	.010	20.34	.30	<b>.00000826</b>
	AD	1.11	.008			
60 Superior Parietal Lobule R	NC	1.05	.010	16.01	.26	<b>.00007337</b>
	AD	1.10	.008			
61 Inferior Parietal Lobule L	NC	1.03	.010	32.34	.44	<b>.00000002</b>
	AD	1.11	.008			
62 Inferior Parietal Lobule R	NC	1.02	.010	33.61	.43	<b>.00000001</b>
	AD	1.10	.007			
63 Supramarginal Gyrus L	NC	.95	.009	21.73	.32	<b>.00000412</b>

	AD	1.00	.007			
64 Supramarginal Gyrus R	NC	.96	.009	23.67	.36	<b>.00000157</b>
	AD	1.02	.007			
65 Angular Gyrus L	NC	.95	.009	33.67	.45	<b>.00000001</b>
	AD	1.02	.007			
66 Angular Gyrus R	NC	.96	.009	26.96	.38	<b>.00000031</b>
	AD	1.02	.007			
67 Precuneus L	NC	1.03	.010	28.89	.38	<b>.00000012</b>
	AD	1.10	.007			
68 Precuneus R	NC	1.04	.010	31.73	.40	<b>.00000003</b>
	AD	1.11	.008			
69 Paracentral Lobule L	NC	1.19	.012	.16	.16	.68940243
	AD	1.19	.009			
70 Paracentral Lobule R	NC	1.12	.011	2.58	.01	.10893285
	AD	1.15	.008			
71 Caudate Nucleus L	NC	1.10	.010	.06	.16	.80577217
	AD	1.10	.008			
72 Caudate Nucleus R	NC	1.06	.010	.23	.20	.63200949
	AD	1.06	.008			
73 Putamen L	NC	1.27	.013	3.87	.10	.04975371
	AD	1.31	.010			
74 Putamen R	NC	1.26	.013	4.98	.14	.02614408
	AD	1.29	.009			
75 Globus Pallidus L	NC	1.19	.011	8.54	.25	.00364387
	AD	1.23	.008			
76 Globus Pallidus R	NC	1.09	.010	1.86	.05	.17356530
	AD	1.11	.007			
77 Thalamus L	NC	1.25	.012	1.19	.39	.27658720
	AD	1.23	.009			
78 Thalamus R	NC	1.22	.012	.74	.32	.38941540

## Chapter 5

---

	AD	1.20	.009			
79 Transverse Temporal Gyrus L	NC	1.07	.010	4.47	.10	.03496709
	AD	1.10	.007			
80 Transverse Temporal Gyrus R	NC	1.07	.010	2.85	.05	.09215691
	AD	1.09	.007			
81 Superior Temporal Gyrus L	NC	1.02	.010	16.02	.32	<b>.00007287</b>
	AD	1.07	.007			
82 Superior Temporal Gyrus R	NC	1.00	.010	21.78	.40	<b>.00000402</b>
	AD	1.06	.007			
83 Superior Temporal Pole L	NC	.88	.008	6.75	.15	.00970352
	AD	.91	.006			
84 Superior Temporal Pole R	NC	.92	.008	4.54	.11	.03373339
	AD	.94	.006			
85 Middle Temporal Gyrus L	NC	.93	.008	19.44	.36	<b>.00001294</b>
	AD	.98	.006			
86 Middle Temporal Gyrus R	NC	.95	.009	15.29	.30	<b>.00010608</b>
	AD	.99	.006			
87 Middle Temporal Pole L	NC	.90	.008	4.31	.08	.03855768
	AD	.92	.006			
88 Middle Temporal Pole R	NC	.92	.008	3.78	.08	.05249867
	AD	.94	.006			
89 Inferior Temporal Gyrus L	NC	.94	.008	7.88	.15	.00520603
	AD	.97	.006			
90 Inferior Temporal Gyrus R	NC	.96	.008	5.76	.12	.01682444

AD .98 .006

Areas showing significantly higher T1-w/T2-w ratios in AD compared to CN subjects are displayed in bold. Abbreviations: AAL, Automated Anatomical Labelling; EMM, Estimated Marginal Means; SE, Standard Error; d, Cohen's d effect size; NC, Normal Cognition; AD, Alzheimer's Disease; Data adjusted for age and sex;  $p < .0005$ .

**Supplementary table 2. Table of mean T1-w/T2-w ratio values for all AAL brain regions compared between AD and NC subjects without image bias correction.**

AAL Region	Diagnosis	No Bias Correction				
		EMM	SE	F	d	p-value
1 Precentral Gyrus L	NC	.94	.008	2.023	.04	.155020929
	AD	.95	.006			
2 Precentral Gyrus R	NC	.97	.009	1.40	.01	.237211492
	AD	.99	.007			
3 Superior Frontal Gyrus L	NC	.86	.008	5.84	.03	.016018675
	AD	.89	.006			
4 Superior Frontal Gyrus R	NC	.87	.008	5.55	.01	.018907383
	AD	.89	.006			
5 Superior Orbital Frontal Gyrus L	NC	.87	.007	.91	.11	.339739884
	AD	.88	.005			
6 Superior Orbital Frontal Gyrus R	NC	.88	.007	1.89	.06	.169540644
	AD	.89	.005			
7 Middle Frontal Gyrus L	NC	.83	.007	3.35	.03	.068037093
	AD	.85	.005			
8 Middle Frontal Gyrus R	NC	.83	.007	4.41	.03	.036204325
	AD	.85	.005			

## Chapter 5

---

9 Middle Orbital Frontal Gyrus L	NC	.85	.007	.03	.16	.860415523
	AD	.85	.005			
10 Middle Orbital Frontal Gyrus R	NC	.85	.007	.21	.13	.649990770
	AD	.86	.005			
11 Inferior Frontal Gyrus Pars Opercularis L	NC	.87	.007	2.16	.01	.142825535
	AD	.88	.006			
12 Inferior Frontal Gyrus Pars Opercularis R	NC	.86	.008	5.08	.09	.024649034
	AD	.89	.006			
13 Inferior Frontal Gyrus Pars Triangularis L	NC	.84	.007	.27	.12	.606964369
	AD	.84	.005			
14 Inferior Frontal Gyrus Pars Triangularis R	NC	.86	.007	1.43	.01	.232716288
	AD	.87	.005			
15 Inferior Frontal Gyrus Pars Orbitalis L	NC	.90	.008	.36	.10	.550841090
	AD	.90	.006			
16 Inferior Frontal Gyrus Pars Orbitalis R	NC	.94	.008	.64	.05	.423350945
	AD	.95	.006			
17 Rolandic Operculum L	NC	.95	.009	2.28	.01	.131725687
	AD	.97	.007			
18 Rolandic Operculum R	NC	.92	.009	7.82	.14	.005389764
	AD	.95	.007			
19 Supplementary Motor Area L	NC	.86	.009	3.16	.02	.076297309

	AD	.88	.007			
20 Supplementary Motor Area R	NC	.87	.009	4.42	.02	.036037633
	AD	.89	.007			
21 Olfactory Cortex L	NC	.92	.008	1.98	.04	.160282515
	AD	.93	.006			
22 Olfactory Cortex R	NC	.91	.008	2.86	.01	.091311768
	AD	.93	.006			
23 Medial Frontal Gyrus L	NC	.85	.008	1.69	.13	.194132696
	AD	.87	.006			
24 Medial Frontal Gyrus R	NC	.85	.008	1.81	.14	.178954335
	AD	.86	.006			
25 Medial Orbitofrontal Cortex L	NC	.84	.008	.49	.12	.483022368
	AD	.85	.006			
26 Medial Orbitofrontal Cortex R	NC	.83	.007	.92	.10	.339125292
	AD	.84	.005			
27 Gyrus Rectus L	NC	.85	.008	1.62	.03	.204172970
	AD	.87	.006			
28 Gyrus Rectus R	NC	.87	.008	2.22	.01	.136696899
	AD	.88	.006			
29 Insula L	NC	.83	.008	4.20	.09	.041002967
	AD	.85	.006			
30 Insula R	NC	.87	.009	8.73	.20	.003289108
	AD	.91	.006			
31 Anterior Cingulate Gyrus L	NC	.84	.008	2.69	.02	.101558857
	AD	.86	.006			
32 Anterior Cingulate Gyrus R	NC	.83	.008	5.66	.07	.017780789

## Chapter 5

---

	AD	.86	.006			
33 Midcingulate Area L	NC	.84	.009	3.94	.15	.047891410
	AD	.86	.006			
34 Midcingulate Area R	NC	.82	.008	7.09	.22	.008004431
	AD	.85	.006			
35 Posterior Cingulate Gyrus L	NC	1.10	.011	5.97	.16	.014947769
	AD	1.14	.008			
36 Posterior Cingulate Gyrus R	NC	1.12	.010	.69	.05	.407780965
	AD	1.13	.008			
37 Hippocampus L	NC	.96	.009	2.35	.35	.125895903
	AD	.94	.006			
38 Hippocampus R	NC	1.01	.009	3.10	.38	.079196357
	AD	.99	.007			
39 Parahippocampal Gyrus L	NC	1.01	.009	1.91	.03	.167365500
	AD	1.03	.007			
40 Parahippocampal Gyrus R	NC	1.03	.009	1.68	.04	.195849941
	AD	1.05	.007			
41 Amygdala L	NC	1.01	.009	1.59	.06	.207938092
	AD	1.02	.007			
42 Amygdala R	NC	1.02	.009	2.51	.01	.113625731
	AD	1.04	.007			
43 Calcarine Sulcus L	NC	1.18	.011	4.65	.08	.031648162
	AD	1.21	.008			
44 Calcarine Sulcus R	NC	1.22	.012	1.26	.06	.262891441
	AD	1.24	.009			
45 Cuneus L	NC	1.10	.011	3.57	.07	.059371934
	AD	1.13	.008			



46 Cuneus R	NC	1.14	.012	.98	.06	.323573151
	AD	1.16	.009			
47 Lingual Gyrus L	NC	1.19	.011	3.14	.05	.077120592
	AD	1.22	.008			
48 Lingual Gyrus R	NC	1.24	.012	.29	.13	.592919523
	AD	1.25	.009			
49 Superior Occipital Gyrus L	NC	1.08	.011	2.06	.01	.151759387
	AD	1.10	.008			
50 Superior Occipital Gyrus R	NC	1.10	.012	.04	.14	.842129890
	AD	1.10	.009			
51 Middle Occipital Gyrus L	NC	1.03	.010	3.01	.02	.083555996
	AD	1.05	.008			
52 Middle Occipital Gyrus R	NC	1.03	.010	.01	.19	.915198686
	AD	1.03	.008			
53 Inferior Occipital Cortex L	NC	1.06	.009	2.60	.05	.107304848
	AD	1.08	.007			
54 Inferior Occipital Cortex R	NC	1.10	.010	.05	.29	.826979009
	AD	1.10	.007			
55 Fusiform Gyrus L	NC	1.01	.010	6.37	.08	.011977785
	AD	1.04	.007			
56 Fusiform Gyrus R	NC	1.04	.010	2.58	.06	.108746931
	AD	1.06	.007			
57 Postcentral Gyrus L	NC	.97	.009	4.13	.09	.042811883
	AD	.99	.007			
58 Postcentral Gyrus R	NC	.99	.010	6.28	.16	.012566381
	AD	1.03	.007			

## Chapter 5

---

59 Superior Parietal Lobule L	NC	1.05	.011	12.24	.23	<b>.000513297</b>
	AD	1.10	.008			
60 Superior Parietal Lobule R	NC	1.06	.011	7.38	.16	.006827863
	AD	1.10	.008			
61 Inferior Parietal Lobule L	NC	1.00	.010	16.17	.29	<b>.000067739</b>
	AD	1.05	.008			
62 Inferior Parietal Lobule R	NC	1.02	.010	17.09	.30	<b>.000042324</b>
	AD	1.07	.008			
63 Supramarginal Gyrus L	NC	.92	.009	8.01	.16	.004849522
	AD	.95	.007			
64 Supramarginal Gyrus R	NC	.93	.009	13.01	.25	<b>.000343865</b>
	AD	.97	.007			
65 Angular Gyrus L	NC	.97	.010	13.05 6	.23	<b>.000335760</b>
	AD	1.02	.007			
66 Angular Gyrus R	NC	1.00	.010	6.05	.10	.014254830
	AD	1.03	.008			
67 Precuneus L	NC	1.05	.011	15.96	.29	<b>.000075372</b>
	AD	1.11	.008			
68 Precuneus R	NC	1.08	.012	15.30	.27	<b>.000105657</b>
	AD	1.14	.009			
69 Paracentral Lobule L	NC	1.08	.014	.30	.09	.586200770
	AD	1.09	.010			
70 Paracentral Lobule R	NC	1.05	.012	2.16	.02	.142390214
	AD	1.07	.009			
71 Caudate Nucleus L	NC	1.13	.011	3.28	.35	.070823615
	AD	1.10	.008			
72 Caudate Nucleus R	NC	1.11	.011	2.16	.31	.142148917

	AD	1.09	.008			
73 Putamen L	NC	1.32	.014	.40	.07	.525618173
	AD	1.34	.010			
74 Putamen R	NC	1.35	.014	3.00	.08	.084216443
	AD	1.38	.010			
75 Globus Pallidus L	NC	1.26	.012	3.75	.13	.053482068
	AD	1.29	.009			
76 Globus Pallidus R	NC	1.15	.011	.10	.05	.755338032
	AD	1.16	.008			
77 Thalamus L	NC	1.44	.014	1.17	.33	.280593715
	AD	1.42	.010			
78 Thalamus R	NC	1.43	.014	.35	.24	.553355306
	AD	1.42	.010			
79 Transverse Temporal Gyrus L	NC	1.07	.010	1.01	.03	.315234797
	AD	1.09	.008			
80 Transverse Temporal Gyrus R	NC	1.07	.010	1.82	.01	.177798976
	AD	1.09	.007			
81 Superior Temporal Gyrus L	NC	.98	.009	6.52	.15	.010981050
	AD	1.01	.007			
82 Superior Temporal Gyrus R	NC	.96	.009	18.01	.30	<b>.000026550</b>
	AD	1.01	.007			
83 Superior Temporal Pole L	NC	.80	.007	4.26	.06	.039648894
	AD	.82	.005			
84 Superior Temporal Pole R	NC	.84	.008	5.07	.10	.024860289
	AD	.87	.006			
85 Middle Temporal Gyrus L	NC	.89	.008	11.56	.22	.000731090
	AD	.93	.006			

86 Middle Temporal Gyrus R	NC	.93	.009	8.71	.12	.003328057
	AD	.96	.007			
87 Middle Temporal Pole L	NC	.78	.007	9.28	.17	.002452176
	AD	.81	.005			
88 Middle Temporal Pole R	NC	.80	.007	11.87	.23	.000621285
	AD	.83	.005			
89 Inferior Temporal Gyrus L	NC	.88	.007	11.14	.14	<b>.000915779</b>
	AD	.91	.006			
90 Inferior Temporal Gyrus R	NC	.92	.008	9.36	.07	.002344465
	AD	.952	.006			

Areas showing significantly higher T1-w/T2-w ratios in AD compared to CN subjects are displayed in bold. Abbreviations: AAL, Automated Anatomical Labelling; EMM, Estimated Marginal Means; SE, Standard Error; d, Cohen's d effect size; NC, Normal Cognition; AD, Alzheimer's Disease; Data adjusted for age and sex;  $p < .0005$ .

**Supplementary table 3. Table of mean T1-w/T2-w ratio values for all AAL brain regions compared between AD and NC subjects using age and sex matched individuals (n=50).**

AAL Region	Diagnosis	Age and sex matched (n=50)				
		EMM	SE	F	d	p-value
1 Precentral Gyrus L	NC	1.09	.021	2.81	.47	.100531524
	AD	1.14	.021			
2 Precentral Gyrus R	NC	1.12	.021	3.56	.52	.065486786
	AD	1.18	.021			
3 Superior Frontal Gyrus L	NC	1.02	.020	5.33	.66	.025504140
	AD	1.08	.020			
4 Superior Frontal Gyrus R	NC	1.03	.020	5.59	.67	.022301262
	AD	1.09	.020			

5 Superior Orbital Frontal Gyrus L	NC	.99	.017	4.19	.57	.046317027
	AD	1.04	.017			
6 Superior Orbital Frontal Gyrus R	NC	1.00	.018	2.77	.46	.103069720
	AD	1.04	.018			
7 Middle Frontal Gyrus L	NC	.99	.020	5.37	.67	.024989283
	AD	1.05	.020			
8 Middle Frontal Gyrus R	NC	1.00	.019	6.26	.71	.015945832
	AD	1.07	.019			
9 Middle Orbital Frontal Gyrus L	NC	.96	.016	5.54	.66	.022958444
	AD	1.01	.016			
10 Middle Orbital Frontal Gyrus R	NC	.97	.016	5.25	.63	.026597171
	AD	1.02	.016			
11 Inferior Frontal Gyrus Pars Opercularis L	NC	.98	.018	6.72	.73	.012754116
	AD	1.05	.018			
12 Inferior Frontal Gyrus Pars Opercularis R	NC	.98	.018	8.20	.81	.006293423
	AD	1.05	.018			
13 Inferior Frontal Gyrus Pars Triangularis L	NC	.97	.019	6.27	.71	.015906473
	AD	1.04	.019			
14 Inferior Frontal Gyrus Pars Triangularis R	NC	.98	.018	6.29	.68	.015767251
	AD	1.05	.018			
15 Inferior Frontal Gyrus Pars Orbitalis L	NC	1.00	.018	4.24	.58	.045083812
	AD	1.05	.018			

## Chapter 5

---

16 Inferior Frontal Gyrus Pars Orbitalis R	NC	1.03	.018	3.98	.55	.052029706
	AD	1.08	.018			
17 Rolandic Operculum L	NC	1.00	.018	4.96	.62	.030863663
	AD	1.06	.018			
18 Rolandic Operculum R	NC	.97	.019	5.98	.68	.018324796
	AD	1.04	.019			
19 Supplementary Motor Area L	NC	1.03	.021	3.93	.55	.053407176
	AD	1.09	.021			
20 Supplementary Motor Area R	NC	1.03	.020	4.92	.62	.031560015
	AD	1.10	.020			
21 Olfactory Cortex L	NC	.95	.016	2.59	.44	.114420632
	AD	.98	.016			
22 Olfactory Cortex R	NC	.93	.017	4.42	.59	.041097325
	AD	.98	.017			
23 Medial Frontal Gyrus L	NC	.97	.019	5.35	.66	.025261761
	AD	1.03	.019			
24 Medial Frontal Gyrus R	NC	.96	.020	5.23	.65	.026843969
	AD	1.03	.020			
25 Medial Orbitofrontal Cortex L	NC	.91	.017	6.27	.71	.015898254
	AD	.97	.017			
26 Medial Orbitofrontal Cortex R	NC	.88	.016	5.68	.67	.021367361
	AD	.94	.016			
27 Gyrus Rectus L	NC	.94	.017	3.05	.48	.087678439
	AD	.98	.017			
28 Gyrus Rectus R	NC	.93	.018	3.95	.56	.052977696

	AD	.98	.018			
29 Insula L	NC	.85	.016	8.33	.82	.005926361
	AD	.92	.016			
30 Insula R	NC	.87	.018	7.68	.76	.008018333
	AD	.94	.018			
31 Anterior Cingulate Gyrus L	NC	.88	.021	8.05	.81	.006753107
	AD	.96	.021			
32 Anterior Cingulate Gyrus R	NC	.86	.020	11.21	.95	.001627435
	AD	.95	.020			
33 Midcingulate Area L	NC	.92	.018	8.63	.83	.005144401
	AD	.99	.018			
34 Midcingulate Area R	NC	.90	.017	9.22	.85	.003940629
	AD	.97	.017			
35 Posterior Cingulate Gyrus L	NC	1.04	.019	11.14	.93	.001682431
	AD	1.13	.019			
36 Posterior Cingulate Gyrus R	NC	1.05	.017	3.48	.51	.068367528
	AD	1.09	.017			
37 Hippocampus L	NC	.88	.015	.02	.05	.889864582
	AD	.88	.015			
38 Hippocampus R	NC	.91	.015	.16	.12	.692153478
	AD	.90	.015			
39 Parahippocampal Gyrus L	NC	.98	.018	.55	.20	.463769480
	AD	1.00	.018			
40 Parahippocampal Gyrus R	NC	.98	.016	.60	.21	.441446363
	AD	1.00	.016			
41 Amygdala L	NC	.99	.018	2.00	.39	.164484821
	AD	1.02	.018			
42 Amygdala R	NC	.99	.016	3.42	.50	.070774037
	AD	1.03	.016			

## Chapter 5

---

43 Calcarine Sulcus L	NC	1.11	.020	6.06	.68	.017650653
	AD	1.18	.020			
44 Calcarine Sulcus R	NC	1.13	.020	8.44	.78	.005621823
	AD	1.21	.020			
45 Cuneus L	NC	1.05	.018	7.73	.73	.007856892
	AD	1.12	.018			
46 Cuneus R	NC	1.09	.018	5.64	.62	.021803137
	AD	1.15	.018			
47 Lingual Gyrus L	NC	1.09	.019	4.18	.57	.046605485
	AD	1.14	.019			
48 Lingual Gyrus R	NC	1.12	.020	2.45	.44	.124173491
	AD	1.16	.020			
49 Superior Occipital Gyrus L	NC	1.04	.017	3.00	.47	.090011250
	AD	1.08	.017			
50 Superior Occipital Gyrus R	NC	1.06	.017	3.05	.46	.087395277
	AD	1.10	.017			
51 Middle Occipital Gyrus L	NC	1.00	.016	7.10	.72	.010601337
	AD	1.06	.016			
52 Middle Occipital Gyrus R	NC	.99	.015	5.69	.63	.021291197
	AD	1.04	.015			
53 Inferior Occipital Cortex L	NC	1.03	.017	2.44	.42	.125470744
	AD	1.07	.017			
54 Inferior Occipital Cortex R	NC	1.05	.017	1.86	.36	.178778637
	AD	1.08	.017			
55 Fusiform Gyrus L	NC	.97	.017	2.76	.47	.103528713
	AD	1.01	.017			
56 Fusiform Gyrus R	NC	.97	.017	2.15	.41	.149632568
	AD	1.01	.017			



57 Postcentral Gyrus L	NC	1.10	.020	3.50	.52	.067908752
	AD	1.16	.020			
58 Postcentral Gyrus R	NC	1.09	.019	7.25	.74	.009843773
	AD	1.16	.019			
59 Superior Parietal Lobule L	NC	1.08	.022	5.52	.65	.023151083
	AD	1.15	.022			
60 Superior Parietal Lobule R	NC	1.07	.020	6.18	.69	.016577580
	AD	1.14	.020			
61 Inferior Parietal Lobule L	NC	1.05	.021	10.34	.91	.002381669
	AD	1.15	.021			
62 Inferior Parietal Lobule R	NC	1.04	.019	15.11	1.08	<b>.000324436</b>
	AD	1.14	.019			
63 Supramarginal Gyrus L	NC	.96	.018	9.35	.85	.003717938
	AD	1.04	.018			
64 Supramarginal Gyrus R	NC	.972	.018	12.68	.98	.000874195
	AD	1.06	.018			
65 Angular Gyrus L	NC	.98	.018	9.85	.88	.002967069
	AD	1.06	.018			
66 Angular Gyrus R	NC	.98	.017	12.52	.96	.000933689
	AD	1.07	.017			
67 Precuneus L	NC	1.04	.020	11.65	.93	.001351056
	AD	1.14	.020			
68 Precuneus R	NC	1.06	.019	12.46	.96	.000955949
	AD	1.15	.019			
69 Paracentral Lobule L	NC	1.18	.023	3.03	.43	.088668724
	AD	1.23	.023			
70 Paracentral Lobule R	NC	1.13	.024	3.00	.46	.090096836
	AD	1.19	.024			

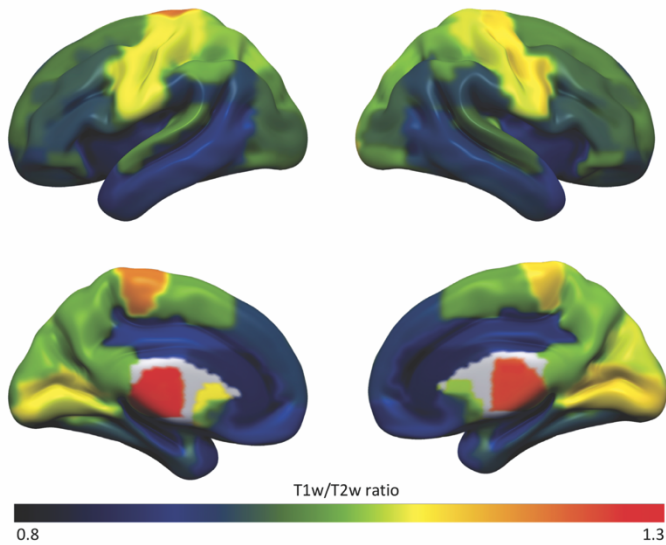
## Chapter 5

---

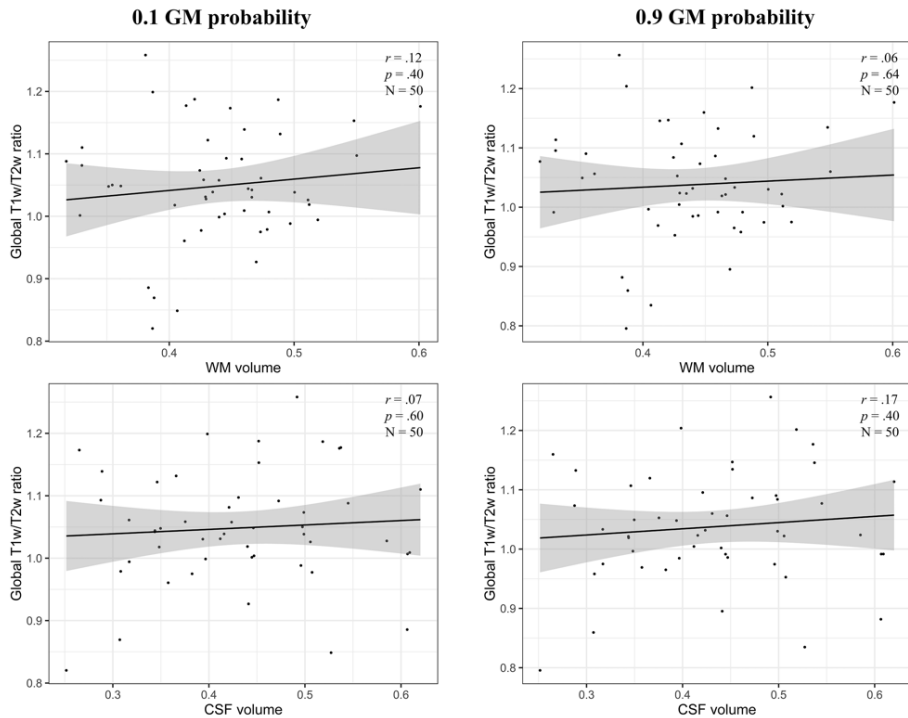
71 Caudate Nucleus L	NC	1.10	.020	.42	.17	.519655032
	AD	1.12	.020			
72 Caudate Nucleus R	NC	1.07	.019	.02	.05	.901061817
	AD	1.07	.019			
73 Putamen L	NC	1.27	.026	6.28	.68	.015776219
	AD	1.37	.026			
74 Putamen R	NC	1.26	.024	6.51	.70	.014145365
	AD	1.35	.024			
75 Globus Pallidus L	NC	1.20	.022	5.31	.65	.025743623
	AD	1.27	.022			
76 Globus Pallidus R	NC	1.10	.019	1.70	.36	.200363290
	AD	1.13	.019			
77 Thalamus L	NC	1.26	.025	.04	.07	.846050600
	AD	1.25	.025			
78 Thalamus R	NC	1.24	.024	.46	.20	.500641987
	AD	1.22	.024			
79 Transverse Temporal Gyrus L	NC	1.05	.020	6.59	.72	.013580909
	AD	1.13	.020			
80 Transverse Temporal Gyrus R	NC	1.06	.018	4.96	.62	.030846464
	AD	1.12	.018			
81 Superior Temporal Gyrus L	NC	1.03	.019	7.27	.77	.009766599
	AD	1.10	.019			
82 Superior Temporal Gyrus R	NC	1.01	.020	12.43	.97	.000967968
	AD	1.11	.020			
83 Superior Temporal Pole L	NC	.89	.017	3.89	.56	.054621381
	AD	.94	.017			
84 Superior Temporal Pole R	NC	.93	.018	2.28	.42	.137545688
	AD	.96	.018			

85 Middle Temporal Gyrus L	NC	.94	.017	7.17	.75	.010233303
	AD	1.00	.017			
86 Middle Temporal Gyrus R	NC	.95	.017	9.55	.86	.003389305
	AD	1.03	.017			
87 Middle Temporal Pole L	NC	.90	.016	3.64	.53	.062842449
	AD	.94	.016			
88 Middle Temporal Pole R	NC	.92	.017	2.29	.42	.137450344
	AD	.96	.017			
89 Inferior Temporal Gyrus L	NC	.95	.015	4.01	.56	.051258928
	AD	.99	.015			
90 Inferior Temporal Gyrus R	NC	.96	.015	6.05	.68	.017765750
	AD	1.02	.015			

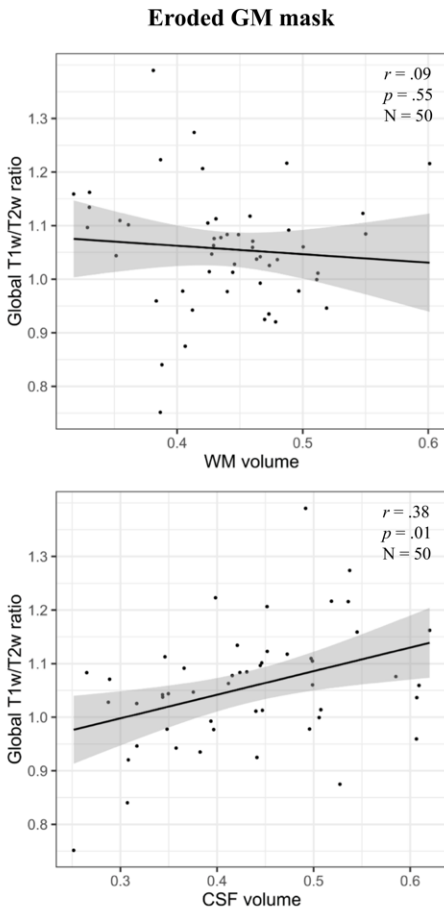
Areas showing significantly higher T1-w/T2-w ratios in AD compared to CN subjects are displayed in bold. Abbreviations: AAL, Automated Anatomical Labelling; EMM, Estimated Marginal Means; SE, Standard Error; d, Cohen's d effect size; NC, Normal Cognition; AD, Alzheimer's Disease; Data adjusted for age and sex;  $p < .0005$ .



**Supplementary figure 1. Whole brain group average T1-w/T2-w ratio surface map of subjects with normal cognition.** The signal strength distribution shows relatively high T1-w/T2-w values (myelin content) in sensory and motor regions and lower values in temporal and frontal areas corresponding with previous literature.



**Supplementary figure 2. Scatterplot of global T1-w/T2-w ratios with CSF and WM volume using different GM probabilities.** In the main analysis the T1-w/T2-w image was masked using a mask with a GM probability of  $>.3$ . In a subset of  $N = 50$  (25 NC; 25 AD) subjects, data was reanalysed using a GM mask probability of  $>.1$  and  $>.9$ . These T1-w/T2-w values were correlated with CSF and WM volumes. The results of both images with different GM probabilities are very similar, and no increase in T1-w/T2-w ratios was seen with higher CSF or WM volume. Therefore, we think it is unlikely that our main results, i.e. higher T1-w/T2-w ratios in AD, can be fully explained by partial volume effects.



**Supplementary figure 3. Scatterplot of global T1-w/T2-w ratios masked with an eroded GM mask with CSF and WM volume.** In a subset of  $N = 50$  (25 NC; 25 AD), the data was re-run using an eroded GM mask to reduce possible partial volume effects from neighbouring GM voxels. Using the erode function in fslmaths, the subject specific GM masks were eroded when zero voxels was found in kernel. The eroded GM mask actually resulted in more PVE, likely associated with atrophy and was therefore not applied in the main analysis.







# CHAPTER 6

## **Grey matter network markers identify individuals with prodromal Alzheimer's disease who will show rapid clinical decline**

Wiesje Pelkmans, Ellen M. Vromen, Ellen Dicks, Philip Scheltens, Charlotte E. Teunissen, Frederik Barkhof, Wiesje M. van der Flier, Betty M. Tijms, for the Alzheimer's Disease Neuroimaging Initiative

*Published in  
Brain Communications, 2022. 4(2)  
DOI:10.1093/braincomms/fcac026*

### **Abstract**

Individuals with prodromal Alzheimer's disease show considerable variability in rates of cognitive decline, which hampers the ability to detect potential treatment effects in clinical trials. Prognostic markers to select those individuals who will decline rapidly within a trial time-frame are needed. Brain network measures based on grey matter covariance patterns have been associated with future cognitive decline in Alzheimer's disease. In this longitudinal cohort study, we investigated whether cut-offs for grey matter networks could be derived to detect fast disease progression at an individual level. We further tested whether detection was improved by adding other biomarkers known to be associated with future cognitive decline (i.e. CSF tau phosphorylated at threonine 181 [p-tau181] levels and hippocampal volume). We selected individuals with mild cognitive impairment and abnormal CSF amyloid  $\beta_{1-42}$  levels from the Amsterdam Dementia Cohort (ADC) and the Alzheimer's Disease Neuroimaging Initiative (ADNI), when they had available baseline structural MRI and clinical follow-up. Outcome was progression to dementia within 2 years. We determined prognostic cut-offs for grey matter network properties (gamma, lambda, and small-world coefficient) using time-dependent Receiver Operating Characteristic analysis in the ADC cohort. We tested generalisation of cut-offs in ADNI, using logistic regression analysis and classification statistics. We further tested whether combining these with CSF p-tau181 and hippocampal volume improved detection of fast decliners. We observed that within 2 years, 24.6% (ADC, n=244) and 34.0% (ADNI, n = 247) of prodromal Alzheimer's disease patients progressed to dementia. Using the grey matter network cut-offs for progression, we could detect fast progressors with 65% accuracy in ADNI. Combining grey matter network measures with CSF p-tau and hippocampal volume resulted in the best

model fit for classification of rapid decliners, increasing detecting accuracy to 72%. These data suggest that single-subject grey matter connectivity networks indicative of a more random network organisation can contribute to identifying prodromal Alzheimer's disease individuals who will show rapid disease progression. Moreover, we found that combined with p-tau and hippocampal volume this resulted in highest accuracy. This could facilitate clinical trials by increasing chances to detect effects on clinical outcome measures.

## **Introduction**

Alzheimer's disease (AD) starts with aggregation of amyloid- $\beta$  ( $A\beta$ ) in the brain, after which it can take up to 20 years for an individual to develop dementia (Jack et al. 2018; Scheltens et al. 2021). It has been proposed that AD clinical trials are most likely to be effective when individuals have biomarker evidence for the presence of  $A\beta$  pathology and do not yet show large scale irreversible neuronal damage (Selkoe 2011; Cummings et al. 2019). This makes  $A\beta$  positive individuals with mild cognitive impairment (MCI), i.e., prodromal AD, a well-suited population for disease-modifying therapies in AD clinical trials. However, a challenge faced in secondary prevention trials is that individuals with prodromal AD show substantial heterogeneity in clinical progression rates (Vos et al. 2015). This heterogeneity hampers the ability to detect treatment effects on cognitive outcomes within a typical 1 to 2 year clinical trial (Jutten et al. 2021). Biomarkers are needed that can help to distinguish individuals with prodromal AD who will show rapid disease progression from those who will remain stable within a trial time-frame.

Previous work has found that disrupted brain grey matter (GM) network measures, reflecting covariance patterns in GM morphology, are related to increased risk of cognitive decline and progression to AD dementia (Pereira et al. 2016; Dicks et al. 2018a; Tijms, ten Kate, et al. 2018; Verfaillie et al. 2018). Across those studies, disrupted whole brain network measures gamma (i.e. normalized values of the clustering coefficient) and small-world, i.e. indicative of an increasingly random network and reduction in small world organisation, were most robustly associated with cognitive decline, adding information to hippocampal volume and/or cerebrospinal fluid (CSF) tau measures. However, it remains unknown to what extent grey

matter networks can be used to identify single individuals who will show fast progression.

Here we studied this question in individuals with prodromal AD from two independent cohorts, i.e., we first established cut-offs in the Amsterdam Dementia Cohort (ADC) and then tested whether these GM network cut-offs could predict if prodromal AD subjects remained stable or progressed to dementia within 2 years in the Alzheimer's Disease Neuroimaging Initiative (ADNI). We then compared the performance of the grey matter network markers with two other biomarkers known to be associated with decline in prodromal AD (i.e., hippocampal volume and CSF phosphorylated tau [p-tau] levels; van Rossum, Visser, et al. 2012; van Rossum, Vos, et al. 2012). and determined an optimal model for detecting fast progressors. Finally, we calculated if stratification of prodromal AD subjects by abnormal GM network markers would reduce sample size requirements in a hypothetical randomised control trial.

## **Materials and Methods**

### *Participants*

We studied two cohorts: the Amsterdam Dementia Cohort (ADC) and the Alzheimer's Disease Neuroimaging Initiative (ADNI). The ADC is a memory clinic-based cohort where participants are re-evaluated on a 6-month basis as part of regular care (Van Der Flier and Scheltens 2018). The patients in the present study visited the memory clinic between November 2003 and July 2019. ADNI is an ongoing longitudinal research cohort, for which criteria are described in more detail at <http://adni.loni.usc.edu/>. It was launched in 2003 as a public-private partnership, led by Principal Investigator Michael W. Weiner, MD. The primary goal of ADNI has been to test whether serial magnetic resonance imaging (MRI), positron emission

tomography (PET), other biological markers, and clinical and neuropsychological assessment can be combined to measure the progression of MCI and early AD. For up-to-date information, see [www.adni-info.org](http://www.adni-info.org). The data used in the present study were collected between December 2005 and April 2016. Diagnosis was evaluated at 3–12-month intervals. For both cohorts, we selected individuals who fulfilled the consensus criteria for MCI as described by Petersen et al. (1999) and Albert et al. (2011), had abnormal levels of CSF  $A\beta_{(1-42)}$ , an available baseline structural MRI scan, and at least one follow-up neuropsychological assessment. In ADNI, conversion from MCI to AD is reviewed by a central review committee that applies the NINCDS-ADRDA diagnostic criteria (McKhann et al. 1984) for diagnosis of AD dementia. In the ADC, AD dementia is also defined according to the NINCDS-ADRDA diagnostic criteria (McKhann et al. 1984) and from 2011 on the NIA-AA criteria were applied (McKhann et al. 2011; Van Der Flier et al. 2014). Disease modifying trials recruiting prodromal AD individuals typically have a trial duration of 24 months or less (Supplementary Table 1; Cummings et al. 2021), therefore we defined individuals as fast progressors when they progressed to dementia within 2 years. In both ADNI and ADC all participants gave written informed consent for participation in the study and for reuse of the data. Ethical approval was given by the regional ethics committees.

### *MRI Acquisition and Pre-processing*

In ADC, structural T1-weighted images were acquired on nine different scanners, using a standardized protocol as part of routine patient care, of which the acquisition parameters are described in detail in the Supplementary material. In ADNI, T1-weighted scans were performed on 1.5T or 3T scanners using previously described standardized protocols (Jack

et al. 2008), typically a sagittal 3D MP-RAGE with a voxel size of 1.2 mm<sup>3</sup>. All images were segmented into grey matter, white matter, and CSF using the Statistical Parametric Mapping (SPM12, <https://www.fil.ion.ucl.ac.uk/spm/software/spm12/>) running in MATLAB (v2011a). The segmented grey matter images were resliced to 2x2x2 mm isotropic voxels to reduce the dimensionality of the data. Total intracranial volume (TIV) was computed as the sum of grey matter, white matter, and CSF volumes. The automated anatomical labelling atlas was used to obtain hippocampal GM volume estimates (Tzourio-Mazoyer et al. 2002). A previously determined cut-off was applied to determine hippocampal abnormality in ADNI with a mean hippocampal volume corrected for TIV of > 3.68 mL (Wisse et al. 2015). All GM segmentations were visually checked for quality.

#### *Single-Subject Grey Matter Networks*

Single-subject grey matter networks were constructed from the native grey matter images as described in the freely available MATLAB scripts: [https://github.com/bettytijms/Single\\_Subject\\_Grey\\_Matter\\_Networks](https://github.com/bettytijms/Single_Subject_Grey_Matter_Networks) and in more detail in Tijms et al. (2012). For each individual, a network was determined from the native space grey matter segmentations. First, nodes were defined as cubes of 3 x 3 x 3 voxels (6x6x6 mm<sup>3</sup>) using an atlas free approach. The nodes keep the 3D structure of the cortex intact, and thereby contain information on GM intensity as well as spatial information between the voxels. Next, connections were defined when nodes showed structural similarity as determined with the Pearson correlation coefficients across corresponding voxels. In order to find the maximum correlation value with a target cube across the curved cortex, each cube was rotated by an angle with multiples of 45° over all axes. The resulting similarity matrix containing

all pairwise correlations was binarized using a threshold that reduced the chance of spurious correlations in the network to 5%. This corresponds to a significance level of  $p < 0.05$  corrected for multiple comparisons using a permutation-based procedure (Noble 2009).

For each individual grey matter network, we calculated  $\gamma$ ,  $\lambda$ , and the small world coefficient, as our previous studies showed that these measures most robustly associated with cognitive decline (Dicks et al. 2018b; Tijms, ten Kate, et al. 2018; Verfaillie et al. 2018). Briefly,  $\gamma$  quantifies how a network's clustering coefficient (the fraction of a node's neighbours that are also neighbours of each other) is higher than that of a random network.  $\lambda$  quantifies how a network's path length (the shortest path length between all pairs of nodes in the network) deviates from a random network. In more detail, in order to determine how the clustering and path length measures deviate from randomly organised networks, we divided the average clustering coefficient and path length values by those values of five randomised reference networks of identical size and degree distribution (Maslov and Sneppen 2002). The ratio of  $\gamma$  to  $\lambda$ , is defined as the small-world coefficient  $\sigma$ , indicative of the optimal balance between information segregation and integration. The network measures were computed with scripts from the Brain Connectivity Toolbox (<https://sites.google.com/site/bctnet/>; Bullmore and Sporns 2009), modified for large scale networks.

### *Cerebrospinal Fluid Analysis*

Lumbar puncture was performed as described in Mulder et al. (2010) and Engelborghs et al. (2017) for ADC, and for ADNI according to the ADNI procedures manual (<http://www.adni-info.org/>). CSF concentrations of  $A\beta_{(1-42)}$  and tau phosphorylated threonine 181 were measured using



sandwich ELISAs (Innotest, Innogenetics, Belgium), at the Neurochemistry laboratory of the department of Clinical Chemistry of the Amsterdam University Medical Center (ADC), and for ADNI with the multiplex xMAP Luminex platform (Luminex Corp, Austin, TX, USA) and INNO-BIA AlzBio3 (Innogenetics, Ghent, Belgium) immunoassay kit-based reagents. The cut-offs for CSF A $\beta$ <sub>(1-42)</sub> and p-tau abnormality have previously been determined and were 813 pg/mL and 52 pg/mL for ADC (Mulder et al. 2010; Tijms, Willemse, et al. 2018), and 192 pg/mL and 23 pg/mL for ADNI (Shaw et al. 2009). Because CSF p-tau was used as one of the predictors for decline, we only used an amyloid marker to define prodromal AD.

### *Statistical Analysis*

Prognostic cut-offs for GM network measures ( $\gamma$ ,  $\lambda$ ,  $\sigma$ ) to predict progression to dementia within 2 years were determined in the ADC cohort through time-dependent receiver operating characteristic (tROC) analysis from censored survival data using nearest neighbour estimation (Heagerty et al. 2000). The advantage of tROC analyses over standard ROC is that tROC takes the time to an event into account when calculating the sensitivity, specificity, and area under the curve (AUC) for a specific marker. For each network measure, we determined the optimal cut-off value in the ADC that best separated prodromal AD patients with a high or low risk for fast clinical decline at two years post baseline. We then used these cut-offs in ADNI to evaluate detecting of fast progressors using logistic regression analysis, and reported accuracy, sensitivity, and specificity. We further evaluated whether GM network measures provide additive information to more commonly used biomarkers for AD, CSF p-tau and hippocampal volume, by adding the latter markers to the logistic regression model and compared model fit using the Akaike's Information Criterion (AIC). Analyses were initially performed

without covariates as such a model would be easiest to apply in practice. We repeated the analyses adding sex, age, education, and MRI scanner as covariates.

Next, we tested the extent to which one, two, or three abnormal biomarkers (small-world, p-tau, hippocampal volume) could predict who progressed to dementia within 2 years using logistic regression. Finally, sample sizes were estimated for a hypothetical 2-year randomized-controlled trial with two arms, showing an expected treatment effect of 25% reduction of decline on the Mini-Mental State Examination (MMSE; Folstein et al. 1983) and the Clinical Dementia Rating scale - Sum of Boxes (CDR-SB; Williams et al. 2013) when stratifying for GM network abnormality using the following formula:

$$\text{Sample size / arm} = 2(z_{1-\alpha/2} + z_{1-\beta})^2 \times (\sigma_b^2 + \sigma_e^2 / \sum(t_i - t_{\text{mean}})^2) / \Delta^2$$

where  $\alpha$  is equal to the type I error of a 2-sided significance test set at 0.05, and the power ( $1-\beta$ ) is 80%. From the linear mixed model,  $\sigma_b^2$  and  $\sigma_e^2$  are the variance in random subject slopes and the residual error variance respectively.  $t_i$  is the measurement at time  $i$  and  $t_{\text{mean}}$  is the average follow-up time,  $\Delta$  is the difference in mean rate of decline in the treatment versus control group using a 25% treatment effect. Analyses were conducted with R version 4.1.1. using the survival and survivalROC packages (Heagerty et al. 2000).

## Results

### *Study Population*

A total of 491 prodromal AD patients were available for this study (Table 1). The participants from ADNI were older and had on average more years of education compared to ADC participants. After 2 years, 60 (24.6%) subjects in ADC and 84 (34.0%) subjects in ADNI showed clinical progression to dementia.

**Table 1. Subject characteristics**

	ADC	ADNI
n	244	247
Age, [y]	67.5 (7.4)	72.9 (7.0)
Sex, [f]	113 (46.3%)	104 (42.1%)
Education, [y]	11.7 (3.2)	15.8 (2.8)
MMSE	26.4 (2.4)	27.5 (1.8)
Progression to dementia, [2y]	60 (24.6%)	84 (34.0%)
<i>APOEε4</i> carrier	157 (73.0%)	164 (66.4%)

Data are presented as mean(SD) or n(%); ADC = Amsterdam Dementia Cohort; ADNI = Alzheimer's Disease Neuroimaging Initiative; y = years; f = female; MMSE = Mini Mental State Examination; APOE = Apolipoprotein E.

### *Cut-Points for Grey Matter Network Measures*

First, we determined cut-points in ADC optimising classification of prodromal AD individuals who remained stable versus those who progressed to dementia within 2 years. Applying the tROC analysis yielded the following cut-offs: 1.627 for  $\gamma$ , 1.106 for  $\lambda$ , and 1.479 for small-world coefficient. These cut-offs resulted in AUCs of 0.60 for  $\gamma$  (sensitivity = 64%, specificity = 54%), 0.51 for  $\lambda$  (sensitivity = 93%, specificity = 16%), and 0.59 for small-world coefficient (sensitivity = 60%, specificity = 63%; Fig. 1). This was comparable to the AUCs of 0.58 for p-tau (sensitivity = 72%, specificity

= 44%) and 0.61 for hippocampal volume (sensitivity = 70%, specificity = 52%).

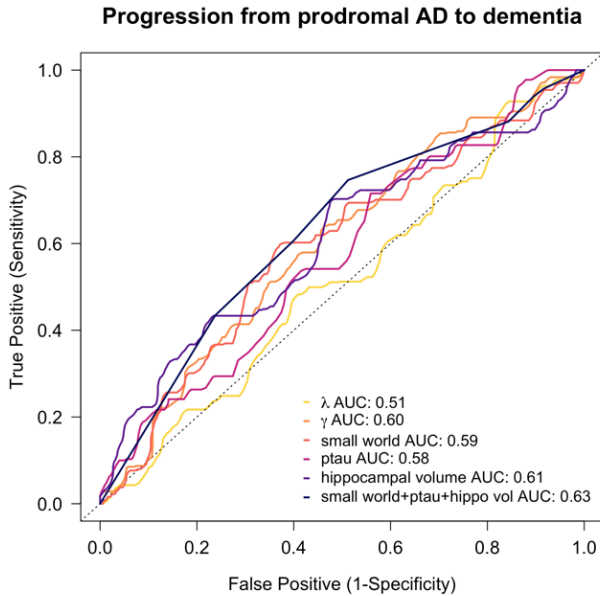


**Figure 1. tROC analyses of prognostic biomarkers for predicting clinical progression within 2 years in ADC.** tROC curves and corresponding areas under the curves to determine the most optimal cut-off for grey matter network markers together and CSF phosphorylated tau and normalised hippocampal volume to assess accuracy when predicting clinical progression to dementia within two years post-baseline in prodromal AD individuals (n=244).

*Predicting Fast Clinical Progression using Grey Matter Network Measures*

We next performed logistic regression analysis in ADNI to evaluate detection of fast progression using ADC determined cut-points. GM network measures ( $\gamma$  and  $\sigma$ ) showed an accuracy of 65% (sensitivity = 33 - 42%, specificity = 77 - 82%) for predicting stable vs progressing individuals. Compared to individuals with normal  $\gamma$  values, those with abnormal  $\gamma$  values were 2.4 times [95% CI= 1.4 - 4.3] more likely to progress to dementia within a 2-year period (Table 2; Fig. 2). Similar odds-ratios (OR) were observed for individuals with abnormal small-world values (Odds=2.2, [95% CI=1.2 - 4.1]), and abnormal hippocampal volume (Odds=2.9, [95% CI= 1.6 - 5.2]; Table 2; Fig. 2). Individuals with abnormal  $\lambda$  and CSF p-tau values showed a higher risk of progression to dementia, that is an odds of 6.5, [95% CI=2.2 - 18.9] and an odds of 3.1, [95% CI=1.0 - 9.4] respectively, however this was accompanied with larger confidence intervals and low accuracy values <.5. When correcting for sex, age, education, and MRI scanner the odds ratios for abnormal biomarkers to predict progression increased (Supplementary Table 3).

In addition, mixed model analysis showed that individuals with abnormal GM network values showed steeper decline on the MMSE ( $\beta \pm SE$ ,  $\gamma$ :-1.00 $\pm$ 0.25;  $\lambda$ :-0.78 $\pm$ 0.30;  $\sigma$ :-0.92 $\pm$ 0.26), and faster deterioration as measured by the CDR-sb ( $\beta \pm SE$ ,  $\gamma$ :0.60 $\pm$ 0.15;  $\lambda$ :0.53 $\pm$ 0.19;  $\sigma$ :0.62 $\pm$ 0.16), compared to individuals with normal GM network metrics (Supplementary Fig. 1).

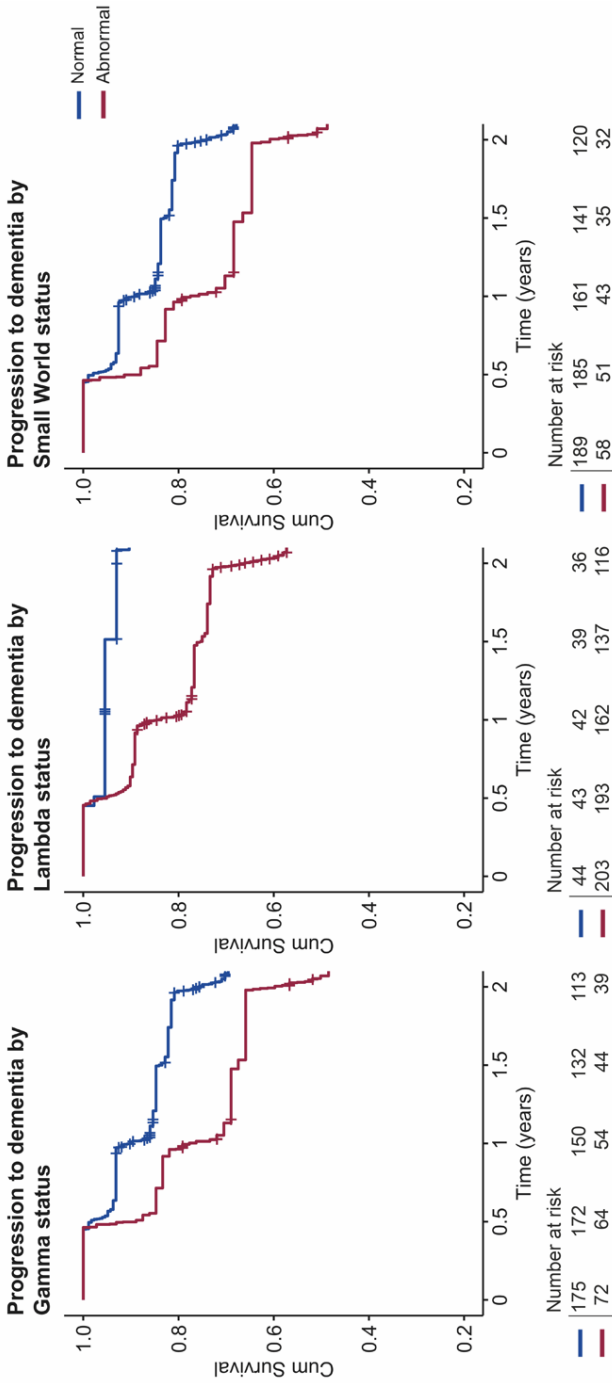


**Figure 2. Kaplan-Meier curves of progression from prodromal AD to dementia within 2 years in ADNI.** Lines represent individuals with normal (blue) and abnormal (red) grey matter network cut-offs were determined in ADC and applied in ADNI.

**Table 2. Odds ratios of abnormal biomarkers to predict clinical progression in ADNI.**

	Odds (CI)	Se	Sp	Acc	p-value
Gamma	2.43 (1.38 - 4.29)	0.42	0.77	0.65	.002*
Lambda	6.50 (2.24 - 18.88)	0.95	0.25	0.49	<.001*
Small-world	2.22 (1.21 - 4.05)	0.33	0.82	0.65	.010*
P-tau	3.12 (1.04 - 9.38)	0.95	0.13	0.41	.043*
Hippocampal vol.	2.90 (1.61 - 5.20)	0.40	0.81	0.67	<.001*

Odds ratios of logistic regression analysis for progression of prodromal AD subjects to dementia within two years. GM network cut-offs were determined in ADC and applied to ADNI. Results are shown for every abnormal biomarker with 95% confidence intervals; CI: confidence interval; Se: sensitivity; Sp: specificity; Acc: accuracy; \*  $p < 0.05$ .

**Table 3. Combining prognostic biomarkers for predicting rapid progression to dementia.**

	Odds (CI)	Se	Sp	Acc	P-value
1 abnormal biomarker	2.40 (0.52 - 11.07)	0.95	0.12	32%	.262
2 abnormal biomarkers	6.40 (1.35 - 30.37)	0.94	0.29	55%	.019*
3 abnormal biomarkers	10.89 (1.99 - 59.72)	0.88	0.61	72%	.006*

Odds ratios of logistic regression analysis in ADNI for the combination of abnormal biomarker predictors. Biomarker combination contains abnormal small-world coefficient, p-tau, and hippocampal volume; Reference category is all normal biomarkers; Se: sensitivity; Sp: specificity; Acc: accuracy; \*  $p < 0.05$ .

### *Optimal Biomarker Model to Identify Fast Progression*

Next, we assessed in ADNI whether GM network measures contained information on disease progression complementary to p-tau and hippocampal volume. For these analyses we assessed the small-world coefficient only, as it can be considered a summary measure of both  $\gamma$  and  $\lambda$ . A model including only p-tau resulted in an AUC of 0.54 (AIC=316), adding hippocampal volume improved the model fit (AUC=0.64; AIC=304,  $p < .001$ ). When adding the small-world coefficient the model did not improve significantly (AUC=0.67; AIC=303,  $p = .082$ ) for classification of rapid

decliners (Supplementary Table 4). Note that the CSF p-tau and hippocampal volume cut-offs were previously established using ADNI-specific cut-points (Shaw et al. 2009; Wisse et al. 2015), while the small-world cut-off was based on the independent ADC, which suggests that the p-tau and hippocampal volume might provide over-optimistic model performance. When the small-world cut-off was also based on ADNI, the model did improve significantly (AUC=0.70; AIC=291,  $p<.001$ ; Supplementary Table 4).

We then tested whether combining the biomarkers would improve detection of fast progressors, by labelling individuals as having no, one, two, or three abnormal predictors. A gradual increase in rapid progression risk was observed with the number of abnormal biomarkers (Table 3; Fig. 3). Showing a 6.4 times increased risk of rapid clinical decline with two abnormal prognostic biomarkers when compared to individuals with abnormal A $\beta$  only. This risk increased steeply to an odds of 10.9 for three abnormal prognostic biomarkers (Table 3; Fig. 3). Rapid progression could be most accurately identified for individuals with all three biomarkers abnormal, with an accuracy of 72% (sensitivity = 88%, specificity = 61%).



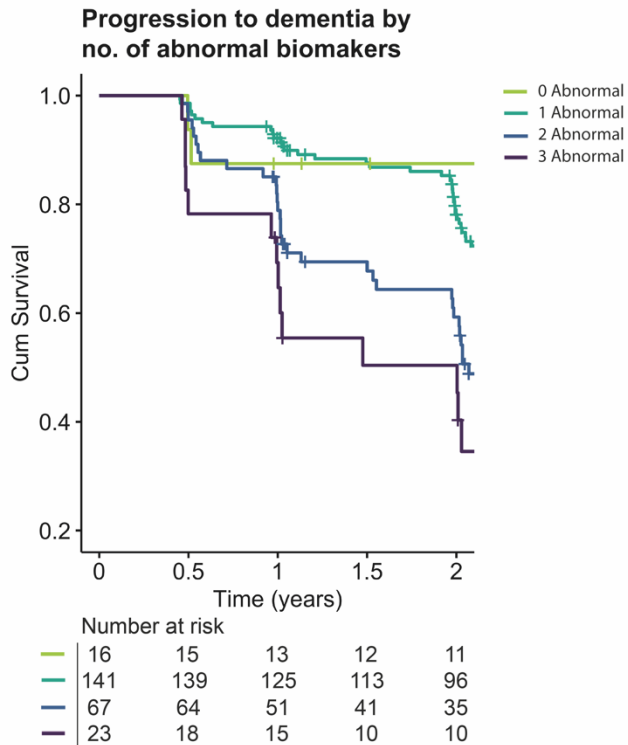


**Figure 3. Kaplan-Meier curves of progression from prodromal AD to dementia within 2 years in ADNI.** Separate lines represent individuals with zero, one, two, or three abnormal biomarkers (grey matter network small-world topology, cerebrospinal fluid phosphorylated tau, and hippocampal volume).

### *Sample Size Estimates*

We next studied if sample size estimates for clinical trials to detect a 25% slowing in rate of decline on the MMSE and CDR-sb would reduce when adding network measures. Table 4 shows for the prodromal AD cohort ( $A\beta^+$  column) without additional markers an estimated sample size of 729 (95% CI=[444 - 1364]) for the MMSE, and 486 (95% CI= [348 - 737]) for the CDR-SB. Estimated sample sizes were smallest when restricting enrolment to prodromal AD participants with abnormal p-tau, abnormal hippocampal volume, and abnormal small-world status ( $A\beta^+ \sigma^+ p\text{-tau}^+ HV^+$ , Table 4).

**Table 4. Sample size estimates for a hypothetical 2-year trial in prodromal AD subjects by biomarker abnormality**

	MMSE	CDR-sb
A $\beta$ <sup>+</sup>	729 [444 - 1364]	486 [348 - 737]
A $\beta$ <sup>+</sup> $\sigma$ <sup>+</sup>	493 [231 - 1530]	370 [214 - 833]
A $\beta$ <sup>+</sup> p-tau <sup>+</sup>	717 [430 - 1377]	445 [318 - 676]
A $\beta$ <sup>+</sup> HV <sup>+</sup>	385 [195 - 965]	310 [192 - 609]
A $\beta$ <sup>+</sup> $\sigma$ <sup>+</sup> p-tau <sup>+</sup>	467 [218 - 1471]	347 [201 - 779]
A $\beta$ <sup>+</sup> $\sigma$ <sup>+</sup> HV <sup>+</sup>	398 [151 - 2162]	263 [133 - 820]
A $\beta$ <sup>+</sup> p-tau <sup>+</sup> HV <sup>+</sup>	392 [194 - 1047]	284 [174 - 569]
A $\beta$ <sup>+</sup> $\sigma$ <sup>+</sup> p-tau <sup>+</sup> HV <sup>+</sup>	358 [138 - 1864]	262 [131 - 853]

Sample size estimates and 95% confidence intervals for a hypothetical 2-year randomised-controlled trial with two arms required to detect a 25% reduction of decline in cognitive outcome measures with a power of 80% using ADNI data. Abbreviations: A $\beta$ <sup>+</sup> = MCI individuals who have abnormal CSF amyloid  $\beta_{1-42}$  levels; A $\beta$ <sup>+</sup>  $\sigma$ <sup>+</sup> = MCI individuals who both have abnormal A $\beta$  and abnormal grey matter network small-worldness; A $\beta$ <sup>+</sup> p-tau<sup>+</sup> = MCI individuals who both have abnormal A $\beta$  and abnormal p-tau<sub>181</sub> CSF levels; A $\beta$ <sup>+</sup> HV<sup>+</sup> = MCI individuals who both have abnormal A $\beta$  and abnormal hippocampal volume; etc.; MMSE = Mini-Mental State Examination; CDR-sb = Clinical Dementia Rating scale - sum of boxes.

## Discussion

The main finding of the present study is that GM network measures can aid in identifying individuals with prodromal AD who are likely to progress to dementia within the next 2 years. Models combining small-world coefficient, p-tau and hippocampal volume showed the best ability to detect progression. These findings could increase power in AD trials by selecting those individuals with abnormal GM network characteristics at high risk for clinical progression within a time frame of 24 months.

Most studies so far that investigated prognostic markers in individuals with MCI, studied also subjects with normal A $\beta$  values (Vos et al. 2015; ben Bouallègue et al. 2017; Hansson et al. 2018; Blennow et al. 2019;

van Maurik et al. 2019; Cicognola et al. 2021; Cullen et al. 2021; Palmqvist et al. 2021). Such an approach makes it difficult to distinguish between the effects caused by A $\beta$ , tau, and neuronal injury on cognition, as abnormalities in tau and neurodegeneration are closely related to A $\beta$  pathology (Sato et al. 2018; Barthélemy et al. 2020; Milà-Alomà et al. 2020). Moreover, it can also inflate accuracy statistics, because abnormal A $\beta$  has a strong predictive effect of decline (Vos et al. 2013; Lim et al. 2014). Predicting progression within A $\beta$  positive individuals is, however, more difficult and the few longitudinal studies that investigated prognostic markers within prodromal AD patients have demonstrated a more modest predictive value over A $\beta$  (van Rossum, Vos, et al. 2012; Jang et al. 2019). This is also reflected by the relatively modest AUC values in the present study.

Moreover, in contrast to previous studies showing that a more disorganised GM network is associated with cognitive decline (Dicks et al. 2018b; Tijms, ten Kate, et al. 2018; Pelkmans et al. 2021), our findings indicate that an individual's GM network measure can be classified as normal or abnormal which is relevant for clinical application and inclusion of subjects in therapeutic trials to select those individuals who will show fast progression over a relatively short time frame (Cummings et al. 2021).

GM network measures start to change early in the disease process: previous studies indicate that the presence of A $\beta$  significantly alters GM networks, and that these alterations may precede tau and neurodegeneration (Oh et al. 2011; Tijms et al. 2016; ten Kate et al. 2018; Voevodskaya et al. 2018), and can predict future hippocampal atrophy (Dicks et al. 2020). It could be hypothesized that the AD neuropathological changes contribute to the observed brain network disruptions, and represent a close biological substrate for disease progression and cognitive decline in AD.

In the current study, we show that individuals with a more random network, as reflected by an abnormal small-world topology, were more than twice as likely to progress to dementia compared to those with normal values. Still, single biomarkers showed modest accuracy to predict fast progression (Pascoal et al. 2017; Blennow et al. 2019). In the present study, we found that the highest predictive accuracy was obtained when the small-world coefficient was combined with both p-tau and hippocampal volume. This resulted in an OR of greater than 10 (sensitivity 88%, specificity 61%, accuracy 72%) for progression to dementia within 2 years for individuals with all three biomarkers abnormal and a 46 - 60% reduction in required sample size to detect at 25% treatment effect in a hypothetical 2-year trial compared to abnormal amyloid alone. This is in line with previous studies (Lorenzi et al. 2010; van Rossum et al. 2010; Bertens et al. 2017) that showed reduced sample size estimates when tau and/or neuronal injury markers are abnormal. We show that GM network measures may further improve predictive models. Together, these studies and our results provide further support for the idea that combining multiple markers may facilitate clinical trials by increasing chances to detect effects on clinical outcome measures.

Strengths of this study include that GM network cut-offs were determined in one cohort and then showed to be generalisable to an independent cohort. Secondly, our approach allows for patient-level application. However, a follow up study is likely needed to further investigate the prognostic value of the determined cut-offs in a larger sample. Another important next step would be to develop more user-friendly software and investigate whether GM network cut-points can be applied to challenges in a clinical setting, such as aiding in short-term care planning for dementia patients.

## **Conclusion**

In conclusion, we showed that GM network measures can be applied to identify individuals with prodromal AD at risk for fast progression. Moreover, when combined with p-tau and hippocampal volume this resulted in the highest prognostic accuracy, which could contribute to detecting treatment effects in AD clinical trials.

## **Funding**

Research at the Alzheimer Center Amsterdam is part of the neurodegeneration research programme of Amsterdam Neuroscience. The Alzheimer Center Amsterdam is supported by Stichting Alzheimer Nederland and Stichting VUmc Fonds. ED is supported by the Race Against Dementia charity ([www.raceagainstdementia.com](http://www.raceagainstdementia.com)). FB is supported by the National Institute for Health Research biomedical research centre at University College London Hospitals.

Data collection and sharing for this project was funded by the Alzheimer's Disease Neuroimaging Initiative (National Institutes of Health Grant U01 AG024904) and DOD ADNI (Department of Defense award number W81XWH-12-2-0012). ADNI is funded by the National Institute on Aging, the National Institute of Biomedical Imaging and Bioengineering, and through generous contributions from the following: AbbVie, Alzheimer's Association; Alzheimer's Drug Discovery Foundation; Araclon Biotech; BioClinica, Inc.; Biogen; Bristol-Myers Squibb Company; CereSpir, Inc.; Cogstate; Eisai Inc.; Elan Pharmaceuticals, Inc.; Eli Lilly and Company; EuroImmun; F. Hoffmann-La Roche Ltd and its affiliated company Genentech, Inc.; Fujirebio; GE Healthcare; IXICO Ltd.; Janssen Alzheimer Immunotherapy Research & Development, LLC.; Johnson & Johnson Pharmaceutical Research & Development LLC.; Lumosity; Lundbeck; Merck

& Co., Inc.; Meso Scale Diagnostics, LLC.; NeuroRx Research; Neurotrack Technologies; Novartis Pharmaceuticals Corporation; Pfizer Inc.; Piramal Imaging; Servier; Takeda Pharmaceutical Company; and Transition Therapeutics. The Canadian Institutes of Health Research is providing funds to support ADNI clinical sites in Canada. Private sector contributions are facilitated by the Foundation for the National Institutes of Health ([www.fnih.org](http://www.fnih.org)). The grantee organization is the Northern California Institute for Research and Education, and the study is coordinated by the Alzheimer's Therapeutic Research Institute at the University of Southern California. ADNI data are disseminated by the Laboratory for Neuro Imaging at the University of Southern California.

### **Competing interests**

W. Pelkmans, E.M. Vromen, and E. Dicks report no disclosures. P. Scheltens reports research support from Alzheimer Nederland, Dioraphte, Stichting VUmc Fonds, and Stichting Alzheimer & Neuropsychiatrie; is a consultant for EIP Pharma, Vivoryon, Toyama Fuji Film, AC Immune, Axon Neuroscience, GemVax, Medavante, Novartis Cardiology, and Green Valley; is co-editor-in-chief of Alzheimer's Research & Therapy; and is a part-time managing partner of the Life Science Partners Dementia Fund. C.E. Teunissen reports research support from European Commission (Marie Curie International Training Network, JPND), Health Holland, the Netherlands Organisation for Health Research and Development (ZonMw), The Weston Brain Institute, and Alzheimer Nederland; and has the following industrial collaborations: collaboration contract with ADx Neurosciences, contract research or received grants from Probiodrug, AC Immune, Biogen-Esai, CogRx, Toyama, Janssen Prevention Center, Boehringer, AxonNeurosciences, Fujirebio, EIP farma, PeopleBio, and Roche, and is on the advisory board of Roche. F.

Barkhof received payment and honoraria from Bayer Genzyme, Biogen-Idec, TEVA, Merck, Novartis, Roche, IXICO Ltd, GeNeuro, and Apitope Ltd for consulting; payment from the IXICOLtd, and MedScape for educational presentations; research support via grants from European Federation of Pharmaceutical Industries and Associations (EFPIA) Innovative Medicines Initiative Joint Undertaking (AMYPAD consortium), European Progression Of Neurological Diseases (EuroPOND H2020), UK MS Society, Dutch MS Society, PICTURE Innovative Medical Devices Initiative - Dutch Research Council (IMDI-NWO), National Institute for Health Research at University College London Hospitals Biomedical Research Centre, and The European Committee for Treatment and Research in Multiple Sclerosis - Magnetic Resonance Imaging in MS (ECTRIMS- MAGNIMS). W.M. van der Flier reports research support from Netherlands Organisation for Health Research and Development (ZonMw), Dutch Research Council (NWO), EU Seventh framework programme (FP7), EU Joint Programme Neurodegenerative Disease Research (JPND), Alzheimer Nederland, CardioVascular Onderzoek Nederland, Health~Holland, Topsector Life Sciences & Health, Stichting Dioraphte, Gieskes-Strijbis Fonds, Stichting Equilibrio, Pasman Stichting, Fujifilm, Boehringer Ingelheim, Life-MI, AVID, Janssen Stellar, Combinostics. W.M. van der Flier is chair of Pasman Stichting. W.M. van der Flier has performed contract research for Biogen and received speaker fees from Biogen and Roche. B.M. Tijms received grant support from ZonMw Memorabel (grant number 73305056).

## References

- Albert MS, DeKosky ST, Dickson D, Dubois B, Feldman HH, Fox NC, Gamst A, Holtzman DM, Jagust WJ, Petersen RC, Snyder PJ, Carrillo MC, Thies B, Phelps CH. 2011. The diagnosis of mild cognitive impairment due to Alzheimer's disease: Recommendations from the National Institute on Aging-Alzheimer's Association workgroups on diagnostic guidelines for Alzheimer's disease. *Alzheimer's & Dementia*. 7:270–279.
- Barthélemy NR, Li Y, Joseph-Mathurin N, Gordon BA, Hassenstab J, Benzinger TLS, Buckles V, Fagan AM, Perrin RJ, Goate AM, Morris JC, Karch CM, Xiong C, Allegrì R, Mendez PC, Berman SB, Ikeuchi T, Mori H, Shimada H, Shoji M, Suzuki K, Noble J, Farlow M, Chhatwal J, Graff-Radford NR, Salloway S, Schofield PR, Masters CL, Martins RN, O'Connor A, Fox NC, Levin J, Jucker M, Gabelle A, Lehmann S, Sato C, Bateman RJ, McDade E. 2020. A soluble phosphorylated tau signature links tau, amyloid and the evolution of stages of dominantly inherited Alzheimer's disease. *Nature Medicine*. 26:398–407.
- ben Bouallègue F, Mariano-Goulart D, Payoux P. 2017. Comparison of CSF markers and semi-quantitative amyloid PET in Alzheimer's disease diagnosis and in cognitive impairment prognosis using the ADNI-2 database. *Alzheimer's Research & Therapy*. 9:32.
- Bertens D, Tijms BM, Vermunt L, Prins ND, Scheltens P, Visser PJ. 2017. The effect of diagnostic criteria on outcome measures in preclinical and prodromal Alzheimer's disease: Implications for trial design. *Alzheimer's and Dementia: Translational Research and Clinical Interventions*. 3:513–523.
- Blennow K, Shaw LM, Stomrud E, Mattsson N, Toledo JB, Buck K, Wahl S, Eichenlaub U, Lifke V, Simon M, Trojanowski JQ, Hansson O. 2019. Predicting clinical decline and conversion to Alzheimer's disease or dementia using novel Elecsys A $\beta$ (1–42), pTau and tTau CSF immunoassays. *Scientific Reports*. 9:19024.
- Bullmore E, Sporns O. 2009. Complex brain networks : graph theoretical analysis of structural and functional systems. *Nature Reviews Neurology*. 10:186–198.
- Cicognola C, Janelidze S, Hertzog J, Zetterberg H, Blennow K, Mattsson-Carlgrén N, Hansson O. 2021. Plasma glial fibrillary acidic protein detects Alzheimer pathology and predicts future conversion to Alzheimer dementia in patients with mild cognitive impairment. *Alzheimer's Research & Therapy*. 13:68.
- Cullen NC, Leuzy A, Palmqvist S, Janelidze S, Stomrud E, Pesini P, Sarasa L, Allué JA, Proctor NK, Zetterberg H, Dage JL, Blennow K, Mattsson-Carlgrén N, Hansson O. 2021. Individualized prognosis of cognitive decline and dementia in mild cognitive impairment based on plasma biomarker combinations. *Nature Aging*. 1:114–123.
- Cummings J, Feldman HH, Scheltens P. 2019. The “rights” of precision drug development for Alzheimer's disease. *Alzheimer's Research & Therapy*. 11:76.



- Cummings J, Lee G, Zhong K, Fonseca J, Taghva K. 2021. Alzheimer's disease drug development pipeline: 2021. *Alzheimer's & Dementia: Translational Research & Clinical Interventions*. 7:1–24.
- Dicks E, Tijms BM, ten Kate M, Gouw AA, Benedictus MR, Teunissen CE, Barkhof F, Scheltens P, van der Flier WM. 2018a. Gray matter network measures are associated with cognitive decline in mild cognitive impairment. *Neurobiology of Aging*. 61:198–206.
- Dicks E, Tijms BM, ten Kate M, Gouw AA, Benedictus MR, Teunissen CE, Barkhof F, Scheltens P, van der Flier WM. 2018b. Gray matter network measures are associated with cognitive decline in mild cognitive impairment. *Neurobiology of Aging*. 61:198–206.
- Dicks E, van der Flier WM, Scheltens P, Barkhof F, Tijms BM. 2020. Single-subject gray matter networks predict future cortical atrophy in preclinical Alzheimer's disease. *Neurobiology of Aging*. 94:71–80.
- Engelborghs S, Niemantsverdriet E, Struyfs H, Blennow K, Brouns R, Comabella M, Dujmovic I, Flier W, Frölich L, Galimberti D, Gnanapavan S, Hemmer B, Hoff E, Hort J, Iacobaeus E, Ingelsson M, Jan de Jong F, Jonsson M, Khalil M, Kuhle J, Lleó A, Mendonça A, Molinuevo JL, Nagels G, Paquet C, Parnetti L, Roks G, Rosa-Neto P, Scheltens P, Skårsgard C, Stomrud E, Tumani H, Visser PJ, Wallin A, Winblad B, Zetterberg H, Duits F, Teunissen CE. 2017. Consensus guidelines for lumbar puncture in patients with neurological diseases. *Alzheimer's & Dementia: Diagnosis, Assessment & Disease Monitoring*. 8:111–126.
- Folstein MF, Robins LN, Helzer JE. 1983. The Mini-Mental State Examination. *Arch Gen Psychiatry*. 40:812.
- Hansson O, Seibyl J, Stomrud E, Zetterberg H, Trojanowski JQ, Bittner T, Lifke V, Corradini V, Eichenlaub U, Batrla R, Buck K, Zink K, Rabe C, Blennow K, Shaw LM. 2018. CSF biomarkers of Alzheimer's disease concord with amyloid- $\beta$  PET and predict clinical progression: A study of fully automated immunoassays in BioFINDER and ADNI cohorts. *Alzheimer's & Dementia*. 14:1470–1481.
- Heagerty PJ, Lumley T, Pepe MS. 2000. Time-Dependent ROC Curves for Censored Survival Data and a Diagnostic Marker. *Biometrics*. 56:337–344.
- Jack CR, Bennett DA, Blennow K, Carrillo MC, Dunn B, Haeberlein SB, Holtzman DM, Jagust W, Jessen F, Karlawish J, Liu E, Molinuevo JL, Montine T, Phelps C, Rankin KP, Rowe CC, Scheltens P, Siemers E, Snyder HM, Sperling R, Elliott C, Masliah E, Ryan L, Silverberg N. 2018. NIA-AA Research Framework: Toward a biological definition of Alzheimer's disease. *Alzheimer's and Dementia*. 14:535–562.
- Jack CR, Bernstein MA, Fox NC, Thompson P, Alexander G, Harvey D, Borowski B, Britson PJ, L Whitwell J, Ward C, Dale AM, Felmlee JP, Gunter JL, Hill DLG, Killiany R, Schuff N, Fox-Bosetti S, Lin C, Studholme C, DeCarli CS, Gunnar Krueger, Ward HA, Metzger GJ, Scott KT, Malloy R, Blezek D, Levy J, Debbins JP, Fleisher AS, Albert M, Green R, Bartzokis G, Glover G, Mugler J, Weiner MW. 2008. The Alzheimer's disease

- neuroimaging initiative (ADNI): MRI methods. *Journal of Magnetic Resonance Imaging*. 27:685–691.
- Jang H, Park J, Woo S, Kim S, Kim HJ, Na DL, Lockhart SN, Kim Y, Kim KW, Cho SH, Kim SJ, Seong J-K, Seo SW. 2019. Prediction of fast decline in amyloid positive mild cognitive impairment patients using multimodal biomarkers. *NeuroImage: Clinical*. 24:101941.
- Jutten RJ, Sikkes SAM, van der Flier WM, Scheltens P, Visser PJ, Tijms BM. 2021. Finding Treatment Effects in Alzheimer Trials in the Face of Disease Progression Heterogeneity. *Neurology*. 96:e2673–e2684.
- Lim YY, Maruff P, Pietrzak RH, Ellis KA, Darby D, Ames D, Harrington K, Martins RN, Masters CL, Szoeker C, Savage G, Villemagne VL, Rowe CC. 2014. A $\beta$  and cognitive change: Examining the preclinical and prodromal stages of Alzheimer's disease. *Alzheimer's & Dementia*. 10:743-751.e1.
- Lorenzi M, Donohue M, Paternicò D, Scarpazza C, Ostrowitzki S, Blin O, Irving E, Frisoni GB. 2010. Enrichment through biomarkers in clinical trials of Alzheimer's drugs in patients with mild cognitive impairment. *Neurobiology of Aging*. 31:1443-1451.e1.
- Maslov S, Sneppen K. 2002. Specificity and Stability in Topology of Protein Networks. *Science* (1979). 296:910–913.
- McKhann G, Drachman D, Folstein M, Katzman R, Price D, Stadlan EM. 1984. Clinical diagnosis of Alzheimer's disease: Report of the NINCDS-ADRDA Work Group\* under the auspices of Department of Health and Human Services Task Force on Alzheimer's Disease. *Neurology*. 34:939–939.
- McKhann GM, Knopman DS, Chertkow H, Hyman BT, Jack CR, Kawas CH, Klunk WE, Koroshetz WJ, Manly JJ, Mayeux R, Mohs RC, Morris JC, Rossor MN, Scheltens P, Carrillo MC, Thies B, Weintraub S, Phelps CH. 2011. The diagnosis of dementia due to Alzheimer's disease: Recommendations from the National Institute on Aging-Alzheimer's Association workgroups on diagnostic guidelines for Alzheimer's disease. *Alzheimer's & Dementia*. 7:263–269.
- Milà-Alomà M, Salvadó G, Gispert JD, Vilor-Tejedor N, Grau-Rivera O, Sala-Vila A, Sánchez-Benavides G, Arenaza-Urquijo EM, Crous-Bou M, González-de-Echávarri JM, Minguillon C, Fauria K, Simon M, Kollmorgen G, Zetterberg H, Blennow K, Suárez-Calvet M, Molinuevo JL. 2020. Amyloid beta, tau, synaptic, neurodegeneration, and glial biomarkers in the preclinical stage of the Alzheimer's continuum. *Alzheimer's & Dementia*. 16:1358–1371.
- Mulder C, Verwey NA, van der Flier WM, Bouwman FH, Kok A, van Elk EJ, Scheltens P, Blankenstein MA. 2010. Amyloid- $\beta$ (1-42), total tau, and phosphorylated tau as cerebrospinal fluid biomarkers for the diagnosis of Alzheimer disease. *Clinical Chemistry*. 56:248–253.
- Noble WS. 2009. How does multiple testing correction work? *Nature Biotechnology*. 27:1135–1137.

- Oh H, Mormino EC, Madison C, Hayenga A, Smiljic A, Jagust WJ. 2011.  $\beta$ -Amyloid affects frontal and posterior brain networks in normal aging. *Neuroimage*. 54:1887–1895.
- Palmqvist S, Tideman P, Cullen N, Zetterberg H, Blennow K, Dage JL, Stomrud E, Janelidze S, Mattsson-Carlgren N, Hansson O. 2021. Prediction of future Alzheimer's disease dementia using plasma phospho-tau combined with other accessible measures. *Nature Medicine*. 27:1034–1042.
- Pascoal TA, Mathotaarachchi S, Shin M, Benedet AL, Mohades S, Wang S, Beaudry T, Kang MS, Soucy J-P, Labbe A, Gauthier S, Rosa-Neto P. 2017. Synergistic interaction between amyloid and tau predicts the progression to dementia. *Alzheimer's & Dementia*. 13:644–653.
- Pelkmans W, Ossenkoppele R, Dicks E, Strandberg O, Barkhof F, Tijms BM, Pereira JB, Hansson O. 2021. Tau-related grey matter network breakdown across the Alzheimer's disease continuum. *Alzheimer's Research & Therapy*. 13:138.
- Pereira JB, Mijalkov M, Kakaie E, Mecocci P, Vellas B, Tsolaki M, Kłoszewska I, Soininen H, Spenger C, Lovestone S, Simmons A, Wahlund LO, Volpe G, Westman E. 2016. Disrupted Network Topology in Patients with Stable and Progressive Mild Cognitive Impairment and Alzheimer's Disease. *Cerebral Cortex*. 26:3476–3493.
- Petersen RC, Smith GE, Waring SC, Ivnik RJ, Tangalos EG, Kokmen E. 1999. Mild cognitive impairment: clinical characterization and outcome. *Arch Neurol*. 56:303–308.
- Sato C, Barthélemy NR, Mawuenyega KG, Patterson BW, Gordon BA, Jockel-Balsarotti J, Sullivan M, Crisp MJ, Kasten T, Kirmess KM, Kanaan NM, Yarasheski KE, Baker-Nigh A, Benzinger TLS, Miller TM, Karch CM, Bateman RJ. 2018. Tau Kinetics in Neurons and the Human Central Nervous System. *Neuron*. 97:1284–1298.e7.
- Scheltens P, de Strooper B, Kivipelto M, Holstege H, Chételat G, Teunissen CE, Cummings J, van der Flier WM. 2021. Alzheimer's disease. *The Lancet*. 397:1577–1590.
- Selkoe DJ. 2011. Resolving controversies on the path to Alzheimer's therapeutics. *Nature Medicine*. 17:1060–1065.
- Shaw LM, Vanderstichele H, Knapik-Czajka M, Clark CM, Aisen PS, Petersen RC, Blennow K, Soares H, Simon A, Lewczuk P, Dean R, Siemers E, Potter W, Lee VMY, Trojanowski JQ. 2009. Cerebrospinal fluid biomarker signature in Alzheimer's disease neuroimaging initiative subjects. *Annals of Neurology*. 65:403–413.
- ten Kate M, Visser PJ, Bakardjian H, Barkhof F, Sikkens SAM, van der Flier WM, Scheltens P, Hampel H, Habert M-O, Dubois B, Tijms BM. 2018. Gray Matter Network Disruptions and Regional Amyloid Beta in Cognitively Normal Adults. *Frontiers in Aging Neuroscience*. 10:1–11.
- Tijms BM, ten Kate M, Wink AM, Visser PJ, Ecury M, Clerigue M, Estanga A, Garcia Sebastian M, Izagirre A, Villanua J, Martinez Lage P, van der Flier WM, Scheltens P, Sanz Arigita E, Barkhof F. 2016. Gray matter network disruptions and amyloid beta in cognitively normal adults. *Neurobiology of Aging*. 37:154–160.

- Tijms BM, Seris P, Willshaw DJ, Lawrie SM. 2012. Similarity-based extraction of individual networks from gray matter MRI scans. *Cerebral Cortex*. 22:1530–1541.
- Tijms BM, ten Kate M, Gouw AA, Borta A, Verfaillie S, Teunissen CE, Scheltens P, Barkhof F, van der Flier WM. 2018. Gray matter networks and clinical progression in subjects with predementia Alzheimer's disease. *Neurobiology of Aging*. 61:75–81.
- Tijms BM, Willemse EAJ, Zwan MD, Mulder SD, Visser PJ, van Berckel BNM, van der Flier WM, Scheltens P, Teunissen CE. 2018. Unbiased approach to counteract upward drift in cerebrospinal fluid amyloid- $\beta$  1–42 analysis results. *Clinical Chemistry*. 64:576–585.
- Tzourio-Mazoyer N, Landeau B, Papathanassiou D, Crivello F, Etard O, Delcroix N, Mazoyer B, Joliot M. 2002. Automated anatomical labeling of activations in SPM using a macroscopic anatomical parcellation of the MNI MRI single-subject brain. *Neuroimage*. 15:273–289.
- Van Der Flier WM, Pijnenburg YAL, Prins N, Lemstra AW, Bouwman FH, Teunissen CE, Van Berckel BNM, Stam CJ, Barkhof F, Visser PJ, Van Egmond E, Scheltens P. 2014. Optimizing patient care and research: The Amsterdam dementia cohort. *Journal of Alzheimer's Disease*. 41:313–327.
- Van Der Flier WM, Scheltens P. 2018. Amsterdam dementia cohort: Performing research to optimize care. *Journal of Alzheimer's Disease*. 62:1091–1111.
- van Maurik IS, Vos SJ, Bos I, Bouwman FH, Teunissen CE, Scheltens P, Barkhof F, Frolich L, Kornhuber J, Wiltfang J, Maier W, Peters O, R  ther E, Nobili F, Frisoni GB, Spuru L, Freund-Levi Y, Wallin AK, Hampel H, Soinen H, Tsolaki M, Verhey F, Kłoszewska I, Mecocci P, Vellas B, Lovestone S, Galluzzi S, Herukka S-K, Santana I, Baldeiras I, de Mendonça A, Silva D, Chetelat G, Egret S, Palmqvist S, Hansson O, Visser PJ, Barkhof J, van der Flier WM. 2019. Biomarker-based prognosis for people with mild cognitive impairment (ABIDE): a modelling study. *The Lancet Neurology*. 18:1034–1044.
- van Rossum IA, Visser PJ, Knol DL, van der Flier WM, Teunissen CE, Barkhof F, Blankenstein MA, Scheltens P. 2012. Injury Markers but not Amyloid Markers are Associated with Rapid Progression from Mild Cognitive Impairment to Dementia in Alzheimer's Disease. *Journal of Alzheimer's Disease*. 29:319–327.
- van Rossum IA, Vos S, Handels R, Visser PJ. 2010. Biomarkers as Predictors for Conversion from Mild Cognitive Impairment to Alzheimer-Type Dementia: Implications for Trial Design. *Journal of Alzheimer's Disease*. 20:881–891.
- van Rossum IA, Vos SJB, Burns L, Knol DL, Scheltens P, Soinen H, Wahlund L-O, Hampel H, Tsolaki M, Minthon L, L'Italiani G, van der Flier WM, Teunissen CE, Blennow K, Barkhof F, Rueckert D, Wolz R, Verhey F, Visser PJ. 2012. Injury markers predict time to dementia in subjects with MCI and amyloid pathology. *Neurology*. 79:1809–1816.
- Verfaillie SCJ, Slot RER, Dicks E, Prins ND, Overbeek JM, Teunissen CE, Scheltens P, Barkhof F, van der Flier WM, Tijms BM. 2018. A more randomly organized grey matter network is associated with deteriorating language and global cognition in

- individuals with subjective cognitive decline. *Human Brain Mapping*. 39:3143–3151.
- Voevodskaya O, Pereira JB, Volpe G, Lindberg O, Stomrud E, van Westen D, Westman E, Hansson O. 2018. Altered structural network organization in cognitively normal individuals with amyloid pathology. *Neurobiology of Aging*. 64:15–24.
- Vos SJ, Xiong C, Visser PJ, Jasielec MS, Hassenstab J, Grant EA, Cairns NJ, Morris JC, Holtzman DM, Fagan AM. 2013. Preclinical Alzheimer's disease and its outcome: a longitudinal cohort study. *The Lancet Neurology*. 12:957–965.
- Vos SJB, Verhey F, Frölich L, Kornhuber J, Wiltfang J, Maier W, Peters O, Rütger E, Nobili F, Morbelli S, Frisoni GB, Drzezga A, Didic M, van Berckel BNM, Simmons A, Soininen H, Kloszewska J, Mecocci P, Tsolaki M, Vellas B, Lovestone S, Muscio C, Herukka S-K, Salmon E, Bastin C, Wallin A, Nordlund A, de Mendonça A, Silva D, Santana I, Lemos R, Engelborghs S, van der Mussele S, Freund-Levi Y, Wallin ÅK, Hampel H, van der Flier W, Scheltens P, Visser PJ. 2015. Prevalence and prognosis of Alzheimer's disease at the mild cognitive impairment stage. *Brain*. 138:1327–1338.
- Williams MM, Storandt M, Roe CM, Morris JC. 2013. Progression of Alzheimer's disease as measured by Clinical Dementia Rating Sum of Boxes scores. *Alzheimer's & Dementia*. 9:1–13.
- Wisse LEM, Butala N, Das SR, Davatzikos C, Dickerson BC, Vaishnavi SN, Yushkevich PA, Wolk DA. 2015. Suspected non-AD pathology in mild cognitive impairment. *Neurobiology of Aging*. 36:3152–3162.

## Supplementary material

**Supplementary Table 1**  
**Overview of current phase 2 and phase 3 disease modifying trials in prodromal AD**

	<i>&lt;1 year</i>	<i>1 year</i>	<i>1.5 years</i>	<i>2 years</i>	<i>&gt;2 years</i>
AMX0035	GV-971	ABvac40	AL002	JNJ-63733657	
BPN14770	Benfotiamine	ACI-35	Blarcamesine		
L-Serine	Curcumin	Aducanumab	Gantenerumab		
Lamivudine	Dasatinib + Quercetin	AGB101	Metformin		
Neflamapimod	Deferiprone	ALZ-801	Tilavonemab		
Nicotinamide	Levetiracetam	Azeliragon	Zagotenemab		
Pepinemab	Liraglutide	Donanemab			
Posiphen	Montelukast	Edonepic (T-817)			
PU-AD	Rapamycin	Gosuranemab (BIIB092)			
Tacrolimus		IVIg			
TEP		Lecanemab			
		Lenalidomide			
		Omega 3 PUFA			
		PQ912			
		Semorinemab			
		Simufilam			
		Solanezumab			
		Valacyclovir			

Source: <https://www.clinicaltrials.gov>

## **Supplementary information 2. MRI acquisition parameters in ADC.**

Structural T1-weighted images were acquired as part of routine patient care from nine different scanners. The following parameters were used: 1.5T Siemens Avanto: Magnetization prepared rapid acquisition gradient echo (MPRAGE), coronal plane, repetition time (TR) 2700 ms, echo time (TE) 5.2 ms, inversion time (TI) 950 ms, flip angle (FA) 8°, voxel size 1×1×1.5 mm<sup>3</sup>; 3T GE Discovery MR750: FSPGR, sagittal plane, TR 7.8 ms, TE 3ms, FA 12°, voxel size 1 mm<sup>3</sup>; 1T Siemens Magnetom Impact: MPRAGE, coronal plane, TR 15 ms, TE 7 ms, TI 300 ms, FA 15°, voxel size 1×1×1.5 mm<sup>3</sup>; 3T Philips Ingenuity PET/MR system: sagittal turbo field echo (TFE), sagittal plane, TR 7 ms, TE 3 ms, FA 12°, voxel size 1×1×1 mm<sup>3</sup>; 1.5T GE SignaHDxt: sagittal fast spoiled gradient echo (FSPGR), sagittal plane, TR 12.4 ms, TE 5.17 ms, TI 450 ms, FA 12°, voxel size 0.98×0.98×1.5 mm<sup>3</sup>; 3T GE SignaHDxt: FSPGR, sagittal plane, TR 708 ms, TE 7 ms, FA 12°, voxel size 0.98×0.98×1 mm<sup>3</sup>; 1.5T Siemens Sonata: MPRAGE, coronal plane, TR 2700 ms, TE 3.97 ms, TI 950 ms, FA 8°, voxel size 1×1×1.5 mm<sup>3</sup>; Toshiba Titan 3T: sagittal fast field echo (FFE) sequence (TR = 9, TE = 3, TI = 800, FA = 7°, 1.00 x 1.00 x 1.00 mm voxels); 1.5T Siemens Vision: MPRAGE, coronal plane, TR 15 ms, TE 7 ms, FA 8°, voxel size 0.98×0.98×1.5 mm<sup>3</sup>.

**Supplementary Table 3. Odds ratios of abnormal biomarkers to predict clinical progression in ADNI**

	<b>Odds (CI)</b>	<b>p-value</b>
Gamma	3.35 (1.65 - 6.80)	.001*
Lambda	7.05 (2.27 - 21.92)	.001*
Small-world coefficient	2.99 (1.43 - 6.25)	.004*
P-tau	3.86 (1.06 - 14.07)	.040*
Hippocampal volume	2.46 (1.22 - 4.95)	.012*

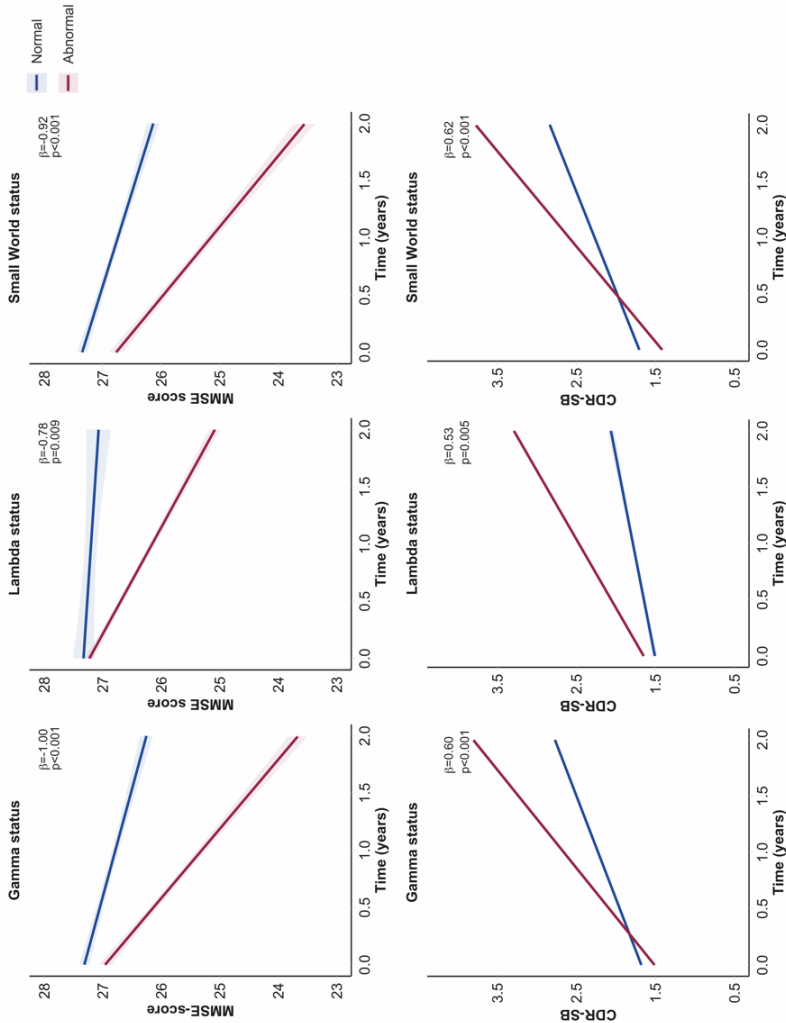
Odds ratios of logistic regression analysis for progression of prodromal AD subjects to dementia within two years. GM network cut-offs were determined in ADC and applied to ADNI. Results are shown for every abnormal biomarker with 95% confidence intervals; Model is adjusted for age, sex, education, and MRI scanner; CI: confidence interval; \*  $p < 0.05$ .

**Supplementary Table 4. Model fit comparisons for predicting rapid progression to dementia.**

	<b>AUC (CI)</b>	<b>AIC</b>	<b>p-value</b>
Model 1: p-tau	0.54 (0.51 - 0.58)	315.6	
Model 2: p-tau + HV	0.64 (0.57 - 0.70)	304.0	<.001*
Model 3a: p-tau + HV + small-world	0.67 (0.60 - 0.73)	303.0	.082
Model 3b: p-tau + HV + small-world	0.70 (0.64 - 0.77)	291.4	<.001*

Output of logistic regression analyses in ADNI. The AIC represents the model fit. The *P*-value for model difference compares a model with a less complex model (that is model 2 vs model 1, and model 3 vs 2). Model3a small-world abnormality cutpoint determined in ADC; Model3b small-world abnormality cutpoint determined in ADNI. Abbreviations: AUC = Area under Curve; CI = Confidence Interval; AIC = Akaike's Information Criterion; HV = Hippocampal Volume.





**Supplementary Figure 1.** Cognitive performance over time by grey matter network status. Linear mixed model analysis with a random intercept and slope. Standardised beta estimates are adjusted for age, sex, education, and scanner type.



# CHAPTER 7

## **Summary & General discussion**



## SUMMARY & GENERAL DISCUSSION

In the following sections, the key findings of this thesis are summarised, and their implications, methodological considerations and future directions are discussed in the light of the current literature.

### *Preclinical pathological changes associated with future cognitive decline*

A $\beta$  positivity in cognitively normal (CN) older individuals has been related to an increased risk of future cognitive decline (Donohue et al. 2017; van der Kall et al. 2020). Moreover, the prevalence of amyloid abnormality in cognitive normal individuals increases with age (from 14% at age 50 to 47% at age 90; Jansen et al. 2022), with an increase in dementia prevalence occurring approximately 20 years later. However, the relationship between amyloid abnormality and cognitive decline in CN oldest-to-old (90+) has been debated (Richard et al. 2012; Herrup 2015; Morris et al. 2018). Mostly by cross-sectional studies that have demonstrated extensive AD pathology at autopsy in CN individuals (Haroutunian et al. 2008; Savva et al. 2009; Corrada et al. 2012), however in order to better understand this relationship repeated cognitive measures are necessary.

In **chapter 2** we observed that CN individuals from the EMIF-AD 90+ study with abnormal A $\beta$  pathology on PET, showed regional cortical thinning and a faster decline on memory and processing speed performance over time. This is in line with the findings of other nonagenarian and centenarian studies (Zhao et al. 2018), indicating that A $\beta$  pathology is not benign and is still associated with cognitive decline, even in individuals who had normal cognition at a very advanced age. Furthermore, we found that neuronal loss in the parahippocampal cortex mediated the effects of A $\beta$  pathology on memory and language decline. This is consistent with previously proposed

independent and synergistic effects of A $\beta$  and neurodegeneration on cognitive impairment in younger populations and in accordance with the amyloid cascade hypothesis (Chételat et al. 2011; Wirth et al. 2013; Bilgel et al. 2018; Svenningsson et al. 2019).

In addition, we observed in CN 90+ individuals that atrophy, predominantly in the medial temporal lobe (MTL), was associated with cognitive decline, regardless of the presence of A $\beta$  pathology. This observation may be explained by the presence of other pathologies besides amyloid plaques. As TDP-43,  $\alpha$ -synuclein, cerebrovascular burden, and hippocampal sclerosis are common in the oldest-old and important factors contributing to non-amyloid neuronal damage and cognitive decline (Yu et al. 2020; Boyle et al. 2021; Kawas et al. 2021). This hypothesis, however, should be further verified by future autopsy studies in this cohort.

The effect of neurodegenerative markers on cognitive decline was examined in greater detail in **chapter 3** by comparing imaging, CSF, and blood-based 'N' biomarkers. Using data from the subjective cognitive impairment cohort (SCIENCE), we found that the N markers CSF t-tau, visual read of medial temporal lobe atrophy (MTA), hippocampal volume (HV), serum neurofilament light (NfL), and serum glial fibrillary acidic protein (GFAP) only moderately correlated with each other. According to expert groups (Jack et al. 2018), different N measures are considered interchangeable. The findings of our study, however, indicate that they cannot be used interchangeably since each marker measures a different aspect of neurodegeneration. As per definition, tau and NfL proteins are important for maintaining axonal integrity, (van Rossum et al. 2012), whereas MTA and HV on MRI reflect a more generic loss of neuronal tissue and neuropil (Bobinski et al. 1999; Barkhof et al. 2007), and GFAP indicates astroglial reactivity (Teunissen et al. 2021). While our study focused on

individuals with intact cognition, other studies have also reported discordances between biomarkers within an ATN category, N in particular, across the AD spectrum (Guo et al. 2020; Mattsson-Carlgren et al. 2020; Lin et al. 2021). Discordances between biomarkers may have significant implications, such as when used as outcome measures in clinical trials.

Furthermore, we investigated the predictive value of different N biomarkers and found that HV, NfL, and GFAP contributed to clinical progression beyond the effects of amyloid and tau. This is in accordance with previous studies demonstrating the predictive value of neurodegeneration markers for cognitive decline, and indicate that the link between HV, NfL, and GFAP pathology with clinical progression is not necessarily dependent on A $\beta$  and tau pathology (Altomare et al. 2019; Jack et al. 2019; Soldan et al. 2019; Ebenau et al. 2020; Ingala et al. 2021).

### *Understanding brain network breakdown in Alzheimer's disease*

Both structural and functional network studies have shown that brain networks of individuals with AD are characterized by a loss of small-world features, i.e. show an increasingly random network topology (Brier et al. 2014; Stam 2014; Yu et al. 2021). Changes in grey matter (GM) networks can be observed early in the course of the disease, when amyloid is becoming abnormal and before overt neuronal damage and clinical symptoms manifest (Tijms et al. 2016; ten Kate et al. 2018; Voevodskaya et al. 2018; Dicks et al. 2020). Investigating brain network changes in response to key pathological aggregates of AD may therefore contribute to a deeper understanding of the pathophysiological processes in pre-dementia stages.

In **chapter 4** we examined the relationship between tau aggregation and GM network alterations in individuals from the bioFINDER study spanning the continuum of CN amyloid negative, CN amyloid positive, MCI

due to AD, and AD dementia. We found that a higher tau-PET load was associated with worse GM network abnormalities. It is possible that the relationship between tau burden and GM network abnormalities could be primarily driven by differences in disease stage, since both are affected by disease severity. However, we observed this association within each disease stage as well, suggesting that tau aggregation and network breakdown are closely interrelated and progressively worsen as the disease progresses. In A $\beta$  negative CN individuals, no relationship was observed between tau signal and GM network changes, suggesting that A $\beta$  positivity is a prerequisite for these changes to occur. At a regional level, we found that default mode network (DMN) regions show the strongest correlation between tau signals and local network disruptions in clustering and path length, whereas tau-associated changes in network degree were most profound in the MTL. We hypothesize that the observed relationship between tau pathology and brain network disruptions may be explained by findings from previous cellular and molecular studies showing that tau aggregates contribute to impaired axonal transport, resulting in further synaptic loss and cortical atrophy, causing substantial network damage and impaired cognition (Ittner et al. 2010; Spires-Jones and Hyman 2014a; Menkes-Caspi et al. 2015). For a better understanding of the underlying mechanism in humans, future studies must combine our measures with different biomarkers. Furthermore, we found that the effect of tau pathology on lower cognitive performance was partially mediated by a decrease in small-world values. Thus, tau and small-world values, although related, also explain unique aspects of cognitive decline.

In **chapter 5** we investigated the hypothesis that cortical myelin is decreased in AD using the T1/T2-weighted ratio in the Amsterdam Dementia Cohort. Contrary to our hypothesis, we observed a higher



T1w/T2w signal in AD dementia patients as compared to healthy controls, with the largest differences observed in DMN regions. Previous studies showing that lower T1w/T2w values are observed frequently in non-AD brain diseases such as multiple sclerosis, suggest that these values reflect a loss of myelin content. In contrast, associations between a higher T1w/T2w ratio and higher amyloid load in preclinical AD subjects has been reported as well (Yasuno et al. 2017).

The T1w/T2w ratio was introduced as a myelin proxy in 2011 and has shown close, albeit qualitative, correspondence with histology-based myelin maps (Glasser and van Essen 2011; Glasser et al. 2014), myelin-associated genes (Ritchie et al. 2018), and sensitivity to myelin disruptions in a variety of diseases including multiple sclerosis, schizophrenia, and bipolar disorder (Iwatani et al. 2015; Ishida et al. 2017; Nakamura et al. 2017; Righart et al. 2017). However, concerns have also been raised regarding the microstructural correlates of the T1w/T2w ratio, including studies showing stronger associations with neurite and dendrite density than with myelin density (Righart et al. 2017; Petracca et al. 2020; Preziosa et al. 2021). Furthermore, studies investigating other pathological conditions, such as Huntington's disease, Parkinson disease, and Multiple System Atrophy have also reported increased T1w/T2w values (Du et al. 2018; Rowley et al. 2018; Ponticorvo et al. 2021; Boaventura et al. 2022). The higher T1w/T2w ratio in our study was associated with higher CSF t-tau concentrations and worse cognition, indicating pathological changes. A possible explanation for the increased T1w/T2w signal in AD is increased iron depositions. As iron colocalizes with myelin and is frequently present around A $\beta$  plaques, it can strongly decrease the T2w signal, which could have contributed to the higher T1w/T2w ratio observed in AD (Fukunaga et al. 2010; Ward et al. 2014). This iron hypothesis is supported by the finding

that brain regions known to be vulnerable in AD and to have a high amyloid burden, such as the precuneus and cingulate cortex, showed the highest T1w/T2w ratios. However, a recent study by Luo et al. (2019) found lower T1w/T2w ratios in the hippocampus and the inferior parietal lobule of AD patients compared to healthy controls, and Rokicki et al. (2021) found no differences between AD dementia patients and healthy controls in cortical T1w/T2w ratios.

Taken together, the heterogeneity of results across studies suggest that the T1w/T2w ratio does not only reflect myelin content. It is likely that factors other than demyelination influence the T1w/T2w signal in AD, since signal intensities can be influenced by a variety of biological and non-biological factors. Combined imaging and histological research is needed since we currently do not have a comprehensive understanding of what the T1w/T2w ratio is measuring and how it may be affected by factors such as iron deposition and inflammation in AD.

### *Predicting clinical progression in pre-dementia Alzheimer's disease*

Preceding sections summarised our findings regarding the relationship between AD pathology and structural brain changes, as well as the association of A $\beta$  plaques, tau tangles, neurodegeneration and GM network disruptions with clinical decline. In **chapter 6** we examined whether this knowledge can be applied to accurate prognosis at the patient level. In prodromal AD individuals, we developed cut-offs for abnormal GM network measures that were predictive of the progression to dementia within 24 months. The cut-offs, which were determined in the Amsterdam Dementia Cohort, were able to detect fast disease progression in an independent cohort with 65% accuracy in MCI patients with biomarker evidence of A $\beta$  pathology. We further showed that when combining GM network measures

with CSF p-tau and hippocampal volume measures, the accuracy of detecting prodromal AD individuals with rapid progression in the validation cohort increased to 72%.

Selection of individuals who are likely to show cognitive decline within a typical AD trial window of 18-24 months is of great importance as this can substantially increase the power to detect treatment effects, which in turn will reduce the required sample size (Cummings et al. 2019). Our work showed that a hypothetical 24-month study to reach 80% power for detecting a 25% slowing in the annual rate of decline on the CDR-sb would require  $\pm$  490 MCI subjects with proven amyloid pathology. Taking into account abnormal small world values, this sample size decreased by 24% to 370 individuals, and by 46% to 262 individuals when hippocampal volume and p-tau values were also abnormal. This suggests that GM network measures might be helpful in addition to p-tau and hippocampal values to select those individuals who will show fast disease progression over a relatively short period of time.

### **Implications and future directions**

In this thesis, a central concept is that different measures of neurodegeneration in Alzheimer's disease play distinct roles in cognitive decline. Additionally, we demonstrated that A $\beta$  abnormality in individuals who remain cognitively intact over the age of 90 is still associated with an increased risk of cognitive decline in the future. A common argument to argue that there is no causal link between amyloid plaques and cognitive decline is that such very old individuals can demonstrate abnormal levels of amyloid while their cognition remains intact. However, this argument is largely based on cross-sectional research from which it is unknown whether cognition will still decline when individuals live long enough. Based on our

findings in the oldest-old, we conclude that A $\beta$  deposition should not be considered to be a part of the 'normal' ageing process, since it was a significant predictor of cognitive decline over time. Furthermore, our results suggest that other pathologies may also contribute to cognitive decline, since atrophy, in addition to A $\beta$ , was also associated with cognitive decline. In order to better study these relationships in the oldest-old, further development of specific markers of other common pathological processes, such as  $\alpha$ -synuclein or TDP-43, is highly anticipated.

The results in this thesis also emphasize the complexity and multifactoriality of the neurobiological mechanisms underlying AD. In order to improve the understanding of these pathophysiological processes, future studies should examine a wide range of biomarkers which cover many of these processes in the same individual. In addition, longitudinal modelling within the same individuals would enhance our understanding of the temporal trajectories and interactions of biomarker changes and their utility in predicting disease progression. This thesis demonstrates, for example, that different 'N' biomarkers reflect different disease aspects, which may be further complicated by the possibility that pathological events may occur at distinct points during disease progression, and their interrelationships may differ depending on disease stage, as well as by individual. Several recent developments in other non-specific markers of synaptic dysfunction (i.e. SV2A-PET, CSF Ng, CSF SNAP-25), and neuroaxonal degeneration (i.e. CSF and plasma NfL) may contribute to an improved determination of an individual's position in the pathophysiological continuum and provide prognostic information, which is highly important when selecting participants and assessing treatment effects in clinical trials. Furthermore, the integration of neuroimaging data with omics data may provide valuable contributions to precision medicine.

Additionally, our research highlights the role of brain networks in further understanding the pathophysiology of AD. GM networks have been found to be sensitive to early disease changes in AD. These changes might not be evident yet from other structural imaging measures such as atrophy and DTI since GM networks also account for the intrinsic organization of cortical morphology (Zhou et al. 2011; Reid and Evans 2013; Guo et al. 2014). A $\beta$  accumulation has previously been related to synaptic dysfunction (Oddo et al. 2003; Spires-Jones and Hyman 2014b) and changes in GM networks already in preclinical AD stages (ten Kate et al. 2018; Voevodskaya et al. 2018). GM network alterations may indicate increased axonal loss (Vermunt 2020) due to tau phosphorylation (Spires-Jones et al. 2009). This is consistent with our work showing a close association between increased tau burden and GM network disruptions. In turn, this leads to an increase in neuronal loss, resulting in cognitive impairments (Figure 1).

Abnormalities in grey matter networks have shown to robustly predict clinical progression. There is a high need for markers able to predict rapid short-term disease progression considering the large heterogeneity in disease progression among individuals with abnormal A $\beta$ , with some individuals remaining stable for several years (Donohue et al. 2017). In addition, for individual-level application of predictive biomarkers, reliable cut-offs must be established. Since imaging markers are largely influenced by interindividual factors such as age and sex, it can be rather difficult to determine abnormality. We demonstrated that robust cut-off determination was possible for GM network measures, since the cut-offs performed similarly in ADNI and ADC, which are two very different cohorts. This opens the door for selecting the best candidates for AD clinical trials, which enrol individuals from different centres that frequently use different scanners and scanner settings. Moreover, our results suggest that one marker is not

sufficient to capture fast decline, since the best predictive accuracy was observed when abnormal GM network measures were combined with hippocampal volume and tau pathology. Further studies are needed to determine which combination of markers is most effective at capturing decline in the short timeframe of a clinical trial.

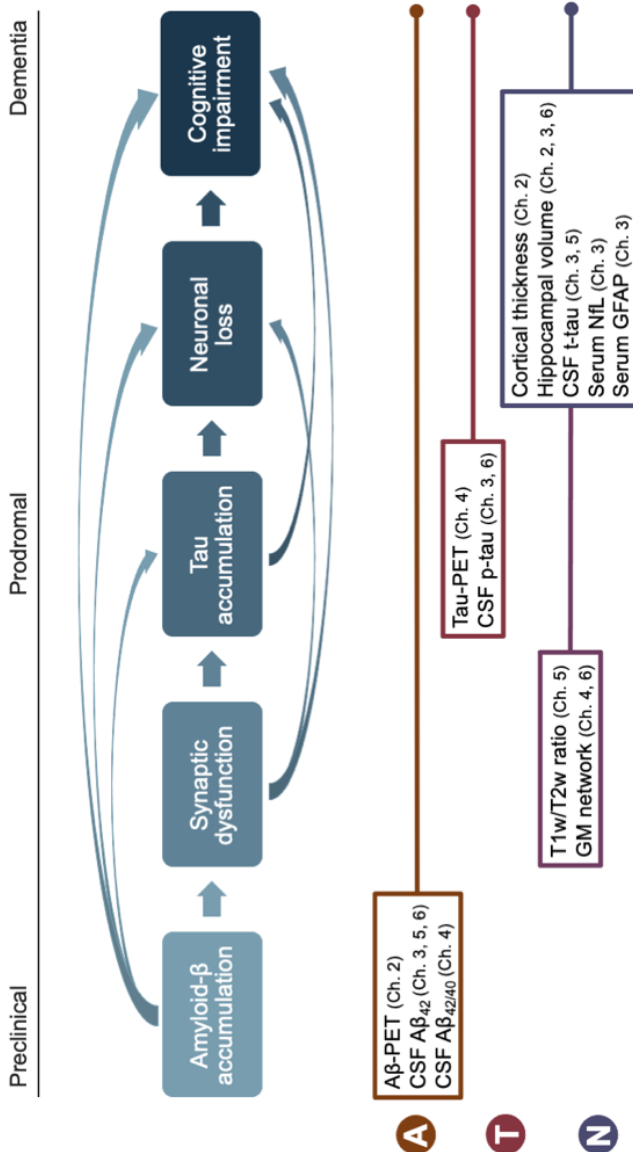


**Figure 1. Hypothetical biomarker model of AD pathophysiology**  
 Boxes represent a temporal pattern of biomarker changes as a function of disease stage (left to right). Arrows indicate a unidirectional effect of one biomarker on another, and show how they contribute directly and indirectly to cognitive dysfunction. Associated biomarkers used in this thesis are classified according to the Amyloid/Tau/Neurodegeneration framework.

## **Methodological considerations**

The results presented in this thesis must be interpreted in light of several methodological considerations. First, we constructed brain networks using a single-subject grey matter network approach, resulting in networks of different size and degree. Although this preserves inter-individual differences, it may also influence the subsequent higher level network measures, which have been shown to be dependent on the total number of connections in a network (van Wijk et al. 2010; van den Heuvel et al. 2017). To overcome this bias, our analyses were performed using normalised network measures, in which the network of interest and the randomised networks are of equal size and degree which may largely cancel out this effect. Furthermore, we included the network's connectivity density (degree/size) as a covariate during statistical analysis to limit the possibility of confounding effects. An alternative approach would have been to normalise all networks to be of the same size and degree. However, in dysconnectivity disorders such as AD, such a procedure could introduce a large number of false positive connections, resulting in an artificially random network (Tijms et al. 2013). It remains a challenging problem how to best deal with this methodological issue in the context of disease. Additionally, GM networks reflect the organisation of grey matter structure in the brain, and their relationship with axonal connectivity as captured with DTI, as well as with functional connectivity as measured with functional MRI, remains largely unclear. It is likely that the different modalities may capture different aspects of dysconnectivity in AD, which remains to be explored in greater depth. Furthermore, the biomarkers presented in this thesis are by no means exhaustive. A large range of other neuronal, axonal and synaptic injury biomarkers are available today, including fluorodeoxyglucose (FDG)-PET, SV2A-PET, structural and functional

connectivity, SNAP-25, VILIP1, and neurogranin (Zetterberg and Bendlin 2021).

### **Conclusion**

Rapid advances in *in vivo* AD pathology biomarkers have tremendously contributed to the understanding of the pathophysiological processes leading to dementia, while also exposing the complexity of the pathophysiology of AD. This thesis investigated the interplay among A $\beta$  deposition, tau aggregation, brain network alterations, and atrophy mechanisms underlying clinical progression. By studying early biomarker changes and their relationship to clinical progression, we are able to gain a better understanding of how these biological processes contribute to AD progression which will be essential to developing early and targeted effective treatments as well as more accurate individual-specific prognoses.



## References

- Altomare D, de Wilde A, Ossenkoppele R, Pelkmans W, Bouwman F, Groot C, van Maurik I, Zwan M, Yaqub M, Barkhof F, van Berckel BN, Teunissen CE, Frisoni GB, Scheltens P, van der Flier WM. 2019. Applying the ATN scheme in a memory clinic population. *Neurology*. 93:e1635–e1646.
- Barkhof F, Polvikoski TM, van Straaten ECW, Kalaria RN, Sulkava R, Aronen HJ, Niinistö L, Rastas S, Oinas M, Scheltens P, Erkinjuntti T. 2007. The significance of medial temporal lobe atrophy: A postmortem MRI study in the very old. *Neurology*. 69:1521–1527.
- Bilgel M, An Y, Helphrey J, Elkins W, Gomez G, Wong DF, Davatzikos C, Ferrucci L, Resnick SM. 2018. Effects of amyloid pathology and neurodegeneration on cognitive change in cognitively normal adults. *Brain*. 141:2475–2485.
- Boaventura M, Sastre-Garriga J, Garcia-Vidal A, Vidal-Jordana A, Quartana D, Carvajal R, Auger C, Alberich M, Tintoré M, Rovira À, Montalban X, Pareto D. 2022. T1/T2-weighted ratio in multiple sclerosis: A longitudinal study with clinical associations. *NeuroImage: Clinical*. 34:102967.
- Bobinski M, de Leon MJ, Wegiel J, DeSanti S, Convit A, saint Louis LA, Rusinek H, Wisniewski HM. 1999. The histological validation of post mortem magnetic resonance imaging-determined hippocampal volume in Alzheimer's disease. *Neuroscience*. 95:721–725.
- Boyle PA, Wang T, Yu L, Wilson RS, Dawe R, Arfanakis K, Schneider JA, Bennett DA. 2021. To what degree is late life cognitive decline driven by age-related neuropathologies? *Brain*. 144:2166–2175.
- Brier MR, Thomas JB, Ances BM. 2014. Network Dysfunction in Alzheimer's Disease: Refining the Disconnection Hypothesis. *Brain Connectivity*. 4:299–311.
- Chételat G, Villemagne VL, Pike KE, Ellis KA, Bourgeat P, Jones G, O'Keefe GJ, Salvado O, Szoek C, Martins RN, Ames D, Masters CL, Rowe CC. 2011. Independent contribution of temporal  $\beta$ -amyloid deposition to memory decline in the pre-dementia phase of Alzheimer's disease. *Brain*. 134:798–807.
- Corrada MM, Berlau DJ, Kawas CH. 2012. A population-based clinicopathological study in the oldest-old: the 90+ study. *Curr Alzheimer Res*. 9:709–717.
- Cummings J, Feldman HH, Scheltens P. 2019. The “rights” of precision drug development for Alzheimer's disease. *Alzheimer's Research & Therapy*. 11:76.
- Dicks E, van der Flier WM, Scheltens P, Barkhof F, Tijms BM. 2020. Single-subject gray matter networks predict future cortical atrophy in preclinical Alzheimer's disease. *Neurobiology of Aging*. 94:71–80.

- Donohue MC, Sperling RA, Petersen R, Sun CK, Weiner M, Aisen PS. 2017. Association between elevated brain amyloid and subsequent cognitive decline among cognitively normal persons. *JAMA - Journal of the American Medical Association*. 317:2305–2316.
- Du G, Lewis MM, Sica C, Kong L, Huang X. 2018. Magnetic resonance T1w/T2w ratio: A parsimonious marker for Parkinson disease. *Annals of Neurology*. 85:1–9.
- Ebenau JL, Timmers T, Wesselman LMP, Verberk IMW, Verfaillie SCJ, Slot RER, van Harten AC, Teunissen CE, Barkhof F, van den Bosch KA, van Leeuwenstijn M, Tomassen J, Braber A den, Visser PJ, Prins ND, Sikkes SAM, Scheltens P, van Berckel BNM, van der Flier WM. 2020. ATN classification and clinical progression in subjective cognitive decline. *Neurology*. 95:e46–e58.
- Fukunaga M, Li T-Q, van Gelderen P, de Zwart JA, Shmueli K, Yao B, Lee J, Maric D, Aronova MA, Zhang G, Leapman RD, Schenck JF, Merkle H, Duyn JH. 2010. Layer-specific variation of iron content in cerebral cortex as a source of MRI contrast. *Proceedings of the National Academy of Sciences*. 107:3834–3839.
- Glasser MF, Goyal MS, Preuss TM, Raichle ME, van Essen DC. 2014. Trends and properties of human cerebral cortex: Correlations with cortical myelin content. *Neuroimage*. 93:165–175.
- Glasser MF, van Essen DC. 2011. Mapping Human Cortical Areas In Vivo Based on Myelin Content as Revealed by T1- and T2-Weighted MRI. *Journal of Neuroscience*. 31:11597–11616.
- Guo X, Chen K, Zhang Y, Wang Y, Yao L. 2014. Regional covariance patterns of gray matter alterations in Alzheimer’s disease and its replicability evaluation. *Journal of Magnetic Resonance Imaging*. 39:143–149.
- Guo Y, Li H, Tan L, Chen S, Yang Y, Ma Y, Zuo C, Dong Q, Tan L, Yu J. 2020. Discordant Alzheimer’s neurodegenerative biomarkers and their clinical outcomes. *Annals of Clinical and Translational Neurology*. 7:1996–2009.
- Haroutunian V, Schnaider-Beeri M, Schmeidler J, Wysocki M, Purohit DP, Perl DP, Libow LS, Lesser GT, Maroukian M, Grossman HT. 2008. Role of the neuropathology of Alzheimer disease in dementia in the oldest-old. *Archives of Neurology*. 65:1211–1217.
- Herrup K. 2015. The case for rejecting the amyloid cascade hypothesis. *Nature Neuroscience*. 18:794–799.
- Ingala S, de Boer C, Masselink LA, Vergari I, Lorenzini L, Blennow K, Chételat G, di Perri C, Ewers M, Flier WM, Fox NC, Gispert JD, Haller S, Molinuevo JL, Muniz-Terrera G, Mutsaerts HJMM, Ritchie CW, Ritchie K, Schmidt M, Schwarz AJ, Vermunt L, Waldman AD, Wardlaw J, Wink AM, Wolz R, Wottschel V, Scheltens P, Visser PJ, Barkhof F. 2021. Application of the ATN classification scheme in a population without dementia: Findings from the EPAD cohort. *Alzheimer’s & Dementia*. 17:1189–1204.

- Ishida T, Donishi T, Iwatani J, Yamada S, Takahashi S, Ukai S, Shinosaki K, Terada M, Kaneoke Y. 2017. Elucidating the aberrant brain regions in bipolar disorder using T1-weighted/T2-weighted magnetic resonance ratio images. *Psychiatry Research: Neuroimaging*. 263:76–84.
- Ittner LM, Ke YD, Delerue F, Bi M, Gladbach A, van Eersel J, Wölfling H, Chieng BC, Christie MJ, Napier IA, Eckert A, Staufenberg M, Hardeman E, Götz J. 2010. Dendritic Function of Tau Mediates Amyloid- $\beta$  Toxicity in Alzheimer's Disease Mouse Models. *Cell*. 142:387–397.
- Iwatani J, Ishida T, Donishi T, Ukai S, Shinosaki K, Terada M, Kaneoke Y. 2015. Use of T1-weighted/T2-weighted magnetic resonance ratio images to elucidate changes in the schizophrenic brain. *Brain and Behavior*. 5:1–14.
- Jack CR, Bennett DA, Blennow K, Carrillo MC, Dunn B, Haeberlein SB, Holtzman DM, Jagust W, Jessen F, Karlawish J, Liu E, Molinuevo JL, Montine T, Phelps C, Rankin KP, Rowe CC, Scheltens P, Siemers E, Snyder HM, Sperling R, Elliott C, Masliah E, Ryan L, Silverberg N. 2018. NIA-AA Research Framework: Toward a biological definition of Alzheimer's disease. *Alzheimer's and Dementia*. 14:535–562.
- Jack CR, Wiste HJ, Therneau TM, Weigand SD, Knopman DS, Mielke MM, Lowe VJ, Vemuri P, Machulda MM, Schwarz CG, Gunter JL, Senjem ML, Graff-Radford J, Jones DT, Roberts RO, Rocca WA, Petersen RC. 2019. Associations of Amyloid, Tau, and Neurodegeneration Biomarker Profiles With Rates of Memory Decline Among Individuals Without Dementia. *JAMA*. 321:2316.
- Jansen WJ, Janssen O, Tijms BM, Vos SJB, Ossenkoppele R, Visser PJ, Aarsland D, Alcolea D, Altomare D, von Arnim C, Baiardi S, Baldeiras I, Barthel H, Bateman RJ, van Berckel B, Binette AP, Blennow K, Boada M, Boecker H, Bottlaender M, den Braber A, Brooks DJ, van Buchem MA, Camus V, Carill JM, Cerman J, Chen K, Chételat G, Chipi E, Cohen AD, Daniels A, Delarue M, Didic M, Drzezga A, Dubois B, Eckerström M, Ekblad LL, Engelborghs S, Epelbaum S, Fagan AM, Fan Y, Fladby T, Fleisher AS, van der Flier WM, Förster S, Fortea J, Frederiksen KS, Freund-Levi Y, Frings L, Frisoni GB, Fröhlich L, Gabryelewicz T, Gertz H-J, Gill KD, Gkatzima O, Gómez-Tortosa E, Grimmer T, Guedj E, Habeck CG, Hampel H, Handels R, Hansson O, Hausner L, Hellwig S, Heneka MT, Herukka S-K, Hildebrandt H, Hodges J, Hort J, Huang C-C, Iriondo AJ, Itoh Y, Ivanoiu A, Jagust WJ, Jessen F, Johannsen P, Johnson KA, Kandimalla R, Kapaki EN, Kern S, Kilander L, Klimkiewicz-Mrowiec A, Klunk WE, Koglin N, Kornhuber J, Kramberger MG, Kuo H-C, van Laere K, Landau SM, Landeau B, Lee DY, de Leon M, Leyton CE, Lin K-J, Lleó A, Löwenmark M, Madsen K, Maier W, Marcusson J, Marquié M, Martinez-Lage P, Maserejian N, Mattsson N, de Mendonça A, Meyer PT, Miller BL, Minatani S, Mintun MA, Mok VCT, Molinuevo JL, Morbelli SD, Morris JC, Mroczko B, Na DL, Newberg A, Nobili F, Nordberg A, Olde Rikkert MGM, de Oliveira CR, Olivieri P, Orellana A,

- Paraskevas G, Parchi P, Pardini M, Parnetti L, Peters O, Poirier J, Popp J, Prabhakar S, Rabinovici GD, Ramakers IH, Rami L, Reiman EM, Rinne JO, Rodrigue KM, Rodríguez-Rodríguez E, Roe CM, Rosa-Neto P, Rosen HJ, Rot U, Rowe CC, Rütger E, Ruiz A, Sabri O, Sakhardande J, Sánchez-Juan P, Sando SB, Santana I, Sarazin M, Scheltens P, Schröder J, Selnes P, Seo SW, Silva D, Skoog I, Snyder PJ, Soininen H, Sollberger M, Sperling RA, Spuru L, Stern Y, Stomrud E, Takeda A, Teichmann M, Teunissen CE, Thompson LI, Tomassen J, Tsolaki M, Vandenberghe R, Verbeek MM, Verhey FRJ, Villemagne V, Villeneuve S, Vogelgsang J, Waldemar G, Wallin A, Wallin ÅK, Wiltfang J, Wolk DA, Yen T-C, Zboch M, Zetterberg H. 2022. Prevalence Estimates of Amyloid Abnormality Across the Alzheimer Disease Clinical Spectrum. *JAMA Neurology*. 1–17.
- Kawas CH, Legdeur N, Corrada MM. 2021. What have we learned from cognition in the oldest-old. *Current Opinion in Neurology*. 34:258–265.
- Lin R-R, Xue Y-Y, Li X-Y, Chen Y-H, Tao Q-Q, Wu Z-Y. 2021. Optimal Combinations of AT(N) Biomarkers to Determine Longitudinal Cognition in the Alzheimer’s Disease. *Frontiers in Aging Neuroscience*. 13:1–14.
- Luo X, Li K, Zeng Q, Huang P, Jiaerken Y, Wang S, Shen Z, Xu X, Xu J, Wang C, Kong L, Zhou J, Zhang M. 2019. Application of T1-/T2-Weighted Ratio Mapping to Elucidate Intracortical Demyelination Process in the Alzheimer’s Disease Continuum. *Frontiers in Neuroscience*. 13:1–13.
- Mattsson-Carlgrén N, Leuzy A, Janelidze S, Palmqvist S, Stomrud E, Strandberg O, Smith R, Hansson O. 2020. The implications of different approaches to define AT(N) in Alzheimer disease. *Neurology*. 94:e2233–e2244.
- Menkes-Caspi N, Yamin HG, Kellner V, Spires-Jones TL, Cohen D, Stern EA. 2015. Pathological Tau Disrupts Ongoing Network Activity. *Neuron*. 85:959–966.
- Morris GP, Clark IA, Vissel B. 2018. Questions concerning the role of amyloid- $\beta$  in the definition, aetiology and diagnosis of Alzheimer’s disease. *Acta Neuropathologica*. 136:663–689.
- Nakamura K, Chen JT, Ontaneda D, Fox RJ, Trapp BD. 2017. T1-/T2-weighted ratio differs in demyelinated cortex in multiple sclerosis. *Annals of Neurology*. 82:635–639.
- Oddo S, Caccamo A, Shepherd JD, Murphy MP, Golde TE, Kaye R, Metherate R, Mattson MP, Akbari Y, LaFerla FM. 2003. Triple-Transgenic Model of Alzheimer’s Disease with Plaques and Tangles. *Neuron*. 39:409–421.
- Petracca M, el Mendili MM, Moro M, Coccozza S, Podranski K, Fleysler L, Inglese M. 2020. Laminar analysis of the cortical T1/T2-weighted ratio at 7T. *Neurology - Neuroimmunology Neuroinflammation*. 7:e900.
- Ponticorvo S, Manara R, Russillo MC, Erro R, Picillo M, di Salle G, di Salle F, Barone P, Esposito F, Pellecchia MT. 2021. Magnetic resonance T1w/T2w ratio and voxel-based morphometry in multiple system atrophy. *Scientific Reports*. 11:21683.

- Preziosa P, Bouman PM, Kiljan S, Steenwijk MD, Meani A, Pouwels PJ, Rocca MA, Filippi M, Geurts JGG, Jonkman LE. 2021. Neurite density explains cortical T1-weighted/T2-weighted ratio in multiple sclerosis. *Journal of Neurology, Neurosurgery & Psychiatry*. 92:790–792.
- Reid AT, Evans AC. 2013. Structural networks in Alzheimer’s disease. *European Neuropsychopharmacology*. 23:63–77.
- Richard E, Schmand B, Eikelenboom P, Westendorp RG, van Gool WA. 2012. The Alzheimer Myth and Biomarker Research in Dementia. *Journal of Alzheimer’s Disease*. 31:S203–S209.
- Righart R, Biberacher V, Jonkman LE, Klaver R, Schmidt P, Buck D, Berthele A, Kirschke JS, Zimmer C, Hemmer B, Geurts JGG, Mühlau M. 2017. Cortical pathology in multiple sclerosis detected by the T1/T2-weighted ratio from routine magnetic resonance imaging. *Annals of Neurology*. 82:519–529.
- Ritchie J, Pantazatos SP, French L. 2018. Transcriptomic characterization of MRI contrast with focus on the T1-w/T2-w ratio in the cerebral cortex. *Neuroimage*. 174:504–517.
- Rokicki J, Wolfers T, Nordhøy W, Tesli N, Quintana DS, Alnæs D, Richard G, Lange AG, Lund MJ, Norbom L, Agartz I, Melle I, Nærland T, Selbæk G, Persson K, Nordvik JE, Schwarz E, Andreassen OA, Kaufmann T, Westlye LT. 2021. Multimodal imaging improves brain age prediction and reveals distinct abnormalities in patients with psychiatric and neurological disorders. *Human Brain Mapping*. 42:1714–1726.
- Rowley CD, Tabrizi SJ, Scahill RI, Leavitt BR, Roos RAC, Durr A, Bock NA. 2018. Altered Intracortical T1-Weighted/T2-Weighted Ratio Signal in Huntington’s Disease. *Frontiers in Neuroscience*. 12:1–9.
- Savva GM, Wharton SB, Ince PG, Forster G, Matthews FE, Brayne C. 2009. Age, Neuropathology, and Dementia. *New England Journal of Medicine*. 360:2302–2309.
- Soldan A, Pettigrew C, Fagan AM, Schindler SE, Moghekar A, Fowler C, Li Q-X, Collins SJ, Carlsson C, Asthana S, Masters CL, Johnson S, Morris JC, Albert M, Gross AL. 2019. ATN profiles among cognitively normal individuals and longitudinal cognitive outcomes. *Neurology*. 92:e1567–e1579.
- Spires-Jones TL, Hyman BT. 2014a. The Intersection of Amyloid Beta and Tau at Synapses in Alzheimer’s Disease. *Neuron*. 82:756–771.
- Spires-Jones TL, Hyman BT. 2014b. The Intersection of Amyloid Beta and Tau at Synapses in Alzheimer’s Disease. *Neuron*. 82:756–771.
- Spires-Jones TL, Stoothoff WH, de Calignon A, Jones PB, Hyman BT. 2009. Tau pathophysiology in neurodegeneration: a tangled issue. *Trends in Neurosciences*. 32:150–159.
- Stam CJ. 2014. Modern network science of neurological disorders. *Nature Reviews Neuroscience*. 15:683–695.

- Svenningsson AL, Stomrud E, Insel PS, Mattsson N, Palmqvist S, Hansson O. 2019. B-Amyloid Pathology and Hippocampal Atrophy Are Independently Associated With Memory Function in Cognitively Healthy Elderly. *Sci Rep.* 9:11180.
- ten Kate M, Visser PJ, Bakardjian H, Barkhof F, Sikkes SAM, van der Flier WM, Scheltens P, Hampel H, Habert M-O, Dubois B, Tijms BM. 2018. Gray Matter Network Disruptions and Regional Amyloid Beta in Cognitively Normal Adults. *Frontiers in Aging Neuroscience.* 10:1–11.
- Teunissen CE, Verberk IMW, Thijssen EH, Vermunt L, Hansson O, Zetterberg H, van der Flier WM, Mielke MM, del Campo M. 2021. Blood-based biomarkers for Alzheimer’s disease: towards clinical implementation. *The Lancet Neurology.* 4422:1–12.
- Tijms BM, Kate M ten, Wink AM, Visser PJ, Ecay M, Clerigue M, Estanga A, Garcia Sebastian M, Izagirre A, Villanua J, Martinez Lage P, van der Flier WM, Scheltens P, Sanz Arigita E, Barkhof F. 2016. Gray matter network disruptions and amyloid beta in cognitively normal adults. *Neurobiology of Aging.* 37:154–160.
- Tijms BM, Möller C, Vrenken H, Wink AM, de Haan W, van der Flier WM, Stam CJ, Scheltens P, Barkhof F. 2013. Single-Subject Grey Matter Graphs in Alzheimer’s Disease. *PLoS ONE.* 8:e58921.
- van den Heuvel MP, de Lange SC, Zalesky A, Seguin C, Yeo BTT, Schmidt R. 2017. Proportional thresholding in resting-state fMRI functional connectivity networks and consequences for patient-control connectome studies: Issues and recommendations. *Neuroimage.* 152:437–449.
- van der Kall LM, Truong T, Burnham SC, Doré V, Mulligan RS, Bozinovski S, Lamb F, Bourgeat P, Fripp J, Schultz S, Lim YY, Laws SM, Ames D, Fowler C, Rainey-Smith SR, Martins RN, Salvado O, Robertson J, Maruff P, Masters CL, Villemagne VL, Rowe CC. 2020. Association of  $\beta$ -Amyloid Level, Clinical Progression, and Longitudinal Cognitive Change in Normal Older Individuals. *Neurology.* 96:10.1212/WNL.0000000000011222.
- van Rossum IA, Vos SJB, Burns L, Knol DL, Scheltens P, Soininen H, Wahlund L-O, Hampel H, Tsolaki M, Minthon L, L’Italien G, van der Flier WM, Teunissen CE, Blennow K, Barkhof F, Rueckert D, Wolz R, Verhey F, Visser PJ. 2012. Injury markers predict time to dementia in subjects with MCI and amyloid pathology. *Neurology.* 79:1809–1816.
- van Wijk BCM, Stam CJ, Daffertshofer A. 2010. Comparing Brain Networks of Different Size and Connectivity Density Using Graph Theory. *PLoS ONE.* 5:e13701.
- Vermunt L. 2020. Secondary Prevention for Alzheimer Disease.
- Voevodskaya O, Pereira JB, Volpe G, Lindberg O, Stomrud E, van Westen D, Westman E, Hansson O. 2018. Altered structural network organization in

- cognitively normal individuals with amyloid pathology. *Neurobiology of Aging*. 64:15–24.
- Ward RJ, Zucca FA, Duyn JH, Crichton RR, Zecca L. 2014. The role of iron in brain ageing and neurodegenerative disorders. *The Lancet Neurology*. 13:1045–1060.
- Wirth M, Oh H, Mormino EC, Markley C, Landau SM, Jagust WJ. 2013. The effect of amyloid  $\beta$  on cognitive decline is modulated by neural integrity in cognitively normal elderly. *Alzheimer's & Dementia*. 9:687.
- Yasuno F, Kazui H, Morita N, Kajimoto K, Ihara M, Taguchi A, Yamamoto A, Matsuoka K, Takahashi M, Nakagawara J, Iida H, Kishimoto T, Nagatsuka K. 2017. Use of T1-weighted/T2-weighted magnetic resonance ratio to elucidate changes due to amyloid  $\beta$  accumulation in cognitively normal subjects. *NeuroImage: Clinical*. 13:209–214.
- Yu L, Boyle PA, Dawe RJ, Bennett DA, Arfanakis K, Schneider JA. 2020. Contribution of TDP and hippocampal sclerosis to hippocampal volume loss in older-old persons. *Neurology*. 94:e142–e152.
- Yu M, Sporns O, Saykin AJ. 2021. The human connectome in Alzheimer disease — relationship to biomarkers and genetics. *Nature Reviews Neurology*. 17:545–563.
- Zetterberg H, Bendlin BB. 2021. Biomarkers for Alzheimer's disease—preparing for a new era of disease-modifying therapies. *Molecular Psychiatry*. 26:296–308.
- Zhao Y, Tudorascu DL, Lopez OL, Cohen AD, Mathis CA, Aizenstein HJ, Price JC, Kuller LH, Kamboh MI, DeKosky ST, Klunk WE, Snitz BE. 2018. Amyloid  $\beta$  Deposition and Suspected Non-Alzheimer Pathophysiology and Cognitive Decline Patterns for 12 Years in Oldest Old Participants Without Dementia. *JAMA Neurology*. 75:88.
- Zhou L, Wang Y, Li Y, Yap P-T, Shen D. 2011. Hierarchical Anatomical Brain Networks for MCI Prediction: Revisiting Volumetric Measures. *PLoS ONE*. 6:e21935.





# APPENDIX

**Nederlandse samenvatting (Dutch summary)**

**List of publications**

**List of author affiliations**

**List of PhD theses Alzheimer Center Amsterdam**

**Portfolio**

**Acknowledgements**

**About the author**



## NEDERLANDSE SAMENVATTING

### Inleiding

#### *Het Alzheimer continuüm*

De ziekte van Alzheimer is een progressieve neurodegeneratieve aandoening en de meest voorkomende vorm van dementie. Van oudsher is de diagnose Alzheimer gebaseerd op de klinische presentatie van de patiënt; progressieve stoornissen in meerdere cognitieve domeinen die interfereren met activiteiten van het dagelijks leven. Een definitieve biologische diagnose was alleen mogelijk door autopsie te verrichten. Bij pathologisch onderzoek bleek echter ongeveer een derde van de patiënten met een klinische Alzheimer dementie diagnose, géén neuropathologische verschijnselen te vertonen die passend zijn bij de ziekte van Alzheimer.

Gedurende de laatste twee decennia heeft de ontwikkeling van biomarkers, die de aanwezigheid van Alzheimer pathologie in levende mensen aan kunnen tonen, het Alzheimer onderzoeksveld getransformeerd. De belangrijkste pathologische kenmerken van de ziekte van Alzheimer, amyloïd- $\beta$  ( $A\beta$ ) plaques en tau neurofibrillaire kluwens, kunnen *in vivo* aangetoond worden met behulp van positron emissie tomografie (PET), in het hersenvocht (liquor) en sinds kort ook in het bloed. Daarnaast kan het afsterven van de hersencellen (neurodegeneratie) goed in kaart worden gebracht met behulp van structurele magnetische resonantie beeldvorming (MRI). Deze ontwikkelingen hebben bijgedragen aan het inzicht dat de eerste pathologische veranderingen al zo'n 20 jaar aanwezig zijn vòòr de presentatie van de eerste dementie symptomen.

Volgens de amyloïd cascade hypothese speelt de ophoping van A $\beta$  een initiërende rol in het ontstaan van de ziekte en ontketent deze een cascade van gebeurtenissen die zorgen voor synaptische disfunctie, de vorming van neurofibrillaire kluwens, inflammatie, verlies van neuronen, cognitieve stoornissen en uiteindelijk dementie. Dit inzicht heeft geleid tot een conceptuele verschuiving van een puur klinisch op symptomen gebaseerde ziekte van Alzheimer, tot een biologisch construct met een continuüm van preklinische, prodromale en dementie fases. Met andere woorden, ongeacht de klinische presentatie definiëren nu biomarkers van de onderliggende pathologie de ziekte van Alzheimer. Deze inzichten hebben geleid tot de publicatie van het 'ATN' onderzoeksmodel dat een binaire classificering van drie Alzheimer biomarkers (A = Amyloïd, T = hypergefosforyleerd Tau, N = Neurodegeneratie) gebruikt, waardoor de ziekte van Alzheimer gedefinieerd kan worden op basis van de aanwezigheid van A<sup>+</sup>T<sup>+</sup> pathologie, terwijl N biomarkers niet specifiek zijn voor de ziekte van Alzheimer maar gebruikt kunnen worden voor stadiëring van de ziekte.

### *Beeldvormende correlaten van neurodegeneratie*

Het toenemende verlies van synapsen en neuronen zijn karakteristieke neurodegeneratieve kenmerken van de ziekte van Alzheimer en deze hangen nauw samen met cognitieve achteruitgang. De grijze stof in de hersenen bestaat uit neuronale cellen en hun verbindingen, veranderingen in de grijze stof kan *in vivo* door middel van structurele MRI in kaart gebracht worden. Verschillende grijze stof integriteit biomarkers laten een nauwe samenhang zien met cognitieve stoornissen en bevatten prognostische waarde om al in een vroeg ziektestadium achteruitgang te voorspellen. Echter kan tot op heden het mechanisme van cognitieve

achteruitgang in de ziekte van Alzheimer niet volledig verklaard worden door de grijze stof integriteit. Ook is het nog niet volledig duidelijk hoe neurodegeneratie samenhangt met Alzheimer pathologie biomarkers in verschillende ziektestadia. In dit proefschrift hebben we vier neurodegeneratieve maten onderzocht die veranderen gedurende de ontwikkeling van de ziekte van Alzheimer: hippocampaal volume, corticale dikte, grijze stof netwerken en corticale myeline. Daarnaast hebben we in kaart gebracht hoe deze maten samenhangen met Alzheimer pathologie biomarkers en klinische progressie.

### **Het doel van dit proefschrift**

Het doel van dit proefschrift is om de complexe relaties tussen Alzheimer pathologie markers (amyloïd en tau) met structurele hersenveranderingen (waaronder maten van neuronale schade en hersennetwerkveranderingen) beter te begrijpen en de samenhang met cognitieve achteruitgang en klinische progressie in verschillende stadia van de ziekte van Alzheimer te onderzoeken.

De onderzoeken richten zich op drie specifieke doelstellingen:

1. Het in kaart brengen van de directe en indirecte effecten van amyloïd pathologie en verschillende neurodegeneratieve maten op cognitieve achteruitgang in de toekomst bij mensen met normale cognitie (H. 2, 3).
2. Een beter begrip van hoe grijze stof netwerken en myeline proxy maten veranderen in reactie op pathologische eiwitten in de ziekte van Alzheimer (H 4, 5).
3. Onderzoeken of grijze stof netwerken, alleen danwel gecombineerd met andere prognostische biomarkers, patiënten met prodromale

Alzheimer kan identificeren die snelle klinische progressie zullen vertonen.

### **De hoofdlijnen**

In **hoofdstuk 2** hebben we onderzocht hoe abnormaal A $\beta$  samenhangt met cognitieve achteruitgang in cognitief normale mensen die ouder zijn dan 90 jaar en in hoeverre deze effecten gemedieerd worden door corticale atrofie.

In **hoofdstuk 3** hebben we verschillende neurodegeneratieve maten vergeleken en hun voorspellende waarde voor klinische progressie berekend in mensen met subjectieve cognitieve achteruitgang.

In **hoofdstuk 4** hebben we de relatie tussen tau deposities en grijze stof netwerkveranderingen onderzocht in patiënten binnen het Alzheimer spectrum.

In **hoofdstuk 5** hebben we T1-w/T2-w ratio waardes vergeleken tussen mensen met normale cognitie en patiënten met Alzheimer dementie, en onderzocht in hoeverre neuronale schade, witte stof hyperintensiteiten en cognitief functioneren leidden tot veranderingen in T1-w/T2-w waarden.

In **hoofdstuk 6** hebben we onderzocht of grijze stof netwerken gebruikt kunnen worden om patiënten met prodromale Alzheimer te identificeren die snelle ziekteprogressie zullen vertonen.

## Samenvatting en discussie

In de volgende sectie worden de belangrijkste bevindingen van dit proefschrift samengevat en geplaatst in de context van de huidige literatuur, mede als de implicaties, methodologische kanttekeningen en toekomstperspectieven.

### *De samenhang van preklinische pathologische veranderingen met cognitieve achteruitgang.*

Abnormaal A $\beta$  in cognitief normale (CN) ouderen is gerelateerd aan een verhoogd risico op cognitieve achteruitgang in de toekomst. De prevalentie van abnormaal A $\beta$  in CN mensen neemt toe met de leeftijd ( $\approx$ 14% 50 jaar tot 47% 90 jaar), gevolgd door een toename in de dementie prevalentie ongeveer 20 jaar later. Echter, in de 'oudste ouderen' (90+ jaar) worden er vraagtekens gezet bij de samenhang tussen abnormaal amyloïd in CN ouderen en cognitieve achteruitgang. Met name als gevolg van resultaten uit cross-sectioneel autopsie onderzoek dat uitgebreide pathologie passend bij de ziekte van Alzheimer laat zien in CN ouderen. Echter, om deze samenhang beter te kunnen begrijpen zijn herhaalde cognitieve metingen noodzakelijk.

In **hoofdstuk 2** hebben we geobserveerd dat CN deelnemers van de EMIF-AD 90+ studie met een abnormale amyloïd PET scan, regionale corticale krimp en een snellere achteruitgang in het geheugen en verwerkingsnelheid lieten zien. Deze bevindingen komen overeen met eerdere studies met negentig- en honderdjarige deelnemers, en suggereert dat A $\beta$  pathologie niet benigne is en geassocieerd is met cognitieve achteruitgang, zelfs in individuen met normale cognitie op zeer oude leeftijd. Bovendien hebben we in dit onderzoek aangetoond dat het verlies van neuronen in de parahippocampale cortex het effect van A $\beta$  pathologie op achteruitgang van het geheugen en taal medieert. Dit is in overeenstemming

met eerder voorgestelde onafhankelijke en synergistische effecten van A $\beta$  en neurodegeneratie op cognitieve stoornissen in jongere populaties en in lijn met de amyloïd cascade hypothese.

Daarnaast observeerden we in CN negentigplussers dat atrofie, voornamelijk in de mediaal temporaal kwab, geassocieerd was met cognitieve achteruitgang ongeacht de aanwezigheid van A $\beta$  pathologie. Deze observatie kan mogelijk verklaard worden door de aanwezigheid van andere pathologieën dan amyloïde plaques. TDP-43,  $\alpha$ -synucleïne, cerebrovasculaire aandoeningen en hippocampale sclerose komen vaak voor in de oudste-ouderen en zijn tevens belangrijke drijvers van niet-amyloïd gerelateerde neuronale schade en cognitieve achteruitgang. Echter dient deze hypothese verder geverifieerd te worden met toekomstig autopsie onderzoek in dit cohort.

In **hoofdstuk 3** hebben we het effect van neurodegeneratieve markers op cognitieve achteruitgang verder in kaart gebracht door verscheidene 'N' biomarkers uit het hersenvocht, bloed en hersenscans te vergelijken. Met behulp van data van het subjectieve cognitieve klachten cohort (SCIENCE), hebben we vastgesteld dat de N markers liquor totaal-tau (t-tau), visuele beoordeling van atrofie in de mediaal temporaalkwab (MTA), hippocampaal volume (HV), serum neurofilament lichte keten (NfL) en serum gliaal fibrillair zuur eiwit (GFAP) maar matig met elkaar correleerden. Op dit moment beschouwen expertgroepen de verschillende N maten als onderling verwisselbaar. Onze bevindingen wijzen er echter op dat deze niet geschikt zijn om uitwisselbaar te gebruiken omdat elke marker een ander aspect van neurodegeneratie meet. Bovendien zijn per definitie tau en NfL belangrijke eiwitten voor axonale integriteit, terwijl MTA en HV op MRI meer generiek het verlies van neuronale weefsel en neuropil weergeven en GFAP als een marker voor reactieve astroglie wordt



beschouwd. Ons onderzoek richtte zich op mensen waarbij de cognitie volledig intact was; andere studies hebben ook binnen het gehele Alzheimer spectrum de discordantie tussen biomarkers binnen een ATN categorie, met name N, aangetoond. Biomarker discordanties kunnen belangrijke gevolgen hebben voor klinische trials, bijvoorbeeld als deze gebruikt worden als uitkomstmaat.

Vervolgens hebben we in deze studie ook de voorspellende waarde van verschillende N biomarkers getest en zagen we dat HV, NfL en GFAP bijdragen aan klinische progressie bovenop het effect van amyloïd en tau. Dit is in lijn met eerdere studies die de voorspellende waarde van neurodegeneratieve markers voor cognitieve achteruitgang aantoonde en laat zien dat het verband tussen HV, NfL en GFAP pathologie met klinische progressie niet afhankelijk hoeft te zijn van A $\beta$  en tau pathologie.

### *Verstoringen in hersennetwerken bij de ziekte van Alzheimer*

Zowel structurele als functionele netwerkstudies hebben laten zien dat hersennetwerken in patiënten met Alzheimer dementie een verminderde 'small-world' organisatie laten zien, m.a.w. in toenemende mate een random netwerk topologie weergeven. Veranderingen in grijze stof (GS) netwerken kunnen al in een vroege fase van de ziekte geobserveerd worden, oftewel op het moment dat amyloïd abnormaal wordt en nog voordat er duidelijke neuronale schade en klinische symptomen zijn. Inzicht in hoe pathologische eiwit aggregaten veranderingen in het hersennetwerk teweegbrengen kan ons daarom meer duidelijkheid geven in de pathofysiologische processen in het pre-dementie stadium van de ziekte.

In **hoofdstuk 4** hebben we de relatie tussen tau aggregatie en GS-netwerkveranderingen onderzocht in deelnemers van de bioFINDER studie die het gehele spectrum van CN amyloïd negatieve, CN amyloïd positieve,

prodromale Alzheimer en Alzheimer dementie omvatten. We vonden dat een hogere hoeveelheid tau pathologie gemeten met PET, gerelateerd was aan meer GS-netwerkafwijkingen. Aangezien zowel de mate van tau pathologie als GS-netwerkafwijkingen toenemen wanneer de ernst van de ziekte toeneemt, kan deze relatie voornamelijk terug te leiden zijn naar verschillen in ziektestadium. Echter, observeerden we deze associatie ook binnen elk ziektestadium, hetgeen suggereert dat tau aggregatie en netwerkverstoring nauw verbonden zijn en verergeren verder in het ziekteproces. We zagen geen relatie tussen tau signaal en GS-netwerkveranderingen in A $\beta$  negatieve deelnemers, wat impliceert dat afwijkend A $\beta$  een vereiste is voor deze geobserveerde veranderingen. Op regionaal niveau vonden we dat hersengebieden in het default mode network (DMN) de sterkste samenhang tussen tau signaal en lokale netwerkverstoringen in 'clustering' en 'path length' maten lieten zien, terwijl veranderingen in netwerk 'degree' door tau voornamelijk zichtbaar waren in de mediaal temporaalkwab. De geobserveerde samenhang tussen tau pathologie en hersennetwerkverstoringen kan mogelijk verklaard worden door bevindingen van eerdere cellulaire en moleculaire studies die aantonen dat tau aggregaten het axonaal transport belemmeren, wat vervolgens tot verder verlies van synapsen en corticale atrofie leidt, resulterend in substantiële netwerkschade en cognitieve stoornissen. Toekomstig onderzoek waarbij deze maten gecombineerd worden met andere biomarkers zijn nodig om de onderliggende mechanismen in mensen beter te kunnen begrijpen. In deze studie hebben we ook door middel van mediatie analyses vastgesteld dat het effect van tau pathologie op slechtere cognitieve prestaties deels gemedieerd wordt door lagere small-world waarden, hetgeen suggereert dat ondanks de samenhang van tau en small-

world waarden deze ook unieke aspecten van cognitieve achteruitgang verklaren.

In **hoofdstuk 5** onderzochten we de hypothese dat er een afname is in corticale myeline in de ziekte van Alzheimer, door gebruik te maken van de ratio van T1 en T2 gewogen beelden uit het Amsterdam Dementie Cohort. In tegenstelling tot onze hypothese, vonden we een hoger T1w/T2w signaal in Alzheimer dementie patiënten ten opzichte van gezonde controles, met de grootste verschillen in DMN-regio's. Deze bevindingen spreken eerder werk tegen dat zich voornamelijk richtte op andere hersenziekten zoals multipale sclerose, deze rapporteerden lagere T1w/T2w waarden in patiënten, wat kenmerkend is voor het verlies van myeline. Daarentegen is in een preklinische Alzheimerstudie, d.w.z. mensen met normale cognitie en abnormaal amyloïd, ook een verhoogd T1w/T2w ratio gevonden.

Toen de T1w/T2w ratio geïntroduceerd werd als proxy maat voor myeline in 2011, werd er, hoewel kwalitatief, grote overeenstemming gevonden met op histologie gebaseerde myeline hersenatlassen, myeline geassocieerde genen en sensitiviteit voor myeline verstoringen in verscheidende ziektebeelden waaronder multipale sclerose, schizofrenie en bipolaire stoornissen. Tegelijkertijd zijn er ook zorgen geuit over de micro-structurele correlaten van de T1w/T2w ratio, waaronder de bevinding van een sterkere samenhang met neuriet en dendriet dichtheid dan met myeline dichtheid. In overeenstemming met onze resultaten, hebben andere studies in pathologische stoornissen tevens verhoogde T1w/T2w waarden gevonden in de ziekte van Huntington, de ziekte van Parkinson en Multipale systeem atrofie. Wij vonden dat een hogere T1w/T2w ratio geassocieerd was met hogere t-tau concentraties in het hersenvocht en slechtere cognitie, hetgeen pathologische verandering impliceert. Een mogelijke verklaring is dat het verhoogde T1w/T2w signaal een weergave is van een verhoogd

aantal ijzer deposities in de ziekte van Alzheimer. IJzer lokaliseert zich samen met myeline en is vaak aanwezig rondom A $\beta$  plaques. IJzer kan het T2w signaal sterk verlagen, hetgeen mogelijk geleid heeft tot de verhoogde T1w/T2w ratio in Alzheimer dementie. Ook werden de hoogste T1w/T2w ratio's geobserveerd in kwetsbare hersenregio's met veel amyloïd stapeling, zoals de precuneus en gyrus cinguli. Maar er is ook recentelijk onderzoek dat lagere T1w/T2w ratio's in de hippocampus en lobulus parietalis inferior heeft gevonden in patiënten met Alzheimer dementie ten opzichte van gezonde controles.

Samengevat, suggereert de grote variëteit in studieresultaten dat de T1w/T2w ratio niet enkel myeline weergeeft. Bij de ziekte van Alzheimer wordt het T1w/T2w signaal waarschijnlijk beïnvloed door andere factoren dan demyelinisatie, aangezien signaalintensiteiten beïnvloed kunnen worden door verscheidene biologische en niet-biologische factoren. Op dit moment is onderzoek waarbij histologisch en beeldvormend onderzoek gecombineerd wordt hard nodig omdat er geen eenduidig beeld is van wat de T1w/T2w ratio meet en hoe deze mogelijk beïnvloed wordt door factoren zoals ijzer deposities en inflammatie in de ziekte van Alzheimer.

### *Klinische achteruitgang voorspellen in de pre-dementie fase van de ziekte van Alzheimer*

In de voorgaande paragrafen heb ik onze bevindingen besproken over de relatie van amyloïd pathologie met structurele hersenveranderingen, en de samenhang van A $\beta$  plaques, tau tangles, neurodegeneratie en GS-netwerk verstoringen met klinische achteruitgang. In **hoofdstuk 6** hebben we vervolgens onderzocht of deze verkregen kennis toegepast kan worden voor prognoses op patiëntniveau. Hiervoor ontwikkelden we afkapwaarden die abnormale GS-netwerk maten in prodromale Alzheimerpatiënten

weergeven en progressie naar dementie binnen 24 maanden voorspelden. Deze afkapwaarden, die waren bepaald in het Amsterdam Dementie Cohort, konden in een ander onafhankelijk cohort snelle ziekteprogressie in MCI-patiënten met biomarker bevestiging van A $\beta$  pathologie vaststellen met 65% zekerheid. Als vervolgens deze GS-netwerkmaten gecombineerd werden met informatie over de status van gefosforyleerd tau en hippocampaal volume, nam de nauwkeurigheid om prodromale Alzheimerpatiënten met snelle progressie te detecteren in het validatie cohort toe naar 72%.

Het selecteren van deelnemers die zeer waarschijnlijk cognitieve achteruitgang zullen laten zien binnen een Alzheimermedicatie trial periode van gemiddeld 18-24 maanden is van groot belang aangezien dit de power om een behandelingseffect aan te kunnen tonen substantieel verhoogt en daarmee de benodigde steekproefomvang verkleint. Ons onderzoek liet zien dat een hypothetische trial van 24 maanden met een power van 80% om een 25% vertraging in jaarlijkse achteruitgang op de CDR-sb te kunnen detecteren ongeveer 490 MCI patiënten met amyloïd pathologie vereist. Wanneer abnormale small-world waarden hierin ook meegenomen werden, nam de steekproefgrootte af met 24% naar 370 deelnemers, en met 46% naar 262 deelnemers als ook hippocampaal volume en p-tau waarden abnormaal waren. Dit suggereert dat in aanvulling op p-tau en hippocampaal volume, GS-netwerkmaten bij kunnen dragen in het selecteren van deelnemers die binnen een relatief kort tijdsbestek snelle ziekteprogressie zullen laten zien.

### **Implicaties en toekomstperspectieven**

In dit proefschrift staan verschillende neurodegeneratieve maten centraal die op verschillende wijze betrokken zijn bij cognitieve achteruitgang bij de

ziekte van Alzheimer. Zo hebben we in ouderen die tot hun negentigste levensjaar cognitief intact bleven aan kunnen tonen dat A $\beta$  abnormaliteit nog steeds samenhangt met een verhoogd risico op cognitieve achteruitgang in de toekomst. Het feit dat deze mensen op zeer late leeftijd abnormaal amyloïd laten zien en tegelijkertijd hun cognitie nog steeds intact is, wordt gebruikt als argument dat amyloïd niet causaal is voor cognitieve achteruitgang. Dit argument is echter voornamelijk gebaseerd op cross-sectioneel onderzoek, waarvan het niet duidelijk is of als mensen lang genoeg zouden leven alsnog achteruit zouden gaan. Een belangrijke implicatie van ons onderzoek in de oudste-ouderen is dat de aanwezigheid van A $\beta$  deposities niet gezien dient te worden als onderdeel van 'normale' veroudering, aangezien het een sterke voorspeller bleek voor cognitieve achteruitgang. Daarnaast tonen onze resultaten dat ook andere pathologieën een belangrijke rol spelen aangezien atrofie gerelateerd was aan cognitieve achteruitgang onafhankelijk van A $\beta$ . Naar de verdere ontwikkeling van specifieke markers voor andere veelvoorkomende pathologische eiwitten waaronder  $\alpha$ -synucleïne en TDP-43 wordt dan ook erg uitgekeken om deze relaties in de oudste-ouderen beter te kunnen bestuderen.

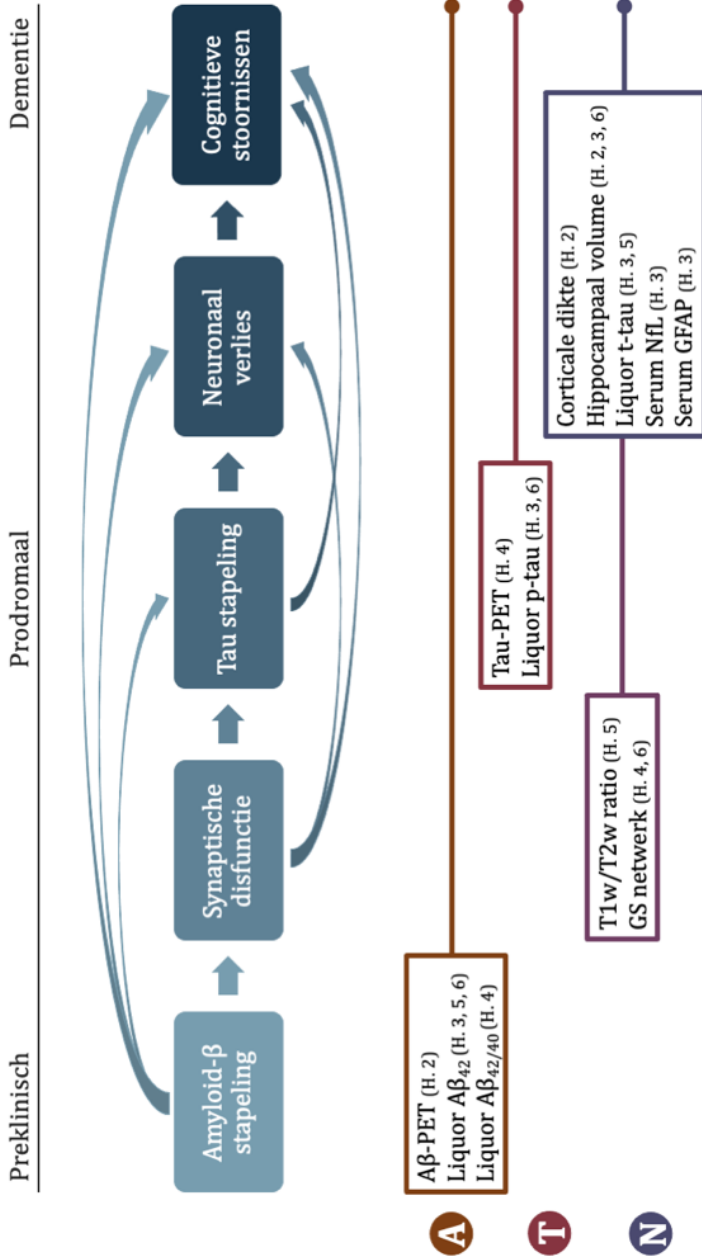
De resultaten van dit proefschrift benadrukken ook de complexiteit van de multifactoriële neurobiologische mechanismen die ten grondslag liggen aan de ziekte van Alzheimer. Om ons begrip van deze pathofysiologische processen te vergroten, is het van groot belang dat toekomstige studies zich richten op een breed scala aan verschillende biomarkers die een groot deel van deze processen beslaan binnen eenzelfde individu. Daarnaast zouden herhaalde metingen binnen dezelfde personen onze kennis over het ziektebeloop, biomarker interacties en het voorspellen van ziekteprogressie aanzienlijk vergroten. Bijvoorbeeld, een van de

resultaten uit dit proefschrift laat zien dat verschillende 'N' biomarkers verschillende ziekte aspecten weergeven, dit wordt verder gecompliceerd doordat pathologische gebeurtenissen op verschillende tijdstippen in het ziekteproces kunnen plaatsvinden en daarnaast mogelijk ook kunnen verschillen tussen individuen. Recente ontwikkelingen in niet-stoornis specifieke markers voor synaptische disfunctie (bv. SV2A-PET, CSF Ng, CSF SNAP-25) en neuroaxonale degeneratie (bv. CSF en plasma NfL) kunnen mogelijk hieraan bijdragen zodat we beter begrijpen op welke positie een patiënt zich bevindt binnen het pathofysiologisch continuüm en kunnen tevens prognostische informatie bieden. Dit is van groot belang voor het selecteren van de meest geschikte studiedeelnemers en voor betere toetsing van behandelingseffecten in klinische trials. Ook kan de integratie van neuroimaging en omics data de ontwikkelingen richting 'precisie geneeskunde' verder bevorderen.

Ons werk toont eveneens de meerwaarde van het toepassen van hersennetwerken bij het doorgronden van de pathofysiologie van de ziekte van Alzheimer, mede omdat GS-netwerken al zeer vroeg veranderingen in het ziekteproces laten zien. Dit wordt nog niet opgepikt door andere structurele beeldvormende maten zoals atrofie en DTI, terwijl GS-netwerken ook rekening houden met de intrinsieke organisatie van de corticale morfologie. A $\beta$  stapeling is gerelateerd aan synaptische disfunctie en aan veranderingen in GS-netwerken al in de preklinische fase van de ziekte van Alzheimer. De schade aan GS-netwerken wordt mogelijk veroorzaakt door het toenemende verlies van axonen als gevolg van tau fosforylatie, deze bevinding komt overeen met ons werk dat een nauw verband laat zien tussen verstoringen in het GS-netwerk en de mate van tau pathologie. Dit resulteert uiteindelijk in nog meer neuronaal verlies en leidt vervolgens tot cognitieve stoornissen (Figuur 1).

Verstoringen in het GS-netwerk zijn een goede voorspeller voor klinische progressie. Aan markers die op korte termijn snelle ziekteprogressie kunnen voorspellen is grote behoefte, gezien de grote heterogeniteit in ziekte beloop waarbij sommige patiënten (ook met abnormaal A $\beta$ ) nog jaren stabiel kunnen blijven. Maar voordat voorspellende biomarkers toegepast kunnen worden op individueel-niveau, dienen er betrouwbare afkapwaarden te worden vastgesteld. Het kan relatief lastig zijn om een afkappunt voor abnormaliteit vast te stellen voor imaging markers omdat deze in zekere mate beïnvloed worden door interindividuele factoren zoals leeftijd en geslacht. In dit proefschrift hebben wij laten zien dat het bepalen van robuuste afkapwaarden voor GS-netwerkmaten mogelijk is, aangezien deze vergelijkbaar presteerden in zowel het ADNI als het ADC cohort, terwijl er wezenlijke cohort verschillen bestaan. Dit opent de deuren voor het selecteren van de meest geschikte kandidaten voor klinische Alzheimer trials, die vaak deelnemers uit verschillende centra includeren en dus ook vaak gebruik maken van verschillende MRI-scanners en scannerinstellingen. Een andere implicatie van onze resultaten is dat één marker waarschijnlijk niet voldoende zal zijn om snelle cognitieve achteruitgang op te pikken, aangezien dat we de best voorspellende waarde vonden wanneer abnormale GS-netwerkmaten gecombineerd werden met hippocampaal volume en tau pathologie. Toekomstige studies dienen zich verder te richten op het samenstellen van de optimale combinatie van markers die het best achteruitgang binnen zo'n kort tijdsbestek kunnen detecteren.





**Figuur 1. Hypothetisch biomarker model van de ziekte van Alzheimer**

De boxen geven het verloop van biomarker veranderingen weer als een functie van ziektestadium (van links naar rechts). De pijlen laten het effect van een biomarker op een andere biomarker zien en hoe deze zowel direct als indirect bijdragen aan het ontstaan van cognitieve stoornissen. Biomarkers die in dit proefschrift gebruikt zijn zijn geclassificeerd volgens het Amyloid/Tau/Neurodegeneratie model.

## **Methodologische kanttekeningen**

Bij de interpretatie van de resultaten uit dit proefschrift is het belangrijk om rekening te houden met een aantal methodologische kanttekeningen. Allereerst hebben wij hersennetwerken berekend volgens een methode waarbij per individu één netwerk berekend wordt, als gevolg hiervan kunnen de netwerken tussen personen verschillen in grootte en aantal verbindingen. Een voordeel van deze methode is het behoud van interindividuele verschillen, maar het kan ook de netwerkmaten beïnvloeden aangezien aangetoond is dat deze afhankelijk zijn van het totaal aantal connecties van een netwerk. Om dit probleem te ondervangen, hebben we gebruik gemaakt van genormaliseerde netwerkmaten waarbij het desbetreffende netwerk en de gerandomiseerde netwerken dezelfde grootte en totaal aantal connecties hebben, waardoor deze effecten grotendeels worden weggenomen. Daarnaast hebben we de connectiviteitsdichtheid (aantal connecties/totaal aantal mogelijke connecties) van een netwerk meegenomen als covariaat tijdens de statistische analyses om op deze manier de invloed van deze variabelen te minimaliseren. Een alternatieve methode zou zijn om alle netwerken te normaliseren naar dezelfde grootte en aantal connecties. Echter, in disconnectiviteitsstoornissen zoals de ziekte van Alzheimer, zou deze aanpak zorgen voor een groot aantal vals positieve verbindingen en daardoor artificieel tot een meer random netwerk kunnen leiden. Hoe het beste om te gaan met deze methodologisch kwestie in een pathologische context is tot op heden niet duidelijk. Daarnaast zijn GS-netwerken een weergave van de organisatiestructuur van de grijze stof in de hersenen, terwijl de relatie met axonale connectiviteit (bv gemeten met DTI), en met functionele connectiviteit (bv gemeten met functionele MRI), nog grotendeels onduidelijk is. Het is aannemelijk dat verschillende

modaliteiten ook verschillende aspecten van disconnectiviteit in de ziekte van Alzheimer weergeven, maar dit dient nog uitgebreider onderzocht te worden. Vervolgens is de lijst van behandelde biomarkers in dit proefschrift lang niet compleet. Er bestaat op dit moment een groot scala aan andere neuronale en axonale biomarkers voor synaptische schade, waaronder fluorodeoxyglucose (FDG)-PET, SVA-PET, structurele en functionele connectiviteit, SNAP-25, VILIP1 en neurogranine.

## **Conclusie**

De snelle ontwikkelingen in Alzheimer pathologie biomarkers hebben een enorme bijdrage geleverd aan een beter begrip van de pathofysiologische processen die leiden tot dementie en geven tegelijkertijd ook de complexiteit van de ziekte van Alzheimer weer. In dit proefschrift hebben we de wisselwerking tussen A $\beta$  deposities, tau aggregaties, hersennetwerkveranderingen en atrofie mechanismen die ten grondslag liggen aan klinische progressie uitgebreid onderzocht. Door het bestuderen van vroege biomarker veranderingen en hoe deze samenhangen met klinische progressie krijgen we de mogelijkheid om deze biologische processen gedurende het ziekteproces beter te begrijpen, wat essentieel is voor toekomstige patiënt-specifieke prognoses en de ontwikkeling van vroege en gerichte effectieve behandelingen.

## List of publications

### *In this thesis*

1. **Pelkmans W**, Vromen EM, Dicks E, Scheltens P, Teunissen CE, Barkhof F, van der Flier WM, and Tijms, BM. *Grey matter network markers identify individuals with prodromal Alzheimer's disease who will show rapid clinical decline*. *Brain Commun*. 2022 Mar 1;4(2):1–9.
2. Ebenau JL, **Pelkmans W**, Verberk IMW, Verfaillie SCJ, van den Bosch KA, van Leeuwenstijn M, Collij LE, Scheltens P, Prins ND, Barkhof F, van Berckel BNM, Teunissen CE, and van der Flier WM. *Association of CSF, Plasma, and Imaging Markers of Neurodegeneration With Clinical Progression in People With Subjective Cognitive Decline*. *Neurology*. 2022 Mar 29;98(13):e1315–26.
3. **Pelkmans W**, Ossenkoppele R, Dicks E, Strandberg O, Barkhof F, Tijms BM, Pereira JB, and Hansson O. *Tau-related grey matter network breakdown across the Alzheimer's disease continuum*. *Alzheimers Res Ther*. 2021 Dec 13;13(1):138.
4. **Pelkmans W**, Legdeur N, Kate M, Barkhof F, Yaqub MM, Holstege H, Berckel BNM, Scheltens P, van der Flier WM, Visser PJ, and Tijms BM. *Amyloid- $\beta$ , cortical thickness, and subsequent cognitive decline in cognitively normal oldest-old*. *Ann Clin Transl Neurol*. 2021 Feb 9;8(2):348–58.
5. **Pelkmans W**, Dicks E, Barkhof F, Vrenken H, Scheltens P, Flier WM, and Tijms BM. *Gray matter T1-w/T2-w ratios are higher in Alzheimer's disease*. *Hum Brain Mapp*. 2019 Sep 3;40(13):3900-9.

### *Not in this thesis*

6. Legdeur N, Moonen JE, Badissi M, Heeman F, Collij L, Sudre CH, **Pelkmans W**, Gordon MF; Novak G, Barkhof F, van Berckel BNM, Scheltens P, Peters M, Visser PJ, Muller M. *Blood pressure in relation to volumetric MRI measures of brain aging in individuals aged 90 years and older*. Submitted.
7. van 't Hooft JJ, **Pelkmans W**, Tomassen J, Smits C, Legdeur N, den Braber A, Barkhof F, van Berckel BNM, Scheltens P, Pijnenburg YAL, Visser PJ, Tijms BM. *Distinct disease mechanisms may underlie*

- cognitive decline due to age related hearing loss in different age groups.* Submitted.
8. van der Doelen DM, Handels RLH, Zwan MD, van Kuijk SMJ, **Pelkmans W**, Bouwman FH, Scheltens P, Dirksen CD, and Verhey FRJ. *The Impact of Amyloid PET Disclosure on Quality of Life in Patients With Young Onset Dementia.* *Alzheimer Dis Assoc Disord.* 2022 Jan;36(1):1–6.
  9. Beentjes KM, Neal DP, Kerkhof YJF, Broeder C, Moeridjan ZDJ, Ettema TP, **Pelkmans W**, Muller MM, Graff MJL, and Dröes RM. *Impact of the FindMyApps program on people with mild cognitive impairment or dementia and their caregivers; an exploratory pilot randomised controlled trial.* *Disabil Rehabil Assist Technol.* 2020 Nov 27;0(0):1–13.
  10. de Wilde A, Ossenkoppele R, **Pelkmans W**, Bouwman F, Groot C, van Maurik I, Zwan M, Yaqub M, Barkhof F, Lammertsma AA, Biessels GJ, Scheltens P, van Berckel BN, and van der Flier WM. *Assessment of the appropriate use criteria for amyloid PET in an unselected memory clinic cohort: The ABIDE project.* *Alzheimer's Dement.* 2019 Nov;15(11):1458–67.
  11. Altomare D, de Wilde A, Ossenkoppele R, **Pelkmans W**, Bouwman F, Groot C, van Maurik I, Zwan M, Yaqub M, Barkhof F, van Berckel BN, Teunissen CE, Frisoni GB, Scheltens P, and van der Flier WM. *Applying the ATN scheme in a memory clinic population.* *Neurology.* 2019 Oct 22;93(17):e1635–46.
  12. van Maurik IS, Visser LNC, Pel-Littel RE, van Buchem MM, Zwan MD, Kunneman M, **Pelkmans W**, Bouwman FH, Minkman M, Schoonenboom N, Scheltens P, Smets EMA, and van der Flier WM. *Development and Usability of ADappt: Web-Based Tool to Support Clinicians, Patients, and Caregivers in the Diagnosis of Mild Cognitive Impairment and Alzheimer Disease.* *JMIR Form Res.* 2019 Jul 8;3(3):e13417.
  13. de Wilde A, van der Flier WM, **Pelkmans W**, Bouwman F, Verwer J, Groot C, van Buchem MM, Zwan M, Ossenkoppele R, Yaqub M, Kunneman M, Smets EMA, Barkhof F, Lammertsma AA, Stephens A, van Lier E, Biessels GJ, van Berckel BN, Scheltens P. *Association of Amyloid Positron Emission Tomography With Changes in Diagnosis and Patient Treatment in an Unselected Memory Clinic Cohort.* *JAMA Neurol.* 2018 Sep 1;75(9):1062.

## List of author affiliations

**Barkhof F:** Department of Radiology & Nuclear Medicine, Amsterdam Neuroscience, Vrije Universiteit Amsterdam, Amsterdam UMC, Amsterdam, The Netherlands; Queen Square Institute of Neurology and Centre for Medical Image Computing, UCL, London, UK

**Berckel BNM van:** Department of Radiology & Nuclear Medicine, Amsterdam Neuroscience, Vrije Universiteit Amsterdam, Amsterdam UMC, Amsterdam, The Netherlands

**Bosch KA van den:** Alzheimer Center Amsterdam, Department of Neurology, Amsterdam Neuroscience, Vrije Universiteit Amsterdam, Amsterdam UMC, Amsterdam, The Netherlands

**Collij LE:** Department of Radiology & Nuclear Medicine, Amsterdam Neuroscience, Vrije Universiteit Amsterdam, Amsterdam UMC, Amsterdam, The Netherlands

**Dicks E:** Alzheimer Center Amsterdam, Department of Neurology, Amsterdam Neuroscience, Vrije Universiteit Amsterdam, Amsterdam UMC, Amsterdam, The Netherlands; Department of Neurology, Mayo Clinic, Rochester, MN, USA

**Ebenau JL:** Alzheimer Center Amsterdam, Department of Neurology, Amsterdam Neuroscience, Vrije Universiteit Amsterdam, Amsterdam UMC, Amsterdam, The Netherlands

**Flier WM van der:** Alzheimer Center Amsterdam, Department of Neurology, Amsterdam Neuroscience, Vrije Universiteit Amsterdam, Amsterdam UMC, Amsterdam, The Netherlands; Department of Epidemiology & Biostatistics, Amsterdam Neuroscience, Vrije Universiteit Amsterdam, Amsterdam UMC, Amsterdam, The Netherlands

**Hansson O:** Clinical Memory Research Unit, Department of Clinical Sciences, Lund University, Malmö, Sweden; Memory Clinic, Skåne University Hospital, Malmö, Sweden

**Holstege H:** Alzheimer Center Amsterdam, Department of Neurology, Amsterdam Neuroscience, Vrije Universiteit Amsterdam, Amsterdam UMC, Amsterdam, The Netherlands; Department of Clinical Genetics, Amsterdam

Neuroscience, Vrije Universiteit Amsterdam, Amsterdam UMC, Amsterdam, The Netherlands

**Kate M ten:** Department of Radiology & Nuclear Medicine, Amsterdam Neuroscience, Vrije Universiteit Amsterdam, Amsterdam UMC, Amsterdam, The Netherlands

**Leeuwenstijn M van:** Alzheimer Center Amsterdam, Department of Neurology, Amsterdam Neuroscience, Vrije Universiteit Amsterdam, Amsterdam UMC, Amsterdam, The Netherlands

**Legdeur N:** Alzheimer Center Amsterdam, Department of Neurology, Amsterdam Neuroscience, Vrije Universiteit Amsterdam, Amsterdam UMC, Amsterdam, The Netherlands; Department of Internal Medicine, Spaarne Gasthuis, Haarlem, the Netherlands

**Ossenkoppele R:** Alzheimer Center Amsterdam, Department of Neurology, Amsterdam Neuroscience, Vrije Universiteit Amsterdam, Amsterdam UMC, Amsterdam, The Netherlands; Clinical Memory Research Unit, Department of Clinical Sciences, Lund University, Malmö, Sweden

**Pereira JB:** Clinical Memory Research Unit, Department of Clinical Sciences, Lund University, Malmö, Sweden; Division of Clinical Geriatrics, Department of Neurobiology, Care Sciences and Society, Karolinska Institute, Stockholm, Sweden

**Prins ND:** Alzheimer Center Amsterdam, Department of Neurology, Amsterdam Neuroscience, Vrije Universiteit Amsterdam, Amsterdam UMC, Amsterdam, The Netherlands

**Scheltens P:** Alzheimer Center Amsterdam, Department of Neurology, Amsterdam Neuroscience, Vrije Universiteit Amsterdam, Amsterdam UMC, Amsterdam, The Netherlands

**Strandberg O:** Clinical Memory Research Unit, Department of Clinical Sciences, Lund University, Malmö, Sweden

**Teunissen CE:** Neurochemistry Laboratory, Department of Clinical Chemistry, Amsterdam Neuroscience, Vrije Universiteit Amsterdam, Amsterdam UMC, Amsterdam, The Netherlands

**Tijms BM:** Alzheimer Center Amsterdam, Department of Neurology, Amsterdam Neuroscience, Vrije Universiteit Amsterdam, Amsterdam UMC, Amsterdam, The Netherlands

**Verberk IMW:** Neurochemistry Laboratory, Department of Clinical Chemistry, Amsterdam Neuroscience, Vrije Universiteit Amsterdam, Amsterdam UMC, Amsterdam, The Netherlands

**Verfaillie SCJ:** Department of Radiology & Nuclear Medicine, Amsterdam Neuroscience, Vrije Universiteit Amsterdam, Amsterdam UMC, Amsterdam, The Netherlands

**Visser PJ:** Alzheimer Center Amsterdam, Department of Neurology, Amsterdam Neuroscience, Vrije Universiteit Amsterdam, Amsterdam UMC, Amsterdam, The Netherlands; Department of Psychiatry & Neuropsychology, School for Mental Health and Neuroscience, Maastricht University, Maastricht, The Netherlands; Department of Neurobiology, Care Sciences and Society, Division of Neurogeriatrics, Karolinska Institutet, Stockholm, Sweden

**Vrenken H:** Department of Radiology & Nuclear Medicine, Amsterdam Neuroscience, Vrije Universiteit Amsterdam, Amsterdam UMC, Amsterdam, The Netherlands

**Vromen EM:** Alzheimer Center Amsterdam, Department of Neurology, Amsterdam Neuroscience, Vrije Universiteit Amsterdam, Amsterdam UMC, Amsterdam, The Netherlands

**Yaqub MM:** Department of Radiology & Nuclear Medicine, Amsterdam Neuroscience, Vrije Universiteit Amsterdam, Amsterdam UMC, Amsterdam, The Netherlands



**Alzheimer Center Hall of Fame**

1. L. Gootjes: Dichotic Listening, hemispherical connectivity and dementia (14-09- 2004)
2. K. van Dijk: Peripheral nerve stimulation in Alzheimer's disease (16-01-2005)
3. R. Goekoop: Functional MRI of cholinergic transmission (16-01-2006)
4. R. Lazeron: Cognitive aspects in multiple sclerosis (03-07- 2006)
5. N.S.M. Schoonenboom: CSF markers in dementia (10-11-2006)
6. E.S.C. Korf: Medial Temporal lobe atrophy on MRI: risk factors and predictive value (22-11-2006)
7. B. van Harten: Aspects of subcortical vascular ischemic disease (22-12-2006)
8. B. Jones: Cingular cortex networks: role in learning and memory and Alzheimer's disease related changes (23-03-2007)
9. L. van de Pol: Hippocampal atrophy from aging to dementia: a clinical and radiological perspective (11-05-2007)
10. 10. Y.A.L. Pijnenburg: Frontotemporal dementia: towards an earlier diagnosis (05-07-2007)
11. A. Bastos Leite: Pathological ageing of the brain (16-11-2007)
12. E.C.W. van Straaten: Vascular dementia (11-01-2008)
13. R.L.C. Vogels: Cognitive impairment in heart failure (11-04-2008)
14. J. Damoiseaux: The brain at rest (20-05-2008)
15. G.B. Karas: computational neuro-anatomy (19-06-2008)
16. F.H. Bouwman: Biomarkers in dementia: longitudinal aspects (20-06-2008)
17. A.A. Gouw: Cerebral small vessel disease on MRI: clinical impact and underlying pathology (20-03-2009)
18. H. van der Roest: Care needs in dementia and interactive digital information provisioning (12-10-2009)
19. C. Mulder: CSF biomarkers in Alzheimer's disease (11-11-2009)
20. W. Henneman. Advances in hippocampal atrophy measurement in dementia: beyond diagnostics (27-11-2009)
21. S.S. Staekenborg: From normal aging to dementia: risk factors and clinical findings in relation to vascular changes on brain MRI (23-12-2009)
22. N. Tolboom: Imaging Alzheimer's disease pathology in vivo: towards an early diagnosis (12-02-2010)
23. E. Altena: Mapping insomnia: brain structure, function and sleep intervention (17-03- 2010)
24. N.A. Verwey: Biochemical markers in dementia: from mice to men. A translational approach (15-04-2010)

25. M.I. Kester: Biomarkers for Alzheimer's pathology; monitoring, predicting and understanding the disease (14-01-2011)
26. J.D. Sluimer: Longitudinal changes in the brain (28-04-2011)
27. S.D Mulder: Amyloid associated proteins in Alzheimer's disease (07-10-2011)
28. S.A.M. Sikkes: measuring IADL in dementia (14-10-2011)
29. A. Schuitemaker: Inflammation in Alzheimer's disease: in-vivo quantification (27-01-2012)
30. K. Joling: Depression and anxiety in family caregivers of persons with dementia (02-04- 2012)
31. W. de Haan: In a network state of mind (02-11-2012) (Cum Laude)
32. D. van Assema: Blood-brain barrier P-glycoprotein function in ageing and Alzheimer's disease (07-12-2012)
33. J.D.C. Goos: Cerebral microbleeds: connecting the dots (06-02-2013)
34. R. Ossenkoppele: Alzheimer PETology (08-05-2013)
35. H.M. Jochemsen: Brain under pressure: influences of blood pressure and angiotensin-converting enzyme on the brain (04-10-2013)
36. A.E. van der Vlies: Cognitive profiles in Alzheimer's disease: Recognizing its many faces (27-11-2013)
37. I.A. van Rossum: Diagnosis and prognosis of Alzheimer's disease in subjects with mild cognitive impairment (28-11-2013)
38. E.I.S. Møst: Circadian rhythm deterioration in early Alzheimer's disease and the preventative effect of light (03-12-2013)
39. M.A.A. Binnewijzend: Functional and perfusion MRI in dementia (21-03-2014)
40. H. de Waal: Understanding heterogeneity in Alzheimer's disease: A neurophysiological perspective (25-04-2014)
41. W. Jongbloed: Neurodegeneration: Biochemical signals from the brain (08-05- 2014)
42. E.L.G.E. Poortvliet-Koedam: Early-onset dementia: Unravelling the clinical phenotypes (28-05-2014)
43. A.C. van Harten: The road less travelled: CSF biomarkers for Alzheimer's disease (07-11-2014)
44. A.M. Hooghiemstra: Early-onset dementia: With exercise in mind (03-12-2014)
45. L.L. Sandberg-Smits: A cognitive perspective on clinical manifestations of Alzheimer's disease (20-03-2015)
46. F.H. Duits: Biomarkers for Alzheimer's disease, current practice and new perspectives (01-04-2015)
47. S.M. Adriaanse: Integrating functional and molecular imaging in Alzheimer's disease (07-04-2015)

48. C. Moller: Imaging patterns of tissue destruction – Towards a better discrimination of types of dementia (01-05-2015)
49. M. del Campo-Milan: Novel biochemical signatures of early stages of Alzheimer’s disease (19-06-2015)
50. M.R. Benedictus: A vascular view on cognitive decline and dementia: relevance of cerebrovascular MRI markers in a memory clinic (20-01-2016)
51. M.D. Zwan: Visualizing Alzheimer’s disease pathology. Implementation of amyloid PET in clinical practice (03-03-2016)
52. E. Louwersheimer: Alzheimer’s disease: from phenotype to genotype (21-06-2016)
53. W.A. Krudop: The frontal lobe syndrome: a neuropsychiatric challenge (23-09- 2016)
54. E.G.B. Vijverberg: The neuropsychiatry of behavioural variant frontotemporal dementia and primary psychiatric disorders: similarities and dissimilarities (22-09- 2017)
55. F.T. Gossink: Late Onset Behavioural Changes differentiating between bvFTD and psychiatric disorders in clinical practice (20-04-2018)
56. M.A. Engels: Neurophysiology of dementia (18-05-2018)
57. S.C.J. Verfaillie: Neuroimaging in subjective cognitive decline: Incipient Alzheimer’s disease unmasked (12-09-2018)
58. M. ten Kate: Neuroimaging in predementia Alzheimer’s disease (13-09-2018)
59. H.F.M. Rhodius-Meester: Optimizing use of diagnostic tests in memory clinics; the next step (24-09-2018)
60. E.A.J. Willemsse: Optimising biomarkers in cerebrospinal fluid. How laboratory reproducibility improves the diagnosis of Alzheimer’s disease (18-10-2018)
61. E. Konijnenberg: Early amyloid pathology – Identical twins, two of a kind? (25- 06-2019)
62. A.E. Leeuwis: Connecting heart and brain; Vascular determinants of cognitive impairment and depressive symptoms (02-07-2019)
63. J. den Haan: Imaging the retina in Alzheimer’s disease (12-09-2019)
64. A.C. van Loenhoud: Cognitive reserve in Alzheimer’s disease. A perspective on the flourishing and withering of the brain (18-09-2019)
65. R.J. Jutten: Capturing changes in cognition; refining the measurement of clinical progression in Alzheimer’s disease (20-09-2019)
66. N. Legdeur: Determinants of cognitive impairment in the oldest-old (08-10-2019)
67. R. Slot: Subjective cognitive decline – predictive value of biomarkers in the context of preclinical Alzheimer’s disease (14-11-2019)

68. N. Scheltens: Understanding heterogeneity in Alzheimer's disease – a data driven approach (17-12-2019)
69. L. Vermunt: Secondary prevention for Alzheimer's Disease – timing, selection, and endpoint of clinical trials (13-03-2020)
70. L.M.P. Wesselman: Lifestyle and brain health – exploring possibilities of an online intervention in non-demented elderly (01-04-2020)
71. I.S. van Maurik: Interpreting biomarker results in patients with mild cognitive impairment to estimate prognosis and optimize decision making (12-05-2020) (Cum Laude)
72. E. Dicks: Grey matter covariance networks in Alzheimer's disease: Edging towards a better understanding of disease progression (09-09-2020)
73. J.J. van der Zande: A sharper image of dementia with Lewy bodies: the role of imaging and neurophysiology in DLB, and the influence of concomitant Alzheimer's disease pathology (21-09-2020)
74. I. van Steenoven: Cerebrospinal fluid biomarkers in dementia with Lewy bodies – towards a biological diagnosis (22-09-2020)
75. N. Beker: Cognition in centenarians – evaluation of cognitive health and underlying factors in centenarians from the 100-plus study (02-10-2020)
76. F. de Leeuw: Nutrition and metabolic profiles in Alzheimer's disease (30-11-2020)
77. T. Timmers: Tau PET across the Alzheimer's disease continuum (02-12-2020)
78. E.E. Wolters: Untangling tau pathology using PET (02-12-2020)
79. A.S. Doorduijn: Nutrition, the unrecognized determinant in Alzheimer's disease (12-01-2021)
80. A. de Wilde: Visualizing Brain Amyloid-beta Pathology (17-03-2021)
81. C. Groot: Heterogeneity in Alzheimer's Disease (06-04-2021)
82. D. Bertens: The use of biomarkers in non-demented AD patients for clinical trial design and clinical practice (14-04-2021)
83. J. Reimand: Discordance between amyloid- $\beta$  PET and CSF biomarkers: Clinical and pathophysiological consequences (12-05-2021)
84. L.E. Colij: The AMYPAD project: Towards the next stage in amyloid PET imaging (01-07-2021)
85. C.T. Briels: Evaluation and implementation of functional cerebral biomarkers in Alzheimer's disease (15-05-2021)
86. N. Tesi: The Genetics of Cognitively Healthy Centenarians (28-09-2021)
87. L.M. Reus: Triangulating Heterogeneity in Dementia (28-09-2021)
88. R. Bapapour Mofrad: The use of Biofluid biomarkers in dementia: implementation in clinical practice and breaking new grounds (08-10-2021)

89. E.H. Thijssen: Blood-based biomarkers for Alzheimer's disease: assay development and clinical validation (15-11-2021)
90. A.C. Baakman: Innovation in cholinergic enhancement for Alzheimer's Disease (17-11-2021)
91. I.M.W. Verberk: Blood-based biomarkers for Alzheimer's disease coming to fruition (08-12-2021)
92. J.F. Leijenaar: Streamlining VCI: Heterogeneity and Treatment Response (11-01-2022)
93. B.D.C. Boon: Deciphering neuropathological heterogeneity in Alzheimer's Disease: Beyond plaques and tangles (14-01-2022)
94. E.H. Singleton: The behavioral variant of Alzheimer's disease: A clinical, neuroimaging and neuropathological perspective (02-06-2022)
95. M. van de Beek: The many faces of dementia with Lewy bodies: impact on clinical manifestation, disease burden and disease progression (09-09-2022)
- 96. W. Pelkmans: Imaging neurodegeneration across the Alzheimer's disease continuum (03-10-2022)**

**Portfolio**

<b>Courses</b>	<b>Year</b>	<b>EC</b>
(f)MRI Toolkit <i>Donders Institute, Nijmegen</i>	2019	2,0
Using R for Data Analysis <i>LUMC, Leiden</i>	2018	1,5
Research Integrity Course <i>VUMC, Amsterdam</i>	2018	2,0
BROK – Good Clinical Practice <i>VUMC, Amsterdam</i>	2017	1,5

**Teaching**

---

Supervision of 2 Bsc and 2 Msc thesis	2020-2021	
Tutor course Neurodegeneration <i>Medicine Bachelor, VU</i>	2018-2021	1,8

**International academic work**

---

Visiting researcher (5m) at Lund University <i>Clinical Memory Research Unit, Lund</i>	2020	8,0
---	------	-----

**International conferences**

---

Alzheimer's Association International Conference <i>Online</i>	2021	1,5
Alzheimer's Association International Conference <i>Online</i>	2020	1,5
Alzheimer's Association International Conference <i>Los Angeles</i>	2019	1,5
Alzheimer's Association International Conference <i>Chicago</i>	2018	1,5
Organisation of Human Brain Mapping <i>Singapore</i>	2018	1,5

**National conferences**

---

---

Amsterdam Neuroscience Annual Meeting	2020-2021	
VUmc Science Exchange Day	2018-2019	3,0
<b>Other</b>		
<hr/>		
Sciencedesk <i>Alzheimercenter Amsterdam</i>	2017-2019	5,0
Participation Friday's educational program <i>Alzheimercenter Amsterdam</i>	2017-2020	8,0

## Acknowledgements

First and foremost, I would like to thank all **patients and research participants** for their participation and dedication, without your contribution the significant developments in Alzheimer's disease research in recent decades would not have been possible.

**Wiesje**, dank voor de kansen die jij mij hebt gegeven. Jouw begeleiding heeft mij enorm gemotiveerd en geïnspireerd. Ik kon altijd rekenen op jouw scherpe analytische blik om mijn werk weer naar een hoger niveau te tillen. **Frederik**, heel veel dank voor jouw input en kritische blik. **Betty**, zonder jou was ik nergens geweest! Jouw inzicht en kennis lijken oneindig en zijn altijd een voorbeeld voor mij geweest. Ik heb echt ontzettend veel van je geleerd én natuurlijk heel fijn samengewerkt. **Philip**, onder jouw vleugels is het AC een toonaangevend instituut geworden. Dank dat ik hier onderdeel van uit mocht maken.

Dear members of the **Thesis Committee**, prof.dr. Liesbeth Reneman, prof.dr. Wiro Niessen, prof.dr. Louise van der Weerd, dr. Joana Pereira, dr. Sietske Sikkes, and dr. Juan Domingo Gispert, many thanks for taking the time to read and evaluate my thesis.

In addition, I would like to thank **Alzheimer Nederland** for their financial support that allowed me to experience the expertise of another research group and to work with the impressive BioFinder dataset. Thanks to **Oscar, Joana, and Rik** for their guidance and giving me this opportunity.



**Juando**, te quiero agradecer también a ti en especial por la oportunidad que me has brindado y espero con ganas nuestra colaboración en los próximos años.

Even though we don't know each other, I would like to thank the **Stack Overflow** community for all their statistical insights and for solving many of my coding problems. If not for them, I would probably still be stuck in an error message. **Femke**, dankjewel dat je mij destijds de kans hebt gegeven om te laten zien wat ik in mijn mars had als assistent. Look where we are now. **Marissa**, ik heb met ontzettend veel plezier jarenlang met jou gewerkt aan onze wetenschapsdesk missie om elke geschikte onderzoekdeelnemer te koppelen aan de juiste studie. **Arno**, dankjewel voor je begeleiding. We hebben die 500 PET-scans toch maar mooi voor elkaar gekregen.

**(Oud) Bunker 2 en een beetje radiologie:** Lianne, Ellen V, Sterre, Heleen, Aniek, Rosha, Frederique, Nina, Els, Casper, Colin, Ellen S, Emma W, Emma C, Ellen D, Tessa, Jurre, Ingrid, Marta, en Lisa dank voor al jullie zin en onzin de afgelopen jaren. Ook al hadden we geen direct daglicht, het was door jullie elke dag weer een feestje om naar werk te gaan.

Lieve **paranimfen**, Aniek & Céline dankjewel dat jullie ook vandaag naast mij willen staan. Jaarband haarband. **Pap, mam & Thomas**, dankjewel voor jullie onvoorwaardelijke steun. **Kersti**, dank voor je betrokkenheid de afgelopen jaren, het hielp om af en toe de ups en downs met je te kunnen delen. **Anna-Sophie**, je hebt me altijd de vrijheid gegeven (en soms gepushed) om te doen wat ik het liefste wilde. Met jou naast me voelt het alsof alles mogelijk is. Jij en ik.



## About the author

Wiesje Pelkmans was born on February 3rd, 1989 and grew up in Oisterwijk. After obtaining her high school atheneum diploma she moved to Maastricht to study Psychology. After completing her bachelor degree specializing in Biological Psychology, she completed a research master degree in Clinical and Cognitive Neuroscience at Maastricht University. As part of this selected two-year program, she had the opportunity to do research for five months at the Sleep Research Centre of the University of Surrey, UK.



After working as a research assistant at the Alzheimercenter Amsterdam, she started her PhD under the supervision of prof.dr W. van der Flier, prof.dr. F. Barkhof and dr. B.M. Tijms. The results of this PhD project are described in this thesis. She received a grant to spend six months at the research group of prof.dr. O. Hansson at Lund University, Sweden.

Currently, Wiesje lives in Amsterdam and in Barcelona with her wife Anna-Sophie where she continues to work on preclinical Alzheimer's disease as a postdoctoral researcher at the Barcelonaβeta Brain Research Center Neuroimaging group.